ANGLIA RUSKIN UNIVERSITY

MODELLING LUNG AND TISSUE GAS TRANSFER USING A MEMBRANE OXYGENATOR CIRCUIT; DETERMINING THE EFFECTS OF A VOLATILE ANAESTHETIC AGENT AND A HAEMOGLOBIN SUBSTITUTE ON OXYGEN, CARBON DIOXIDE AND NITRIC OXIDE DIFFUSION

HELEN DUNNINGHAM

A Thesis in partial fulfilment of the
requirements of Anglia Ruskin University for the degree of Doctor of Philosophy.

This research programme was carried out in collaboration with Cambridge Perfusion Services and the Papworth NHS Trust at Papworth Hospital, Cambridge, UK.

Submitted: April 2011

ANGLIA RUSKIN UNIVERSITY

Acknowledgements

FACULTY OF SCIENCE AND TECHNOLOGY

DOCTOR OF PHILOSOPHY

MODELLING LUNG AND TISSUE GAS TRANSFER USING A MEMBRANE OXYGENATOR CIRCUIT; DETERMINING THE EFFECTS OF A VOLATILE ANAESTHETIC AGENT AND A HAEMOGLOBIN SUBSTITUTE ON OXYGEN, CARBON DIOXIDE AND NITRIC OXIDE DIFFUSION

By HELEN DUNNINGHAM
April 2011

I have much gratitude to so many people who have helped and supported me in my doctorate journey.

Firstly, to my supervisory team Dan Gordon, Dr. Colin Borland and Dr. Alain Vuylsteke who have encouraged and supported me with every step of this work. They have never lost faith in my ability to complete despite one baby closely followed, unexpectedly, by twins! A thesis with three children under the age of two was a major accomplishment.

To my three babies, I wanted you to know that despite this huge task, your needs always came first. When you were sleeping, your mummy worked long evenings to get this done. I hope one day that you will be proud and inspired by this achievement.

To my parents, for tirelessly proof-reading chapter after chapter. You have always been supportive of my quest to fulfil my dream.

Lastly, to my husband who has accepted second place to my doctorate while I spend the evenings with my laptop. He has listened and consoled me during many frustrations regarding this work. Without my husband's support this endeavour may not have been realised.

Thank you!

ANGLIA RUSKIN UNIVERSITY

Abstract

FACULTY OF SCIENCE AND TECHNOLOGY

DOCTOR OF PHILOSOPHY

MODELLING LUNG AND TISSUE GAS TRANSFER USING A MEMBRANE OXYGENATOR CIRCUIT; DETERMINING THE EFFECTS OF A VOLATILE ANAESTHETIC AGENT AND A HAEMOGLOBIN SUBSTITUTE ON OXYGEN, CARBON DIOXIDE AND NITRIC OXIDE DIFFUSION

By HELEN DUNNINGHAM

April 2011

A novel *in vitro* membrane oxygenator circuit was developed to test gas exchange where particular elements could be examined whilst keeping other variables constant. The circuit comprises two membrane oxygenators connected to form a continuous blood circuit resembling venous and arterial blood conditions. The effects of Isoflurane, a volatile anaesthetic, on oxygen transfer were investigated. RBC resistance to nitric oxide diffusion (DNO) was tested in this circuit by haemolysis and addition of the haemoglobin-based-oxygen-carrier (HBOC) Oxyglobin.

The circuit was primed with equine blood flowing at 2.5 l/min. The oxygenator was ventilated with 5 l/min air/oxygen/N_2 mix providing a range of FiO_2. The deoxygenator received 5 l/min 5% CO_2 in N_2 with 0.2-0.3 l/min CO_2. Isoflurane 1%, NO 4000-16000 ppb and CO 0.03% were added to the oxygenator gas. Uptake of O_2, CO_2, CO and NO were calculated by gas inlet and outlet concentrations and flow rates. Arterial and venous oxygen dissociation curve (aODC and vODC) comparisons were made.

Isoflurane uptake by the circuit blood was evident and 1% Isoflurane did not affect oxygen uptake ($p=0.981$), aODC or vODC ($p=0.311$ and $p=0.751$). Haemolysis did not affect O_2 or CO_2 transfer but increased DNO ($p<0.001$). 250ml free Hb solution addition to the circuit increased DNO by 91% ($p<0.0001$). Addition of 250ml Oxyglobin increased DNO by 143% from 7.41±2.77 to 17.97±1.83 ml/min/mmHg. Oxyglobin caused a right shift of aODC and vODC ($p<0.0001$) but NO-bound Oxyglobin caused a left vODC shift ($p<0.0001$).

Conclusion: Isoflurane administered via a membrane oxygenator does not affect O_2 uptake or carriage in the blood. RBC surroundings provide significant resistance to DNO in circuit tests. Significant uptake of NO by Oxyglobin supports the potential of HBOCs to scavenge endothelial NO *in vivo,* causing vasoconstriction. Oxyglobin binding NO shifts the ODC left resulting in poor oxygen delivery to tissues.

Keywords: Membrane Oxygenator, Deoxygenator, Isoflurane, Nitric Oxide, HBOC, Oxyglobin

ANGLIA RUSKIN UNIVERSITY

Table of Contents

II. Tables

Chapter 1 Tables

Chapter 3 Tables

Chapter 4 Tables

ANGLIA RUSKIN UNIVERSITY

Copyright of Thesis

FACULTY OF SCIENCE AND TECHNOLOGY

DOCTOR OF PHILOSOPHY

MODELLING LUNG AND TISSUE GAS TRANSFER USING A MEMBRANE OXYGENATOR CIRCUIT; DETERMINING THE EFFECTS OF A VOLATILE ANAESTHETIC AGENT AND A HAEMOGLOBIN SUBSTITUTE ON OXYGEN, CARBON DIOXIDE AND NITRIC OXIDE DIFFUSION

By HELEN DUNNINGHAM

April 2011

ANGLIA RUSKIN UNIVERSITY

Declaration

FACULTY OF SCIENCE AND TECHNOLOGY

DOCTOR OF PHILOSOPHY

MODELLING LUNG AND TISSUE GAS TRANSFER USING A MEMBRANE OXYGENATOR CIRCUIT; DETERMINING THE EFFECTS OF A VOLATILE ANAESTHETIC AGENT AND A HAEMOGLOBIN SUBSTITUTE ON OXYGEN, CARBON DIOXIDE AND NITRIC OXIDE DIFFUSION

By HELEN DUNNINGHAM

April 2011

I declare that all work presented in this thesis is a result of my own work. Assistance was sought for the calculation of DO_2 via a computerised Bohr Integration method devised by Dr. C Borland (Appendix 2).

Symbols and Abbreviations List

AAMI	Association for the Advancement of Medical Instrumentation
aODC	Arterial oxygen dissociation curve
ARDS	Adult respiratory distress syndrome
ATP	Adenosine triphosphate
BMI	Body Mass Index
BP	Barometric pressure millibars
CaO_2	Arterial oxygen content ml/dl
$CaCO_2$	Arterial carbon dioxide content mmol/l
CcO_2	End pulmonary capillary oxygen content (usually substituted by CAO_2) ml/dl
CJD	Creutzfeldt-Jakob-Disease
CO	Carbon monoxide
CO_2	Carbon dioxide
COin	Concentration of CO in oxygenator inlet gas (%)
$ContO_2$	Oxygen content of blood ml/dl
COout	Concentration of CO in oxygenator outlet gas (%)
CPB	Cardiopulmonary Bypass
$C\bar{v}O_2$	Venous oxygen content ml/dl
$C\bar{v}CO_2$	Venous carbon dioxide content mmol/l
DCO	Carbon monoxide transfer ml/min/mmHg
DCO_2	Carbon dioxide transfer ml/min/mmHg
Deoxy	Deoxygenator
Deoxy F	Deoxygenator gas flow ml/min
D_L	Lung diffusion
D_LCO	Lung diffusing capacity for carbon monoxide ml/min/mmHg
D_LNO	Lung diffusing capacity for nitric oxide ml/min/mmHg
D_LO_2	Lung diffusing capacity for oxygen ml/min/mmHg
D_M	Membrane diffusion
D_MNO	Membrane diffusing capacity for nitric oxide ml/min/mmHg
DNO	Nitric oxide transfer ml/min/mmHg
DO_2	Oxygen transfer ml/min/mmHg
EEG	Electroencephalography
EU	European Union
FDA	US Food and Drug Administration
Fe^+	Iron
$FeCO_2$	Expired fractional carbon dioxide content
FeISO	Expired fractional Isoflurane content
FeO_2	Expired fractional oxygen content
$FiCO_2$	Inspired fractional carbon dioxide content
FiISO	Inspired fractional Isoflurane content
FiO_2	Inspired fractional oxygen content
g/dl	Grams per decilitre
Hb	Haemoglobin g/dl
HBOC	Haemoglobin-based-oxygen-carrier
HCO_3	Bicarbonate concentration in blood mmol/l
Hct	Haematocrit %
HIV	Human-Immunodeficiency-Virus
IV	Intravenous
K^+	Potassium mmol/l

l/min	Litres per minute
$\dot{M}CO$	Carbon monoxide uptake ml/min
$\dot{M}CO_2$	Carbon dioxide uptake ml/min
MI	Myocardial infarction
ml/dl	Millilitres per decilitre
ml/min	Millilitres per minute
ml/min/mmHg	Millilitres per minute per millimetre of mercury
MMC	South African Medical Control Council
mmHg	Millimetres of mercury
mmol/l	Millimols per litre
$\dot{M}O_2$	Oxygen uptake ml/min
N_2	Nitrogen
NaCl	Sodium chloride
NO	Nitric oxide
NO_2	Nitrogen dioxide
NOin	Concentration of NO in oxygenator inlet gas (ppb)
NOout	Concentration of NO in oxygenator outlet gas (ppb)
O_2	Oxygen
O_2sat	Oxygen saturation of the blood %
ODC	Oxygen dissociation curve
Oxy	Oxygenator
Oxy F	Oxygenator gas flow ml/min
P_{50}	Measure of oxygen affinity; oxygen partial pressure at 50% saturation
PACO	Alveolar carbon monoxide partial pressure mmHg
$PaCO_2$	Arterial carbon dioxide partial pressure mmHg
PaO_2	Arterial oxygen partial pressure mmHg
PAO_2	Alveolar oxygen partial pressure mmHg
$P\bar{c}CO_2$	Pulmonary capillary carbon dioxide partial pressure mmHg
$P\bar{c}O_2$	Pulmonary capillary oxygen partial pressure mmHg
PCO_2	Partial pressure of carbon dioxide in blood mmHg
PFC	Perfluorocarbon based oxygen therapeutics
PH_2O	Saturated water vapour pressure (for a given laboratory temperature) mmHg
pHa	Arterial pH
pHv	Venous pH
PO_2	Partial pressure of oxygen in blood mmHg
ppb	Parts per billion
ppm	Parts per million
PVC	Polyvinyl chloride
$P\bar{v}CO_2$	Venous carbon dioxide partial pressure mmHg
$P\bar{v}O_2$	Venous oxygen partial pressure mmHg
$\dot{Q}$	Blood flow or ‘cardiac output’ ml/min
$\dot{Q}g$	Gas flow ml/min
$\dot{Q}s$	Blood flow shunt ml/min
$\dot{Q}t$	Total blood flow ml/min
RBC	Red blood cell
SA	Surface area m^2
SaO_2	Arterial blood oxygen saturation %

sO_2	Blood oxygen saturation %
STPD	Standard temperature, pressure and dry gas
SvO_2	Venous blood oxygen saturation %
t	Laboratory temperature $^{\circ}C$
$t½$	Half-life min
Vc	Pulmonary capillary blood volume ml
vODC	Venous oxygen dissociation curve
0.93	Membrane absorption correction factor (for half membrane) as minor NO uptake was noted in a saline primed membrane oxygenator (Borland, 2006)
$1/ D_L$	Lung diffusion resistance
1 cell	One membrane oxygenator compartment
¼"	Quarter of an inch internal diameter tubing
⅜"	Three eighths of an inch internal diameter tubing
½"	Half of an inch internal diameter tubing
2,3-DPG	2,3-diphosphoglycerate
2 cells	Whole membrane oxygenator (2 compartments)
Θ	'theta' Specific conductance of a gas per 1 ml blood
β	'beta' gas content in the blood ml/min/mmHg
µm	Micrometre

Chapter 1 Introduction

1.1. Membrane Oxygenators

An oxygenator functions as the patient's lungs during cardiothoracic surgery requiring cardiopulmonary bypass (CPB). It can also provide respiratory support in acute respiratory disorders. An oxygenator only performs gas exchange so functions such as endocrine are suspended during the operative procedure. The oxygenator allows passage of gases (oxygen, carbon dioxide and anaesthetics) between inspired gas and blood so the term 'oxygenator' is incorrect although commonly used. In clinical practice, a patient's venous circulation is pumped through the bypass circuit where it is oxygenated and carbon dioxide removed by the oxygenator before arterialised blood is returned to the aorta. Normally, an oxygenator adds oxygen to venous blood by ventilating the gas side with oxygen rich gas and removes carbon dioxide from venous blood by ventilating the gas side with carbon dioxide depleted gas. The oxygenator uses basic gas diffusion whereby gas moves from a higher to a lower concentration.

Oxygenators have been classified as bubble, film or membrane depending on the method of gas exchange. Bubble oxygenators allowed bubbles to be generated in the patients' blood within the device where the surface of the bubble served as the membrane for gas transfer. With film oxygenators blood was passed over gaseous discs in a thin film for gas transfer to occur. Both bubble and film oxygenators were assembled per case using sterilised reusable glass and stainless steel parts. Both oxygenator types caused blood damage due to direct blood-gas interface. Membrane oxygenators imitate the lungs as a membrane separates the blood and gas flowing on either side allowing gas transfer. Membrane separation of blood and gas phases aids haemocompatibility. Membrane

materials used are silicone or poly-4-methyl-1-pentene (true membranes) or microporous polypropylene where tiny holes are manufactured into the membrane for gas diffusion. The membrane can be a flat sheet or hollow fibres woven into a bundle. In this study, a microporous polypropylene sheet membrane oxygenator was used as an example of a current clinical device. The thesis will concentrate solely on polypropylene membrane oxygenators.

1.1.1 Comparison to lungs

Modern day membrane oxygenators aim to transfer maximum amounts of gas (oxygen and carbon dioxide) at a given blood flow rate, thus maximising efficiency. Despite the manufacturers aiming for large gas exchange surface areas, the devices are kept compact for ease of use and to minimise blood trauma and priming (fill) volume.

There are many differences between a membrane oxygenator and the lungs. Structurally, the lungs contain 300 million alveoli separated from gas by alveolar epithelium and capillary endothelium of combined thickness 0.3 μm (Cotes 1993) whereas a membrane oxygenator (e.g. Cobe Duo) has two oxygenator cells separated from gas by 100-150 μm polypropylene membrane containing multiple micropores (<0.1 μm). The blood pathway diameter through the membrane oxygenator is very different to the pulmonary capillaries of the alveoli. In alveoli, blood passes one RBC at a time with high vascular compliance avoiding resistance to blood flow hence gas transfer distance is very small. It has not been possible to construct a narrow blood pathway in membrane oxygenators due to excessive pressure resistance exerted by blood flow. A much larger blood channel is required resulting in greater distance for gas transfer. Larger blood channels create laminar flow where the outer RBC layers exchange gas but are stagnant and the middle layers move quickly with less time and greater distance for gas transfer. Manufacturers induced

secondary blood flows to aid mixing within the blood channel thus reducing laminar flow but avoiding blood trauma from excessive turbulence. The surface area for gas exchange is very different between the membrane oxygenator at 2.6 m^2 (Cobe Duo CML) and the lungs at 70 m^2 (Guyton 1976). To compensate for the smaller membrane surface area, manufacturers increased the blood pathway length, keeping blood in contact with the membrane for longer (9.6 seconds) allowing gas exchange to occur. In lungs, the pulmonary capillary blood transit time is expected to be 0.3 seconds (Cotes 1993). The gas used to ventilate the membrane oxygenator is continuous, at high velocity and utilises a high inspired oxygen fraction (FiO_2 65-80%) to achieve high arterial blood saturations. In the lungs, gas is inspired and expired, yet the design of airways with multiple branches reduces the velocity of the gas flow with diffusion dominating in the alveoli. The simplistic oxygenator gas channel facilitates easier calculation of alveolar oxygen tensions based on a semi-logarithmic decline between inlet and outlet concentrations. The V/Q ratio (ventilation/perfusion ratio) in a normal adult lung equals 1 but in the membrane oxygenator ratios can be in excess of 2. The higher gas flow required (i.e. 5 l/min) to achieve normoxia for a given blood flow (i.e. 2.5 l/min) compensates for reduced gas transfer efficiency. In this model, the membrane surface area and pulmonary capillary volume is fixed whereas in the lung there are changes in these parameters such as pulmonary capillary recruitment and distension with increased blood flow.

In the membrane oxygenator, oxygen uptake by the blood from the gas uses both convective and diffusive processes. There is convective mixing of the blood in the blood channel to reduce stagnant layers compared to pulmonary capillaries with diameter approximating the RBC. Diffusive distances are greater in the membrane oxygenator with wider gas and blood channels and thicker membrane compared to the lesser diffusive distance of the alveolar to pulmonary capillaries.

The anatomical shunt in the lungs comprises venous blood entering the arterial circulation without being exposed to ventilated areas of the lung, so is considered a perfusion limited shunt. This differs from the shunt within the membrane oxygenator. The principle is the same, where venous blood not exposed to the membrane mixes with the arterial blood; however, the shunt is most likely due to the laminar flow characteristics of a larger diameter blood channel.

1.1.2 Suitability

The membrane oxygenator is an alternative device for experimental gas diffusion studies compared to rapid reaction apparatus or *in vivo* work. Previous *in vitro* diffusion work has utilised rapid reaction apparatus, first reported by Hartridge and Roughton (1923) who discovered that O_2 and Hb combination was very rapid at 100^{th} of a second. The apparatus comprised two pressurised vessels, one containing dilute O_2 free Hb solution and the other O_2 exposed tap water. The two fluids were forced under pressure into a mixing chamber and down a long, thin observation tube. Spectroscopy determined oxyHb and deoxyHb ratios at known distances along the tube. The oxygenation time of blood was calculated by the distance (cm) divided by fluid velocity (cm/sec). Similarly, CO and Hb reactions were monitored via dissociation of CO and Hb, facilitated by bright light exposure at the tube entry (Hartridge and Roughton 1923b). Modernising modifications were made to the original apparatus (i.e. syringe drivers, photoelectric spectroscopy) however, large amounts of blood was required for very short run times due to the flow velocities needed to observe such quick reactions. Increased flow velocities induce turbulent flow which can cause RBC shear stress. A stopped-flow methodology was reported (Gibson 1954) where the flow is halted abruptly close to the mixing chamber (<1.0 ms) and a complete kinetic curve established. This method allowed observation of change and less reagent

use, but stopping flow induced settling of RBCs and formation of an unstirred layer. The unstirred layer may impede gas diffusion (Hughes and Bates 2003). This proposed circuit would comprise two oxygenators acting as the lungs and the tissues, thus a continuously operating circuit could be developed resembling venous and arterial blood gas parameters. The 'lung' oxygenator could be used for testing gas diffusion theories. The compactness of the circuit would limit the blood needed to run a battery of experiments, whilst the continuous operation would limit unstirred layer formation. The circuit design would facilitate changes in membrane surface area/blood volume, blood flow, gas flow, oxygen tensions, haematocrit and red cell integrity whilst keeping other variables constant. A membrane oxygenator circuit would allow diffusion experiments to be conducted in conditions that would otherwise be impossible *in vivo* i.e. haemolysis and low haemoglobin states. Whilst the physiological differences are apparent with *in vitro* work, including rapid reaction apparatus, they provide a functional model of gas transfer. The membrane oxygenator circuit provides an alternative gas diffusion testing apparatus.

1.2 Using a Membrane Oxygenator Circuit to Model Gas Exchange

The aim was to create a compact, efficient and continuously perfused membrane oxygenator circuit to replicate arterial and venous blood conditions. Hypotheses of gas exchange were tested using a system where a single variable could be altered over a supraphysiological range while keeping the remaining variables unchanged.

The literature review was restricted to peer reviewed journals applicable to the field. The search terms were "*in vitro* membrane oxygenator modelling" thus excluding older oxygenator types, clinical assessments or *ex vivo* studies whereby the patient or animals

provide the venous blood conditioning. Studies detailing methods for membrane oxygenator gas diffusion testing were primarily used as these were likely to include both arterial and venous circuitry rather than other studies such as drug testing and effects of circuit coatings.

1.2.1 Circuit Design

Membrane oxygenators undergo rigorous testing by the manufacturers in accordance with the AAMI (2009) guidelines prior to commercial approval but manufacturers rarely publish this methodology or data. The AAMI guidelines methodology criteria are not specific allowing large variations in test conditions yielding commercially favourable results (Fried and Mohamed 1994). Once approved for clinical use, a device often undergoes comparison studies to older devices in the clinical setting which will be subject to patient variables i.e. BMI, oxygen consumption, temperature, acid-base balance and pre-existing conditions. *In vivo* tests are favoured over *in vitro* testing as ethical considerations are less once a product has been approved for clinical use. To obtain comparable gas diffusion data between different membrane oxygenators under simulated clinical conditions, several researchers have developed testing circuits.

Vocelka *et al* (1993) published an *in vitro* protocol for evaluating and comparing membrane oxygenators. Their circuit compared oxygen and carbon dioxide transfer of oxygenators from different manufacturers under the same operating conditions. The circuit was a single-pass system utilising vast quantities of bovine blood (24 litres). This methodology has been used by several researchers with varying quantities of blood (Van Meurs *et al* 1991**,** Rais-Bahrami *et al* 1992, Griffiths 1994, Gourlay and Taylor 1994, Beckley *et al* 1996, Matsuda and Sakai 2000, Maeda *et al* 2000, Kawahito *et al* 2001 and Motomura *et al* 2003). Single-pass systems comprise a reservoir of blood deoxygenated

to venous blood parameters before being held in another reservoir. Venous blood is pumped through the test membrane oxygenator where it is arterialised and returned back to the first reservoir. Some minor variations such as extra shunting loops, directional changes and additional reservoirs may be included. This creates a large and complex circuit which requires blood to be repeatedly reconditioned to venous parameters. The disposables and volumes of blood for these circuits make them expensive. They were popular in the early 1990s when membranes were less efficient and larger in capacity so complex circuitry was required to achieve the gas exchange data.

Single-pass systems cannot run for a lengthy duration before exhausting the volume of preconditioned venous blood. In Vocelka's study (1993), 24 litres of bovine blood was needed to allow a testing duration of 4-12 minutes at typical blood flow rates of 2-6 l/min. Single-pass systems do not facilitate changes in gas or haematological parameters during the experiment as equilibrium takes a few minutes to achieve. For example, increasing Hb levels during the test run would be difficult to achieve as the blood volumes needed to increase the Hb from 1-10g/dl would be vast. Hb increases are easier to achieve in smaller circuits with less amounts of blood. The main purpose of single-pass methodology is for determining overall gas transfer at predetermined conditions. This single-pass methodology was inflexible for this research project. The circuit design was for a compact, continuously run circuit allowing for controlled changes in operating conditions. A later study by Walczak *et al* (2005), a modified Vocelka method, described methodology where the deoxygenating and test circuits ran in parallel with both feeding into the same reservoir of blood allowing continuous circulation. He demonstrated that a continuous circuit was feasible but the deoxygenating component comprised many units so failed to be compact. It was considered that a compact system with less disposables and smaller blood usage was possible for this research.

The size and number of deoxygenator units required for the circuit was a concern. The deoxygenator removes O_2 from the blood whilst adding CO_2. Transfer of CO_2 is very efficient as it readily crosses the membrane but O_2 liganded with haemoglobin is more difficult to remove. Many researchers cited two or more deoxygenator units or had substantially larger deoxygenator membranes compared to the test membranes. Studies conducted by Vocelka *et al* (1993), Griffiths (1994) and Beckley *et al* (1996) described two oxygenator units whereas Walczak *et al* (2005) used four units and Gourlay and Taylor (1994) utilised "a series of deoxygenating units": quantity was not specified. Van Meurs *et al* (1991) and Rais-Bahrami *et al* (1992) used one deoxygenating unit but the deoxygenator membrane surface area was $3.3m^2$ compared to the oxygenator membrane surface area of 0.5, 0.6 or $0.8m^2$ thus a 6, 5 or 4 times membrane diffusing area. This difference in deoxygenating and oxygenating membrane number and size reflects the inefficient membrane technology in the 1990s. The volume of blood to deoxygenate was large determining deoxygenator membrane size. Often details of the exact membrane oxygenators used for deoxygenation are omitted. Kawahito *et al* (2001) demonstrated that a smaller deoxygenating to oxygenating membrane surface area was adequate to remove O_2 from blood: 1.9 m^2 deoxygenator: $1.0m^2$ prototype oxygenator membrane. This study was a later publication indicating the efficiency of newer membrane oxygenators, i.e. Cobe Optima. These studies show that deoxygenation may be difficult with a single unit of an equal membrane surface area to the arterialising unit. Ideally, this circuit would utilise one deoxygenator unit for system compactness and cost.

To replicate tissues and provide venous blood, the deoxygenator must remove O_2 from the blood and add CO_2. The deoxygenator ventilating gas needs to comprise CO_2 but exclude O_2 for appropriate gas exchange. Vocelka *et al* (1993) detailed a deoxygenator gas mix of

100% CO_2, 100% N_2 and 5% CO_2 in N_2. Preconditioning of the blood commenced with 100% CO_2 for 12-15 seconds before switching to 5% CO_2 in N_2. Additional CO_2 or N_2 was added as necessary by constant adjustment. This adjustment was considered unsuitable for this work as a stable deoxygenation method was required for a continuous system. Griffiths *et al* (1994) modified Vocelka *et al*'s (1993) methods with 7% CO_2 in N_2 at 10 l/min with a venous blood flow of 4 l/min. This demonstrated a stable approach although the gas flow to blood flow ratio was high suggesting difficultly in deoxygenating. Other studies described the use of CO_2 and N_2 but concentrations and gas flows were omitted (Gourlay *et al* 1990, Gourlay and Taylor 1994, Matsuda and Sakai 2000 and Walczak *et al* 2005). To precondition vast quantities of venous blood for single-pass systems, higher CO_2 gas concentrations are needed compared to a smaller continuously run circuit. The concentration of CO_2 added would be dependent on deoxygenator surface area, gas flows and blood flows. Van Meurs *et al* (1991), Rais-Bahrami *et al* (1992) and Beckley *et al* (1996) described using CO_2, N_2 and O_2 for their deoxygenator yet removal of O_2 is the primary role of the deoxygenator unit. To effectively remove O_2, an anoxic gas mix maximizes the diffusion gradient for O_2 transfer. However, if the deoxygenator was for preconditioning venous blood prior to use through the test membrane oxygenator, O_2 may be needed to achieve venous saturation of 65%. In this circuit the deoxygenator would be used to continuously remove O_2 and add CO_2 to the blood. The initial deoxygenator gases would be 5% CO_2 in N_2 (Vocelka *et al* 1993) and if continuous normocapnia was not achieved, additional low flow 100% CO_2 would be added.

Previous studies utilised bovine blood as vast quantities were required coupled with ease of procurement from abattoirs. The single-pass methodology requires large volumes of blood to run the system before exhausting the preconditioned venous blood, i.e. 24 litres

pumped at 2 l/min equals 12 minutes operation. Four studies detailed high blood volumes; 24 litres (Vocelka *et al* 1993), 18 litres (Griffiths *et al* 1994), 12 litres (Gourlay and Taylor 1994) and 20 litres (Beckley *et al* 1996). Implications of large blood volumes would be cost, procurement and storage prior to use. In Walczak *et al*'s (2005) study five litres of bovine blood was used to run the complex parallel venous and test circuit but this exceeded blood volume expectations. This compact circuit would require 1-2 litres of blood based on volume capacity of the components. Despite this smaller volume per circuit, human donation would be ethically ambiguous. Several donors of the same blood group would need to donate 500 ml of blood each. Expired human blood donations from NHS stock would have storage damage (Liumbruno and Aubuchon 2010) rendering it unsuitable for extrapolation of gas diffusion data. In-date human bank blood would be unethical to use due to shortages of blood for medical use. Animal blood donations are commercially available and were acquired for this research allowing for reproducibility. The equine donor was selected due to body surface area and blood volume enabling three litres of blood donation per experimental session. Donor gender and age specifications can be realised to reduce variations in the data.

1.2.2 Calculations

Literature for both clinical and *in vitro* oxygenator assessments was reviewed for oxygen uptake ($\dot{M}O_2$) and carbon dioxide uptake ($\dot{M}CO_2$) calculations. Most authors cite reverse Fick approach to $\dot{M}O_2$ calculations. Fick principle, named after Adolf Eugen Fick, determines cardiac output by knowing the concentration of a marker substance into and out of an organ per unit of time. This marker substance was oxygen and the organ was the whole body represented as:

$$Q = MO_2 \div (CaO_2 - CvO_2)$$

Where $\dot{Q}$ = cardiac output (ml/min)

$\dot{M}O_2$ = oxygen uptake (ml/min)

CaO_2 = pulmonary vein blood O_2 content (mg/dl)

$C\overline{v}O_2$ = pulmonary artery blood O_2 content (mg/dl)

Assuming cardiac output is known the equation can be rearranged to calculate oxygen uptake:

$$MO_2 = (CaO_2 - CvO_2) \times Q$$

The oxygen content of the arterial (CaO_2) or venous ($C\overline{v}O_2$) blood is calculated from the following equation:

$$ContO_2(ml/dl) = (Hb \times 1.36 \times O_2 sat) + (0.003 \times PO_2)$$

Where $ContO_2$ = oxygen content of blood (ml/dl)

Hb = Haemoglobin concentration in the blood (g/dl)

1.36 = ml of O_2 carried by 1g fully saturated Hb

O_2 sat = O_2 saturation of the blood (arterial or venous as appropriate)

0.003 = O_2 solubility correction factor for plasma (0.003ml O_2 /dl /mmHg PO_2)

PO_2 = partial pressure of O_2 in the blood (arterial or venous as appropriate)

Slight variations of these calculations are presented in the published literature, i.e. for 'O_2 content' the initial bracketed section determines the content of O_2 bound to Hb for a given Hb and associated saturation. The second bracketed section adds the amount of dissolved O_2 within plasma proportional to the partial pressure (Henrys Law). Some publications assume the plasma O_2 content negligible and is not included in the total O_2 content calculation. Variation in the 1.36 mlO_2/gHb is often presented as $1.34mlO_2/gHb$. This is due to pure Hb having the capacity to carry 1.39ml O_2/gHb but under normal bodily conditions Hb is present in alternative non O_2 carrying forms such as methaemoglobin, so a corrected value is used.

The alternative $\dot{M}O_2$ calculation utilises inspired and expired gas O_2 concentrations to provide direct O_2 uptake data through the oxygenator, using the following equation:

$$MO_2 = (FiO_2 - FeO_2) \times F$$

Where $\dot{M}O_2$ = oxygen uptake (ml/min)

FiO_2 = fractional inspired O_2 concentration

FeO_2 = fractional expired O_2 concentration

F = gas flow through the oxygenator (ml/min)

This approach was not well documented compared to the reverse Fick method. FiO_2 and FeO_2 values where detailed have been determined via mass spectrometry. Portable FiO_2 meters were used in this work rather than a mass spectrometer as it is large, subject to interference from water vapour and unavailable in many establishments (including Papworth.) The gas method historically had errors in recording patient data so reverse Fick was popular. However, reverse Fick $\dot{M}O_2$ is calculated from multiple calculations

encompassing correction factors, all of which could add error to the overall result. The gas method was chosen for this work as the margins of error were considered less and the methodology suited the oxygenator.

$\dot{M}O_2$ calculations were used alone with the exception of Visser and de Jong (1997) and Segers *et al* (2001). $\dot{M}O_2$ provides values of total oxygen uptake across the membrane from gas phase to blood phase. Oxygen diffusion is dependent on the concentration gradient between gas and blood phases with increased transfer over larger gradients. Comparison of oxygen diffusion in changing conditions cannot be made with the $\dot{M}O_2$ equation alone. Visser and de Jong (1997) devised an equation to measure the driving force needed to transfer 1ml O_2 per minute based on the partial pressure difference of O_2 in the gas and venous blood phases. Segers *et al* (2001) equated the oxygen transfer to the pressure gradient between the gas phase and resultant PaO_2. These were both non standard variations. Researchers have measured DO_2 and DCO in humans for over a hundred years (Bohr 1909, Krogh 1915 and Hughes and Bates 2003). Piiper and Scheid (1980) devised an equation (DO_2) where oxygen uptake is adjusted for the concentration gradient between 'alveoli' and blood phases thus facilitating comparison of oxygen transfer in changing conditions. Lilienthal *et al* (1946) divided oxygen uptake by the membrane oxygen partial pressure difference determined from the alveolar and mean capillary oxygen tensions. Both Lilienthal and Piiper equations were incorporated in this data evaluation to give comparative oxygen uptake analysis.

CO_2 transfer is less widely published as in clinical practice oxygen delivery is more important. CO_2 is more soluble and readily transferred across a membrane than O_2. Few papers have cited equations for CO_2 transfer in the membrane oxygenator. Of these publications, $\dot{M}CO_2$ is calculated using a version of Fick's principle (Gourlay *et al* 1990,

Visser and de Jong 1997, Niimi *et al* 1997, Kawahito *et al* 2001 and 2002, Karimova *et al* 2005) or a gas method (Van Meurs *et al* 1991, Kawak *et al* 1991, Vocelka *et al* 1993 and 1997, Griffiths *et al* 1994, Beckley *et al* 1996). The commonly used equation for $\dot{M}CO_2$ reflecting Fick's principle is:

$$MCO_2 = 22.4 \times (CvCO_2 - CaCO_2) \times Q$$

Where $\dot{M}CO_2$ = CO_2 uptake (ml/min)

22.4 = conversion factor from mmol to ml

$C\bar{v}CO_2$ = content of CO_2 in venous blood (mmol/l)

$CaCO_2$ = content of CO_2 in arterial blood (mmol/l)

$\dot{Q}$ = blood flow (ml/min)

The CO_2 content of the arterial ($CaCO_2$) or venous ($C\bar{v}CO_2$) blood is calculated from the following equation:

$$TotalCO_2 = HCO_3 + (0.03 \times PCO_2)$$

Where $TotalCO_2$ = total CO_2 in the blood (arterial or venous) (mmol/l)

HCO_3 = Bicarbonate concentration in the blood (mmol/l)

0.03 = solubility coefficient of CO_2 in plasma (mmol/l/mmHg)

PCO_2 = partial pressure of CO_2 in the arterial or venous blood (mmHg)

$\dot{M}CO_2$ calculated using the gas method takes the expired CO_2 fractional concentration multiplied by the gas flow. These studies calculated the removal rate of CO_2 from the blood so the inspired ventilating gas was void of CO_2. i.e.

$$MCO_2 = FeCO_2 \times F$$

Where $\dot{M}CO_2$ = CO_2 uptake (ml/min)

$FeCO_2$ = expired fractional CO_2 concentration

F = gas flow (ml/min)

The deoxygenator was being used to actively add CO_2 throughout this continuously running circuit. The gas method of $\dot{M}CO_2$ would involve determining the inspired and expired CO_2 concentration difference multiplied by gas flow. Anaesthetics commonly use infrared technology for analysing expired CO_2 concentrations which could be adapted for the membrane oxygenator. Error in the gas $\dot{M}CO_2$ method occurs when the inspired gas flow does not equal the expired gas flow i.e. the amount of O_2 passing into the lungs being greater than the amount of CO_2 being removed. Occasionally, a marker gas such as helium is utilised to determine patient inspired and expired gas volumes. The oxygenator environment requires higher continuous gas flows for effective gas transfer and this error loses significance compared to lung ventilation. The reverse Fick $\dot{M}O_2$ calculation limitations also apply to the Fick based $\dot{M}CO_2$ equation. For consistency, the $\dot{M}CO_2$ gas method would be used with infrared CO_2 gas sensors. DCO_2 was calculated from $\dot{M}CO_2$ for comparative CO_2 transfer under varying conditions using a modification of both Lilienthal and Piiper equations.

Literature reviewed shows no previously described simple, compact and continuously run circuit designed for gas diffusion extrapolation. This work sought to create a compact circuit comprising one membrane oxygenator to model the lungs and a second membrane oxygenator to deoxygenate the blood and model the tissues. Both oxygenator and

deoxygenator would be run in sequence within the circuit continuously for several hours. The blood volume would be kept minimal at 1.5-2.0 litres. Commercially available components and blood would be used facilitating reproducibility of the circuit by this and other research groups. The simplicity of the circuit would allow effects of isolated experiments on gas diffusion data to be observed.

1.3 Isoflurane Use in Cardiopulmonary Bypass

1.3.1 Isoflurane Anaesthesia

Isoflurane is a clear, colourless volatile anaesthetic used to induce and maintain anaesthesia by depressing the central nervous system. It acts on receptors of the nervous system but its specific mode of action is unclear. Isoflurane is within the halogenated anaesthetic group being halogenated with fluorine and chlorine (Figure 1.1). Isoflurane has a mildly pungent ether-like odour.

Patients are administered Isoflurane via a vaporiser through the ventilator inspired gas. It rapidly passes across the lungs into the blood. In 4-6 minutes, arterial blood concentrations are 50% of the inspired concentrations due to the low solubility of Isoflurane in blood and tissues. This aids a rapid onset of anaesthesia. Inspired induction concentrations are 0.5% and anaesthetic maintenance 1.0-2.5% with supplemental doses of muscle relaxants (Rhodia NZ Ltd 1999). Isoflurane is rapidly cleared from the blood once terminated. The majority of the Isoflurane is expired unchanged via the lungs. Its poor solubility means little Isoflurane is metabolised (0.2%) with small amounts of metabolite (trifluoracetic acid) being detected in urine.

Isoflurane can be used as an antihypertensive (Alston 1989). Hypertension can be managed using other antihypertensive drugs such as sodium nitroprusside but these can cause tachycardia and subsequent rebound hypertension. Isoflurane decreases hypertension by reducing peripheral vascular resistance with minimal cardiac depressant effects.

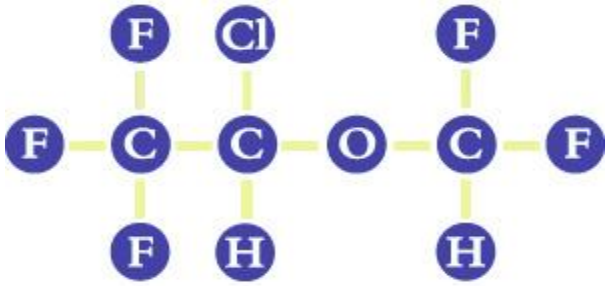

Figure 1.1 Chemical structure of Isoflurane (source; Anaesthesia UK).

Anaesthesia is maintained by volatile agents or IV drug infusions. In cardiothoracic surgery, IV anaesthetics are commonplace but volatile anaesthetics have remained popular. Use of cardiopulmonary bypass during cardiothoracic surgery leads to altered pharmacokinetic effects of IV drugs (Gedney and Ghosh 1995) and subsequent clearance due to haemodilution, hypothermia and changes in visceral perfusion (Marks 2003). Poor solubility of volatile anaesthetics limits metabolism and renal elimination so they are not subjected to the same pharmacokinetic considerations of IV anaesthetics. Some establishments combine IV and volatile anaesthetic use to ensure adequate anaesthesia is maintained.

During cardiopulmonary bypass, the lungs are deflated to avoid obscuring the surgeon's field. Isoflurane administration via the lungs is not possible and so many hospitals administer Isoflurane through the membrane oxygenator component of the bypass machine. Isoflurane is added via the inlet gas lines connected to the membrane oxygenator. The volatile agent passes down the concentration gradient across the membrane to the patient's blood. Once Isoflurane is terminated the fresh gas flowing through the membrane oxygenator aids elimination from the blood via the reverse gradient.

1.3.2 Isoflurane and Membrane Oxygenators

Isoflurane and other volatile agents have been studied in older 'bubble' types of oxygenators (Price *et al* 1988, Henderson *et al* 1988, Nussmeier *et al* 1988 and 1989). This literature review encompasses "Isoflurane and membrane oxygenators". Most manufacturers of membrane oxygenators warn against the use of volatile anaesthetic agents through the devices as they have not tested their products for gas transfer and device integrity in the presence of such drugs.

There have been concerns regarding the ability to deliver adequate levels of anaesthetic to the patient via membrane oxygenators. The membrane material may provide resistance to Isoflurane transfer. Subsequently, *in vitro* and *in vivo* studies have been conducted to investigate anaesthetic transfer in membrane oxygenators. Loomis *et al* (1986) investigated the transfer of Isoflurane across the Cobe membrane oxygenator in relation to its hypotensive properties and subsequent adverse effect of EEG suppression. Patients were administered inspired Isoflurane concentrations of 1.5 to 3.0% which yielded adequate arterial blood concentrations (36.6 to 84.4µg/ml) indicating the ability of Isoflurane transfer in microporous polypropylene membranes. Further studies examine

the wash-in and wash-out durations of Isoflurane in membrane oxygenators (Henderson *et al* 1988, Stern *et al* 1989, Hickey *et al* 1996, Lockwood *et al* 1999 and Wiesenack *et al* 2002). Anaesthetic transfer was verified while gaining knowledge of the duration taken to establish adequate blood levels for anaesthesia and the time needed for clearance. Isoflurane concentrations increase rapidly within a few minutes of administration followed by a slower increase to equilibrium. The reverse is seen in the wash-out period after the vaporiser was turned off. Isoflurane t½ was quoted as 18.8 minutes (hypothermia) (Loomis *et al* 1986), 14.9 minutes (hypothermia) and 12.2 minutes (warm) (Henderson *et al* 1988). Wash-in and wash-out times can be influenced by the gas flow rate through the device and the type of study. *In vitro* studies are not subjected to distribution of Isoflurane in tissues, such as muscle and fat, seen in *in vivo* studies. Membrane material can affect Isoflurane transfer where diffusion type membranes constructed from poly-(4-methyl-1-pentene) material (Wiesenack *et al* 2002, Philipp *et al* 2002) or silicone (Stern *et al* 1989) showed limited transfer of Isoflurane. They demonstrated a limited loss of Isoflurane from the gas flow and poor blood levels being achieved. The diffusion type membranes are not microporous and are considered more biocompatible due to the lack of gas/blood interface. Therefore diffusion of Isoflurane is subject to solubility, concentration gradients and gas permeability of the membrane material. These studies have shown that the membrane material plays a fundamental role in Isoflurane transfer. For this circuit, the microporous polypropylene membrane oxygenator that has proven Isoflurane transfer properties (Yang *et al* 2004, Liu and Dhara 2005) was used. This type of membrane is commonly used clinically so effects of Isoflurane on oxygen transfer will be reflective of clinical practice.

Halogenated anaesthetic agents can damage the polycarbonate housing of membrane oxygenators by weakening the plastic after spillages (Maltry and Eggers 1987, Cooper and

Levin 1987 and Walls *et al* 1988). Isoflurane effects on the structure and efficiency of the membrane within the oxygenator could impact on gas transfer. Crosbie *et al* (1998) studied polypropylene fibres of the Maxima Plus membrane oxygenator exposed to concentrated Isoflurane for 3 hours or one week. Membrane fibres examined via light microscopy showed no change in structure or integrity. Lanquetot (2005) evaluated 634 patients undergoing cardiopulmonary bypass with Isoflurane anaesthesia concluding no affects of Isoflurane on the membrane. Neither of these studies quantified O_2 transfer to support this conclusion. Muhle *et al* (2001) determined the effects of Isoflurane on O_2 transfer in the membrane oxygenator. The *in vitro* circuit had a preconditioning venous system and a single pass through the test microporous polypropylene membrane oxygenator (Affinity). Experimental design included varying gas flows, O_2 tensions and Isoflurane concentrations but had a constant blood flow of 2 l/min. The O_2 transfer calculation was not detailed. Muhle concluded that O_2 transfer in the presence of Isoflurane (1, 3 and 5%) was not significantly different to baseline data. The major limitation of this study was the single-pass circuit design with a subsequent run time of 30 seconds. Lockwood *et al* (1999) demonstrated up to five minutes for equilibrium of Isoflurane between gas and blood phases. The wash-in and wash-out studies reviewed have shown similar findings with blood concentrations rising to a plateau over the first few minutes of administration (Henderson *et al* 1988, Hickey *et al* 1996 and Wiesenack *et al* 2002). A run time of 30 seconds was not considered adequate or clinically representative.

Literature demonstrates an understudied area of research regarding the effect of Isoflurane on O_2 transfer in the microporous polypropylene membrane oxygenator. Despite this the practice of administering volatile anaesthetic agents via the membrane oxygenator is still common practice today. This work was designed to evaluate the effects of Isoflurane on

O_2 transfer in the membrane oxygenator and the effects on the oxygen dissociation curve (ODC). The circuit would be designed to enable longer and continuous running times for each experimental change to allow equilibrium between the gas and blood phases to take place. It is hoped that O_2 transfer data from this study will add clarification to the current clinical practice.

1.4 Nitric Oxide

1.4.1 What is Nitric Oxide?

Nitric oxide (NO) is a colourless gas also known as nitrogen monoxide. NO gas is relatively safe within the therapeutic range of 1-80 ppm, with a half-life of 15-30 seconds in air. High NO concentrations (5,000 to 20,000 ppm) exert toxic side effects such as pulmonary oedema and methaemoglobinemia. Methaemoglobin is formed when Hb binds NO in the presence of oxygen causing the iron atom to become ferric (Fe^{3+}) rather than the ferrous (Fe^{2+}) state. Methaemoglobin cannot bind and release oxygen affecting the oxygen carriage of blood. Conversion of methaemoglobin back to haemoglobin occurs via the NADH-dependent enzyme methaemoglobin reductase (diaphorase I).

NO undergoes spontaneous oxidation to form nitrogen dioxide (NO_2) in oxygen rich environments. NO_2 is a pulmonary irritant, so exposure should be limited to 5 ppm (Weinberger *et al* 2001). NO gas administered via a patient ventilation system is at risk of forming NO_2 if the inspired oxygen concentration is high and the dwell time sufficient (Sokol *et al* 1999). To limit NO_2 formation, NO (<1000 ppm) is mixed with N_2 in cylinders. NO is added into the ventilation system close to the patient and mixed with oxygen only during administration. NO_2 formation is monitored throughout NO therapy.

NO is biologically important as the 'endothelium-derived relaxing factor'. Blood vessel endothelium (inner lining) uses NO to signal the surrounding smooth muscle to relax, resulting in vasodilation and increased blood flow. In lungs, NO regulates pulmonary vascular resistance by governing respiratory smooth muscle. NO has other biological functions such as inhibiting platelet adhesion to the vascular endothelium which can be extended to protect platelets during extracorporeal circulation. In long-term membrane oxygenator circuits, platelets can be activated by the artificial surface leading to adhesion and aggregation on the membrane. This results in post operative hemorrhage due to low platelet counts (thrombocytopenia). Trans-membrane NO (20 ppm) therapy has demonstrated reduction in thrombocytopenia and increased platelet reactivity during *in vitro* extracorporeal circulation (Keh *et al* 1999). Additionally, NO has anti-inflammatory effects of inhibiting leukocyte adhesion to vascular endothelium.

Inhaled NO is used therapeutically to treat pulmonary hypertension in neonates with congenital heart defects or meconium aspiration and in adults with Adult Respiratory Distress Syndrome (ARDS) (Beck *et al* 1999). Pulmonary hypertension can cause right ventricular dysfunction compromising cardiac output. Systemic treatment of pulmonary hypertension (nitroglycerin or nitroprusside) results in pulmonary vasodilation but this increases blood flow through non-ventilated alveoli. Pulmonary capillary blood is exposed to anoxic alveoli increasing perfusion-ventilation mismatching. Additionally, these drugs result in systemic vasodilation which may be undesirable. Inhaled NO is distributed throughout ventilated alveoli causing dilatation of the pulmonary blood vessels partaking in gas exchange. NO that passes into the blood is inactivated once bound to haemoglobin limiting the effects on the systemic circulation.

Recently NO has emerged as an alternative gas to CO for lung function testing in pulmonary disease.

1.4.2 D_L

Diffusing capacity measurement (transfer factor) of the lungs (D_L) is an important diagnostic tool to determine lung disease in patients. The current lung function testing protocols utilise carbon monoxide gas (CO), as it is highly reactive with haemoglobin and is diffusion limited. The diffusing capacity test does not use oxygen (D_LO_2) as it is a perfusion limiting gas, influenced by inspired oxygen concentrations and pulmonary blood flow (Vc). D_LO_2 calculation is simplistic but the end pulmonary capillary oxygen partial pressure ($P_{\bar{c}}O_2$), known as back tension, is difficult to ascertain.

$$D_LO_2 = \frac{MO_2}{PAO_2 - PcO_2}$$

Where D_LO_2 is the lung diffusing capacity for oxygen, $\dot{M}O_2$ is oxygen uptake in ml/min, PAO_2 is the alveolar partial pressure of oxygen (mmHg) and $P_{\bar{c}}O_2$ is the mean pulmonary capillary oxygen partial pressure (mmHg).

CO was used to demonstrate that gas transfer in lungs was by passive diffusion from the alveoli to the pulmonary capillary blood (Krogh 1915). It is an alternative gas to oxygen in lung function testing as the back tension of carbon monoxide is considered zero (with the exception of smokers) due to tight binding of CO to Hb. The equation for D_LCO is a simplified version of D_LO_2.

$$D_LCO = \frac{MCO}{PACO}$$

Where D_LCO is the lung diffusing capacity for carbon monoxide, $\dot{M}$CO is uptake of carbon monoxide in ml/min and PACO is the alveolar partial pressure of carbon monoxide (mmHg).

Roughton and Forster (1957) demonstrated that D_LCO comprises both alveolar membrane diffusion and the reaction of CO with pulmonary capillary blood. Diffusion resistance to D_LCO is expressed as the reciprocal ($1/D_L$).

$$\frac{1}{D_L CO} = \frac{1}{D_M CO} + \frac{1}{\theta CO \times Vc}$$

Where D_LCO is the lung diffusing capacity for carbon monoxide, D_MCO is the membrane diffusing capacity, θCO is the specific transfer conductance of blood for CO and Vc is pulmonary capillary volume (ml). Transfer of gas from alveolar air to blood encompasses several separate stages. Firstly, gas in alveolar air must transfer across the alveolar-capillary membrane to the blood. Gas passes through plasma to the RBC where it crosses the RBC membrane before passing through the RBC interior for binding with Hb. Roughton and Forster's equation compartmentalised these stages into two areas; the first part of the equation details diffusion limitation and the latter part details CO reaction with blood.

An alternative gas for lung function testing has emerged as nitric oxide (NO) (Guenard *et al* 1987, Borland 1989). NO has stronger binding to haemoglobin, is independent of inspired oxygen concentrations and its reaction rate with haemoglobin is effectively infinity. NO has not replaced CO in lung function testing due to issues regarding the

length of breath holding, sensitivity of the NO analysers and the potential toxicity of NO. The lung diffusing capacity of NO (D_LNO) is calculated in the same way as D_LCO. Roughton and Forster's equation (1957) has been applied to D_LNO. Due to the rapid and irreversible nature of binding between NO and Hb, θNO was considered infinite. This being the case, D_LNO would equal D_MNO (Guenard *et al* 1987). Consistent with this, Heller and Schuster (1998) reported that the diffusion element (D_MNO) accounted for 98 ±6% of the overall resistance to alveolar-capillary NO transfer.

Other groups have questioned the importance of the RBC on D_LNO suggesting that D_LNO is not just D_MNO but also includes diffusion of NO within the capillary plasma and the RBC (Borland *et al* 2006 and 2010). Sakai *et al* (2008) investigated the affects of the RBC membrane and interior on DNO by stopped-flow and computer simulation of NO uptake in Hb vesicles with different intracellular Hb concentrations. They determined that the vesicle membrane provided no resistance to DNO as vesicles containing low Hb concentrations had similar DNO to acellular Hb. They concluded that the RBC interior provided resistance to DNO as vesicles with a high Hb concentration had a reduced DNO. The Hb at the membrane surface bound NO providing a barrier to further NO transfer within the vesicle. Sakai *et al* (2008) work did not include the extracellular diffusion barrier resistance. Using Hb vesicles as representation of RBCs is a limitation of their study. Vaughn *et al* (2000 and 2001) used competition experiment methodology with mathematical modelling comparing free Hb to RBCs exposed to NO donors in solution. By providing NO uniformly throughout the test solution coupled with the mixing method, the influence of an extracellular diffusion barrier was removed, attributing resistance to DNO by the RBC membrane or intracellular resistance. Mathematical modelling assumed that RBCs are spherical or planar, RBCs are uniformly spaced and NO donor concentrations do not vary spatially. Liu *et al* (1998 and 2002) previously determined red

cell resistance to DNO, sought to test theories published by Vaughn *et al* (2000). Using similar competition experiments with mathematical modelling and low RBC concentrations, they determined that the boundary layer does exist in competition methodology. Liu (2002) demonstrated that resistance to DNO at varying haematocrit was attributed to the unstirred boundary layer of the RBC.

Literature review relating to DNO resistance exerted by the RBC has revealed an understudied area with equivocal conclusions. Much of the published work utilises computer modelling techniques (Vaughn *et al* 2000 and 2001, Liu 2002, Sakai *et al* 2008) which are based on assumptions that may lead to inaccuracies in results and conclusions obtained. Using the model oxygenator circuit, resistance of the RBC to DNO can be directly measured and assessed in a simulated, continuously running circuit. Experimental design can be varied by haemolysis or addition of free Hb (such as a haemoglobin-based-oxygen-carrier) to determine the role of the RBC membrane, RBC interior and the RBC surroundings in providing resistance to DNO. This novel approach will contribute to the battery of equivocal results in determining the role of the RBC in resistance to DNO.

1.5 Haemoglobin-Based-Oxygen-Carriers (HBOC) and Oxyglobin

'Oxygen therapeutics' is used to describe a transfusion fluid that mimics human blood's oxygen transport ability. Oxygen therapeutics is sub-classified into two categories based on the mode of oxygen transportation. Perfluorocarbon (PFC) based oxygen therapeutics are short term man-made emulsions that carry oxygen, and haemoglobin-based-oxygen-carriers (HBOCs) are made of modified haemoglobins. In this work, the only commercially available oxygen therapeutic (Oxyglobin) was used, an HBOC which would

facilitate comparison to blood being haem based. Literature review was solely focused on HBOCs. Oxyglobin was to be added to the circuit blood to determine if free haemoglobin enhances DNO, while establishing RBC resistance to DNO.

1.5.1 What are HBOCs?

HBOCs are extracted haemoglobin (Hb) in solution that has the ability to transport oxygen to the tissues. HBOCs were developed as an alternative to donated packed red blood cells with lengthy shelf-life (up to 36 months compared to RBC 42 days) and ambient storage conditions, benefitting pre-hospital and operational theatre survival. Development of HBOCs could lead to a sustainable, infection free blood source used in circumstances where blood is not readily available, or where blood transfusion poses a serious infection risk. In some parts of the world, donated blood carries high risk of disease transmission i.e. many countries in sub-Saharan Africa have an adult HIV-positive prevalence of up to 30%. Estimates suggest that at least 25% of transfused blood in Africa is not screened leading to a high HIV transmission rate (Jenkins 2007). The allogenic nature of Hb would eradicate the need for meticulous blood grouping and the associated mortality and morbidity risk. The small size of Hb compared to RBCs allows oxygenated blood to travel through capillaries where RBCs cannot pass thus theoretically increasing tissue perfusion and oxygen availability in ischaemic areas.

Hb is a tetrameric structure comprising two alpha and two beta polypeptide chains each bound to a haem unit. Each unit of haem can bind one molecule of oxygen. As each oxygen molecule is bound to a haem unit, the tetramer undergoes conformational change increasing affinity for the next oxygen molecule. The sources of Hb used to create HBOCs include human, bovine and swine. Alternative recombinant production has yielded Hb cultured from bacteria (*Escherichia Coli*), yeast (*Saccharomyces cerevisiae*), tobacco

plant (*Nicotiana tabacum*) or sea lugworm sources (*Arenicola marina*) (Standl 2004, Lowe 2006 and Clark 2007). Extracted Hb is modified to produce oxygen carrier molecules with desirable characteristics such as altered oxygen affinity and increased intravascular shelf-life.

The initial extracted Hb undergoes an extensive modification process to enable the HBOC to have desirable characteristics (Figure 1.2). Stroma free Hb has demonstrated a high affinity for oxygen with poor offloading in the tissues, due to loss of 2,3-DPG and dissociation of the Hb tetramer into diamers. The dissociated α and β chains are readily excreted by the kidneys reducing intravascular half-life. To compare, the P_{50} of whole blood is 26.5mmHg but in 2, 3-DPG depleted stroma free Hb the P_{50} is 12-14mmHg (Grethlein *et al* 2007). To minimise renal excretion of Hb, researchers cross-link the α or β chains with covalent bonding which stabilises the haem tetramer unit e.g. diaspirin connection. Hb tetramer stabilisation also increases the P_{50}. Examples of cross-linked HBOCs are Hemolink and HemAssist. Another technique of chemically modifying the Hb at the 2, 3-DPG site can also increase the P_{50} (Chen *et al* 2009).

Poor intravascular half-life of HBOCs can be further improved by increasing the molecular size of the covalently bonded Hb tetramer by conjugation techniques. Hb is conjugated with a biocompatible polymer such as dextran, polyethylene glycol or gluteraldehyde, increasing the molecular weight e.g. Hemospan. Alternatively, linking the individual covalently bonded Hb tetramers creates polymerized Hb of greater molecular weights. Four or five Hb tetramers can be polymerised with substances such as gluteraldehyde e.g. PolyHeme, Hemopure, Oxyglobin and Oxyvita.

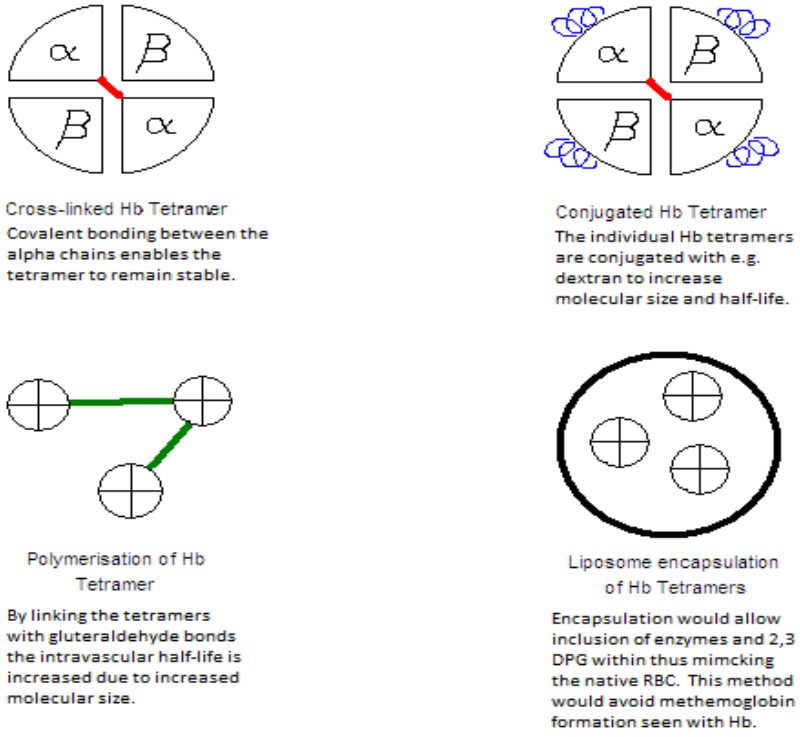

Figure 1.2 Schematic diagrams of HBOC production processes (Brown University 2005). Cross-linking provides stabilisation of the Hb tetramer from dissociation to diamers. Conjugation of the stabilised tetramer increases molecular size and intravascular life. Similarly, polymerisation of several Hb tetramers further increases molecular size. Encapsulation would be the ultimate HBOC process.

The ultimate HBOC method would involve Hb encapsulation recreating the natural membrane characteristics of native RBCs. 2, 3-DPG and reduction enzymes could be added to manipulate oxygen affinity and delay oxidation of the Hb to methaemoglobin. This methodology is likely to have a good intravascular half-life.

1.5.2 Brief history of HBOCs

In 1916, Wilson Sellards and George Minot first attempted blood transfusion giving Hb in saline to anaemic patients but they developed nephrotoxicity due to transfusion impurities (Lowe 2006 and Clark 2007). World War II stimulated Amberson *et al* (1949) to administer bovine Hb solution to animals and a human Hb solution to a postpartum

haemorrhage patient who subsequently died of renal complications. This approach was abandoned with workers believing that RBC stroma deposits in the renal tubules and free Hb causes vasoconstriction, resulting in reduced renal blood flow, renal failure and hypertension. Rabiner *et al* (1967) demonstrated that stroma-free Hb had no renal effects when infused into dogs.

Diseases such as Human-Immunodeficiency-Virus (HIV) in 1985 and Creutzfeldt-Jakob-Disease (CJD) have added enormous interest into blood substitutes. In 1985, the US military and Baxter Healthcare Corp created the HBOC HemAssist. Baxter Healthcare Corp continued with the first HBOC clinical trials (Chen *et al* 2009) despite animal study results being discouraging. The phase III clinical trials were suspended in 1998 due to increased predicted mortality rates in trauma patients receiving HemAssist. Baxter Healthcare Corp is now developing Optro.

In 1998 FDA, and in 1999 EU, approval was granted for Biopure's Oxyglobin for treatment of anaemia in dogs. In 2001, approval was granted from South Africa's Medical Control Council (MCC) for Hemopure (Biopure Corp) use solely for anaemic surgical patients since the HIV infection rate amongst the general population and hence donated blood was high. However, evidence against the use of blood substitutes including Hemopure (Natanson *et al* 2008) halted use of Hemopure by the MCC. In 2009, Biopure Corporation ceased operation and sold remaining Oxyglobin stocks to its distributors.

Sangart was founded in 1998 to develop MP4OX (Hemospan). Phase II and III trials continue (2002-2010) with expected US Navy collaboration.

PolyHeme ™ (Northfield Laboratories) followed the Vietnam War for use in trauma and has been studied in a hospital based trauma trial (Gould *et al* 2002) and a multicentre pre-hospital phase III trauma trial (http://www.northfieldlabs.com/polyheme.html accessed 29th March 2010). A phase II multicentre pre-hospital trauma trial completed in June 2006 was surrounded by controversy over the patient selection. The unpublished results showed unfavourable survival in the PolyHeme group compared to usual resuscitation (13.4% vs. 9.3%). Following removal of participants falling outside protocol requirements, the data was published showing 11.1% mortality in the PolyHeme group with an increased risk of myocardial infarction (3% vs. 1% control) (Moore *et al* 2009). In 2009, the FDA denied approval of PolyHeme due to the associated risks prompting Northfield Laboratories to close.

OxyVita Inc was formed in 2003, producing a new generation of polymerised haemoglobin (OxyVita ®) reported by the company not to elicit the vasoactivity seen with other HBOCs. Being available as a powder formulation allows reconstitution in remote situations. These products are in the preclinical testing phase (www.oxyvita.us accessed 14th May 2010).

To date no HBOC has achieved FDA approval for human clinical use due to complications (pulmonary and vascular hypertension, gastrointestinal disturbances) and increased incidences of MI and strokes. Safety and efficacy guidelines were drafted by the FDA (FDA, 2004) for future HBOC testing. Research continues to identify the mechanism of these complications and thus develop HBOCs.

1.5.3 Current Clinical Situation and Problems Limiting Their Use

Several HBOCs have progressed to phase II and III clinical trials; HemAssist, Hemolink, Hemospan, Hemopure and PolyHeme have published trials. HemAssist, Hemolink, Hemopure and PolyHeme have since been abandoned but Hemospan was undergoing trials during 2010 (www.sangart.com/newsroom accessed 8th December 2010). No approval for clinical use has been obtained from the FDA to date.

Review of the phase II and III trials have shown an increased risk of MI and death associated with HBOC use (Natanson *et al* 2008). The study reviewed trials encompassing the HBOCs Hemolink, PolyHeme, HemAssist, Hemopure and Hemospan in surgical, trauma or stroke patients. All HBOCs have had incidences of MI or mortality in study groups compared to controls. Despite the high risk patient selection, HBOCs contributed to detrimental outcomes with a stated 30 % increase in overall mortality and a 2.7 fold increase in MI (Natanson *et al* 2008) however the data reviewed was limited by the availability of publications. This publication was associated with withdrawal of HBOC trials as the risks of MI and mortality raised concerns over enlisting low risk patients to studies.

The mechanism for HBOC associated MI or stroke has been linked to HBOC related vasoconstriction. Yu *et al* (2009) suggested that coronary vasoconstriction reduces myocardial blood supply resulting in MI. HBOC transfused patients have reported gastrointestinal side effects, abdominal and chest pain which was linked to vasoconstriction (Winslow 2003). Two principle mechanisms for causing vasoconstriction have been cited; nitric oxide (NO) scavenging or increased oxygen delivery.

NO scavenging occurs when the HBOC binds endothelial nitric oxide, a natural vasodilator (Irwin *et al* 2008). It is hypothesised that HBOCs have a high affinity for NO which determines the hypertensive effect (Doherty *et al* 1998, Olson *et al* 2004). Tetrameric Hb can extravasate through the vasculature where it scavenges NO from smooth muscle cells (Tsai *et al* 2006). Low molecular weight HBOCs have resulted in vasoconstriction regardless of oxygen affinity supporting extravasation (Hare *et al* 2006). Increased molecular size could reduce extravasation of the HBOC (Tsai *et al* 2006, Baudin-Creuza *et al* 2008, Hu and Kluger 2008). To further support NO scavenging, Doherty *et al* (1998) synthesized recombinant haemoglobin with genetic alteration of the haem pockets which showed reduced affinity for NO. Mice deficient in the enzyme NO synthase did not exhibit hypertension when transfused with HBOC compared to normal mice (Yu *et al* 2009). Infusion of sodium nitrite, a metabolite of NO, can block the vasoconstrictive effects exerted by HBOC transfusion (Yu *et al* 2009, Arnaud *et al* 2010). Inspired NO treatment prior to or during HBOC administration can reduce vasoconstrictive effects in mice and lambs (Yu *et al* 2008, Yu *et al* 2009). Research by Yu *et al* has given a convincing argument to support NO scavenging as the cause of HBOC related vasoconstriction. Secondary to NO scavenging are two other theories. Desaturated RBCs release ATP (vasodilator mediator) simulating NO production but HBOC release of O_2 results in less RBC desaturation with reduced ATP release and increased vasoconstriction (Cole *et al* 2009). Their study associated ATP release to the oxygen affinity of HBOCs. Alternatively, haemoglobin reduces nitrite to NO which compensates for reduced endogenous NO vasodilation in hypoxia but HBOC replacement of RBC will limit this secondary NO production (Gladwin *et al* 2009).

The alternative theory for HBOC induced vasoconstriction involves elevated oxygen arteriolar partial pressures which stimulate autoregulation resulting in arteriolar

vasoconstriction (Winslow 2003, Cole *et al* 2008). RBC travel centrally within the vessel lumen creating a boundary effect for O_2 transfer whereas the small size of HBOCs increases O_2 release nearer the vessel wall. This coupled with a weak affinity for oxygen i.e. an elevated HBOC P_{50}, results in hyperoxaemia resulting in autoregulatory responses. HBOCs with low P_{50} and increased molecular weight are beneficial in reducing O_2 delivery (Rohlfs *et al* 1998, Winslow *et al* 1998, McCarthy *et al* 2001, Tsai *et al* 2003, Cole *et al* 2007). Newer generation HBOCs processed with low P_{50} values shift the ODC leftwards, decreasing oxygen offloading thus targeting ischaemic tissue oxygenation (Hemospan and PolyHeme). Sangart (Hemospan) claim that their product is not vasoactive (Vandegriff *et al* 2003, Winslow *et al* 2005). PolyHeme was associated with pulmonary hypertension with resultant reduction in cardiac output (Yu *et al* 2010) and increased risk of MI in clinical trials (Moore *et al* 2009). Natanson's study (2008) incorporated data from HBOCs with varying P_{50} (Hemospan and PolyHeme having lower P_{50} and Hemopure, Hemolink and HemAssist having higher P_{50}) indicating that P_{50} does not influence HBOC vasoconstriction, casting doubt on this theory.

Current research favours NO scavenging theories for HBOC related vasoconstriction. HBOCs are essentially free Hb, so the NO scavenging potential coincides with the debate that RBC integrity provides resistance to D_LNO. HBOCs are thought to scavenge NO from the vasculature or by extravasation of the vessel wall, manifesting as vasoconstriction, yet the affinity of an HBOC to bind NO has not been quantified. Contrastingly, in D_LNO research, RBC integrity appears to provide resistance to DNO, but the mechanism has not been established. The two areas of research, blood substitutes and D_LNO, are dissimilar yet the debate regarding RBC/Hb binding NO has implications in both areas. Development of HBOCs may provide a better understanding of RBC integrity in D_LNO.

Yu *et al* (2008, 2009) described the use of inhaled NO prior to HBOC administration to offset vasoactivity. Therapeutic NO is limited in cardiopulmonary bypass during cardiothoracic surgery as the lungs are deflated. NO administration would be via the membrane oxygenator within the cardiopulmonary bypass circuit. HBOCs remain structurally stable and efficacious for oxygen delivery during extracorporeal circulation for 5 hr at 2 l/min flow (Neya *et al* 1998). For this research, NO transfer across a membrane oxygenator within an experimental circuit was investigated and the NO binding potential of a HBOC (Oxyglobin) assessed. Concurrently, RBC resistance to DNO was investigated via Oxyglobin addition to the circuit blood. The impact of NO and Oxyglobin on oxygen transfer including the ODC were investigated. No previous study quantifies NO uptake by an HBOC or explores the impact of NO and HBOC on the ODC. Oxyglobin was the only licensed HBOC at the time of the experimental phase, licensed for canine use allowing direct comparison of this work to that completed with dogs in collaboration with this research.

Table 1.1 HBOC information Summary

This table details the HBOC manufacturers and their products, with information on the manufacturing process, oxygen affinity, half-life and shelf-life. Lastly, the clinical trials conducted and the status of the HBOC at the end of 2010 has been included.

Product	Company	HBOC type	P_{50}	t½	Shelf-life	Clinical Trials	Status
PolyHeme	Northfield USA	Pyridoxylate Polymerized human Hb	20-22 mmHg	24 hr	18 months refrigerated	II and III	Abandon
Hemopure	Biopure, USA	Polymerized bovine Hb	40 mmHg	19 hr	≥36 months refrigerated or room temperature	II and III License for SA, 2001 to 2008	Abandon
Oxyglobin (canine)	Biopure, USA	Polymerised bovine Hb	34 mmHg	30-40 hr	36 months refrigerated or room temperature	License for anaemic dogs, 1998 to date	Stock sold off
Hemolink	Hemosol, USA	O-raffinose cross-linked Human Hb	34 mmHg	18 hr	≥12 months refrigerated	II and III	Abandon
Hemospan	Sangart, USA	Conjugated Human Hb	5-6 mmHg	24-36 hr		I and II	Ongoing
Optro ™	Baxter Healthcare Corp	Cross-linked human Hb genetically modified from *E.Coli*		2-19 hr	18 months refrigerated	II and III	Ongoing
OxyVita®	OxyVita, USA	Polymerised bovine Hb	Low P_{50}	≥10 hr	12 months room temperature or estimated 10 years frozen	Pre-clinical trials	Ongoing
HemAssist	Baxter Healthcare corp	Cross-linked human Hb	32mm Hg	6-12 hr	≥12 months refrigerated	II and III	Abandon

Sources: Stollings and Oyen 2006, Oxyglobin licence data (2006). Lowe 2006, Chen *et al* 2009. Company website press releases.

1.6 Aims and Objectives of the Thesis

The aim of this research was to design a compact, continuously running membrane oxygenator circuit for evaluation of gas diffusion theories. The circuit would comprise commercially available membrane oxygenators, PVC tubing and equine blood to allow reproducibility by this or other groups. The circuit would undergo a battery of experiments designed to validate the circuit and to provide baseline data and trends. The circuit would be used for the following gas transfer experiments.

- The circuit would be used to investigate the effects of Isoflurane on oxygen transfer in the membrane oxygenator. Clinically, Isoflurane anaesthetic is administered via the membrane oxygenator of cardiopulmonary bypass circuits against the advice of the manufacturers. There is little data on the effects of Isoflurane on gas transfer in the device.
- The effects of red cell integrity on nitric oxide transfer would be investigated in this circuit. The red cell may provide resistance to nitric oxide transfer which is important for lung function tests using nitric oxide. Experimental design incorporates haemolysis and haemoglobin-based-oxygen-carrier (HBOC) addition to test the impact of red cell integrity on nitric oxide transfer.
- The nitric oxide scavenging potential of the HBOC Oxyglobin would be assessed in this circuit. HBOC transfusion results in vasoconstriction which has been associated with endothelial nitric oxide scavenging. This study sought to quantify this scavenging potential.

Ethics approval was granted by ARU Research and Ethics Sub-Committee and Papworth Hospital Research and Development, as the protocol was deemed to have no material ethical issues.

Chapter 2: Data Handling

2.1 ODC Data Conversion to Hills Plot

The Hills plot was used to transform the sigmoid curve of the ODC to a straight line plot (linearised) with the ability to test for an observed deviation in the ODC from the calculation of the P_{50} (Hill 1910). For the Hills plot log PO_2 was calculated (x axis) and plotted against saturation in the form log (S/1-S) (y axis).

$$logPvO_2 = \log(PvO_2)$$

$$\log PaO_2 = \log(PaO_2)$$

$$SvO_2\left(\frac{S}{1-S}\right) = \log\left(\left(\frac{SvO_2}{100}\right) \div \left(\frac{1-SvO_2}{100}\right)\right)$$

$$SaO_2\left(\frac{S}{1-S}\right) = \log\left(\left(\frac{SaO_2}{100}\right) \div \left(\frac{1-SaO_2}{100}\right)\right)$$

P_{50} can be calculated from the intercept and slope of the Hills plot linear trend line for each group i.e. Isoflurane versus no Isoflurane, using the following equation.

$$P_{50} = antilog\ (\frac{Intercept}{Slope})$$

2.2 Statistical Analysis

The data was computed and calculations made via Microsoft Excel Spreadsheet (Microsoft Office 2007 software). The Excel spreadsheet data was imported into SPSS software v.16.0 for statistical analysis. Where quoted, the means have been presented with standard deviations (±SD) which will have included inter-run variation with donor blood and membrane tolerances, unless stated.

Linear correlations were analysed using linear regression with R^2 values and statistical significance reported. Curvilinear correlations have been analysed using Spearman test for non-parametric data or Pearson test for parametric data with *r* and p values quoted. Mean comparison statistics were carried out using the independent *t* test with *t* and p values presented. Data summary tables present 'statistical values' as R^2, *r* or *t*, corresponding to linear regression, curvilinear correlation or means comparison tests, as appropriate.

Effects of an experimental group on the ODC compared to the control blood was statistically analysed by first converting the data to a Hills plot (section 2.1). From this linear data a *t* test could be performed to analyse for shift changes in the presence of the experimental treatment compared to the control.

Statistical significance was achieved when the alpha level was ≤ 0.05. Specific p=values have been quoted unless p=0.000. In this instance the p value has been classified as $p<0.001$ or $p<0.0001$ to verify the level of significance.

Chapter 3: Circuit Design and Validation

Aims

To devise a compact *in vitro* continuously running experimental circuit that replicates the arterial and venous blood circulation oxygen and carbon dioxide tensions using commercially available components. To run a battery of tests with varying parameters i.e. varying blood flow, gas flow, haematocrit, to provide baseline data and trends for this circuit. Subsequently, the circuit could be used for exploring gas transfer hypotheses.

3.1 Setting Up the Circuit Design

The circuit comprises two membrane oxygenators, one acting as the 'lungs' (termed oxygenator) and the other as the 'tissues' (termed deoxygenator). Blood is continuously pumped around the two devices via PVC tubing passing through a positive displacement roller pump (Stockert, Sorin Group, Milano, Italy) that compresses the tubing forcing forward blood flow. Gas transfer occurs via passive diffusion through the microporous membrane down the partial pressure gradients. To create arterialised blood the oxygenator is ventilated with oxygen in balanced nitrogen. Oxygen in the gas will passively diffuse across the membrane oxygenating the blood to arterial parameters as it passes through the device. The oxygenator gas, devoid of carbon dioxide, is set at an adequate flow rate (5 l/min determined in pilot test) in order for carbon dioxide to diffuse from the blood across the membrane into the ventilating gas. These processes occur simultaneously within the oxygenator unit. The deoxygenator unit ventilating gas comprises carbon dioxide in balanced nitrogen utilising the same principles as the oxygenator. Carbon dioxide within the ventilating gas passes across the membrane

entering the blood to create venous blood carbon dioxide tensions. The deoxygenator gas, devoid of oxygen, is set at an adequate flow rate (5 l/min determined in pilot test) for oxygen to diffuse from the blood across the membrane into the ventilating gas. In order to complete the experimental protocol extra gases were added to the oxygenator ventilating gas. Nitric oxide (NO), carbon monoxide (CO) and the inhaled anaesthetic Isoflurane were added as appropriate.

3.1.1 Basic Circuit Set-Up

The circuit described is based on the standard adult cardiopulmonary bypass circuit where one membrane oxygenator takes over from the lungs and the pump replaces cardiac function. The deoxygenator in this circuit replaces the patient who ordinarily would be the generator of venous blood. All lines were kept very short to aid the compactness of the circuit and to reduce the blood volume needed to run the circuit. Monitors and analysers used for blood gas analysis, blood saturations and gas oxygen concentrations are all equipment used clinically.

All hardware and disposables listed in Appendix 1 were required for this circuit set-up. PVC tubing can be cut with sterile scissors or a sterile blade using aseptic techniques.

On both of the Cobe Duo Oxygenators with integral hardshell reservoirs (Sorin Group, Milano, Italy) the loose Luer Lock connections were tightened. The ¼" red lockable cap by the oxygenator outlet port was closed. To one of the Cobe Duo membrane oxygenators with integral reservoir (designated 'deoxygenator' and 'venous reservoir') a length of the ⅜" PVC tubing was attached to the outlet port of the reservoir (located at the bottom). The ⅜" PVC tubing was directed through the Stockert pump raceway checking for correct direction of blood flow. This ⅜" PVC tubing exiting from the Stockert pump outlet was

fed downwards towards the second Cobe Duo membrane oxygenator (designated ‘oxygenator’) and attached to the oxygenator inlet port (top burgundy cap) (Figure 3.1). As the circuit only comprised one reservoir, the additional reservoir was removed as it was surplus, however the recirculation line from the oxygenator needed to be reattached to the venous reservoir. The ⅜” PVC tubing between the Stockert pump outlet and the oxygenator inlet was cut centrally and a ⅜” x ⅜” connector with Luer Lock was used to reconnect this tubing. A pressure dome was screwed on to this Luer Lock (Figure 3.2). Another length of ⅜” PVC tubing was attached to the ‘oxygenator’ outlet port (lower red cap) and cut to length before the other end was attached to the ‘deoxygenator’ inlet port (upper burgundy cap) (Figure 3.3). This short section of tubing between the oxygenator and the deoxygenator was cut centrally and a ⅜” Cobe Sat/Hct Sensor connector was inserted into the tubing (Figure 3.4). Further ⅜” PVC tubing was connected to the ‘deoxygenator’ outlet port (lower red cap) and directed half way up towards the central inlet port located on top of the venous reservoir. A ⅜” x ½” Luer Lock connector was attached onto the end of the ⅜” PVC tubing (that had been cut to length) with a section of ½” PVC tubing from the connector following through to attach to the venous reservoir central inlet port (Figure 3.5). Calibrated CDI 500 sensors were screwed onto the purge lines from both the deoxygenator and the oxygenator before returning to the venous reservoir. The ‘arterial’ Cobe Sat/Hct sensor cable was connected to the ⅜” Cobe Sat/Hct Sensor connector between the oxygenator and the deoxygenator. The ‘venous’ Cobe Sat/Hct sensor cable was connected to the port on the venous reservoir inlet connection (Figure 3.6). The Spectrum Medical M2 ‘arterial’ wrap-around sensor was placed on the tubing between the oxygenator and the deoxygenator and the ‘venous’ wrap-around sensor was located on the deoxygenator outlet tubing.

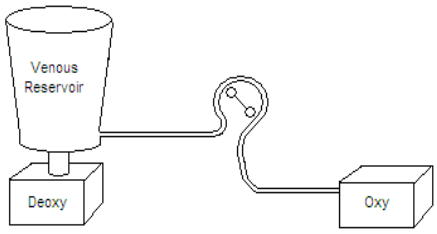

Figure 3.1

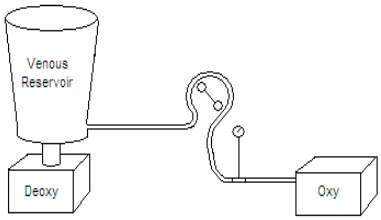

Figure 3.2

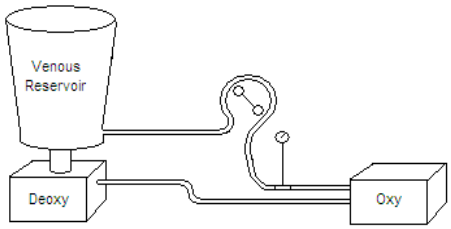

Figure 3.3

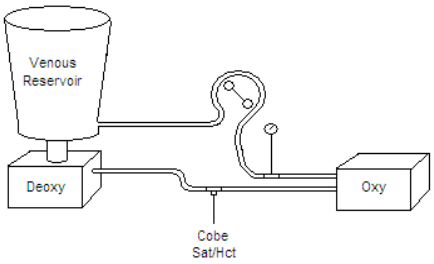

Figure 3.4

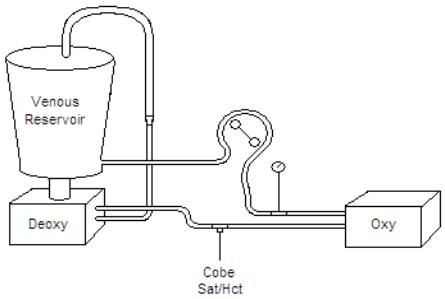

Figure 3.5

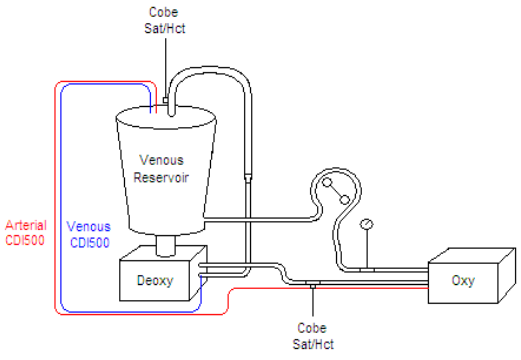

Figure 3.6

Figures 3.1 to 3.6 Step-By-Step Schematic Representation of the Basic Circuit Set-up.

Finally a fluid administration line was added to one of the Luer Lock connections on the top of the reservoir and another one was screwed onto the ⅜" X ½" Luer Lock connector. This completed the basic circuit set-up.

The ventilating gas tubing needed to be assembled using a series of ¼"x ¼" Luer Lock, ¼" Y connectors and some ¼" tubing. For the oxygenator a Y section of ¼" tubing was attached to the two gas inlet ports on the device. A long length of ¼" tubing was cut close to the device to incorporate a ¼"x ¼" Luer Lock connector allowing for gas sampling. The ¼" tubing was cut further along to facilitate the anaesthetic vaporiser manifold (Isotec 3, Datex-Ohmeda GE Healthcare, Chalfont Saint Giles, UK). The final section of ¼" tubing was divided using a series of ¼" Y connectors and ¼" tubing to attach to the individual air, O_2, N_2, CO and NO regulators (Figure 3.7).

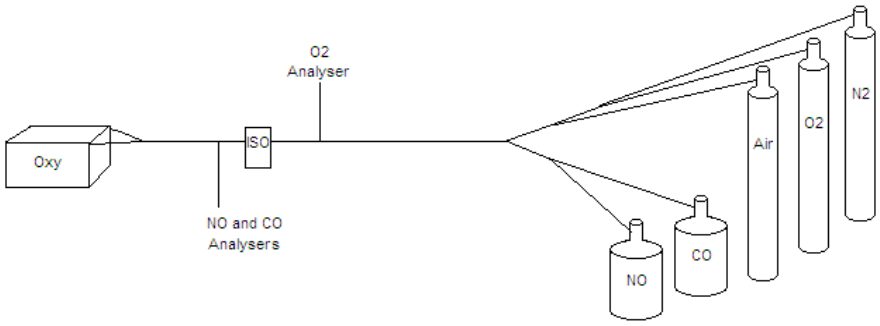

Figure 3.7 Schematic Diagram of the Oxygenator Gas Inlet Tubing.

Finally the oxygenator gas line was cut upstream of the anaesthetic regulator to accommodate the Teledyne AX300 O_2 sensor. The deoxygenator gas line was made in a similar way to the oxygenator line, with a gas sampling port made from a ¼" x ¼" Luer Lock connector and connection to 5% CO_2 in balanced N_2, CO_2 and N_2 regulators utilising a series of ¼" Y connectors. For both oxygenator and deoxygenator, separate scavenging

tubing were made using ⅜” tubing and a ⅜” Y connector to allow passive removal of the exhaust gases to a safe atmosphere. Gas sampling of the exhaust gases was facilitated by inserting a ⅜” x ⅜” Luer Lock connector into each of the exhaust lines close to the individual devices. The oxygenator exhaust tubing was additionally cut near to the device to integrate a second Teledyne AX300 O_2 sensor.

The Medtronic heater/cooler unit (Medtronic, Minneapolis USA) outlet water pipe was pushed onto the heat exchanger inlet of the deoxygenator. The heater/cooler inlet water pipe was attached to the deoxygenator heat exchanger outlet. The water lines were unclamped and the heater/cooler switched to run, visually checking for a watertight connection. The heater/cooler temperature was adjusted to 37 ˚C and the heater enabled. During the experiments the circulating blood temperature was monitored via CDI 500 sensors and the heater/cooler adjusted, if necessary, to maintain a circuit temperature of 37 ˚C.

3.1.2 Priming the Circuit

The term ‘prime’ is used to describe the addition of physiological fluid (priming fluid) to the circuit in order to displace air.

Two litres of 0.9% sodium chloride (NaCl) was administered into the venous reservoir via the fluid administration line attached to the top. One emptied 0.9% NaCl bag was placed onto the other fluid administration line with it clamped off. The second emptied 0.9% NaCl bag was kept for later use. The Stockert pump was set to a low flow (1 l/min flow rate) in order to control the de-airing process. As fluid moved through the circuit the tubing was tapped with a clamp to dislodge bubbles. Where a connector had been cut into the tubing it was gently manipulated to work the tubing further over the connector creating

a firm connection. A 30ml syringe was pushed onto the end of the pressure dome and by gently using the plunger of the syringe, air from inside the dome was expelled. Once visually de-aired the syringe was used to set the inner dome membrane to the middle. The syringe was removed and the dome attached to a pressure gauge. The circuit tubing was checked for air by following the flow pathway into the oxygenator, tapping the tubing and device to remove air via the purge line. The connections between the oxygenator and the deoxygenator were checked for tightness and air bubbles trapped on the connector edges were dislodged. The deoxygenator was de-aired by allowing expelled air to be vented through the purge line. Finally the return line from the deoxygenator through to the venous reservoir was de-aired. The pump flow was then turned up to 4 l/min to de-air the circuit under pressure (<300mmHg). Once air was no longer seen exiting the oxygenator and deoxygenator purge lines these lines were closed off. The pump flow was then switched off.

The experiments that were run with equine blood in the circuit were initially primed with 0.9% NaCl for ease of de-airing. Clinical experience has highlighted that priming with whole blood makes de-airing difficult as blood is prone to frothing. Once the circuit was fully primed with 0.9% NaCl, blood was added by displacement of the prime fluid. The PVC tubing between the deoxygenator and the venous reservoir above the fluid administration line was clamped. This fluid administration line was opened and the pump turned on slowly to gently pump prime fluid into the bag until the reservoir level reached minimum (i.e. 50ml). The pump was stopped. Two litres of equine blood was added to the reservoir via the administration line on top of the reservoir. Once the blood was added, the pump was set on a slow flow to continue filling the fluid bag with prime until blood was seen entering the bag. During this process the bag filled before blood was seen so the pump was stopped in order to replace the bag with the second empty 0.9% NaCl

fluid bag. The procedure was continued until blood was seen entering the bag at which point the pump was stopped and the fluid administration line clamped off. If there was less than 300ml of blood in the reservoir, additional fluid (equine blood or 0.9% NaCl) was added. Finally, the clamp from the PVC tubing above the fluid administration line was removed and the pump restarted at a high flow (4 l/min) to allow mixing of the blood. The circuit was recirculated for five minutes with the CDI 500 sensor lines open to allow the CDI 500 analyser to reach equilibrium. Gases for both the deoxygenator and oxygenator were switched on, tailoring the settings until optimum blood gas parameters were seen on the CDI 500 monitor. Typical oxygenator gas settings were 5 l/min of air with 0.3 l/min oxygen resulting in an approximate FiO_2 26%. For the deoxygenator approximately 5l/min 5% CO_2 in N_2 with 0.2 l/min CO_2 was used. (Figure 3.8)

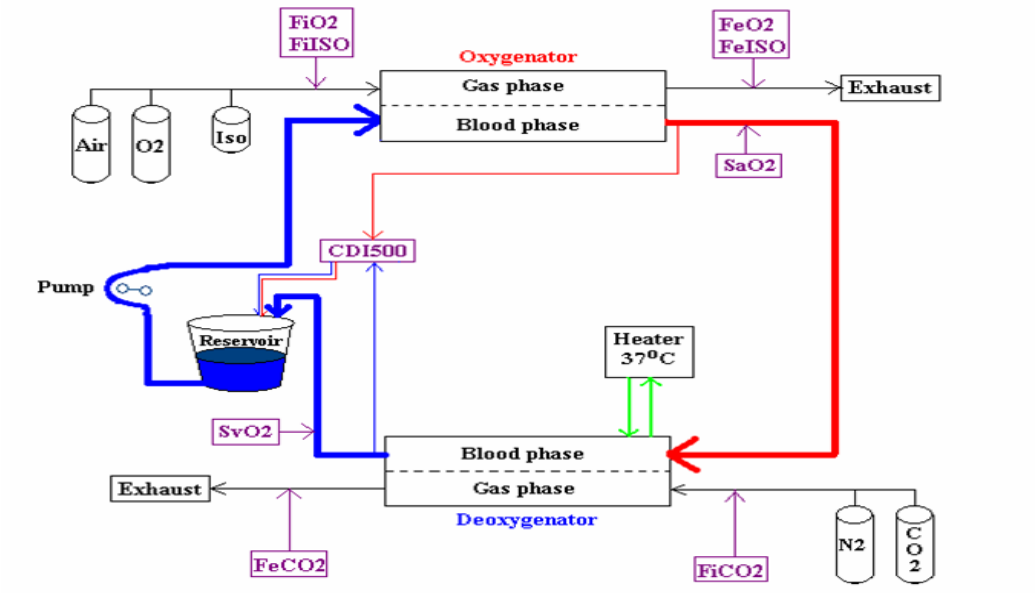

Figure 3.8 Schematic Diagram of the Circuit Blood and Gas Phases

3.1.3 Gas Mixtures

All gases were obtained from British Oxygen, Manchester, UK. For the oxygenator, stock cylinders of air and oxygen were connected via Y gas tubing to produce a FiO_2 24-26% to

achieve normoxic blood gas parameters. For experiments where the FiO_2 was varied, stock cylinders of oxygen and nitrogen were connected to the oxygenator gas lines. Stock cylinders of NO (1000ppm) in nitrogen and CO (0.3%) in oxygen (19%) and Helium (11%) were also connected to the oxygenator gas lines. In the initial experiments this was via a therapeutic NO mixing device (Nomius 305, MTA Sahlgrewska, Goteburg, Sweden and Bronkhorst Hi Tech, 7261 AK Ruurlo, Netherlands). The mixing device was set to give 5ppm of NO and 0.02% of CO and this gas was further diluted by the oxygenator gas mix as the CO and NO was added to the oxygenator gas line via a side arm downstream. In later experiments the NO and CO gases were connected into the oxygenator gas line via individual calibrated rotameters and the gases adjusted according to the inlet concentrations required.

The volatile anaesthetic agent Isoflurane (Abbott Laboratories Ltd, Maidenhead, UK) was delivered via a calibrated Isotec 3 vaporiser (Datex-Ohmeda GE Healthcare, Chalfont Saint Giles, UK) located in the oxygenator gas line.

For the deoxygenator a cylinder containing 5% CO_2 in N_2 and a stock cylinder of CO_2 were connected via Y gas tubing to provide adequate CO_2 concentration (8%) in order to achieve normocapnia. During the basic experiments where the test involved varying the $FiCO_2$, stock cylinders of CO_2 and N_2 were connected to the deoxygenator gas lines.

3.1.4 Blood

Commercially available defibrinated horse blood (TCS Biosciences, Buckingham, UK) was used within twenty-eight days of collection. No specification of gender or age was made for the preliminary experiments but was later specified as gelding age range 6-13 years. It was guaranteed free of haemolysis and adjusted by adding and withdrawing

serum to a constant haematocrit of between 40 to 50 % by the manufacturers. It was refrigerated at 4°C prior to use.

3.1.5 Equipment Details

Blood gas analysis was made using the CDI Blood Parameter Monitoring System 500, an in-line optical fluorometric analyser which requires a minimum blood flow rate of 35 ml/min (Terumo Cardiovascular Systems, Surrey, UK). The blood sample shunt lines exiting the oxygenator and the deoxygenator were each connected to a calibrated shunt sensor which continually monitored pH, PO_2, PCO_2 and K. The sensors used for each circuit were calibrated at the start of the session with manufacturer supplied calibration gases.

Haemoglobin, methaemoglobin and carboxyhaemoglobin concentrations were measured using a bench-top analyser Rapidlab 800 (Bayer, Berks, UK). This analyser was calibrated daily in accordance with the manufacturer's recommendations by a suitably trained member of hospital staff. Blood samples (1.5ml) were withdrawn from the oxygenator sample shunt line (used for the CDI 500 sensor) into heparinised syringes and either analysed immediately or kept refrigerated prior to analysis at the end of the experimental run. The concentration of methaemoglobin was less than 3% and carboxyhaemoglobin less than 7.5% in all experiments.

Blood oxygen saturation was determined by either the Cobe Sat/Hct analyser (Cobe Cardiovascular, Arvada, USA) or the Spectrum Medical M2 analyser (Spectrum Medical Ltd, Cheltenham, UK). Both of these devices automatically undertook an internal calibration run when switched on. The Cobe Sat/Hct utilises infrared spectroscopy to determine blood saturation whereas the newer Spectrum Medical M2 uses white light

technology. For the earlier work the Cobe Sat/Hct analyser was the available technology but for the later work the newer Spectrum Medical M2 was used in conjunction with the Cobe Sat/Hct analyser.

The gas analysis was performed by different analysers. Oxygen in the gas phase (FiO_2 and FeO_2 measurements) was initially analysed using the Datex digital oxygen meter (5120, Datex Ohmeda, Louisville 80027-9560 USA) calibrated with 19%, 21% and 100% oxygen, and later a medical oxygen analyser AX300 (Teledyne Analytical Instruments, Cambridge, UK) calibrated with 100% or 21% oxygen. The Teledyne AX300 was predominantly used due to its oxygen analysis range and sensitivity. For all oxygen sensors, volatile anaesthetic agents can interfere with oxygen readings. The manufacturers for the Teledyne AX300 quote a reading error of <1.5% in the presence of Isoflurane but that these performances meet or exceed the sensitivity requirements of ISO 7767: 1997 (E). The FiISO and FeISO were analysed using an in-built infrared analyser on the Datex anaesthetic monitor (Datex-Ohmeda, Hatfield, UK). CO_2, NO and CO were all analyzed using the chemiluminescent Logan LR 2000 analyser (Logan Research, Rochester, UK) to which a manufacturer custom-built CO analyser was bolted on in series "upstream."

Temperature, relative humidity and barometric pressure were recorded for each experimental session. The humidity of the oxygenator outlet was determined by wet and dry bulb thermometer (Met-check, Milton Keynes, UK). The barometric pressure was determined by the local weather station located at RAF Wittering.

3.2 Pilot Experiments With This Circuit Design

Aim

The focus of these initial experiments was to determine if a single oxygenator and a single deoxygenator were adequate to establish oxygenation and deoxygenation of the circulating equine blood. The literature review demonstrated that either several membrane units or a linked but separately operating deoxygenating circuit was required. The CDI 500 sensors were to be assessed for the time taken for equilibrium to be reached upon each experimental change to the circuit.

The venous reservoir to be used was a hardshell type with vent holes around the top to allow for volume expansion within the holding device. This allows blood to come into contact with air within the reservoir. A blood/air interface is a potential source of oxygen transfer which may influence the results obtained for oxygenator gas transfer. To determine the possible effects of a reservoir blood/air interface on gas transfer, a bypass loop was incorporated into the circuit allowing the venous reservoir to be bypassed. Data was collected for comparison with and without the venous reservoir.

3.2.1 Pilot Circuit Set-Up

The circuit was assembled as described previously (3.1.1) but an extra recirculation loop was integrated to allow circulation of the venous blood from the venous reservoir via a second stockert positive displacement pump to the deoxygenator (Figure 3.9).

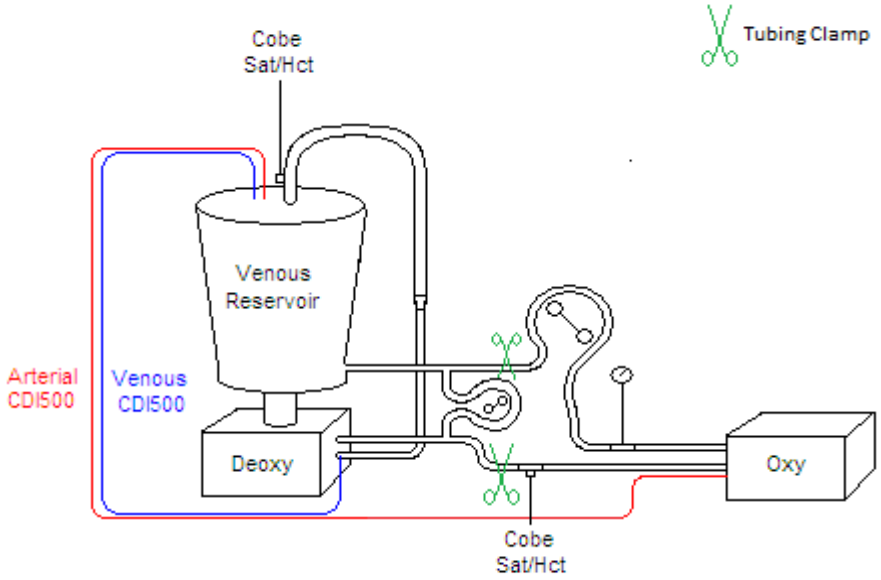

Figure 3.9 Schematic Diagram of the Venous Bypass Pumping Loop.

If a single deoxygenator was not efficient at deoxygenating the blood, there was a facility available for venous conditioning as per previous published works (Van Meurs *et al* 1991, Rais-Bahrami *et al* 1992, Vocelka *et al* 1993, Griffiths *et al* 1994, Gourlay and Taylor 1994, Beckley *et al* 1996, Matsuda and Sakai 2000, Maeda *et al* 2000, Kawahito *et al* 2001 and Motomura *et al* 2003). To facilitate this additional circuitry, two ⅜" Y connectors and an extra length of ⅜" tubing was required. The circuit was primed as described previously (3.1.2) with the exception that prime fluid was recirculated through the loop and the secondary pump left switched off so that fluid did not pass through the loop.

3.2.2 Pilot Methodology

1. Gas Flow Test

   The circuit pump was set at 2.5 l/min. The oxygenator received air (oxygen 21%). To determine the appropriate oxygenator gas flow for oxygenation of the blood, the flow was adjusted to 0.5, 1.0, 2.5 or 5.0 l/min of air. The deoxygenator received 5 l/min 5% CO_2 in balanced N_2.

2. CDI 500 Sensor Equilibration Test

   The blood flow rate was set at 2.5 l/min. The deoxygenator gas flow was 5l/min of 5% CO_2 in balanced N_2. The oxygenator gas flow was set from 0.5 l/min to 2.5l/min of air and the stopwatch started. The pH, PO_2 and PCO_2 values from the CDI 500 monitor for both venous and arterial blood were recorded at time 0, 1, 1.5, 2, 2.5, 3, 3.5, 4, 4.5 and 5 minutes to assess the equilibration duration.

3. Optimum Gas Settings

   To determine the optimal gas settings for both the oxygenator and the deoxygenator at a blood flow rate of 2.5 l/min, the standard gas was initially used for each device i.e. 5 l/min air (determined in the Gas Flow Test) for the oxygenator and 5 l/min 5% CO_2 in balanced N_2 for the deoxygenator. To these standard gases, oxygen was added to the oxygenator and carbon dioxide was added to the deoxygenator. The blood gas changes were recorded until optimum arterial and venous blood gas parameters were observed.

4. Open versus Closed Venous Reservoir

   A bypass loop was added between the deoxygenator outlet and the pump to bypass the venous reservoir. The closed reservoir test incorporated clamping the venous reservoir out and the circuit continuously run utilising the bypass loop. With the open reservoir test the bypass loop was clamped out allowing blood to pass through the reservoir with the blood/air interface. The blood flow was set at 2.5 l/min. The oxygenator gas flow was set to 5 l/min air with 0.3 l/min O_2 and the deoxygenator gas flow was set to 5 l/min 5% CO_2 in balanced N_2 with 0.2 l/min CO_2. The pH, PO_2 and PCO_2 values from the CDI 500 monitor for both venous and arterial blood were

recorded for the open reservoir and closed reservoir circuit so that gas transfer data could be compared.

3.2.3 Pilot Experimental Results

1. Gas Flow Test

With the blood flow set to 2.5 l/min the oxygenator gas flow required to adequately oxygenate the blood was 5 l/min (Table 3.1). This produced a PaO_2 81.00 mmHg with a $P\overline{v}O_2$ 34.50 mmHg. The deoxygenator gas flow of 5 l/min was sufficient to deoxygenate the blood. Due to the low $FiCO_2$ levels to the deoxygenator in this early experimental work it was not possible to determine the efficiency of the circuit with regards to CO_2.

Table 3.1 Preliminary Experimental Results for Optimal Oxygenator Gas Flows

Oxy Gas Flow l/min	pHa	pHv	PaO_2 mmHg	$P\overline{v}O_2$ mmHg
0.5	7.39	7.38	47.30	29.25
1.0	7.42	7.41	63.76	33.75
2.5	7.48	7.44	74.26	34.50
5.0	7.53	7.48	81.00	34.50

2. CDI 500 Sensor Equilibration Test

During the first 4.5 minutes, PaO_2 from the oxygenator outlet was seen to equilibrate from 47.25 mmHg to 70.50 mmHg after the air flow to the oxygenator was increased from 0.5 l/min to 2.5 l/min. The CDI 500 analyser specification indicates a response time of 24 seconds to display 90% of a step change in PO_2 so it is concluded that most of the equilibrium time was for the blood to stabilise rather than the sensors.

$P_{\bar{c}}O_2$ took only 3.5minutes to reach equilibrium from 36.58 mmHg to 45.94 mmHg. DO_2 mirrored this response time reaching 0.95 ml/min/mmHg. The rate of oxygen uptake remained at 93.10 ml/min throughout from time 0 onwards indicating an instantaneous gas change.

3. Optimum Gas Settings

The oxygenator and deoxygenator gas settings were adjusted until more physiological arterial and venous readings were achieved. The optimal oxygenator gas was 5 l/min air with 0.3 l/min O_2 and the optimal deoxygenator gas was 5 l/min 5% CO_2 in balanced N_2 with 0.2 l/min CO_2. The blood gases are presented in Table 3.2.

Table 3.2 Pilot Experimental Results for Optimum Gas Settings

	Arterial	Venous
pH	7.27-7.29	7.13-7.15
PO_2 mmHg	76-86	36-38
PCO_2 mmHg	35-37	59-62

4. Open versus Closed Venous Reservoir

There were no changes in pH, PO_2 or PCO_2 when the venous reservoir was clamped out compared to the presence of the blood/air interface within the reservoir. $\dot{M}O_2$ and DO_2 showed no difference between open or closed reservoir circuitry (Table 3.3).

Table 3.3 Pilot Experimental Results for Open and Closed Venous Reservoir

Reservoir	pHa	pHv	PaO_2 mmHg	$P\bar{V}O_2$ mmHg	$PaCO_2$ mmHg	$P\bar{V}CO_2$ mmHg	$\dot{M}O_2$ ml/min	DO_2 ml/min/mmHg
Open 1	7.28	7.14	81	38	37	62	148.32	1.11
Closed 1	7.28	7.15	83	39	36	60	119.61	0.88
Open 2	7.28	7.15	83	39	37	61	119.61	0.88
Closed 2	7.29	7.15	86	39	35	59	119.61	0.89
Open 3	7.27	7.13	76	36	36	62	110.41	0.83
Closed 3	7.28	7.14	78	37	36	60	110.41	0.84

3.2.4 Pilot Experimental Outcomes

For each experiment the CDI 500 sensors were left to equilibrate for 5 minutes prior to recording the monitor readings.

A deoxygenator gas flow of 5 l/min was efficient in deoxygenating 2.5 l/min blood flow so the additional venous conditioning loop was not required in this circuit design.

The optimal gas settings determined from the pilot test were set at the start of each experiment, i.e. 5 l/min air with 0.3 l/min O_2 for the oxygenator and 5 l/min 5% CO_2 in balanced N_2 with 0.2 l/min CO_2 for the deoxygenator. From these initial settings, gases may need some slight adjustment to accommodate for small variations in the donated blood and membrane efficiency. Actual oxygenator and deoxygenator gas settings used for each experiment were recorded and reported in the methodology.

The open and closed reservoir test indicated that the blood/air interface present within the hardshell venous reservoir had no impact on gas transfer. The circuit design retained the hardshell type venous reservoir as it adds flexibility with volume addition for varying Hb.

3.3 Basic Gas Transfer Properties of this Circuit Design: Methodology

To establish the gas transfer properties of this circuit, a series of basic experiments were conducted varying blood flow ($\dot{Q}$), oxygenator gas flow (F), oxygenator inspired oxygen (FiO_2), deoxygenator inspired carbon dioxide ($FiCO_2$) and haemoglobin concentration (Hb). The results of these experiments provided this model with baseline data. Each experiment was duplicated with a different circuit each time (denoted as run 1, run 2 etc). The methodology for these experiments may have been modified on subsequent runs in order to rectify any issues raised during the first run, as described under each experimental heading.

Each circuit was assembled and primed as previously described (3.1.1-3.1.2) for all but the varying Hb experiment. For the varying Hb experiment once the circuit was primed with 0.9% NaCl the test started with slow addition of equine blood to the circuit. The pH, PO_2 and PCO_2 values from the CDI 500 analyser for both venous and arterial blood were recorded for each experimental change after 5 minutes equilibration. The oxygenator inspired and expired oxygen content was also established.

3.3.1 Effects of Varying Blood Flow ($\dot{Q}$) and Surface Area (SA)

The oxygenator gas flow was 5 l/min air (run 1) or 5 l/min air with 0.2-0.4 l/min O_2 (runs 2 and 3). The deoxygenator gas flow was 5 l/min 5% CO_2 in balanced N_2 with addition of

0.2-0.4 l/min CO_2. The blood flow was randomly varied to include 0.1, 0.2, 0.5, 1.0, 2.0 and 2.5 l/min for one oxygenator cell and two oxygenator cells.

3.3.2 Effects of Varying Oxygenator Gas Flow (F)

The blood flow was set to 2.5 l/min. The deoxygenator gases were set to 5 l/min 5% CO_2 in balanced N_2 (run 1) or 5 l/min 5% CO_2 in balanced N_2 with 0.2 l/min CO_2 (run2). The oxygenator received varying flows of air at 0.5, 1.0, 2.5, 5.0, 7.5, 10.0, 12.5 and 15.0 l/min in a randomized order.

3.3.3 Effects of Varying Oxygenator FiO_2

The blood flow was set to 2.5 l/min. The deoxygenator gases were set to 5 l/min 5% CO_2 in balanced N_2 with 0.2 l/min CO_2. The oxygenator received 5 l/min of a mixture of air, N_2 and O_2 to provide a range of FiO_2 between 4.9% and 98% in a randomized order. For the hypoxic gas mixtures, N_2 was mixed with O_2 at the following l/min ratios; 4.0+1.0, 4.1+0.9, 4.2+0.8, 4.3+0.7, 4.4+0.6, 4.5+0.5, 4.6+0.4, 4.7+0.3, 4.8+0.2 and 4.9+0.1. For the hyperoxic gas mixtures, air and O_2 were mixed in the following l/min gas ratios; 0+5.0, 0.5+4.5, 1.0+4.0, 1.5+3.5, 2.0+3.0, 2.5+2.5, 3.0+2.0, 3.5+1.5, 4.0+1.0, 4.5+0.5 and 5.0+0.

3.3.4 Effects of Varying Deoxygenator $FiCO_2$

The blood flow was set to 2.5 l/min. The oxygenator gases were set to 5 l/min air with 0.1-0.3 l/min O_2. The deoxygenator received approximately 5 l/min (4.7-5.3 l/min) of a mixture of 5% CO_2 in balanced N_2, 100% CO_2 and N_2 to achieve $FiCO_2$ ranging between 1.78% and 23.82%. The deoxygenator inspired and expired carbon dioxide content was established for each change.

3.3.5 Effects of Varying Haemoglobin Concentration (Hb)

The circuit was primed with 0.9% NaCl. The pump flow was set to 2.5 l/min. The oxygenator gases were 5 l/min air (run 1) or 5 l/min air with 0.3 l/min O_2 (run 2 and 3). The deoxygenator gases were 5 l/min 5% CO_2 in balanced N_2 with 0.2 l/min CO_2.

For the first and second runs equine blood was held in a second reservoir with ⅜" tubing attached to the reservoir outlet directed through a second roller pump which pumped the blood into the top of the venous reservoir. The second roller pump was set to 60 ml/min to facilitate a slow increase in Hb concentration. The Hb achieved in runs 1 and 2 were 2.4-10.3 g/dl and 2.2-9.0 g/dl, respectively.

For the third run, equine blood was added in 25 ml aliquots via syringe into the top of the venous reservoir. This approach was utilised to achieve results at the lower Hb concentrations where data appeared to be incomplete from the first two runs. The Hb concentration range achieved was 0.26-2.29 g/dl.

At one minute intervals or five minutes after every aliquot of equine blood data was recorded.

3.3.6 Blood Shunt

Using the data from the varying blood flow experiments, shunt fraction was calculated. Using the varying FiO_2 data the calculated shunt was interpreted as diffusion or perfusion limiting.

3.3.7 Circuit Variation

The same equine donation was divided and used to run two separate circuits comprising the same type of membrane oxygenators but of different batches. Blood flow was set to 2.5 l/min. The same gas settings of 5 l/min air with 0.3 l/min oxygen for the oxygenator and 5 l/min 5% CO_2 in balanced N_2 with 0.2 l/min CO_2 for the deoxygenator were applied to each circuit. DO_2, DNO and DCO were calculated and compared.

3.3.8 Calculations

Barometric pressure acquired in millibars was converted to mmHg.

$$BP\ mmHg = \frac{BP\ millibars \div 1000}{750}$$

Calculations based on measurements of absolute amounts of gas were subjected to STPD conversion by correction for water vapour, pressure and temperature.

$$Water\ vapour\ pressure = PH_2O \times Relative\ Humidity$$

$$Temperature\ correction = \frac{273 + t}{273}$$

1. $P_{\bar{c}}O_2$

The mean pulmonary capillary oxygen partial pressure ($P_{\bar{c}}O_2$)(mmHg) is derived from PaO_2 and $P\overline{v}\ O_2$ using Bohr Integration method. It is not possible to directly measure $P_{\bar{c}}O_2$ therefore the value is calculated based on assumptions of the PO_2 changes along the length of the pulmonary capillaries. Bohr (1909) devised a method of calculating $P_{\bar{c}}O_2$ by assuming that the rate of oxygen diffusion is proportional to the PO_2 difference

between the alveolar gas and the pulmonary capillary at that point. A spreadsheet was created in Microsoft Excel, by C. Borland, recreating the Bohr integration to aid calculation of $P_{\bar{c}}O_2$ from the circuit PaO_2 and $P\overline{V}O_2$ data (Appendix 2).

2. PAO_2

Alveolar oxygen partial pressure (PAO_2) (mmHg) was calculated by taking the logarithmic mean of inlet and outlet gas oxygen concentrations. This approach was based on an assumed semi-logarithmic decline in oxygen within the gas phase of the oxygenator mirroring the semi-logarithmic incline in blood uptake of oxygen within the blood phase. The equation was corrected for BP and water vapour.

$$PAO_2 = \left(antilog\left(\frac{\log FiO_2 + logFeO_2}{2}\right)\right) \times \left(\left(\frac{BP\ millibars \div 1000}{750}\right) - (PH_2O \times Relative\ Humidity)\right)$$

3. $\dot{M}O_2$

Rate of oxygen uptake by the oxygenator (ml/min) was calculated via the gas phase method (as previously described in chapter 1) by taking the difference between the oxygenator inlet and outlet oxygen concentrations. The gas oxygen concentration difference was multiplied by the oxygenator gas flow to give a total uptake of oxygen, corrected for water vapour, pressure and temperature.

$$MO_2 = (FiO_2 - FeO_2) \times Oxy\ F \times \left(\frac{273}{273+t}\right) \times \left(\left(\frac{BP\ millibars \div 1000}{750}\right) - (PH_2O \times Relative\ Humidity)\right) \div 760)$$

4. DO_2

Oxygen diffusion (DO_2) (ml/min/mmHg) was calculated using Lilienthal *et al* formula (1946) whereby oxygen uptake ($\dot{M}O_2$) is divided by the membrane oxygen partial pressure difference, determined as the difference between alveolar oxygen tension and capillary oxygen tension (PAO_2-PcO_2). This method is not commonly used in clinical practice due to the calculation not accounting for uneven lung function. For this method the simplicity of the oxygenator gas and blood pathways allow the use of direct DO_2 calculation.

$$DO_2 = \frac{MO_2}{PAO_2 - P\bar{c}O_2}$$

5. DO_2 (Piiper method)

Oxygen diffusion (ml/min/mmHg) using Piiper method (1980) was used to compare with the Lilienthal formula above in the DO_2 calculation for the varying FiO_2 experiment. Piiper's DO_2 equation was a simplified version of the Lilienthal method as the pulmonary capillary O_2 tension was omitted, however the simplification was only valid over the linear portion of the ODC.

$$DO_2 = \frac{MO_2}{PaO_2 - P\bar{v}O_2} \times log_e\left(\frac{PAO_2 - P\bar{v}O_2}{PAO_2 - PaO_2}\right)$$

6. $P\bar{c}CO_2$

Pulmonary capillary carbon dioxide partial pressure ($P\bar{c}CO_2$) (mmHg) was calculated as the mean of the inlet and outlet deoxygenator blood carbon dioxide tensions ($PaCO_2$ and $P\bar{v}CO_2$ respectively). Carbon dioxide reacts rapidly with blood therefore a simpler

formula was used assuming a linear increase in carbon dioxide from the gas phase of the deoxygenator.

$$P\bar{c}CO_2 = \frac{PaCO_2 + P\bar{v}\,CO_2}{2}$$

7. $PACO_2$

The alveolar carbon dioxide tension (mmHg) within the deoxygenator gas phase was calculated as the mean of the inlet and outlet gas carbon dioxide concentrations ($FiCO_2$ and $FeCO_2$ respectively). This was based on the assumption that carbon dioxide declines linearly within the gas phase of the deoxygenator due to the rapid reaction of carbon dioxide with the blood. Correction for BP and water vapour was applied.

$$PACO_2 = \left(\frac{FiCO_2 - FeCO_2}{2}\right) \times \left(\left(\frac{BP\ millibars \div 1000}{750}\right) - (PH_2O \times Relative\ humidity)\right)$$

8. $\dot{M}CO_2$

Carbon dioxide uptake (ml/min) via the deoxygenator was calculated using the $\dot{M}O_2$ formula but substituting the inlet and outlet oxygen concentrations for inlet and outlet carbon dioxide concentrations. The carbon dioxide inlet and outlet difference was multiplied by the deoxygenator gas flow, and corrected for water vapour, temperature and pressure.

$$MCO_2 = (FiCO_2 - FeCO_2) \times Deoxy\ F \times \left(\frac{273}{273+t}\right) \times \left(\left(\frac{BP\ millibars \div 1000}{750} - (PH_2O \times Relative\ Humidity\right) \div 760\right)$$

9. DCO_2

For consistency Lilienthal DO_2 formula was modified for DCO_2.

$$DCO_2 = \frac{MCO_2}{PACO_2 - P\bar{c}CO_2}$$

10. Piiper 'style' DCO_2

This is a modification of Piiper's DO_2 method for calculating DCO_2 to use as a comparison to the DCO_2 described previously.

$$DCO_2 = \frac{MCO_2}{P\bar{v}CO_2 - PaCO_2} \times log_e\left(\frac{PACO_2 - PaCO_2}{PACO_2 - P\bar{v}CO_2}\right)$$

11. Shunt Fraction

This equation determines the venous admixture effect through the oxygenator, i.e. the blood not partaking in gas exchange that leaves the oxygenator deoxygenated. The shunted blood ($\dot{Q}s$) is taken as the difference between pulmonary capillary O_2 content and arterial O_2 content (CcO_2-CaO_2), divided by the total O_2 content ($\dot{Q}t$) achieved (CcO_2-$C\bar{v}O_2$).

$$Shunt\ fraction = \frac{\dot{Q}s}{\dot{Q}t} = \frac{CcO_2 - CaO_2}{CcO_2 - C\bar{v}O_2}$$

12. Respiratory Exchange Ratio

The RER is the ratio of the rate of carbon dioxide leaving the oxygenator ($FeCO_2$) to the rate of oxygen uptake in the oxygenator (FiO_2-FeO_2), thus making an allowance for movement of gas across the membrane or lungs. RER in man at rest is typically 0.8.

$$RER = \frac{FeCO_2}{FiO_2 - FeO_2}$$

13. Circuit Haematocrit

This calculation is used to predict the circuit haematocrit after blood addition to a crystalloid primed circuit. Haematocrit was estimated in the varying haematocrit experiments due to difficulties in measuring such low values. Haematocrit was calculated from the total volume in the circuit, the volume of blood added and the known haematocrit of the blood entering the circuit.

$$Circuit\ Hct\ = \frac{Volume\ of\ blood\ added\ ml\ x\ Hct\ of\ blood\ added}{Total\ circuit\ volume\ \ ml}$$

3.3.9 Statistical Analysis

Statistical analysis has been detailed in Chapter 2, section 2.2.

3.4 NO and CO Gas Transfer Methodology

3.4.1 NO and CO addition

NO and CO were added to the circuit via a stock cylinder of NO (1000 ppm) in nitrogen and a stock cylinder of CO (0.3%) in oxygen (19%) and Helium (11%). These two cylinders were incorporated into the oxygenator gas tubing via either a therapeutic NO mixing device or via individual rotameters. NO and CO were diluted by the oxygenator gas mix so concentrations were titrated to give the desired amounts at the oxygenator inlet. NO was delivered at a concentration of 5000 ppb unless the outlet amount was likely to drop below the detectable limit and therefore the inlet concentration was increased to maintain uptake data. CO was delivered at a concentration of 0.03%.

3.4.2 Experiments

The experiments for varying blood flow/surface area, oxygenator gas flow, oxygenator FiO_2, deoxygenator $FiCO_2$ and haemoglobin concentration, previously described (Section 3.3), were conducted with NO and CO administration via the oxygenator gas mix.

For each experimental change, NO and CO concentrations were established at the oxygenator gas inlet and oxygenator gas outlet, to be known as NOin, NOout, COin and COout.

3.4.3 Calculations

The DCO calculation is derived from the D_LCO equation described by Marie Krogh (1915). LN(COin/COout) is the membrane uptake rate constant multiplied by the oxygenator gas flow with STPD correction. The DNO calculation was based on the same formula, replacing COin and COout with NOin and NOout. DNO was further adjusted by

a membrane absorption correction factor (0.93 for half membrane) as minor NO uptake was noted in a saline primed membrane oxygenator (Borland, 2006).

$$DCO = \frac{Oxy\ F \times \left(\frac{273}{273+t}\right) \times \left(\frac{BP}{1000}\right)}{\left(\frac{BP}{1000} \times 750\right) - (PH_2O \times Relative\ Humidity)} \times LN\left(\frac{COin}{COout}\right)$$

$$DNO = \frac{Oxy\ F \times \left(\frac{273}{273+t}\right) \times \left(\frac{BP}{1000}\right)}{\left(\frac{BP}{1000} \times 750\right) - (PH_2O \times Relative\ Humidity)} \times LN\left(\frac{NOin}{NOout}\right) - (0.93 \times 2)$$

3.4.4 Statistical Analysis

The statistical analysis is described in Chapter 2, section 2.2.

3.5 Basic Gas Transfer Properties of This Circuit Design: Results and Discussion

3.5.1 Varying Blood Flow and Surface Area; Results

At very low blood flows, the accuracy of the CDI 500 sensors was questioned due to the minimum blood flow of 35ml/min required. Blood flow rates of 0.1 l/min highlighted sensor issues with lack of machine response to blood flow changes. Later work incorporated a larger bore sample tubing for the sensors to optimise blood flow through them.

Generally PaO_2 showed a very slight decrease over the blood flow range 0.1- 2.5 l/min whereas $P\overline{v}O_2$ showed a very slight increase. As a result $P_{\bar{c}}O_2$ remained static throughout the blood flow range. There were no differences in these trends when the surface area was halved (Figures 3.10 and 3.11, Figure section pg 191). PaO_2 averaged 63.44 ±33.57 mmHg for 1 cell and 81.45 ±34.66 mmHg for 2 cells. $P\overline{v}O_2$ averaged 21.51 ±7.97 mmHg for 1 cell and 27.36 ±8.58 mmHg for 2 cells. $P_{\bar{c}}O_2$ calculated from $P\overline{v}O_2$ and PaO_2 was 34.37 ±5.83 mmHg for 1 cell and 41.75 ±6.85 mmHg for 2 cells. Overall 2 cells resulted in slightly higher $P\overline{v}O_2$ ($p=0.042$), PaO_2 ($p=0.122$) and resultant $P_{\bar{c}}O_2$ ($p=0.001$) when compared to just 1 oxygenator cell.

Increasing blood flow from 0.2 to 2.5 l/min for 1 cell and 2 cells corresponded with a linear increase in $\dot{M}O_2$ and DO_2. $\dot{M}O_2$ and DO_2 for both 1 cell and 2 cells revealed inter-run variations in data (Figures 3.12 and 3.13). $\dot{M}O_2$ for 1 cell ranged 23.28 to 93.11 ml/min (run 1, $p=0.018$), 229.46 to 321.24 ml/min (run 2, $p=0.004$) and 34.35 to 137.40 ml/min (run 3, $p=0.002$). The resultant DO_2 for 1 cell ranged 0.21 to 0.90 ml/min/mmHg (run 1, $p=0.011$), 1.91 to 2.63 ml/min/mmHg (run 2, $p=0.008$) and 0.22 to 0.95 ml/min/mmHg (run 3, $p=0.002$). For two oxygenator cells the same inter-run variation

was noted with $\dot{M}O_2$ ranges of 23.28 to 93.11 ml/min (run 1, p=0.050), 183.57 to 275.35 ml/min (run 2, p=0.032) and 49.07 to 161.93 ml/min (run 3, p=0.006). The resultant DO_2 for 2 cells was calculated as 0.23 to 0.99 ml/min/mmHg (run 1, p=0.017), 1.54 to 2.36 ml/min/mmHg (run 2, p=0.014) and 0.31 to 1.20 ml/min/mmHg (run 3, p=0.005). The surface area size did not affect $\dot{M}O_2$ or DO_2 (p=0.896 and p=0.927).

CO_2 data was only collected during run 3 as the analyser CO_2 range was increased for this run. Statistical analysis was not performed on this small sample size. $PaCO_2$ increased in a curvilinear manner with increasing blood flow from 10 mmHg at 0.1 l/min to a mean 36.25 ± 2.22 mmHg at 1.0-2.5 l/min for 1 cell. $P\bar{v}CO_2$ similarly decreased over the blood flow range from 63 mmHg at 0.1 l/min to a mean 48.25 ±2.36 mmHg over 1.0 – 2.5 l/min for 1 cell. $P_{\bar{c}}CO_2$ was calculated from $P\bar{v}CO_2$ and $PaCO_2$ and averaged 40.83 ±2.48 mmHg for 1 cell (Figure 3.14). Both $\dot{M}CO_2$ and DCO_2 increased linearly from 51.03 to 137.40 ml/min and 2.28 to 14.52 ml/min/mmHg respectively (Figures 3.16 and 3.17).

With two oxygenator cells the CO_2 data showed very similar trends and results as that for 1 cell concluding no effect of surface area on CO_2. $PaCO_2$ increased curvilinearly with increasing blood flow from 10 mmHg at 0.1 l/min to a mean 31.75 ±5.38 mmHg at 1.0-2.5 l/min for 2 cells. $P\bar{v}CO_2$ similarly decreased over the blood flow range from 65 mmHg at 0.1 l/min to a mean 47.25 ±0.96 mmHg over 1.0-2.5 l/min for 2 cells. $P_{\bar{c}}CO_2$ was calculated from $P\bar{v}CO_2$ and $PaCO_2$ and averaged 39.00 ±2.28 mmHg (Figure 3.15). Both $\dot{M}CO_2$ and DCO_2 increased linearly from 52.51 to 140.83 ml/min and 2.46 to 11.78 ml/min/mmHg respectively (Figure 3.16 and 3.17).

Table 3.4 Effects of Blood Flow and Surface Area Data Summary

Varying Blood Flow and Surface Area					
	$\dot{Q}$				***SA***
Parameter	*Trend*	*Statistical value*	*d.f. or n*	*p value*	*Trend*
PaO_2	Slight decrease	1 cell R^2=0.249 2 cells R^2=0.098	17 17	p=0.035 p=0.207	Slight increase *t*=-1.584 d.f.=34 p=0.122
$P\bar{v}O_2$	Slight increase	1 cell R^2=0.326 2 cells R^2=0.275	17 17	p=0.013 p=0.026	Slight increase *t*=-2.118, d.f.=34 p=0.042
1 cell $\dot{M}O_2$	Linear increase	R^2=0.786, 0.894, 0.928	d.f.=5, 5, 5	p=0.018, 0.004, 0.002	No effect *t*=0.131 d.f.=34 p=0.896
2 cell $\dot{M}O_2$	Linear increase	R^2=0.659, 0.722, 0.873	d.f.=5, 5, 5	p=0.050, 0.032, 0.006	
1 cell DO_2	Linear increase	R^2=0.831, 0.858, 0.002	d.f.=5, 5, 5	p=0.011, 0.008, 0.002	No effect *t*=-0.092 d.f.=34 p=0.927
2 cell DO_2	Linear increase	R^2=0.797, 0.811, 0.890	d.f.=5, 5, 5	p=0.017, 0.014, 0.005	

Varying Blood Flow and Surface Area; Discussion

The effect of blood flow on $P\bar{v}O_2$ and PaO_2 showed increased arterial-venous oxygen tension difference at low flows which decreased as the blood flow increased. This phenomenon was expected as low blood flow results in slower blood transit through both the oxygenator and the deoxygenator. This provides more time to oxygenate and deoxygenate the blood, hence the results seen in this model at low flows. As the blood flow through the circuit increases, transit time reduces through the devices thus the

arterial-venous difference decreases. This same theory can be applied to the $P\bar{v}CO_2$ and $PaCO_2$ as the blood flow through the circuit equally affects carbon dioxide transfer.

The effect of increasing blood flow on $\dot{M}O_2$ and $\dot{M}CO_2$ is a linear increase with a slight plateau evident at higher flows (2-2.5 l/min). Despite increased arterial-venous partial pressure difference in oxygen and carbon dioxide at low flow, the amount of blood circulating will restrict gas transfer. Hence, the amount of deoxyhaemoglobin arriving at the oxygenator is very low thus limiting oxygen uptake via the oxygenator. As the amount of deoxyhaemoglobin entering the oxygenator increases, as denoted by increased blood flow, oxygen uptake increases. Similarly, increasing amounts of arterial blood entering the deoxygenator increases carbon dioxide transfer. The potential $\dot{M}O_2$ and $\dot{M}CO_2$ plateau effect at higher blood flows through the circuit is likely to be related to the increasing $P\bar{v}O_2$ and $PaCO_2$ thus less pressure gradient to drive oxygen and carbon dioxide transfer across the membrane. DO_2 and DCO_2 showed the same trend as $\dot{M}O_2$ and $\dot{M}CO_2$.

Surface area did not affect $\dot{M}O_2$, $\dot{M}CO_2$, DO_2 or DCO_2. Oxygen and carbon dioxide are considered perfusion limited gases (in resting healthy man) which is evident here in this apparatus. Perfusion limited gases reach equilibrium quickly between the gas channel and blood channel. Diffusion of a perfusion limited gas is affected by the blood available and blood partial pressures will readily increase in response to increasing gas concentrations. An effect on oxygen or carbon dioxide uptake associated with a reduction in membrane surface area would imply a diffusion limitation. Carbon dioxide has a very quick reaction with blood due to its increased solubility so although the pressure gradient between the blood partial pressure and gas concentration is low, equilibrium is easily reached. Oxygen however has a slower rate of reaction with blood but with a greater pressure gradient

between the alveolar gas and venous blood to drive the transfer, equilibrium is reached readily.

The model circuit has shown expected trends in the effects of blood flow and surface area on oxygen and carbon dioxide transfer. From this experiment the circuit has been validated for a blood flow of 2.5 l/min as a standard for all other experiments.

3.5.2 Effects of Varying Oxygenator Gas Flow (F); Results

Over the oxygenator gas flow range 0.5 to 15.0 l/min, the optimal gas flow was confirmed as 5 l/min coinciding with preliminary work.

PaO_2 increased initially from 47.25 mmHg (0.5 l/min) to 65.25 mmHg (2.5 l/min) after which the PaO_2 averaged 69.88 ±5.46 mmHg over the gas flow range 5 to 15 l/min. Similarly $P\bar{v}O_2$ increased from 29.25 mmHg (0.5 l/min) to 37.5 mmHg (2.5 l/min) before averaging 36.63 ±1.10 mmHg over the 5 to 15 l/min gas flow range. $P_{\bar{c}}O_2$ followed the same trend with increases from 37.00 mmHg (0.5 l/min) to 47.48 mmHg (2.5 l/min) before averaging 48.19 ±0.29 mmHg for gas flows 5 to 15 l/min. (Figure 3.22)

$\dot{M}O_2$ and DO_2 both showed a positive linear relationship with increasing oxygenator gas flow. $\dot{M}O_2$ increased from 41.90 ml/min at 0.5 l/min to 139.67 ml/min at 15 l/min ($p=0.004$). DO_2 rose from 0.50 ml/min/mmHg at 0.5 l/min to 1.25 ml/min/mmHg at 15 l/min ($p=0.007$). (Figures 3.23 and 3.24)

$PaCO_2$ was assessed as the increasing oxygenator gas flow would impact on the removal of CO_2 from the 'venous' blood. $PaCO_2$ was noted to slightly decrease curvilinearly with

increasing oxygenator gas flow. In run 1, $PaCO_2$ reduced from 30 mmHg at 0.5 l/min to 15.75 mmHg at 5 l/min (p=0.042). In run 2, $PaCO_2$ reduced from 48 mmHg at 2.5 l/min down to 30 mmHg at 15 l/min (p=0.008). (Figure 3.25)

Table 3.5 Varying Oxygenator Gas Flow Summary Table

Varying oxygenator Gas Flow 0.5-15.0 l/min				
Parameter	***Trend***	***Statistical value***	***p value***	***d.f. or n***
PaO_2	Initial increase to plateau	*r*=0.284	p=0.427	n=10
$P\bar{v}O_2$	Initial increase to plateau	*r*=0.567	p=0.087	n=10
$P_{\bar{c}}O_2$	Initial increase to plateau	*r*=0.507	P=0.135	n=10
$\dot{M}O_2$	Linear increase	R^2=0.661	p=0.004	d.f.=9
DO_2	Linear increase	R^2=0.614	p=0.007	d.f.=9
$PaCO_2$	Slight decrease	*r*=-0.958 and *r*=-0.928	p=0.042, p=0.008	n=5 and 6

Effects of Varying Oxygenator Gas Flow (F); Discussion

This experiment was designed to give information on the impact of gas flow on oxygenation within the circuit and to determine the ideal gas flow.

PaO_2 and $P\bar{v}O_2$ were seen to increase slightly with gas flows of 0.5-2.5 l/min before plateauing over the higher gas flows (5-15 l/min). This indicated that gas flows up to 2.5 l/min were limiting the oxygenation of the blood within the circuit. At low gas flows the diffusion gradient between the gas channel and the blood channel was not great enough to drive diffusion to equilibrium. At higher gas flows the fresh gas resulted in a higher diffusion gradient with equilibrium being reached between the gas and blood channels.

This was reflected in the $\dot{M}O_2$ and DO_2 which showed a linear increase with increasing oxygenator gas flow.

The oxygenator within the circuit not only oxygenates the blood but also removes carbon dioxide from the blood. A change in oxygenator gas flow will impact on $PaCO_2$ values as a higher oxygenator gas flow will remove more carbon dioxide from the blood. This was demonstrated by a curvilinear decrease in $PaCO_2$ with increasing oxygenator gas flows.

From this experimental data, an oxygenator gas flow of 5 l/min was optimal for achieving the desired PaO_2, $P\overline{v}O_2$ without compromising $PaCO_2$.

3.5.3 Effects of Varying Oxygenator FiO_2; Results

The oxygenator FiO_2 range of 4.9% to 98.0% was achieved over two experimental runs.

Over the FiO_2 range achieved, PaO_2 increased linearly from 19 mmHg up to 527 mmHg ($p<0.0001$). In contrast $P\overline{v}O_2$ ($p<0.0001$) and $P_{\bar{c}}O_2$ ($p<0.0001$) displayed a curvilinear increase. $P\overline{v}O_2$ increased initially from 16 mmHg at FiO_2 4.9% up to 40 mmHg at a FiO_2 17.3% after which $P\overline{v}O_2$ averaged 48.98 ±3.64 mmHg. $P_{\bar{c}}O_2$ followed a similar trend with an initial increase from 17.5 mmHg at FiO_2 4.9% up to 50.1 mmHg at FiO_2 21%, after which $P_{\bar{c}}O_2$ averaged 72.80 ±4.58 mmHg. (Figure 3.27)

$\dot{M}O_2$ when plotted against FiO_2 displayed a statistically significant linear increase ($p<0.0001$) ranging from 18.48 ml/min at FiO_2 4.9% up to 229.46 ml/min at FiO_2 98% (Figure 3.28). DO_2 showed a more complex relationship with FiO_2 (Figure 3.29). DO_2 sharply increasing from 0.77 ml/min/mmHg at FiO_2 7.4% up to 1.66 ml/min/mmHg at FiO_2 8.9%. The DO_2 then followed a steep decrease down to 0.91 ml/min/mmHg at FiO_2

21% before averaging 0.45 ±0.17 ml/min/mmHg at the higher FiO_2 range 25 to 98%. Using Piiper's DO_2 calculation the same trend was observed. Piiper's DO_2 increased sharply from 0.77 ml/min/mmHg at FiO_2 7.4% up to 1.66 ml/min/mmHg at FiO_2 8.9%. The DO_2 then followed a steep decrease down to 0.97 ml/min/mmHg at FiO_2 21% before averaging 0.67 ±0.13 ml/min/mmHg at the higher FiO_2 range 25 to 98%. At the lower FiO_2 there was no significant difference between the two calculation methods (p=0.910) however at the higher FiO_2 25-98% Piiper DO_2 was slightly higher than the Lilienthal DO_2 (p=0.012).

Table 3.6 Varying Oxygenator FiO_2 Data Summary Table

Varying oxygenator FiO_2 4.9% to 98%				
Parameter	***Trend***	***Statistical value***	***p value***	***d.f. or n***
PaO_2	linear increase	R^2=0.994	p<0.0001	d.f.=21
$P\bar{v}O_2$	Curvilinear increase	*r*=0.935	p<0.0001	n=21
$P_{\bar{c}}O_2$	Curvilinear increase	*r*=0.945	p<0.0001	n=21
$\dot{M}O_2$	Linear increase	R^2=0.896	p<0.0001	d.f.=20
DO_2	Unique trend	-	-	-

Effects of Varying Oxygenator FiO_2; Discussion

With increasing FiO_2 a close linear correlation with increasing PaO_2 was observed which is also expected in life. This experiment provided reference data for the required FiO_2 needed to achieve a desired PaO_2. In this model the data has shown that a FiO_2 of 26% was required to give $P\bar{v}O_2$ and PaO_2 within a clinical range compared to 21% in life. This can be attributed to the differences between the membrane oxygenator and the lungs which include smaller membrane surface area, larger diameter 'pulmonary capillaries', thicker membrane and heterogeneity of blood and gas flow which all contribute to resistance to gas exchange.

The linear relationship seen between increasing FiO_2 and resultant $\dot{M}O_2$ showed that as more oxygen was available in the gas phase, oxygen transfer increased corresponding with an increasing blood oxygen partial pressure (PaO_2). DO_2 showed a unique trend with a steep rise over the lower FiO_2 4.9-8.9% as the oxygen uptake rises rapidly over the corresponding steep portion of the ODC (β) where sO_2 was approximately 45-85%. The specific conductance of O_2 (θ) per 1 ml blood is also increased at low PO_2 due to the ease of O_2 binding. These findings are supportive of the historical diffusion resistance (1/D) equation published by Roughton and Forster (1957), modified by Cotes and Meade (1993), where membrane (D_M), blood flow ($\dot{Q}$) and pulmonary capillary volume (Vc) remain unchanged in this model, attributing affects of O_2 uptake to β and θ.

$$\frac{1}{D} = \frac{1}{D_M} + \frac{1}{\beta Q + \theta Vc}$$

FiO_2 8.9% to 26% was associated with a less steep decline in DO_2 covering the ODC sO_2 range 85-95% where the oxygen binding rate slows. The plateau in the DO_2 at FiO_2 >26% corresponded with sO_2 >98% so the transfer of oxygen based on the sigmoid shape of the ODC will be at its lowest. This finding validates the requirement for FiO_2 26% to achieve normoxia in this circuit.

The DO_2 calculation method used in this project was based on that described by Lilienthal (1946). It is a simplistic calculation of gas uptake divided by the membrane partial pressure difference. The difficulty with this equation is determining PAO_2-$P\bar{c}O_2$ with accuracy. Bohr determined that PAO_2-$P\bar{c}O_2$ increases non-linearly from PAO_2-$P\bar{v}O_2$ to PAO_2-PaO_2. He derived a method of calculating this from SaO_2 and $S\bar{v}O_2$ of the ODC. This is thought to provide an accurate PAO_2-$P\bar{c}O_2$. Piiper's DO_2 calculation is a more

complex calculation which simplifies the Bohr process. However, Piiper uses PaO_2-P$\overline{V}O_2$ for the partial pressure gradient difference which does not give the partial pressure gradient directly across the membrane as in Lilienthal DO_2. DO_2 for varying FiO_2 was calculated via both Lilienthal and Piiper methods and compared. Over the hypoxic and normoxic conditions the results were virtually the same, however in the hyperoxic range Piiper's DO_2 was significantly higher than the Lilienthal DO_2. The pressure gradient difference PaO_2-P$\overline{V}O_2$ used in Piiper's DO_2 equation will be affected by the venous admixture effect i.e. PaO_2 will be lower than the end pulmonary capillary partial pressure. At the lower FiO_2 Piiper's use of PaO_2-P$\overline{V}O_2$ will not be affected significantly by the venous admixture affect as at lower blood oxygen saturations the effect on PaO_2 is less. At higher FiO_2 the lower blood oxygen saturations of the venous admixture will have a more diluting effect on the highly saturated blood exiting the pulmonary capillaries. By dividing oxygen uptake by PaO_2-P$\overline{V}O_2$ for the pressure gradient difference the overall DO_2 will be overestimated particularly at higher FiO_2.

The varying oxygenator FiO_2 experiment has demonstrated a reference range of PaO_2 for a given FiO_2. From the data, FiO_2 26% has been established as the standard oxygenator oxygen concentration required to achieve normoxic arterial blood in this circuit. The DO_2 to be used for further experimental work will be that described by Lilienthal *et al* (1946) combined with the Bohr integration method.

3.5.4 Effects of Varying Deoxygenator $FiCO_2$; Results

The $FiCO_2$ range achieved via the deoxygenator in this apparatus was 1.78 to 23.8%.

pH decreased with increasing $FiCO_2$ over the range 1.78 to 23.8%. pHa decreased from 7.73 to 7.12 ($p<0.0001$) and pHv decreased from 7.71 to 6.93 ($p<0.0001$). (Figure 3.34)

Both $P\bar{v}CO_2$ ($p<0.0001$) and $PaCO_2$ ($p<0.0001$) increased linearly in response to increasing $FiCO_2$ (Figure 3.35). At the lower $FiCO_2$ 1.78%, $PaCO_2$ and $P\bar{v}CO_2$ was below the detection limit of the CDI 500 analyser at <10 mmHg. For the $FiCO_2$ range 2.26 to 23.8%, $P\bar{v}CO_2$ was 12 to 125 mmHg and $PaCO_2$ ranged 11 to 67 mmHg. $P_{\bar{c}}CO_2$ was calculated from $P\bar{v}CO_2$ and $PaCO_2$ so subsequently increased linearly from 11.5 to 96 mmHg ($p<0.0001$).

$\dot{M}CO_2$ increased linearly with increasing $FiCO_2$ from 34.06 ml/min (at 2.26%) to 221.16 ml/min (at 23.8%) ($p<0.0001$) (Figure 3.36). DCO_2 started high at 11.65 ml/min/mmHg at $FiCO_2$ 2.26% and then gradually decreased curvilinearly to 3.29 ml/min/mmHg at $FiCO_2$ 23.8% ($p=0.031$). Comparing the modified Piiper method for calculating DCO_2 versus modified Lilienthal formula showed no significant difference ($p=0.173$) with modified Piiper DCO_2 starting high at 11.76 ml/min/mmHg at $FiCO_2$ 2.26% and then gradually decreasing to 3.52 ml/min/mmHg at $FiCO_2$ 23.8%. (Figure 3.37)

PaO_2 was noted to curvilinearly ($p<0.0001$) decrease from 135 mmHg ($P\bar{v}CO_2$ 13 mmHg) to 96 mmHg ($P\bar{v}CO_2$ 43 mmHg) in response to increasing $P\bar{v}CO_2$, plateauing at 90 ±2.89 mmHg ($P\bar{v}CO_2$ 43 to 125 mmHg). $P\bar{v}O_2$ increased curvilinearly ($p<0.0001$) from 26 mmHg ($P\bar{v}CO_2$ 12 mmHg) to 48 mmHg ($P\bar{v}CO_2$ 125 mmHg). (Figure 3.38) Despite the decrease in PaO_2 there was a linear increase in $\dot{M}O_2$ with increasing $P\bar{v}CO_2$ ($p<0.001$) from 104.70 ml/min ($P\bar{v}CO_2$ 15 mmHg) to 190.36 ml/min ($P\bar{v}CO_2$ 125 mmHg). (Figure 3.39) Similarly DO_2 increased linearly with increasing $P\bar{v}CO_2$ ($p<0.0001$) from 0.74 ml/min/mmHg ($P\bar{v}CO_2$ 15 mmHg) to 1.62 ml/min/mmHg ($P\bar{v}CO_2$ 125 mmHg). (Figure 3.40)

Table 3.7 Varying Deoxygenator $FiCO_2$ Data Summary Table

Varying deoxygenator $FiCO_2$ 1.78% to 23.8%				
Parameter	***Trend***	***Statistical value***	***p value***	***d.f. or n***
pHa	Linear decrease	R^2= -0.751	p<0.0001	d.f.=24
pHv	Linear decrease	R^2= -0.908	p<0.0001	d.f.=24
PaO_2	Curvilinear decrease	*r*=-0.907	p<0.0001	n=22
$P\bar{v}O_2$	Curvilinear increase	*r*=0.992	p<0.0001	n=22
$\dot{M}O_2$	Linear increase	R^2=0.872	p<0.001	d.f.=15
FeO_2	Linear decrease	R^2= -0.904	p<0.0001	d.f.=15
DO_2	Linear increase	R^2=0.872	p<0.0001	d.f.=15
RER	Linear increase	R^2=0.892	p<0.0001	d.f.=15
$PaCO_2$	Linear increase	R^2=0.959	p<0.0001	d.f.=22
$P\bar{v}CO_2$	Linear increase	R^2=0.950	p<0.0001	d.f.=22
$P_{\bar{c}}CO_2$	Linear increase	R^2=0.962	p<0.0001	d.f.=22
$\dot{M}CO_2$	Linear increase	R^2=0.715	p<0.0001	d.f.=23
DCO_2	Curvilinear decrease	*r*=-0.466	p=0.031	n=23

To investigate the apparent impact of $P\bar{v}CO_2$ on PaO_2 the FeO_2 was plotted against $P\bar{v}CO_2$ (Figure 3.41). FeO_2 decreased linearly with increasing $P\bar{v}CO_2$ (p<0.0001) from 23.4% ($P\bar{v}CO_2$ 12 mmHg) to 21.6% ($P\bar{v}CO_2$ 125 mmHg). The RER was seen to increase from 0.30 ($P\bar{v}CO_2$ 12 mmHg) to 1.59 ($P\bar{v}CO_2$ 125 mmHg) in response to increasing $P\bar{v}CO_2$ (p<0.0001) (Figure 3.42).

Effects of Varying Deoxygenator $FiCO_2$; Discussion

The increase in $FiCO_2$ corresponded with a linear rise in $P\bar{v}CO_2$ as the partial pressure gradient increased between the gas and blood channels, also driving a linear increase in $\dot{M}CO_2$. Subsequently, pH was seen to decrease in response to the acidity in the blood

generated by the increased carbon dioxide partial pressures. $PaCO_2$ increased as oxygenator gas flows were not adjusted to remove the extra carbon dioxide in the venous blood. The DCO_2 decreasing curvilinear trend was consistent with a higher carbon dioxide uptake at the lower $P\bar{V}CO_2$ where the partial pressure difference would aid carbon dioxide transfer. As the blood carbon dioxide levels increase the rate of carbon dioxide transfer will decrease.

Hypercapnia is known to cause a right shift in the ODC resulting in increased $P\bar{V}O_2$ which was evident in this experiment by the curvilinear increase in response to increasing deoxygenator $FiCO_2$. PaO_2 was noted to decrease curvilinearly which caused some speculation. $\dot{M}O_2$, and subsequently DO_2, apparently increased with increasing deoxygenator $FiCO_2$ which conflicted with the decrease in PaO_2-$P\bar{V}O_2$ difference. During hypercapnia there is a resultant shift in the respiratory exchange ratio (RER) due to the extra carbon dioxide leaving the blood and entering the 'alveolar' gas. In this experiment, the oxygenator FeO_2 was found to decrease with increasing deoxygenator $FiCO_2$ which was a result of the increasing carbon dioxide moving across the membrane into the gas phase. The decrease in FeO_2 would account for the increase in $\dot{M}O_2$ and DO_2 by creating a calculation error. An RER shift in man from the normal 0.8 can be at the expense of DO_2 where hypercapnia occurs, which this model simulates. If a correction factor is applied to the FiO_2 values, corresponding to the increasing oxygenator $FeCO_2$, the oxygenator FiO_2 significantly decreases with increasing $P\bar{V}CO_2$ (R^2=0.841, d.f.=14, $p<0.0001$) (Figure 3.44). The reduced FiO_2 would correspond with a decrease in PaO_2, as the driving partial pressure gradient across the membrane reduces. The resultant corrected $\dot{M}O_2$ shows no significant change with increasing $P\bar{V}CO_2$ (R^2=0.217, d.f.=14, p=0.080)(Figure 3.45).

$$Corrected\ Oxy\ FiO_2 = Oxy\ FiO_2 \times (1 - Oxy\ FeCO_2)$$

The varying deoxygenator $FiCO_2$ experimental data provided a reference of the $FiCO_2$ required for a given $P\overline{v}\ CO_2$. In further research where the deoxygenator $FiCO_2$ is to be varied, correction would be needed for calculation of $\dot{M}O_2$ and DO_2. The data in this work has confirmed the initial deoxygenator $FiCO_2$ 8% as the standard gas setting for this circuit.

3.5.5 Effects of Varying Haemoglobin Concentration (Hb); Results

The haematocrit ranges achieved were 7.3-31.0% (run 1), 6.5-27.1% (run 2) and 0.66-5.7% (run 3) (Figure 3.46). Run 3 utilised a slower blood addition in order to achieve data in the lower Hct range <6% as this data was absent with the faster blood addition rates of runs 1 and 2.

pHv ($p<0.0001$) and pHa ($p<0.001$) were seen to increase linearly during the blood addition for the experimental runs encompassing Hb 6.5 to 31.0 g/dl. In the first run pHv ranged 6.66-7.10 and pHa ranged 6.73-7.13. Similarly in the second run, pHv ranged 6.64-7.17 and pHa ranged 6.84-7.31. For the third run with lower Hct levels, the pHv values were below that detected by the analyser <6.5. The pHa was initially out of range until a Hct of 2.5 was reached where the pH ranged 6.55-6.79 up to Hct 5.71. (Figure 3.47)

PaO_2 ($p<0.0001$) and $P\overline{v}\ O_2$ ($p=0.023$) when plotted against Hb concentration showed a curvilinear relationship (Figure 3.48). The PaO_2 was reading high initially with the saline prime (run 3 = 169mmHg) but reduced until the Hct was approximately 20% where the

PaO_2 stabilised between 50 to 60 mmHg (run 1) or 80-90 mmHg (run 2). The $P\bar{v}O_2$ was reading very low initially with the saline prime at 10 mmHg (run 3) but this increased as blood was added until a Hct of 15% where $P\bar{v}O_2$ stabilised between 35-38 mmHg (run 1) and 40-45 mmHg (run 2). The resultant calculated $P_{\bar{c}}O_2$ at the lower Hct range of 0-5.71 showed a curvilinear increase from 34.56 to 45.31 mmHg. In runs 1 and 2 where the Hct range was 7.3-31.0 and 6.5-27.1, $P_{\bar{c}}O_2$ was stable at 43.86 ±4.42 mmHg and 56.70 ±2.64 mmHg, respectively.

The $\dot{M}O_2$ ($p<0.0001$) and DO_2 ($p<0.0001$) showed a curvilinear increase over the Hct range where the values increased significantly from Hct 0 to 15% before plateauing (Figures 3.49 and 3.50). In run 1, with lesser FiO_2 (21%) $\dot{M}O_2$ and DO_2 started at 71.7 ml/min and 0.56 ml/min/mmHg at 0% rising to a mean of 252.43 ±46.47 ml/min and 2.51 ±0.58 ml/min/mmHg, respectively. In run 2 with a FiO_2 26.3%, $\dot{M}O_2$ and DO_2 started at 63.39 ml/min and 0.33 ml/min/mmHg at 0% increasing to a mean of 151.17 ±0 ml/min and 1.17 ±0.02 ml/min/mmHg, respectively. Run 3 revealed a gradual increase in both $\dot{M}O_2$ and DO_2 over the Hct range 0.66-5.71. $\dot{M}O_2$ and DO_2 rose from 63.66 ml/min and 0.75 ml/min/mmHg to 146.92 ml/min and 0.98 ml/min/mmHg with an oxygenator FiO_2 26.5%.

$\dot{M}CO_2$ data was only taken from runs 2 and 3 as the CO_2 delivery for run 1 was interrupted during the experiment (Figure 3.51). At lower Hct range 0.66-5.71 $\dot{M}CO_2$ increased curvilinearly from 259.46 ml/min to 297.90 ml/min ($p=0.004$). At the higher Hct range 6.5-27.1 $\dot{M}CO_2$ started at 119.34 ml/min at the start of the run (Hb=0) but maintained a mean $\dot{M}CO_2$ 182.71 ±4.43 ml/min thereafter in the presence of RBC. DCO_2 similarly increased from 6.77 ml/min/mmHg to 8.36 ml/min/mmHg over the Hct range 0.66-5.71. At the higher Hct range DCO_2 was 4.94 ml/min/mmHg with the saline prime

and maintained a mean 8.82 ±0.66 ml/min/mmHg over the Hct range 6.45-27.1. Across the whole Hct range 0.66-27.1 DCO_2 increased curvilinearly (p=0.002) (Figure 3.52).

Table 3.8 Varying Hb Concentration Data Summary Table

Varying Hb concentration Hct 0.66% to 31.0%				
Parameter	***Trend***	***Statistical Value***	***p value***	***d.f. or n***
pHa	Linear increase	R^2=0.576	p<0.001	d.f.=19
pHv	Linear increase	R^2=0.870	p<0.0001	d.f.=19
PaO_2	Curvilinear decrease	*r*= -0.913	p<0.0001	n=32
$P\bar{v}O_2$	Curvilinear increase	*r*=0.401	p=0.023	n=32
$\dot{M}O_2$	Curvilinear increase	*r*=0.726	p<0.0001	n=33
DO_2	Curvilinear increase	*r*=0.699	p<0.0001	n=33
$\dot{M}CO_2$	Curvilinear Increase at low Hb	*r*=0.790	p=0.004	n=11
DCO_2	Increasing trend	*r*=0.623	p=0.002	n=22

Effects of Varying Haemoglobin Concentration (Hb); Discussion

The varying haemoglobin experiment allowed gas transfer at very low haemoglobin concentrations to be examined. This work could not be conducted in living species due to the extreme anaemic state. The haematocrit range covered was conducted using three experimental runs which have shown some inter-run variations attributed to the different oxygenator circuits used. The data trends were comparable even if the exact data values were not fully comparable.

The prime used for the circuit was 0.9% NaCl which has a pH 5.5. At very low Hct the pH was too acidotic and below the analyser limit (<6.5) but once the Hct reached 2.5% the pH showed a linear increase. The undetectable pH was due to the acidotic prime influencing the pH and as blood entered the circuit the pH was buffered. An alternative

prime of lactated ringers (pH 6.5) would have resulted in pH above the detection threshold.

PaO_2 was high at very low Hct concentrations whereas $P\bar{v}O_2$ was low. Dissolved oxygen would be removed by the deoxygenator more readily than oxygen bound to haemoglobin. As Hct levels increased the PaO_2-$P\bar{v}O_2$ difference decreased as oxygen was liganded to haemoglobin. At Hct 15-20% the oxygen partial pressures stabilised.

$\dot{M}O_2$ and DO_2 increased curvilinearly corresponding with increasing Hct, plateauing at Hct >15%. As more haemoglobin became available in the circuit, more oxygen was taken up via the oxygenator. Additionally, the haemoglobin being added to the circuit was deoxygenated. Conversely, in this model the threshold Hct for a reduction in $\dot{M}O_2$ was 15% (Hb 5 g/dl) which has been shown to cause an increase in cardiac output in acutely anaemic (human) volunteers (Weiskopf *et al* 1998). In anaemic subjects, cardiac output would increase to maintain oxygen delivery thus $\dot{M}O_2$ and DO_2 would not decrease but in this model the pump flow was not adjusted to compensate. Additionally, in the first run a FiO_2 21% was used in the oxygenator gas compared to 26.5% in the subsequent runs and it is noted that the $\dot{M}O_2$ and DO_2 were higher in the lower oxygen gas mix than the higher mix. This corresponded with the findings for the varying oxygenator FiO_2 experiment.

The CO_2 data was limited due to a gas interruption in the initial experiment rendering the CO_2 data unreliable. The data available is small but shows good trends. $\dot{M}CO_2$ and DCO_2 were seen to gradually increase at the low Hct range (0.66-5.71) but then plateau after Hct >6. The initial rise in $\dot{M}CO_2$ would be a result of the need for CO_2 for buffering of the circulating blood until more clinical Hct and $P\bar{v}CO_2$ were achieved. After this time

CO_2 would still be taken up by the blood due to the concentration gradient across the membrane and utilised in the buffering reactions but at a slower uptake.

From the increasing haemoglobin experiment the data showed that an Hct >15% was the threshold for stabilisation of the oxygen partial pressures and oxygen uptake. The subsequent work in this research was to encompass Hct within the clinical range 27-36 g/dl.

3.5.6 Blood Shunt; Results

The shunt fraction was seen to increase linearly with increasing blood flow (p=0.009). Shunt fraction ranged from 0.084% at 0.1 l/min up to 37% at 2.5 l/min (Figure 3.18). Shunt fraction for 1 cell and 2 cells was not significantly different (p=0.051).

Shunt fraction was plotted against varying oxygenator FiO_2 (Figure 3.33) for a standard blood flow rate (2.5 l/min) revealing a decreasing curvilinear relationship (p<0.0001). At low FiO_2 4.9% the shunt was calculated as 82.2% reducing to 18.5% at FiO_2 21%. At higher FiO_2 (38-98%) the shunt fraction averaged 0.93 ±0.007%.

Table 3.9 Shunt Fraction Data Summary

Shunt Fraction				
Parameter	***Trend***	***Statistical value***	***p value***	***d.f. or n***
$\dot{Q}$	Linear increase	R^2=0.183	p=0.009	d.f.=35
SA	No statistical change	*t*=2.021	p=0.051	d.f.=34
FiO_2	Curvilinear decrease	*r*= -0.988	p<0.0001	n=22

Blood Shunt; Discussion

Physiological blood shunting is due to venous blood from the bronchial artery supply draining into the left atrium and the coronary artery supply draining into the left ventricle. Pulmonary capillary blood from the lungs will be desaturated slightly by this venous blood to become the arterial blood. The shunt fraction is usually 1-2% in healthy adults (Cotes, 2006) but can increase with ventilation-perfusion mismatches and cardiac abnormalities. In the oxygenator, the shunt fraction is likely to be due to the wide blood channel and the laminar flow characteristics of the device. With increasing blood flow, shunt fraction was seen to increase up to 37% which suggests there is a large amount of blood not in contact with the membrane. The surface area change did not influence the shunt fraction which was expected, as the flow pathway through each side of the membrane is the same.

To determine if the shunt fraction is attributed to poor ventilation-perfusion matching or is related to a blood flow pathway, shunt fraction was plotted against FiO_2. In this case the shunt fraction was seen to be extremely high (82%) at low FiO_2 (4.9%) reducing steeply to 18.5% at FiO_2 21%. In hyperoxia the shunt fraction reduced to 0.93% which is more comparable to the physiological shunt fraction. The virtual elimination of the shunt fraction in hyperoxia indicates that the shunt seen with increasing blood flow can be attributed to blood not partaking in the gas exchange due to the blood flow characteristics through the device i.e. there is a substantial PO_2 gradient decreasing from the immediate area of the membrane to the centre of the blood channel.

Early work by Lilienthal (1946) detailed A-a (Alveolar-arterial) PO_2 gradient and its impact on D_LO_2 during normoxic and anoxic conditions. The shunt fraction was assumed to be equal during normoxia and anoxia. Therefore any difference in A-a gradient would be attributed to the lung diffusion. From this experimental work the theory appears to be

incorrect as in hypoxia the shunt fraction increases steeply. Therefore a difference in the A-a gradient used in their work may actually be due to increasing shunt and may underestimate D_LO_2. The original work went unchallenged until 1973 when questioned by Dr J B West, prompting Riley and Permutt (1973) to reinvestigate the assumption. They confirmed West's findings that the shunt fraction increases during low O_2 breathing. This later publication confirms the findings in this experimental data.

From this experiment, it was found that at FiO_2 21% the shunt fraction is elevated which could cause a diffusion limitation in the experimental work. At FiO_2 26% the shunt fraction was comparable to that seen in life. This coupled with the normoxic blood partial pressures achieved with FiO_2 26% are evidence that this FiO_2 should be the standard oxygenator gas setting.

3.5.7 Circuit variation; Results

DO_2 results from two different circuits run with the same blood donation averaged 0.89 ±0.01 ml/min/mmHg (circuit 1) and 1.06 ±0.00 ml/min/mmHg (circuit 2). There was a significant difference in DO_2 ($p<0.0001$) which was attributed to membrane oxygenator variation.

Similar variations were observed with DNO and DCO ($p=0.001$ and $p<0.0001$, respectively). DNO averaged 13.52 ±4.76 ml/min/mmHg and 17.25 ±5.62 ml/min/mmHg. DCO averaged 1.20 ±0.00 ml/min/mmHg and 1.88 ±0.05 ml/min/mmHg.

Table 3.10 Circuit Variation Data Summary

Circuit Variation				
Parameter	***Trend***	***Statistical value***	***p value***	***d.f. or n***
DO_2	Significant difference	*t*=-5.107	p<0.0001	d.f.=19
DNO	Significant difference	*t*=-3.755	p=0.001	d.f.=19
DCO	Significant difference	*t*=-9.614	p<0.0001	d.f.=19

Circuit variation; Discussion

The membrane oxygenators used were manufactured by perforating the polypropylene in order to create a microporous membrane through which gas transfers. The process is a mechanical one which is likely to elicit some variation. The circuit variation test has quantified this as a significant variation which may have an impact on between-run comparative experiments.

The marked between-run variation observed with blood from a single horse donor used in two circuits shows that the variation observed is between oxygenators. To limit this variation impact, any comparative work would need to be conducted during the same experimental run, i.e. using the same circuit set-up and blood donation. Repeated experimental runs can be conducted using a different circuit and blood donation.

3.6 NO and CO Gas Transfer Data in This Circuit Design: Results and Discussion

3.6.1 Effects of Varying Blood Flow ($\dot{Q}$) and Surface Area (SA)

DNO was not affected by changes in blood flow from 0.1 to 2.5 l/min (p=0.333). There was a significant increase in DNO with increasing surface area (p=0.002). DNO for 1 cell

averaged 5.72 ±1.61 ml/min/mmHg and for 2 cells averaged 9.71 ±3.62 ml/min/mmHg. (Figure 3.19)

DCO was not significantly affected by changes in blood flow from 0.1 to 2.5 l/min (p=0.079). DCO was significantly affected by changes in surface area with 1 cell averaging 1.07 ±0.21 ml/min/mmHg and 2 cells averaging 1.46 ±0.35 ml/min/mmHg for run 1 (p=0.039). In run 2 DCO for 1 cell averaged 0.81 ±0.17 ml/min/mmHg and for 2 cells averaged 1.13 ±0.25 ml/min/mmHg (p=0.026). (Figure 3.20)

3.6.2 Effects of Varying Oxygenator Gas Flow (F)

DNO increased linearly with increasing oxygenator gas flow 2.5 to 15.0 l/min (p<0.001). DNO increased from 4.76 ml/min/mmHg at 2.5 l/min gas flow up to 11.19 ml/min/mmHg at 15 l/min gas flow. (Figure 3.26)

DCO showed no change in response to increasing oxygenator gas flow (p=0.932). DCO averaged 1.36 ±0.28 ml/min/mmHg over the oxygenator gas flow range 2.5 to 15.0 l/min. (Figure 3.26)

3.6.3 Effects of Varying Oxygenator FiO_2

DNO was unaffected by increasing FiO_2 in the hyperoxic range 21-98% with DNO averaging 10.00 ±0.94 ml/min/mmHg (p=0.639) (Figure 3.32). Similarly DNO was unaffected by FiO_2 in the hypoxic range 4.9-20% with DNO averaging 5.08 ±0.30 ml/min/mmHg (p=0.617) (Figure 3.31). The hypoxic and hyperoxic data were achieved with two separate experimental runs so inter-run variation was noted.

DCO significantly decreased linearly from 1.98 ml/min/mmHg to 0.50 ml/min/mmHg with increasing FiO_2 over the range 4.9-98% (p=0.011) (Figure 3.30).

Table 3.11 DNO and DCO Data Summary Table

Parameter	***DNO***			
	Trend	***Statistic***	***p value***	***d.f. or n***
Blood Flow	No change	R^2=0.043	p=0.333	d.f.=23
Surface Area	Increased	t=3.491	p=0.002	d.f.=22
Oxy gas Flow	Linear increase	R^2=0.978	p<0.001	d.f.=5
Oxy FiO_2	No change	R^2=0.025 R^2=0.033	p=0.639 p=0.617	d.f.=10 d.f.=9
Deoxy $FiCO_2$	No change	R^2=0.116	p=0.509	d.f.=5
Hct	Linear increase	R^2=0.964	p<0.0001	d.f.=19
Parameter	***DCO***			
	Trend	***Statistic***	***p value***	***d.f. or n***
Blood Flow	No change	R^2=0.134	p=0.079	d.f.=23
Surface Area	Increased	t=-2.369 t=-2.602	p=0.039 p=0.026	d.f.=10 d.f.=10
Oxy gas Flow	No change	R^2=0.002	p=0.932	d.f.=5
Oxy FiO_2	Linear decrease	R^2=0.295	p=0.011	d.f.=21
Deoxy $FiCO_2$	Linear increase	R^2=0.767	p=0.022	d.f.=5
Hct	Curvilinear increase	r=0.782	p<0.0001	n=22

3.6.4 Effects of Varying Deoxygenator $FiCO_2$

DNO was unaffected by increasing deoxygenator $FiCO_2$ ranging 7.8-23% with DNO averaging 6.19 ±0.89 ml/min/mmHg (p=0.509) (Figure 3.43).

DCO increased linearly with increasing deoxygenator $FiCO_2$ ranging 7.8-23% with DCO increasing from 0.45 ml/min/mmHg to 3.24 ml/min/mmHg (p=0.022) (Figure 3.43).

3.6.5 Effects of Varying Haemoglobin Concentration (Hb)

DNO significantly increased with rising Hct (p<0.0001) from 0.68 ml/min/mmHg at Hct 0.66 up to 7.08 ml/min/mmHg at Hct 27.1 (Figure 3.53).

DCO significantly increased curvilinearly with increasing Hct (p<0.0001) from 0.34 ml/min/mmHg (saline prime) up to 1.09 ml/min/mmHg at Hct 27.1 (Figure 3.53).

3.6.6 DNO and DCO Discussion

NO and CO are both diffusion limited gases as evident from the data in this series of experiments. Both NO and CO were unaffected by blood flow whereas surface area did influence NO and CO uptake which was expected with diffusion limited gases.

Carbon monoxide is a competitive inhibitor to haemoglobin binding oxygen (Roughton *et al* 1957). Both gases will compete for the same haemoglobin binding site but carbon monoxide is preferentially bound as the affinity is greater. Although the affinity for carbon monoxide is greater the reaction with haemoglobin is slower than that for oxygen. When the oxygenator FiO_2 was increased DCO was seen to decrease. The high amount of oxygen was successfully competing with carbon monoxide and the displacement of this

bound oxygen makes the reaction rate with carbon monoxide much slower. More interestingly, DCO increased with increasing deoxygenator $FiCO_2$. As carbon monoxide is delivered via the oxygenator, this seemed an odd finding. Reviewing the experimental data for oxygen, it was noted that PaO_2 decreased due to an increase in the oxygenator respiratory quotient which suggested a dilutionary effect on O_2 as the CO_2 transfers from the blood into the oxygenator gas. This would account for the increase in DCO as the respiratory quotient shifts favouring the competitive binding of carbon monoxide by haemoglobin. In future work where the respiratory quotient may be varied from the clinical 0.7-0.75 range, data must be interpreted with this consideration.

Increasing gas flow through the oxygenator resulted in an increase in DNO but not DCO. The reaction rate of NO with haemoglobin is very rapid compared to CO. When the inlet and outlet NO concentration data were compared, it revealed a decrease in NO inlet concentration with increasing gas flow, while the outlet concentrations increased as the bulk flow carries NO through the gas pathway. The inlet-outlet difference significantly decreased with increasing gas flow to a minimal difference. The increasing DNO was therefore attributed to a mathematical enhancement as the NO concentration difference is multiplied by gas flow. Increasing gas flow through the oxygenator results in quicker gas transit time that mathematically enhances DNO but limits DCO.

Rising haemoglobin concentrations increased both DNO and DCO curvilinearly. The prominent increase in diffusion corresponded with the preclinical Hct range <15g/dl. As CO binds to the haemoglobin molecule it is evident that an increase in haemoglobin will increase DCO at such low haemoglobin concentrations. NO binds to the β globin chain of haemoglobin but the decreased DNO in low haemoglobin concentrations has been

attributed to diffusion resistance of RBCs or plasma (Chapter 5). Low haemoglobin levels provide chemical limitation to DCO and diffusion resistance to DNO.

From this battery of NO and CO experiments, both gases responded to the changing conditions with expected results given historical data. The circuit provides an insight into the diffusion of NO and CO under varying conditions where one parameter may be studied in isolation. With this flexibility of the circuit the next phase was to determine the effects of haemolysis on DNO and DCO as speculation grows regarding RBC resistance to DNO.

3.7 Model Suitability; Overall Discussion

From the data it is evident that a reliable model of gas exchange over physiological blood partial pressure ranges can be achieved with two commercially available oxygenators. This model has demonstrated that a deoxygenator membrane surface area of equal size to the oxygenator is adequate to provide deoxygenation.

These experiments revealed some inter-run variations in the data so that some experimental data taken on different days were not wholly comparable. However, the trends of the data were significant which adds validity to the circuit design. The inter-run variations were considered to be a result of either the initial broad blood donor pool or the membrane oxygenator manufacturing process. Subsequently, the donor selection was narrowed to geldings aged 5-12 years rather than including younger or female donors that seemed to have skewed earlier data. The membrane oxygenators used were from clinical stock so they will have imposed manufacturing tolerances. Experiments to clarify the differences in gas diffusion across the membrane oxygenators within the circuit added a

significant inter-run variation. Based on this unexpected finding, work involving comparative experiments was subsequently conducted using the same blood and circuitry.

Carbon dioxide transfer is less widely investigated probably due to the complex way in which carbon dioxide is present within the blood and red blood cell. In patients, tissues produce carbon dioxide and the transfer across the lungs is purely an elimination process. In this model, carbon dioxide is actively added to the blood via a membrane deoxygenator in order to provide venous blood to the circuit. Data regarding influences upon carbon dioxide transfer is integral to these investigations.

The model can be used to investigate gas transfer with regards to diffusion laws. Vapour density and water solubility denotes the diffusion ratio DCO_2>DNO>DO_2>DCO. This was demonstrated during the varying blood flow experiment (graph 3.21). The limiting mechanisms of gas transfer were established in this experimental model which reflected that previously reported. Oxygen and carbon dioxide were both considered perfusion limited with NO and CO exhibiting diffusion limited characteristics.

A wide range of gas exchange data can be extrapolated from this model and adaptations of the methodology can be made for investigating both clinical and non-clinical parameters. This circuit has been used to model gas exchange in the presence of nitric oxide and carbon monoxide with publication of results (Borland *et al* 2006 and 2010). The methodology of this model has been previously described (Dunningham *et al* 2007) but in this work the methodology has been extended to enable investigations into the effects of a volatile anaesthetic agent (Isoflurane) and a blood substitute (Oxyglobin) on gas diffusion.

CHAPTER 4: Effects of the Volatile Anaesthetic Isoflurane on Gas Transfer

Aims

To test the hypothesis, that a volatile anaesthetic agent (Isoflurane) affects oxygen uptake in the membrane oxygenator. Isoflurane is commonly added to the oxygenator gas flow during cardiopulmonary bypass, to provide either anaesthetic to the patient or to control hypertension. It is important to establish if the presence of Isoflurane results in altered gas exchange properties of the oxygenator. There is limited data on the impact of Isoflurane on oxygen transfer in the membrane oxygenator and most studies are confined to the adequacy of anaesthesia to avoid patient awareness during cardiopulmonary bypass (Henderson *et al* 1988, Hickey *et al* 1996, Philipp *et al* 2002 and Wiesenack *et al* 2002). In this study, the effects of Isoflurane on oxygen transfer and the oxygen dissociation curve (ODC) within the membrane oxygenator were investigated, using a continuously running oxygenator and deoxygenator model circuit.

4.1 Addition of Isoflurane to the Oxygenator: Circuit Set-Up.

Isoflurane is a volatile anaesthetic in liquid form at room temperature. The molecules of the liquid have low cohesion (poor attraction to other molecules) and a high kinetic energy which enable the molecules to pass across the surface of the liquid, known as vaporisation. A liquid is considered volatile if it vaporises easily. A large surface area of the Isoflurane liquid will enable rapid vaporisation until equilibrium is reached between the liquid and gas. Therefore, if fresh gas is passed over the surface area of the Isoflurane liquid, vapour will be carried away enabling more vapour to form. Vaporisation is proportional to the

gas flow across the surface. An anaesthetic vaporiser is designed to use these properties to mix the volatile agent with a carrier gas such as air and oxygen.

4.1.1 Isoflurane Vaporiser

The vaporiser type used for this research was the Ohmeda Isotec 3 (Ohmeda, Hatfield, UK). Fresh gas passes through this vaporiser via two channels controlled by an integrated flow-splitting valve. A proportion of the gas is diverted to be exposed to vapour given off from the Isoflurane saturated wicks, whilst the remainder of the gas passes through a bypass channel. This design safely regulates the amount of Isoflurane administered into the gas flow. If all of the gas were to pass through the vaporiser the end concentration would be too potent. The concentration setting on the vaporiser controls the flow-splitting valve. Isoflurane liquid is affected by temperature whereby the amount of vapour increases with rising temperature. A temperature-compensating valve is incorporated which generates resistance to flow through the vapour chamber with varying temperature. The temperature-compensating valve provides a constant concentration of Isoflurane in the carrier gas despite temperature fluctuations.

4.1.2 Incorporation of Isoflurane into the Circuit

The Isoflurane vaporiser was situated in the oxygenator gas inlet tubing (Figures 3.7 pg 44 and 3.8 pg 47), sited on a mounting bracket that had specifically sized reducing connectors to fit into the ¼" gas inlet tubing. The vaporiser was located initially downstream of the FiO_2 analyser but was relocated upstream of the FiO_2 analyser following the preliminary experiments. In the preliminary work (Borland *et al* 2007b) Isoflurane was associated with an increased oxygen uptake across the membrane oxygenator. The calculation relies upon FiO_2 and FeO_2 differences, which increased when the vaporiser was switched on due to an increase in FiO_2. To verify the data, the FiO_2 pre vaporiser and at the oxygenator gas

inlet were compared (section 4.2.3). This work showed that the vaporiser setting switch increased the FiO_2 of the oxygenator pre vaporiser gas for 1-5% compared to 0% Isoflurane. The FiO_2 analyser positioning post vaporiser represented actual oxygen concentrations delivered to the oxygenator.

The Isoflurane concentration within the oxygenator gas flow was set to 0.5, 1, 2, 3, 4 and 5% for the preliminary work or 1% for the main experimental work, using the percentage setting dial on the vaporiser. The circuit was otherwise assembled as described in chapter 3, section 3.1.

4.1.3 Isoflurane Analyser

Isoflurane concentrations are analysed via gas chromatography or infrared technology. Clinically, the latter has emerged as the current standard analyser due to the compact size, rapid response to concentration changes and reliability. The inspired gas Isoflurane concentration (FiISO) and expired gas Isoflurane concentration (FeISO) in this work were analysed using an in-built infrared analyser on the Datex anaesthetic monitor (Datex-Ohmeda, Hatfield, UK).

4.2 Pilot Experiments With Isoflurane

Aims

The pilot experiments were designed to clarify the experimental protocol.

The anaesthetic agent was administered via a vaporiser so the initial test was to clarify the actual concentration achieved for a particular percentage setting. This would verify the

accuracy of the calibrated vaporiser used in this work. Then, the actual Isoflurane concentration passing across the oxygenator membrane was determined to establish that the membrane was permeable to Isoflurane. Following some initial preliminary tests on oxygen transfer in the presence of Isoflurane (Borland *et al* 2007b) a non dose related increase in $\dot{M}O_2$ was observed which raised concerns over the circuitry. The FiO_2 and FeO_2 difference appeared to be the determining factor in the $\dot{M}O_2$ increase so the location of the vaporiser to the FiO_2 analyser within the gas tubing was investigated. These tests were performed on a circuit assembled dry (without priming).

During a preliminary experimental run with Isoflurane, the time to wash-out was determined. This would be of importance in following experiments where the Isoflurane concentration was to be randomised. Knowledge of the time needed to allow the Isoflurane to be removed from the circuit would be critical where 0% Isoflurane followed an Isoflurane group.

4.2.1 Pilot Circuit Set-up and Methodology

1. Isoflurane Vaporiser Test – Concentration versus Setting

   The circuit was set up dry (Chapter 3, section 3.1). The oxygenator gas flow was set to 5 l/min with a FiO_2 26%. The Isoflurane vaporiser was randomly set at 1, 2, 3, 4 or 5% and the concentration delivered into the gas line determined via analyser. This was repeated five times.

2. Isoflurane Concentrations Pre and Post Oxygenator Membrane

   The circuit was set up dry (Chapter 3, section 3.1). The blood inlet tubing was clamped so that gas passing across the membrane could exit via the blood outlet tubing (arterial line) only. Gas flowing into the oxygenator gas channel would either pass

through the gas channel and exit via the exhaust or pass across the membrane exiting via the arterial line. FiO_2 was set to 26% and the gas flow randomised to 1, 2, 3, 4 or 5 l/min. The Isoflurane vaporiser concentration was randomly set to 0.5, 1, 2 or 3%. The Isoflurane concentration was measured pre (FiISO), post oxygenator membrane (arterial line) and in the oxygenator exhaust (FeISO).

3. FiO_2 Analyser Positioning With Isoflurane

   The circuit was set up dry (Chapter 3, section 3.1). Two FiO_2 analysers (AX300) were placed into the oxygenator gas inlet tubing, one pre and another post Isoflurane vaporiser. The oxygenator gas was set to 5.5 l/min with a FiO_2 27%. The Isoflurane vaporiser setting was randomly adjusted to 0, 1, 2, 3, 4 or 5% and the pre and post vaporiser FiO_2 recorded for each change. This was repeated five times.

4. Isoflurane Wash-out

   The circuit was set-up and primed with equine blood (Chapter 3, section 3.1). The oxygenator gas settings were 5 l/min air with 0.3 l/min O_2. The deoxygenator gas settings were 5 l/min 5% CO_2 in balanced N_2 with 0.2 l/min CO_2. The blood flow of the circuit was 2.5 l/min. The Isoflurane vaporiser was set to 1% (based on the outcomes from the FiO_2 Analyser Positioning Experiment section 4.2.3) and this was confirmed by FiISO and FeISO measurements. The Isoflurane vaporiser was turned to 0% and the FeISO recorded at 5, 25, 30, 35, 40, 45, 60, 70 and 80 seconds. The Isoflurane washout time for 1% concentration was calculated from this data.

4.2.2 Pilot Experimental Results

1. Isoflurane Vaporiser Test – Concentration versus Setting

   The actual mean Isoflurane concentrations versus the vaporiser settings are given in Table 4.1. There was good correlation between the Isoflurane concentration achieved versus the Isoflurane concentration setting (Figure 4.1, R^2=0.998). For each change in Isoflurane concentration it was noted to take three minutes for the concentration reading to stabilise on the Datex analyser.

Table 4.1 Isoflurane Concentration Setting Versus Analyser Concentration

Isoflurane Vaporiser Conc. %	***Analyser Isoflurane Conc. % Mean (SD)***	***% Difference***
1.0	0.93 (0.00)	7%
2.0	1.8 (0.00)	10%
3.0	2.9 (0.00)	3.3%
4.0	3.8 (0.00)	5%
5.0	5.0 (0.00)	0%

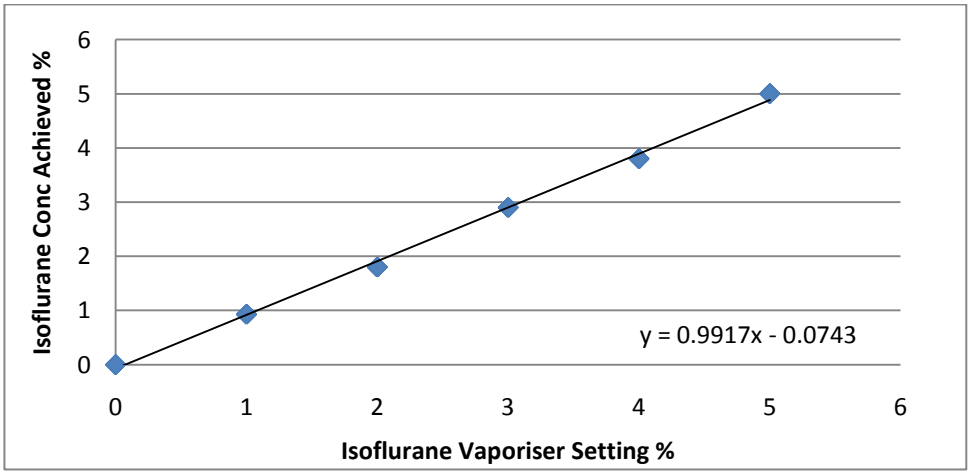

Figure 4.1 Isoflurane oxygenator inlet concentration versus the vaporiser setting; There was a good correlation between the Isoflurane concentration achieved versus the Isoflurane vaporiser concentration setting (R^2=0.998).

Table 4.2 Pre and Post Membrane Isoflurane Concentrations.

The FeISO and arterial line Isoflurane concentrations were compared (*t*-test) to the FiISO for each concentration setting to determine significant differences in Isoflurane distribution within the circuit. No differences in distribution were observed

	Mean	***SD***	***t-test value***	***p value***	***d.f.***
0.5% FiISO	0.46	0.001	-	-	-
0.5% FeISO	0.44	0.001	0.955	p=0.352	18
0.5% Arterial line	0.44	0.002	1.197	p=0.247	18
1% FiISO	0.90	0.004	-	-	-
1% FeISO	0.89	0.004	0.412	p=0.686	18
1% Arterial line	0.88	0.007	0.684	p=0.504	18
2% FiISO	1.91	0.010	-	-	-
2% FeISO	1.88	0.006	0.747	p=0.464	18
2% Arterial line	1.86	0.009	1.140	p=0.269	18
3% FiISO	2.91	0.028	-	-	-
3% FeISO	2.84	0.012	1.187	p=0.251	18
3% Arterial line	2.81	0.017	1.504	p=0.150	18

2. Isoflurane Concentrations Pre and Post Membrane

   The FiISO, FeISO and arterial line Isoflurane concentrations were unaffected by the gas flow. There was no notable difference in the inlet gas Isoflurane concentrations compared to both the outlet gas and arterial line concentrations (Table 4.2).

3. FiO_2 Analyser Positioning With Isoflurane

   The difference between pre vaporiser and post vaporiser FiO_2 was 0.4% at 0% Isoflurane up to 2.3% at 4% Isoflurane. The data showed statistically significant pre

and post vaporiser FiO_2 differences in the Isoflurane concentration range 1-5%. The actual mean pre and post vaporiser values are presented in Table 4.3.

Table 4.3 Pre and Post Isoflurane Vaporiser FiO_2 Data

FiO_2 was measured pre and post vaporiser to determine effects of vaporiser positioning within the gas line. The pre vaporiser FiO_2 increased when Isoflurane (1-5%) was switched on. Post vaporiser values decreased with Isoflurane presence with *t*-test values highlighting the pre-post vaporiser FiO_2 significance.

Isoflurane Conc. %	***Pre Vaporiser FiO_2***	***Post Vaporiser FiO_2***	***Pre-Post % Difference***	***t-test value***	***p value***	***d.f.***
0	0.265 (SD 0.006)	0.261 (SD 0.004)	0.4%	1.233	p=0.252	8
1	0.273 (SD 0.005)	0.259 (SD 0.005)	1.4%	4.185	p=0.003	8
2	0.272 (SD 0.004)	0.254 (SD 0.005)	1.8%	6.114	p<0.001	8
3	0.271 (SD 0.004)	0.254 (SD 0.006)	1.7%	5.743	p<0.001	8
4	0.272 (SD 0.003)	0.249 (SD 0.003)	2.3%	11.387	p<0.0001	8
5	0.272 (SD 0.003)	0.250 (SD 0.003)	2.2%	12.080	p<0.0001	8

4. Isoflurane Wash-out

With the Isoflurane vaporiser set to 1%, the FiISO and FeISO were 1.30% and 1.00% respectively. The time to completely wash out 1% Isoflurane from the circuit was 80 seconds. The t½ was calculated as 25.4 seconds. (Figure 4.2)

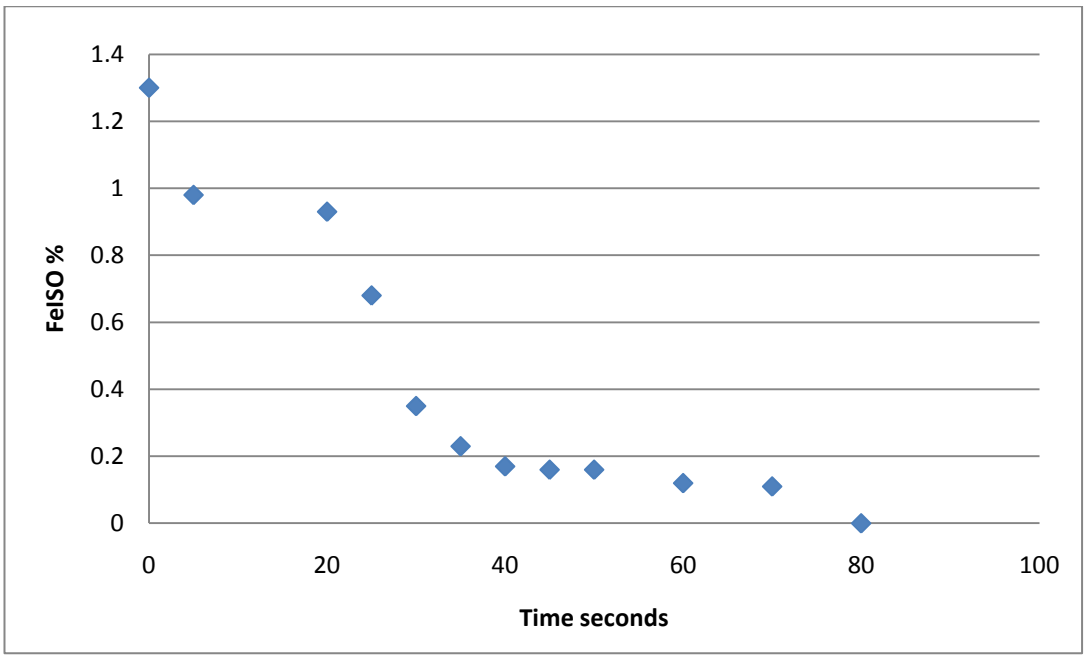

Figure 4.2 Oxygenator wash out time for 1% Isoflurane; The time to completely wash out 1% Isoflurane from the circuit was 80 seconds. The t½ was calculated as 25.4 seconds.

4.2.3 Pilot Experimental Outcomes

The Isoflurane concentration measured in the gas was lower than the vaporiser concentration setting for all but the 5% setting. According to the manufacturer's specifications, the Isotec 3 vaporiser has an acceptable calibration tolerance of 10% of the percentage dial setting. The vaporiser used in this experiment was within the acceptable tolerances. Whilst this test has highlighted a reduction in Isoflurane concentrations the relevance would be negligible as inlet and outlet concentrations were subsequently analysed for each experiment. The time taken for Isoflurane concentrations to stabilise on the Datex analyser was 3 minutes. In the circuit pilot tests (Chapter 3, section 3.2) PaO_2 on the CDI 500 analyser took 4.5 minutes to reach equilibrium resulting in a 5 minute run after each experimental change before recording data.

The Isoflurane concentrations measured in the outlet gas (FeISO) and arterial line were found to be marginally less than the inlet gas (FiISO) although not significantly different.

The gas inlet and outlet were continuous with little resistance to flow so no variation in Isoflurane concentration between FiISO and FeISO was expected or observed. For Isoflurane to pass into the arterial line it had to cross the microporous membrane and there was potential for the membrane to cause a degree of resistance to the gas flow. However, as indicated by the Isoflurane concentration difference between FiISO and the arterial line, a membrane resistance to the varying gas flow was not observed. This result also demonstrated that Isoflurane was not absorbed by the membrane material polypropylene.

The difference in FiO_2 pre and post vaporiser was marked with a notable increase (2.6%) in pre vaporiser FiO_2 when Isoflurane was switched on (1-5%). Manufacturers of oxygen sensors state that volatile anaesthetic agents can interfere with the oxygen reading. The manufacturer of this oxygen analyser (Teledyne AX300) stated a reading error of <1.5% in the presence of Isoflurane but in this test we found greater reading errors of up to 2.6%. For subsequent work the FiO_2 analyser was placed post Isoflurane vaporiser to ensure accurate FiO_2 data collection at oxygenator inlet. If the FiO_2 was measured prior to the vaporiser, it would always be higher than the actual FiO_2 delivered to the oxygenator as the Isoflurane concentration itself would reduce the FiO_2. The Isoflurane was subsequently used at 1% throughout this work in order to represent a clinical concentration. At 1% Isoflurane there was minimal FiO_2 reading error based on this work.

The Isoflurane 1% wash out t½ was calculated as 25.4 seconds which was much quicker than that cited by Henderson *et al* (1988) at 12.2 minutes in normothermic conditions. The work carried out by Henderson *et al* was conducted in patients on cardiopulmonary bypass. The times will be increased *in vivo* due to retention and release of the anaesthetic agent by tissues (Eger 2004). This *in vitro* work was not subjected to these influential factors hence the much quicker clearance of Isoflurane. The t½ for this *in vitro* circuit was

important for experiments conducted in the absence and presence of Isoflurane in a random order to ensure adequate recirculation time was applied for the anaesthetic to be removed. In the following experiments where Isoflurane was discontinued, a minimum period of ten minutes elapsed prior to further experimental work commencing.

4.3 Effects of Isoflurane on O_2 Transfer: Methodology

The experimental circuit was set-up and primed as described in Chapter 3, section 3.1. For each experimental change, the pH, PO_2 and PCO_2 values from the CDI 500 monitor for both venous and arterial blood were recorded after 5 minutes equilibration. Venous and arterial blood saturations were noted from the Spectrum Medical M2 analyser. The oxygenator FiO_2 and FeO_2 were established for each change. Inspired Isoflurane and expired Isoflurane concentrations were also measured via the Datex analyser in either the oxygenator or the deoxygenator gases as appropriate.

4.3.1 Effects of Oxygenator Isoflurane on DO_2

The blood flow was set at 2.5 l/min. The oxygenator was ventilated with 5 l/min mixture of N_2 and O_2 giving FiO_2 ranging 5.9 to 34.7%. Isoflurane was administered via the oxygenator gas line at 0% or 1% for each FiO_2 range. The deoxygenator was ventilated with 5 l/min 5% CO_2 in balanced N_2 and 0.2 l/min CO_2. The test was repeated five times on different days using a new circuit and equine donor each time.

4.3.2 Effects of Deoxygenator Isoflurane on DO_2

The blood flow was set at 2.5 l/min. The oxygenator gas was 5 l/min N_2 and O_2 at varying mixtures to give a FiO_2 ranging 3.3 to 31.8%. Isoflurane was initially delivered via the

oxygenator at 1% concentration for the FiO_2 range. The deoxygenator received 5 l/min 5% CO_2 in balanced N_2 with 0.2 l/min CO_2. The circuit was run for a period of 15 minutes without Isoflurane administration prior to switching the Isoflurane vaporiser to the deoxygenator gas inlet line. The oxygenator and deoxygenator received the same gas regime as previously stated with the deoxygenator gas delivering 1% Isoflurane, via the deoxygenator membrane, to the circuit blood.

4.3.3 Effects of Isoflurane on ODC

The blood flow was set to 2.5 l/min. The deoxygenator gas was 5 l/min 5% CO_2 in balanced N_2 with 0.2 l/min CO_2. The oxygenator was ventilated with a total gas flow of 5 l/min comprising O_2 and N_2 mix achieving FiO_2 ranging 5.9 to 34.7%. Isoflurane was administered via the oxygenator gas inlet line and was set to 0% or 1%. For each Isoflurane setting, ten FiO_2 concentrations within the range 5.9 to 34.7% were randomly tested.

4.3.4 Calculations

The calculations are detailed in Chapter 3, section 3.3.8. Details of Hills Plots are given in Chapter 2, section 2.1.

4.3.5 Statistical Analysis

The statistical analysis has been described in Chapter 2, section 2.2.

4.4 Effects of Isoflurane on the Membrane Diffusion Ability: Methodology

To determine if Isoflurane has an effect on the diffusion ability of the membrane, tests were conducted in the presence of NO and CO. NO and CO are both diffusion limited gases so if Isoflurane exerted an effect on the diffusion capabilities of the membrane, a change in DNO and DCO would be evident.

4.4.1 Effects of Isoflurane on DNO and DCO

The circuit was run with varying blood flow of 0.5, 1.0, 2.0 and 3.0 l/min. The deoxygenator received 5 l/min 5% CO_2 in balanced N_2 with 0.3 l/min CO_2. The oxygenator gas was set to 5 l/min air with 0.3 l/min O_2 resulting in FiO_2 24.8%. NO and CO were added to the oxygenator gas at 5000 ppb and 0.03% respectively. The Isoflurane was randomly set to 0, 1, 2, 3, 4 and 5% in the oxygenator gas and for each of these Isoflurane settings the blood flow was randomly tested at the flow rates detailed above. Inspired and expired NO and CO were established for each change of Isoflurane concentration and blood flow.

4.4.2 Calculations

The DNO and DCO calculations are detailed in Chapter 3, section 3.4.3.

4.5 Effects of Isoflurane on O_2 Transfer: Results

Isoflurane was taken up by the blood as indicated by a reduction in FeISO concentrations compared to FiISO concentrations (Figure 4.3).

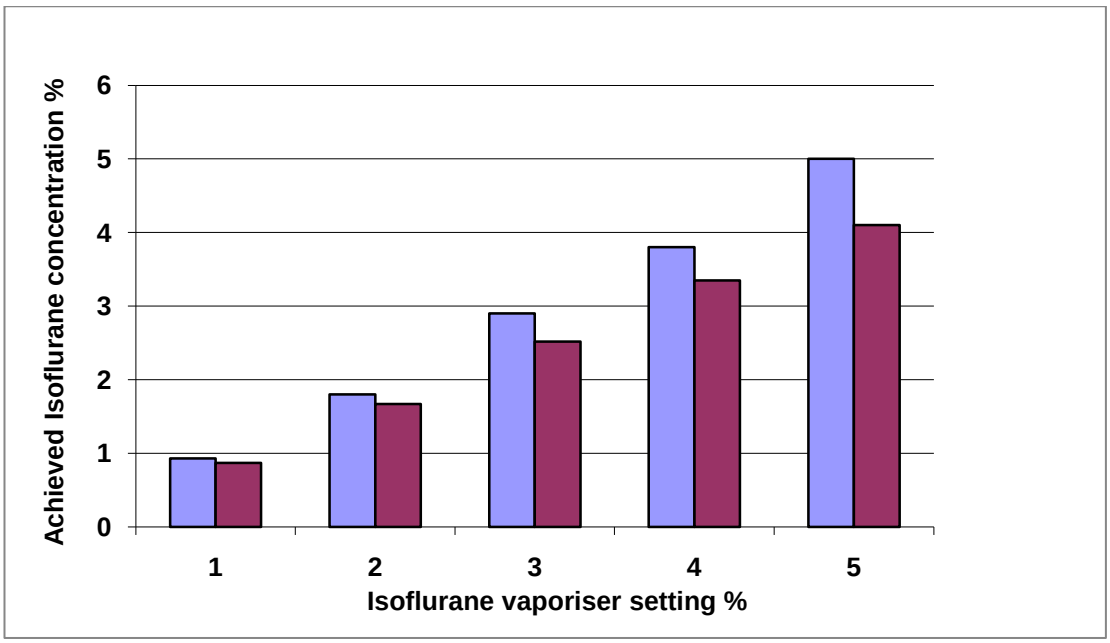

Figure 4.3 FiISO and FeISO values for each vaporiser setting; Reduction of FeISO ■ for each corresponding FiISO ■ demonstrates the uptake of Isoflurane across the membrane oxygenator.

4.5.1 Effects of Oxygenator Isoflurane on DO_2

There was no significant change in PaO_2 (p=0.380) and $P\overline{v}O_2$ (p=0.475) in the presence of 1% Isoflurane when compared to the control (0% Isoflurane). PaO_2 averaged 50.60 ±24.12 mmHg at 0% Isoflurane compared to 46.64 ±21.33 mmHg at 1% Isoflurane (Figure 4.4). $P\overline{v}O_2$ averaged 33.77 ±7.06 mmHg with 0% Isoflurane compared to 32.78 ±6.99 mmHg in the presence of 1% Isoflurane (Figure 4.5).

The addition of Isoflurane to the oxygenator gas flow did not affect $\dot{M}O_2$ (p=0.981). At 0% Isoflurane $\dot{M}O_2$ was 136.83 ±85.40 ml/min compared to 137.24 ±88.12 ml/min at 1% over the FiO_2 range. (Figure 4.6)

The addition of Isoflurane to the oxygenator gas flow did not affect DO_2 (p=0.605). DO_2 was calculated as 2.09 ±1.09 ml/min/mmHg at 0% Isoflurane compared to 2.20 ±1.18 ml/min/mmHg for 1% Isoflurane. (Figure 4.7)

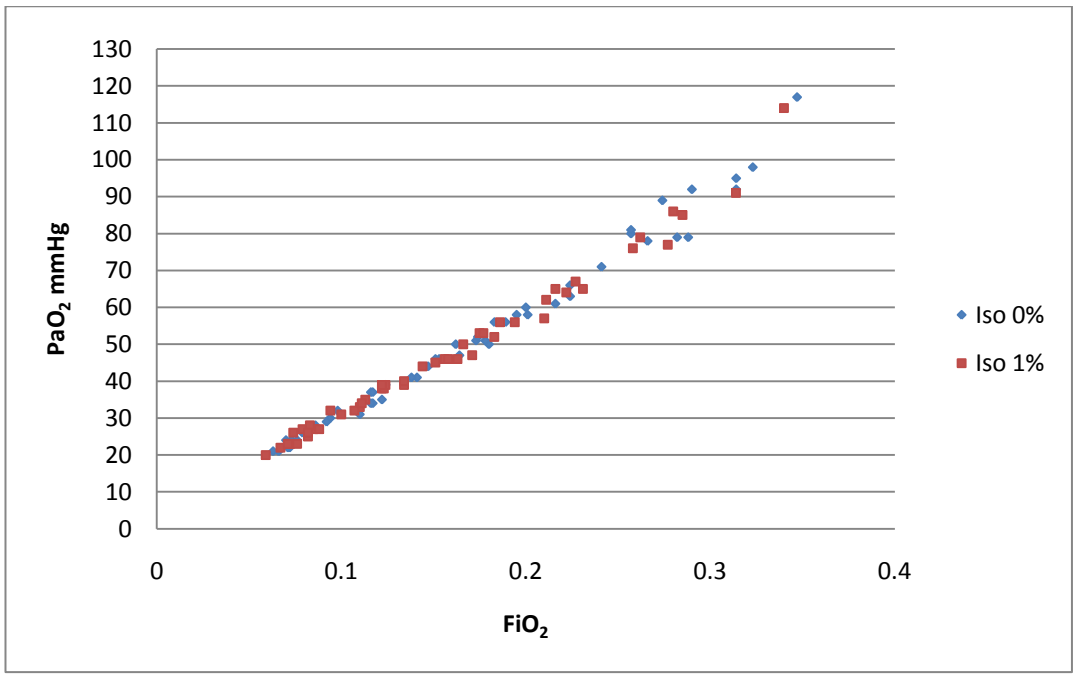

Figure 4.4 Effects of Isoflurane on PaO_2 at varying FiO_2; There was no significant change in PaO_2 (p=0.380) in the presence of 1% Isoflurane ■ when compared to 0% Isoflurane ♦. PaO_2 averaged 50.60 ±24.12 mmHg (range 20 to 117 mmHg) at 0% Isoflurane compared to 46.64 ±21.33 mmHg (range 20 to 114 mmHg) at 1% Isoflurane.

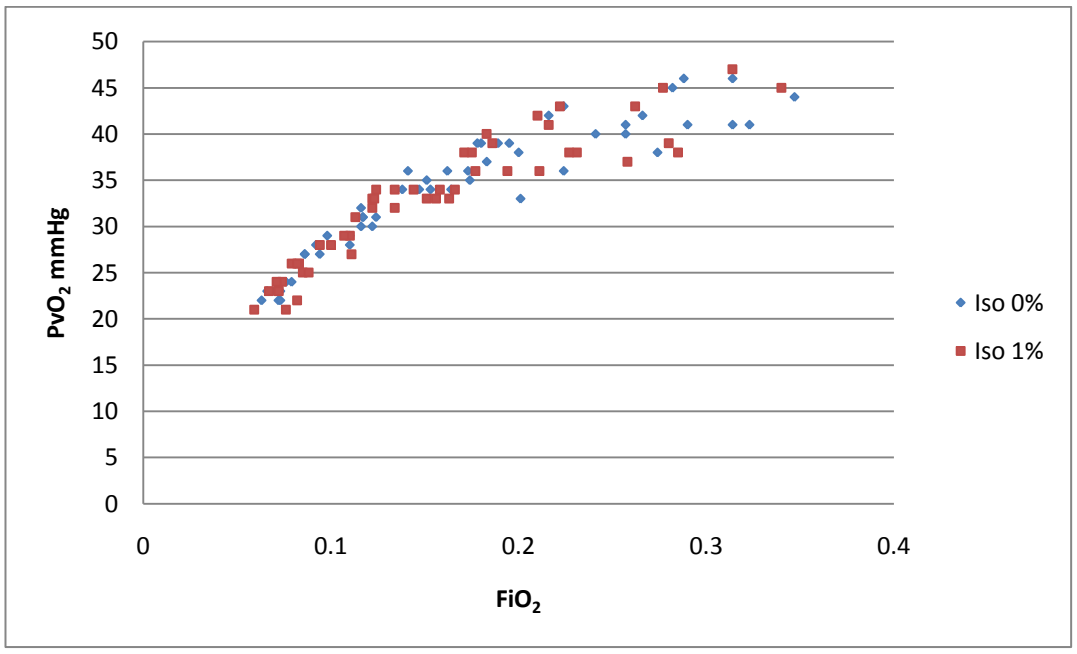

Figure 4.5 Effects of Isoflurane on $P\overline{V}O_2$ with varying FiO_2; There was no significant change in $P\overline{V}O_2$ (p=0.475) in the presence of 1% Isoflurane ■ when compared to 0% Isoflurane ♦. $P\overline{V}O_2$ averaged 33.77 ±7.06 mmHg (range 21 to 44 mmHg) with 0% Isoflurane compared to 32.78 ±6.99 mmHg (range 21 to 45 mmHg) in the presence of 1% Isoflurane.

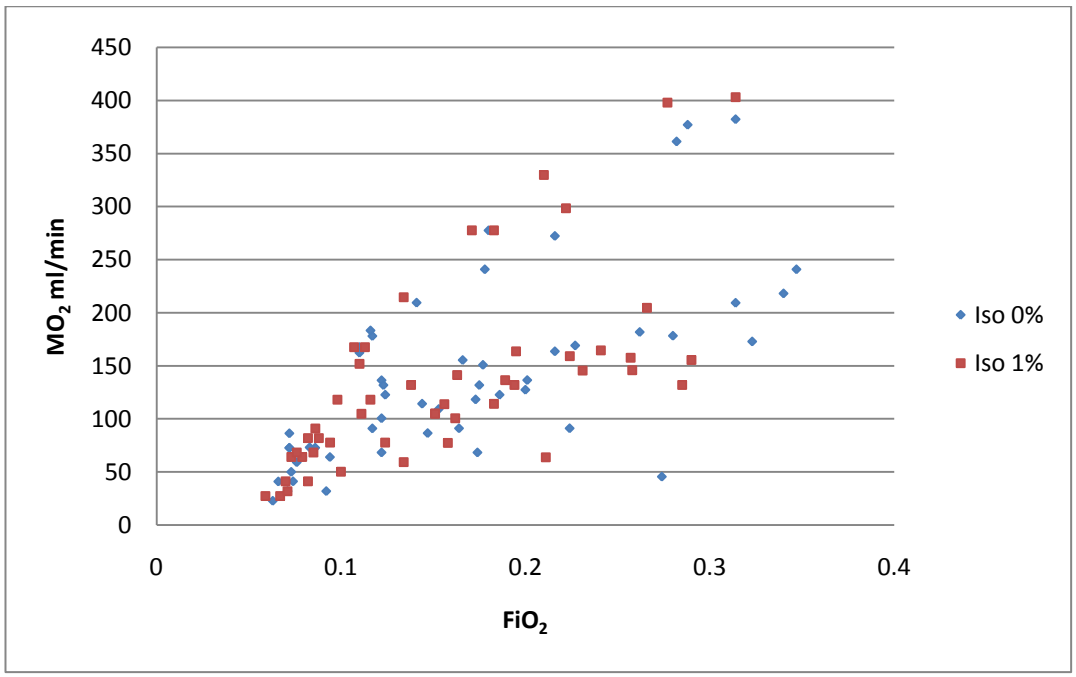

Figure 4.6 Effects of Isoflurane on $\dot{M}O_2$ at varying FiO_2; Addition of Isoflurane to the oxygenator gas flow did not affect $\dot{M}O_2$ (p=0.981). At 0% Isoflurane ♦ $\dot{M}O_2$ was 136.83 ±85.40 ml/min compared to 137.24 ±88.12 ml/min at 1% ■ over the FiO_2 range.

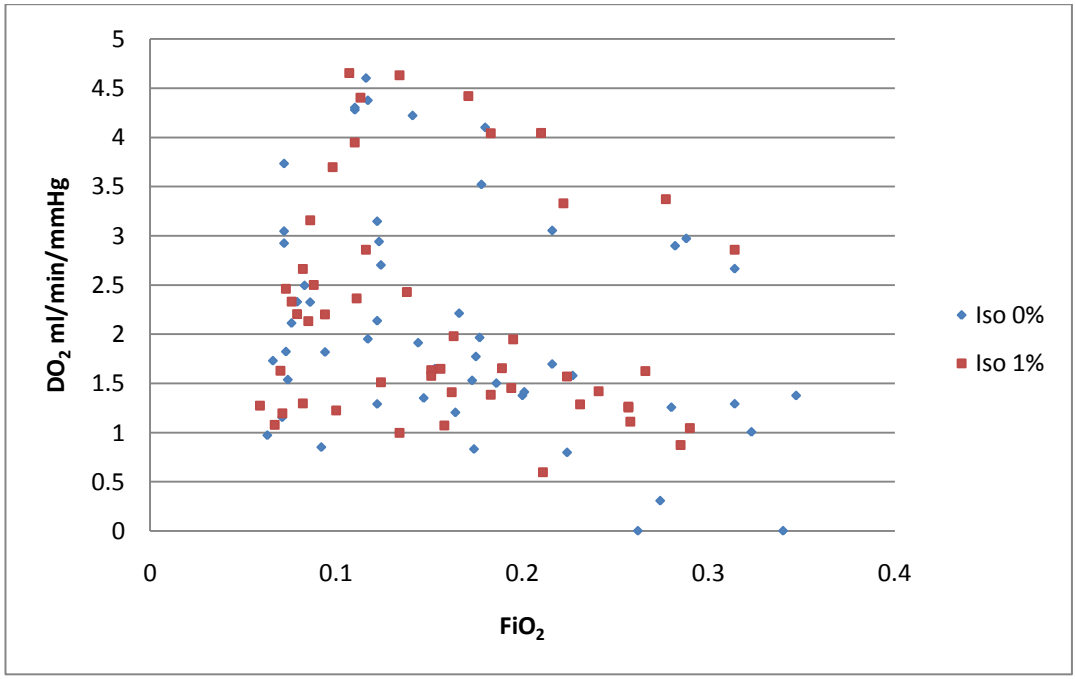

Figure 4.7 Effects of Isoflurane on DO_2 at varying FiO_2; Addition of Isoflurane to the oxygenator gas flow did not affect DO_2 (p=0.605). DO_2 was calculated as 2.09 ±1.09 ml/min/mmHg at 0% Isoflurane ♦ compared to 2.20 ±1.18 ml/min/mmHg for 1% Isoflurane ■.

4.5.2 Effects of Deoxygenator Isoflurane on DO_2

There was no significant difference in DO_2 when Isoflurane (1%) was delivered via the oxygenator or the deoxygenator ($p=0.405$). DO_2 ranged 0.93 to 2.80 ml/min/mmHg (mean 1.68 ±0.35 ml/min/mmHg) for the oxygenator Isoflurane and ranged 0.92 to 2.95 ml/min/mmHg (mean 1.91 ±0.40 ml/min/mmHg) for the deoxygenator Isoflurane.

4.5.3 Effects of Isoflurane on ODC

SaO_2 was plotted against PaO_2 to highlight the arterial ODC (Figure 4.8). The arterial ODC presented as a Hills plot (Figure 4.9) showed good correlation between log PaO_2 and SaO_2 (S/1-S) ($p<0.0001$). The arterial ODC showed no significant shift in the presence of 1% Isoflurane compared to the control group (0% Isoflurane) ($p=0.311$).

$S\bar{v}O_2$ was plotted against $P\bar{v}O_2$ to form the venous ODC (Figure 4.10). When plotted as a Hills plot (Figure 4.11) there was good correlation between the log $P\bar{v}O_2$ and $S\bar{v}O_2$ (S/1-S) ($p<0.0001$). There was no significant shift of the ODC in the presence of 1% Isoflurane compared to the control group (0% Isoflurane) ($p=0.751$).

The P_{50} was calculated from the venous ODC Hills plot as 24.23 mmHg for blood exposed to 0% Isoflurane compared to 24.00 mmHg for blood exposed to 1% Isoflurane.

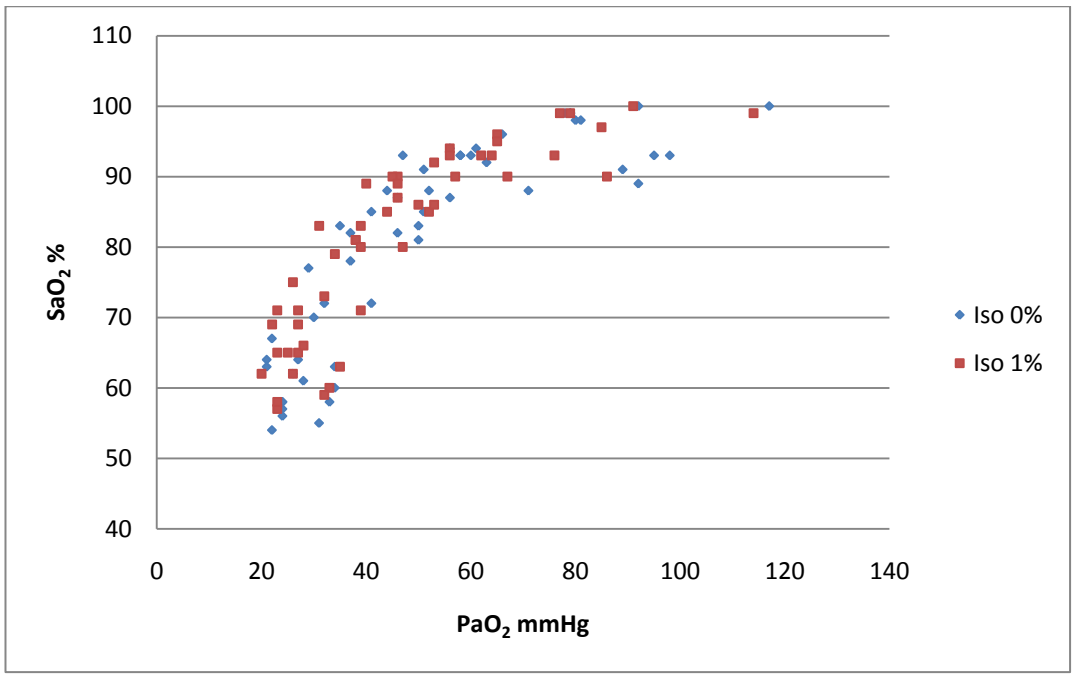

Figure 4.8 Effects of Isoflurane on the Arterial ODC; The arterial ODC showed no significant shift in the presence of 1% Isoflurane ■ compared to the control group ♦ (0% Isoflurane) (p=0.311).

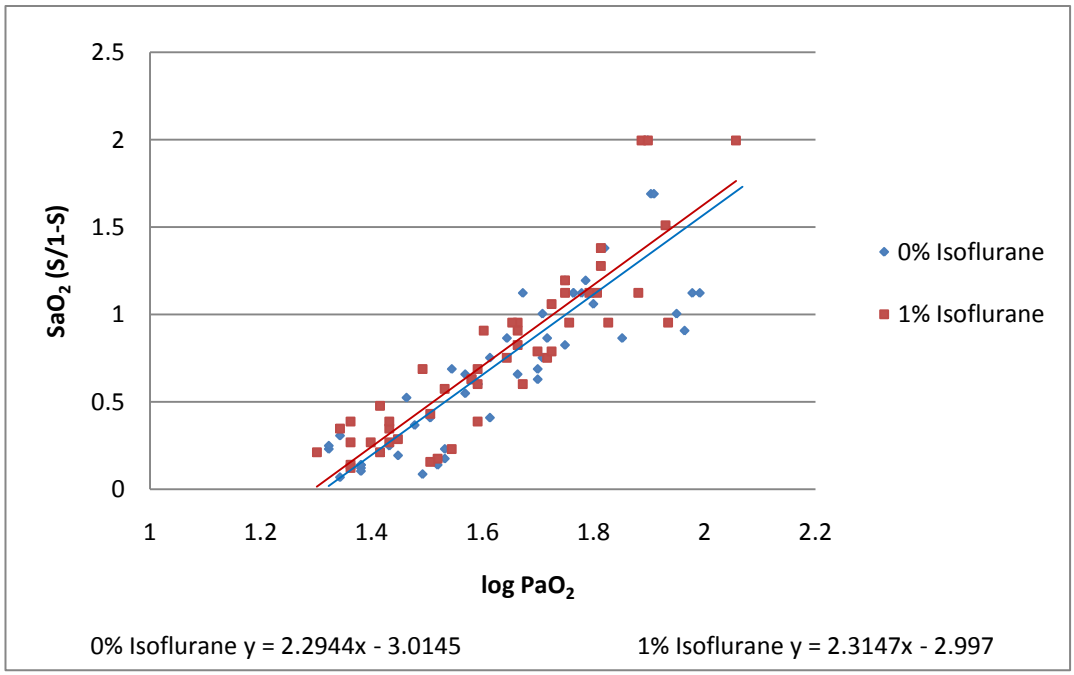

Figure 4.9 Effects of Isoflurane on the arterial ODC – Hills plot; The arterial ODC presented as a Hills plot showed good correlation between log PaO_2 and SaO_2 (S/1-S) ($p<0.0001$). The arterial ODC showed no significant shift in the presence of 1% Isoflurane ■ compared to the control group ♦ (0% Isoflurane) (p=0.311).

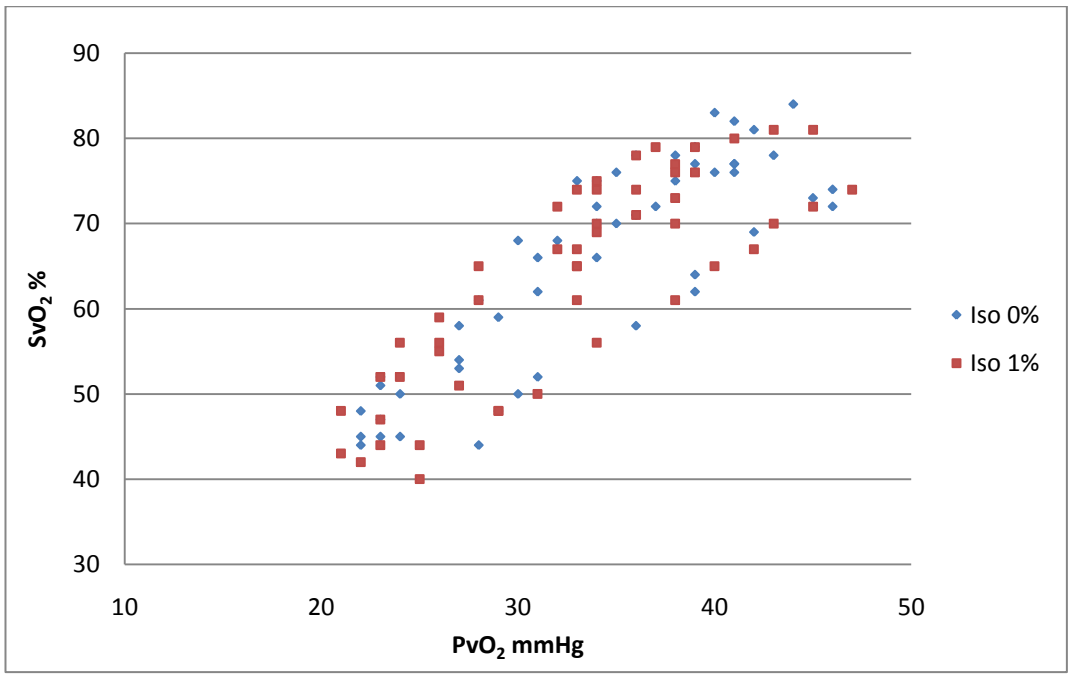

Figure 4.10 Effects of Isoflurane on the Venous ODC; There was no significant shift of the ODC in the presence of 1% Isoflurane ■ compared to the control group ♦ (0% Isoflurane) (p=0.751).

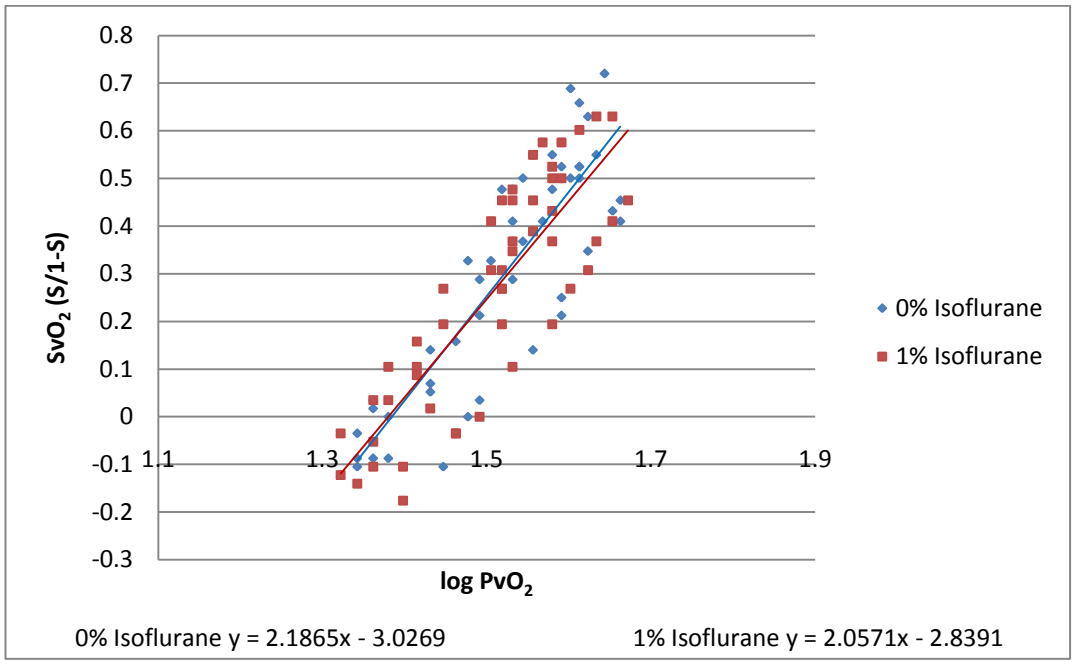

Figure 4.11 Effects of Isoflurane on the Venous ODC – Hills plot; When plotted as a Hills plot there was good correlation between the log P $\overline{V}$ O_2 and S $\overline{V}$ O_2 (S/1-S) (p<0.0001). There was no significant shift of the ODC in the presence of 1% Isoflurane ■ compared to the control group ♦ (0% Isoflurane) (p=0.751).

Table 4.4 Effects of Isoflurane on DO_2 Data Summary

Effects of Isoflurane on DO_2				
Parameter	***Trend***	***Statistical value***	***p value***	***d.f. or n***
PaO_2	No change	*t*=0.881	p=0.380	d.f.=101
$P\bar{v}O_2$	No change	*t*=0.718	p=0.475	d.f.=101
$\dot{M}O_2$	No change	*t*=-0.024	p=0.981	d.f.=101
DO_2	No change	*t*=-0.518	p=0.605	d.f.=101
Deoxy Iso DO_2	No change	*t*=-0.852	p=0.405	d.f.=18
Art ODC	Hills Correlation No ODC shift	R^2=0.762 *t*=1.019	p<0.0001 p=0.311	d.f.=99 d.f.=99
Ven ODC	Hills Correlation No ODC shift	R^2=0.729 *t*=-0.318	p<0.0001 p=0.751	d.f.=102 d.f.=102

4.6 Effects of Isoflurane on the Membrane Diffusion Ability: Results

4.6.1 Effects of Isoflurane on DNO and DCO

DNO (p=0.001) and DCO (p<0.0001) increased curvilinearly in the presence of Isoflurane 0% to 5% (Figure 4.12). Table 4.5 shows the mean and SD values for DNO and DCO for each Isoflurane concentration. The effect was predominantly seen at the 4% and 5% Isoflurane concentrations. If the test was conducted on the 0 to 3% 'clinical' Isoflurane concentration range neither DNO (p=0.622) or DCO (p=0.340) were significantly increased.

Table 4.5 Effects of Isoflurane Concentration on Mean DNO and DCO

Mean DNO and DCO values for each Isoflurane concentration showed a curvilinear increase statistically significant over the range 0-5% but not the clinical range 0-3%.

Isoflurane Concentration %	DNO ml/min/mmHg Mean (SD)	DCO ml/min/mmHg Mean (SD)
0 %	4.50 (1.42)	0.74 (0.14)
1 %	3.76 (0.30)	0.76 (0.14)
2 %	3.83 (0.16)	0.82 (0.17)
3 %	3.96 (0.20)	0.83 (0.16)
4 %	5.35 (0.25)	1.07 (0.16)
5 %	6.15 (0.44)	1.22 (0.08)
0-5% stats	*r*=0.620, n=24 p=0.001	*r*=0.721, n=24 p<0.0001
0-3% stats	*r*=0.133, n=16 p=0.622	*r*=0.255, n=16 p=0.340

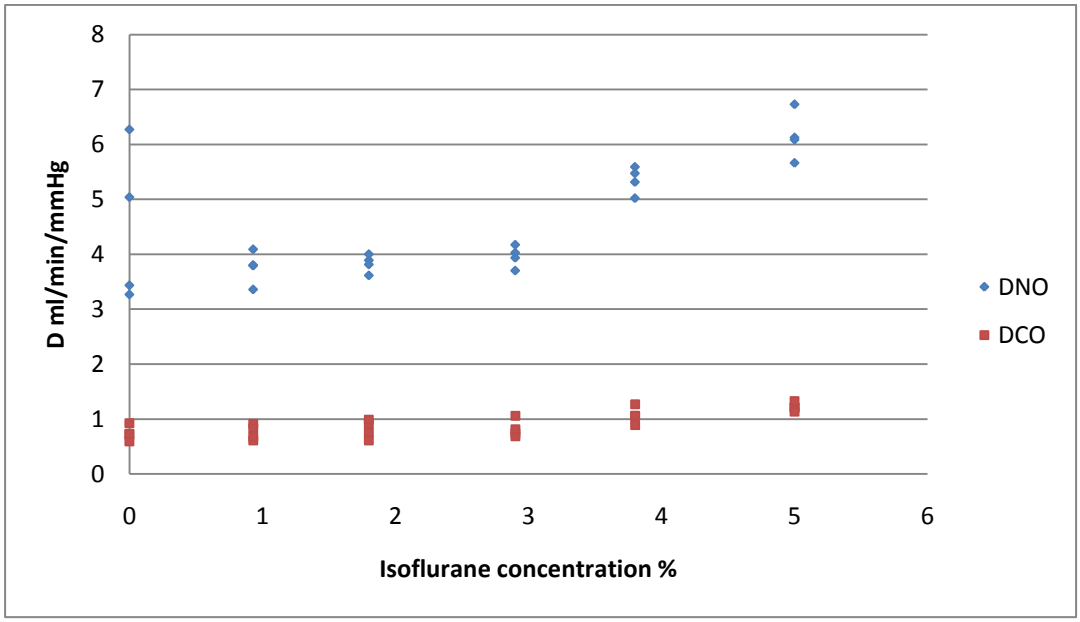

Figure 4.12 Effects of Isoflurane on DNO and DCO; DNO ♦ (p=0.001) and DCO ■ (p<0.0001) increased curvilinearly in the presence of Isoflurane 0% to 5%. The effect was predominantly seen at the 4% and 5% Isoflurane concentrations. In the 0 to 3% 'clinical' Isoflurane concentration range neither DNO (p=0.622) or DCO (p=0.340) were significantly increased.

4.7 Implications of Isoflurane Use in the Membrane Oxygenator: Discussion.

During cardiopulmonary bypass, Isoflurane is added to the oxygenator gas providing either anaesthetic to the patient or hypertension treatment (Alston 1989). Oxygenator manufacturers discourage the use of volatile anaesthetic agents in their devices yet the practice is commonplace. It is important to establish if Isoflurane may result in altered gas exchange properties of the oxygenator. This study investigated the effects of Isoflurane on oxygen transfer within a membrane oxygenator using a continuously running oxygenator and deoxygenator model.

Previously, preliminary results indicated that Isoflurane in the oxygenator gas caused an increase in oxygen uptake ($\dot{M}O_2$), significant at all concentrations but not dose related (1 to 5%). The data showed a venous ODC left shift although the arterial ODC was unaffected. The apparent left shift of the venous ODC corresponded with the observed increase in oxygen uptake (Borland *et al* 2007b). Further investigation in this work suggested that the FiO_2 analyser was affected by Isoflurane vaporiser interference. The $\dot{M}O_2$ equation is based upon the FiO_2 and FeO_2 difference, multiplied by gas flow. Therefore, any interference of FiO_2 analysis may inadvertently affect $\dot{M}O_2$. Manufacturers of the FiO_2 analyser (AX300) have cited an interference rate of <1.5% however in this work it was seen to increase to 2.6% at 1-5% Isoflurane concentrations. Following the pilot study, the AX300 was repositioned downstream of the vaporiser to minimise interference and to establish accurate FiO_2 delivery at the oxygenator. After this change no effects on $\dot{M}O_2$ were evident. The results of the experiments detailed in this chapter were repeated with consistency validating these findings rather than the presented preliminary work (Borland *et al* 2007b). Muhle *et al* (2001) conducted a similar study in a hollow fibre microporous polypropylene membrane oxygenator concluding no effect of

Isoflurane on $\dot{M}O_2$. Muhle's study involved venous conditioning of bovine blood before passing through the test oxygenator exposed to gas containing Isoflurane. It was a single-pass experiment of thirty seconds duration. Based on this work, the circuit run time for Muhle's study was not adequate for Isoflurane to equilibrate between the blood and gas phases. In this experiment, the washout phase t½ was calculated as 25.4 seconds and therefore five minutes were allowed to elapse after each settings change. Despite this, the conclusions reached by Muhle and this group are the same. The FiO_2 analyser placement was a significant influence in this work. Clinically, these analysers are often placed prior to the vaporiser so patients will receive less inspired oxygen than the analyser displays.

There was no significant change in PaO_2 or $P\overline{v}O_2$ in the presence of Isoflurane compared to controls. This coupled with an absence of an Isoflurane effect on $\dot{M}O_2$ adds validity to the conclusion that Isoflurane does not affect oxygen transfer in the membrane oxygenator. An ODC experiment was conducted to determine if Isoflurane affected the carriage of oxygen in blood. The circuit equipment was modified to simulate a tonometer, a novel approach not published by any other group. By simultaneously measuring arterial and venous PO_2 and arterial and venous sO_2, the ODC was determined. Addition of 1% Isoflurane had no significant effect on arterial or venous PO_2 or sO_2 in the membrane oxygenator. Subsequently, the venous and arterial ODCs were unaffected by 1% Isoflurane. This finding concluded that 1% Isoflurane did not affect oxygen carriage in the blood.

To determine if Isoflurane affected gas transfer properties of the membrane oxygenator, the circuit was run with nitric oxide (NO) and carbon monoxide (CO) present in the oxygenator gas. NO and CO are both diffusion limited gases which could indicate changes in membrane porosity or permeability. In this work, there was no statistically

significant difference in DNO or DCO between control and Isoflurane groups for clinical concentrations of 1 to 3%. This concluded that the membrane gas transfer properties are unaffected by 1-3% Isoflurane, corresponding with the lack of effect in oxygen transfer across the membrane where 1% Isoflurane was used. 1% Isoflurane was selected as it represented the clinical Isoflurane concentration for the membrane oxygenator (Rhodia NZ Ltd 1999). At higher Isoflurane concentrations (4 and 5%) DNO and DCO both significantly increased. The reason for this apparent membrane effect exerted by high Isoflurane concentrations remains unclear. It is speculated that in higher Isoflurane concentrations the membrane pores are surrounded by a vapour barrier rather than a water barrier which may aid NO and CO transfer. Although DNO and DCO increases observed at higher Isoflurane concentrations suggest an effect on the membrane, this does not account for the DO_2 increase in the preliminary data at all concentrations. The FiO_2 analyser placement in relation to the Isoflurane vaporiser was deemed accountable for the enhanced DO_2 rather than a membrane effect. In this work, clinical Isoflurane concentrations did not affect the membrane oxygenator gas transfer ability.

An interaction between the membrane and Isoflurane (4 and 5%) was considered. FiISO and FeISO data demonstrated uptake of Isoflurane from the gas. Hickey *et al* (1996) investigated the effects of uptake and elimination of Isoflurane in different membrane oxygenators, concluding that microporous polypropylene membranes have low affinity for Isoflurane. A FiISO concentration of 1.15% administered via the oxygenator gas resulted in bovine blood concentrations of 2.6-2.9mg/dl after five minutes of exposure (Hickey *et al* 1996). FiISO 1% would achieve similar Isoflurane blood concentrations in this study. The pilot work showed the same Isoflurane concentrations present in the oxygenator inlet gas, in the exhaust gas and arterial line. If the membrane absorbed Isoflurane a reduction in Isoflurane concentration in the arterial line would have been observed. Based on this

work and previously reviewed studies (Crosbie *et al* 1998 and Lanquetot *et al* 2002), it is concluded that Isoflurane does not interact with the polypropylene membrane.

The circuit developed for this work can be used to investigate the effects of a volatile anaesthetic agent on gas transfer. Manufacturers of membrane oxygenators would need to seek approval from the regulatory bodies to permit use of volatile anaesthetic agents in their devices. Extensive tests would have to be conducted, with this work being an example of that requirement. This work demonstrates that Isoflurane used within the clinical range has no effect on oxygen transfer in polypropylene microporous membrane oxygenators or oxygen carriage in the blood. Administration of Isoflurane via polypropylene microporous membrane oxygenators during cardiopulmonary bypass will not adversely affect patient care.

Chapter 5: Effects of Haemolysis on DO_2 DCO_2 DNO and DCO

Aims

To test the hypothesis that haemolysis of whole blood does not affect DO_2, DCO_2, DNO and DCO in the membrane oxygenator circuit. There is little data on the effects of haemolysis on DO_2 and DCO_2 due to ethical issues of inducing gross haemolysis in living species. Patients exhibiting clinical haemolysis are likely to have secondary effects such as altered lung physiology which may preclude reliable gas transfer data. The membrane oxygenator model designed in this work facilitates the investigation into the effects of haemolysis on gas transfer. NO is used in conjunction with CO for lung function testing whereby DNO is considered to reflect alveolar-capillary diffusion (Heller and Schuster 1998). NO is a diffusion limited gas which has an instantaneous reaction with oxyhaemoglobin in contrast to CO. Based on this D_LNO would be equal to D_MNO (Guenard *et al* 1987). There has been speculation that the specific conductance of NO within the blood (θ_{NO}) may not be infinite as previously assumed (Borland 1990, 2003, 2005, 2006, 2010). If this is the case then the values for D_LNO do not represent D_MNO as the NO reaction with blood may influence the results. To determine the effects of gross haemolysis on DO_2, DCO_2, DNO and DCO the circuit was primed with equine blood and gradually haemolysed by addition of water to the circuit volume. To reflect clinical levels of haemolysis (up to 2.1 g/dl in long term dialysis patients, Rother *et al* 2005) a free Hb solution was prepared and gradually added to the circuit blood where DO_2, DNO and DCO were evaluated.

5.1 Altering the Circuit Blood via Gross Haemolysis: Circuit Set-Up.

To achieve haemolysis, a quantity of water was to be added to the circuit blood to cause the RBC to swell and lyse. The venous reservoir facilitates the addition of volume to the circuit via access ports on the top. Three types of port were available, Luer lock, ¼" and ⅜". The Luer lock allows attachment of a syringe or a fluid administration line whereas the ¼" and ⅜" ports attach appropriate sized tubing. In the first pilot experiment, water was added via a fluid administration line attached to a Luer lock on top of the reservoir. A 500 ml tap water aliquot was measured using a measuring cylinder and added via the fluid administration line. A second 500 ml aliquot of tap water was added in the same way. In total, 1000 ml of water was added which achieved visual haemolysis, also confirmed by a potassium increase from 5.4 to 9.5 mmol/l measured via the CDI 500 analyser. The volume to be added in subsequent experiments was likely to be 1000 ml but over a slower flow rate such as 60 ml/min so a gradual haemolysis would occur. Therefore, a more consistent volume addition methodology was required.

A second reservoir was added to the circuit. ⅜" PVC tubing was attached to the reservoir outlet, directed around a second calibrated stockert positive displacement pump (water pump) and attached to the available ⅜" access port on the venous reservoir. The second reservoir was filled with 1500 ml of tap water via a fluid administration line. The second (water) pump was utilised to administer the water to the circuit at a designated flow rate i.e. 60 ml/min.

Haemolysis in the circuit blood was determined by an increase in blood potassium levels as potassium is released from the red blood cell (RBC) when lysed by water. Potassium

levels were analysed using the CDI 500 analyser with a potassium range 1.0 to 10.0 mmol/l (bias 0.12 mmol/l).

5.2 Free Hb Solution Addition to the Circuit Blood: Circuit Set-Up.

5.2.1 Free Hb Solution Preparation

For preparation of free Hb solution, 500 ml of horse blood (PCV 50% and 44%, Hb 17.0 and 15.2 g/dl) was stored upright overnight, refrigerated, to allow the separation of RBCs from the plasma. The following morning, plasma was expressed from the top of the blood bag by a separating clamp leaving the RBCs in the bottom of the bag. Tap water was added to a total volume of 500ml to achieve complete haemolysis. The blood bag containing the free Hb solution was agitated by hand prior to removal of the free Hb solution into a syringe.

5.2.2 Addition of the Free Hb Solution to the Circuit

The circuit was set-up and primed (Chapter 3, section 3.1). A single equine blood donation was used to prime the circuit and to create the free Hb solution for that circuit. While the circuit was operating, free Hb solution was added into the top of the venous reservoir via syringe in measured aliquots of 25 or 30 ml. In the first experiment, 330 ml total free Hb solution was added to ensure adequate DNO data was accomplished. After data examination, subsequent experiments received 250 ml total free Hb solution to allow for comparisons with an Oxyglobin transfusion (250 ml). The free Hb solution added to the circuit was calculated to give a free Hb concentration of between 0.19 to 2.4 g/dl in the circulating blood.

5.3 Pilot Experiments With Gross Haemolysis

Aims

The pilot experiments were designed to clarify the experimental protocol. The initial preliminary experiment was conducted to assess what amount of water addition to the circuit was necessary to create haemolysis as determined by an increase in K^+.

The second pilot test was conducted to establish methodology for a gradual haemolysis to fully investigate the effects on gas transfer. A set amount of water was to be pumped into the circuit reservoir at a low flow rate per minute to achieve gradual haemolysis of the circuit blood.

5.3.1 Pilot Circuit Set-up and Methodology

Following all experimental changes to the circuit, the blood was allowed to recirculate for 5 minutes to allow equilibrium to occur between the blood and analysers as discussed in Chapter 3, section 3.2.

1. Quantifying the Total Water Addition for Haemolysis Induction

The circuit was set up and primed with equine blood (Chapter 3, section 3.1). The blood pump was set at 2.5 l/min. The oxygenator gases were set to 5 l/min air with 0.3 l/min O_2 and the deoxygenator gases were set to 5 l/min 5% CO_2 in balanced N_2 with 0.2 l/min CO_2. 500 ml of circuit blood was removed by pumping out via a giving line attached to the venous reservoir return tubing. This was replaced by 500 ml of water into the top of the venous reservoir via another fluid administration line. After 5 minutes of recirculation the CDI 500 results were recorded before another 500 ml of water was added to the circuit

via the venous reservoir. The CDI 500 results were recorded after five minutes of circulation.

2. Verification of Gradual Water Addition Methodology for Inducing Haemolysis

The circuit was set-up and primed with equine blood (Chapter 3, section 3.1). The blood pump was set at 2.5 l/min. A second reservoir was filled with water, which was pumped via a second Stockert roller pump (water pump) into the top of the venous reservoir. The water pump was set to 60 ml/min to achieve a gradual addition of 1500 ml of water into the circuit over 25 minutes. The oxygenator gases were set to 5 l/min air and the deoxygenator gases were set to 4.5 l/min 5% CO_2 in balanced N_2 with 0.1 l/min CO_2.

For each pilot run the potassium levels were monitored as they indicated the level of haemolysis within the circuit. The pH, PO_2, PCO_2 and K^+ values from the CDI 500 monitor for both venous and arterial blood were recorded at 5 minute intervals during the volume addition. The oxygenator inspired and expired oxygen content was also established.

5.3.2 Pilot Experimental Results

1. Quantifying the Total Water Addition for Haemolysis Induction

The starting Hb of the circuit blood was 11.3 g/dl. The potassium level was 5.4 mmol/l prior to water addition. After the first 500 ml of water was added to the circuit via displacement the potassium rose to 7.2 mmol/l. The second aliquot of 500 ml water increased potassium to 9.5 mmol/l. The pHa and pHv both decreased with addition of water to the circuit from 7.41 to 7.19 and 7.34 to 7.08 respectively. PaO_2, $P\overline{v}O_2$, $PaCO_2$ and $P\overline{v}CO_2$ all remained stable during haemolysis averaging 89.33 ±5.69 mmHg, 30.67

±1.15 mmHg, 31.33 ±0.57 mmHg and 46.33 ±0.57 mmHg, respectively. $\dot{M}O_2$ and $\dot{M}CO_2$ showed no change, averaging 111.25 ±14.17 ml/min and 137.89 ±4.37 ml/min, respectively. DO_2 and DCO_2 followed the same trend and averaged 0.77 ±0.12 ml/min/mmHg and 10.76 ±0.58 ml/min/mmHg respectively. No statistics were performed on this data as the sample size (n=3) was too small.

2. Verification of Gradual Water Addition Methodology for Inducing Haemolysis

The Hb at the start of the experiment was 10.1 g/dl. 1500ml of water was added to the circuit at 60 ml/min over 25 minutes duration. Haemolysis was indicated by a curvilinear rise in potassium levels (r=0.986, n=6, p<0.001) from 6.5 mmol/l up to 10 mmol/l achieved after 1200 ml of water addition. At 1200 ml water addition, the upper limit of the CDI 500 sensors (10 mmol/l) was reached with this level indicating a significant presence of haemolysis.

The pHv (R^2=0.962, d.f.=5, p<0.01) and pHa (R^2=0.945, d.f.=5, p<0.01) were seen to decrease linearly with increasing addition of water to the circulating blood from 7.09 to 6.91 and 7.12 to 6.95, respectively.

PaO_2 was seen to slightly decrease from 58.5 mmHg to 48.0 mmHg over the duration of the experiment. Similarly $P\overline{v}O_2$ decreased from 39.5 mmHg to 24.75 mmHg. Both $PaCO_2$ and $P\overline{v}CO_2$ remained stable at 56.36 ±2.34 mmHg and 66.50 ±0.61 mmHg, respectively.

$\dot{M}O_2$ increased from 215.22 ml/min with no water addition to a mean of 272.62 ±21.39 ml/min throughout the haemolysis. DO_2 was initially 2.02 ml/min/mmHg with no addition of water but then averaged 2.52 ±0.10 ml/min/mmHg during haemolysis. Piiper

DO_2 showed the same trend as Lilienthal DO_2 at 2.05 ml/min/mmHg with no water added and then averaged 2.58 ±0.10 ml/min/mmHg during haemolysis. $\dot{M}CO_2$ remained stable throughout the addition of water to the circuit at 101.94 ±0.95 ml/min. DCO_2 similarly stabilised at 17.71 ±3.56 ml/min/mmHg throughout.

5.3.3 Pilot Experimental Outcomes

From the pilot experiments, the methodology was adequate in providing significant haemolysis in the circuit blood as determined by an increase in K^+. The maximum threshold for K^+ analysis by the CDI 500 was 10 mmol/l and the water addition needed to achieve this was approximately 1000 ml. The circuit blood volume was usually 2000 ml so to achieve gross haemolysis 1000 ml of water was added to give a total circulating volume of 3000 ml. The addition of water via the second reservoir and water pump worked well. The results showed a curvilinear rise in K^+ indicating a gradual lysis leading to gross haemolysis. This methodology was easy to execute with consistency in results. For the main experiments, the water was to be added via a second 'water' pump or via individual syringe aliquots at a slow flow rate.

For the free Hb solution addition, the methodology would incorporate syringe aliquots followed by 5 minutes recirculation, facilitating a slow increase in free Hb. Based on the previous haemolysis pilot work no specific experiments were required for free Hb.

5.4 Effects of Haemolysis on O_2 Transfer: Methodology

The circuit was set up and primed with equine blood (Chapter 3, section 3.1). For each experimental change, the circuit was allowed to run for 5 minutes for equilibrium to be

achieved as discussed in Chapter 3, section 3.2. Following this, the pH, PO_2 and PCO_2 values from the CDI 500 analyser were noted. Venous and arterial blood saturations were recorded from the Spectrum Medical M2 analyser. The oxygenator FiO_2 and FeO_2 were established for each change. Potassium levels were recorded from the CDI 500 analyser as an indicator for haemolysis.

5.4.1 Effects of Gross Haemolysis on O_2 Transfer

The blood flow was set at 2.5 l/min. A second reservoir was filled with water and pumped via a second Stockert roller pump (water pump) into the top of the main venous reservoir. The oxygenator gases were 5 l/min air with 0.3 l/min O_2 and the deoxygenator received 5 l/min 5% CO_2 in balanced N_2 with 0.2-0.3 l/min CO_2. In the first circuit set-up the water pump was set to 30 ml/min in order to investigate a slower rate of haemolysis. Data from the analysers was noted every 5 minutes. In the subsequent circuit set-up, water was added in 60 ml syringe aliquots into the top of the venous reservoir.

5.4.2 Effects of Free Hb Solution on O_2 Transfer

The blood flow was set at 2.5 l/min. The oxygenator received 5 l/min air with 0.3 l/min O_2. The deoxygenator gases were set to 5 l/min 5% CO_2 in balanced N_2 with 0.2 l/min CO_2. At five minute intervals 25 or 30 ml aliquots of free Hb Solution were added into the top of the venous reservoir up to a total of 250 or 330ml, respectively.

5.4.3 Effects of Free Hb Solution on ODC

The blood flow was set at 2.5 l/min. The oxygenator was ventilated with 5 l/min N_2 and O_2 at varying mixtures to give a FiO_2 ranging 5.0 to 43.5%. The deoxygenator gases were set to 5 l/min 5% CO_2 in balanced N_2 with 0.2 l/min CO_2. The ODC experiment was conducted with whole equine blood in the absence or presence of 250 ml free Hb solution.

The blood saturations were plotted against the blood oxygen partial pressures for both the venous and arterial blood to achieve the venous and arterial ODCs.

5.4.4 Shunt Fraction in Gross Haemolysis

Using the same methodology as that described for the effects of gross haemolysis on O_2 transfer (section 5.4.1), the shunt fraction was calculated from the data achieved.

5.4.5 Calculations

The calculations used for the data generated in this chapter were those detailed in Chapter 3, section 3.3.8. Hills plots are described in Chapter 2, section 2.1.

5.4.6 Statistical Analysis

Statistical analysis is described in Chapter 2, section 2.2.

5.5 Effects of Haemolysis on DNO and DCO: Methodology

5.5.1 Effects of Gross Haemolysis on DNO and DCO

The same methodology was used as that described in section 5.4.1. NO was added to the oxygenator gas at 4500-5000 ppb for the first experimental run, rising to 6100-6300 ppb for the second experimental run. The increase in NO addition was to ensure that the NOout concentration did not drop below a detectable amount so that DNO was calculable. The CO was also added to the oxygenator gas at a concentration of 0.03%. At five minute intervals NOin, NOout, COin and COout were established.

5.5.2 Effects of Free Hb Solution on DNO and DCO

The same methodology as that described in section 5.4.2 was used. NO was added to the oxygenator gas at 7200, 14700, 12300 and 17900 ppb for each run to ensure that the inlet concentration exceeded that crossing the membrane. CO was added to the oxygenator gas at 0.03%. Five minutes after each aliquot of free Hb solution, the NOin, NOout, COin and COout were determined.

5.5.3 Effects of DNO on the ODC

The same methodology as that described in section 5.4.3 was used. NO was added to the oxygenator gas at 10000 ppb. The ODC in the absence and presence of NO was plotted and compared.

5.5.4 Calculations

The DNO and DCO calculations are detailed in Chapter 3, section 3.4.3.

5.6 Effects of Haemolysis on O_2 Transfer: Results

5.6.1 Effects of Gross Haemolysis on O_2 Transfer

The initial Hb concentrations of the two circuits were 8.9 g/dl and 10.6 g/dl. In run 1, 1300 ml of water was added at a flow rate of 30 ml/min over fifty minutes. In the second run, 800 ml of water was added using 60 ml aliquots over sixty minutes. K^+ was seen to increase curvilinearly with increasing water addition to the circuit for both experimental runs ($p<0.0001$). K^+ increased from 3.3 up to 9.9 mmol/l where the upper threshold of the CDI 500 analyser was exceeded after 900ml of water addition (Figure 5.1).

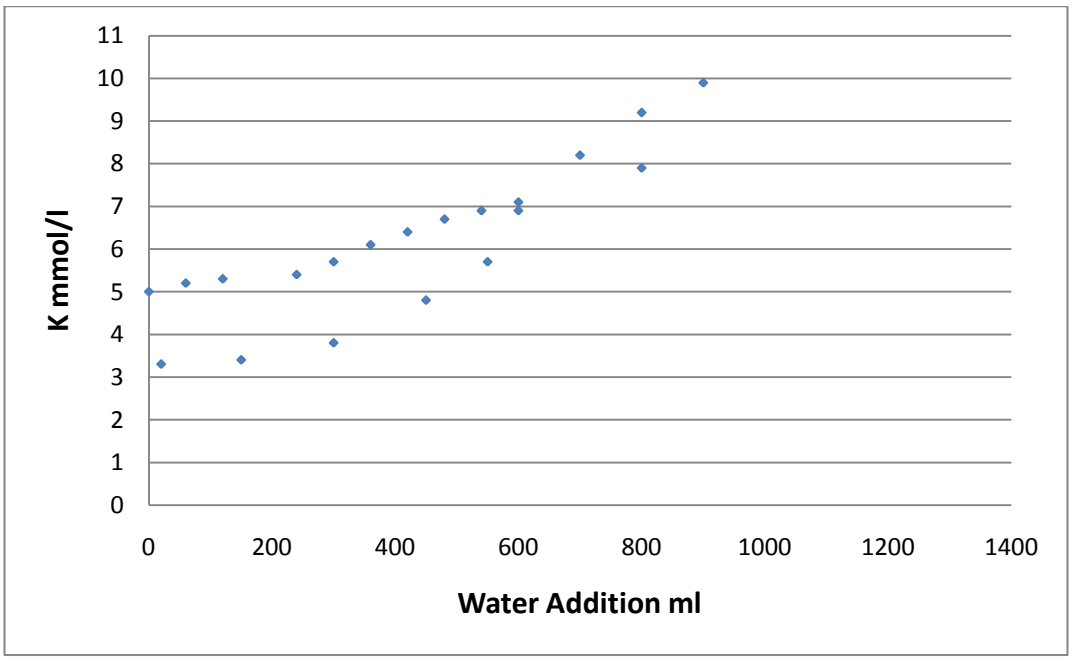

Figure 5.1 Effects of Water Addition on Potassium; K^+ increased from 3.3 up to 9.9 mmol/l where the upper threshold of the CDI 500 analyser was exceeded after 900ml of water addition.

pHv and pHa gradually decreased with water addition and potassium increase (p=0.005 and p=0.023, respectively). In the first circuit, pHa reduced from 7.27 to 7.12 and pHv decreased from 7.13 to 6.95. In the second circuit, pHa was reduced from 7.42 to 7.31 and pHv decreased from 7.24 to 7.16.

PaO_2 remained stable (p=0.070) which differed to that seen in the pilot work where a slight decrease was observed (section 5.3.2.2). $P\overline{v}O_2$ slightly decreased over the haemolysis (p=0.046). PaO_2 averaged 79.54 ±3.49 mmHg and $P\overline{v}O_2$ averaged 29.63 ±3.65 mmHg (Figure 5.2). There was no significant change in $PaCO_2$ and $P\overline{v}CO_2$ during the haemolysis (p=0.298 and p=0.601, respectively). $PaCO_2$ was 35.00 ±5.19 mmHg and $P\overline{v}CO_2$ was 60.50 ±2.93 mmHg (Figure 5.3).

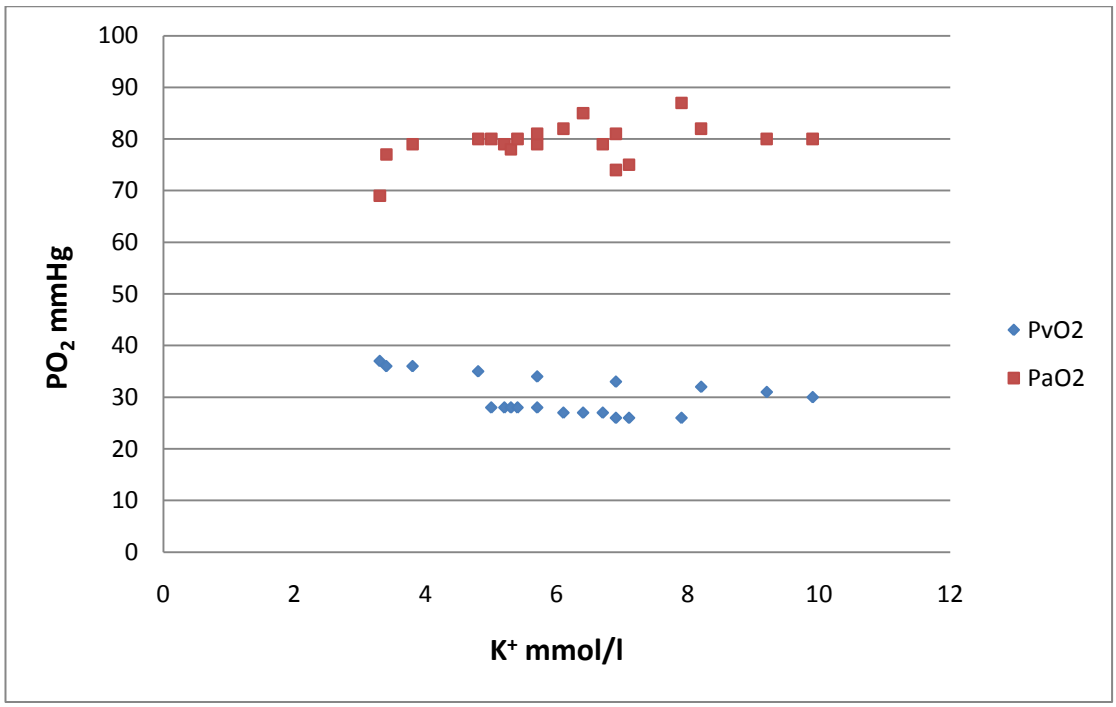

Figure 5.2 Effects of Haemolysis on PO_2; PaO_2 ■ averaged 79.54 ±3.49 mmHg and P $\overline{V}$ O_2 ♦ averaged 29.63 ±3.65 mmHg.

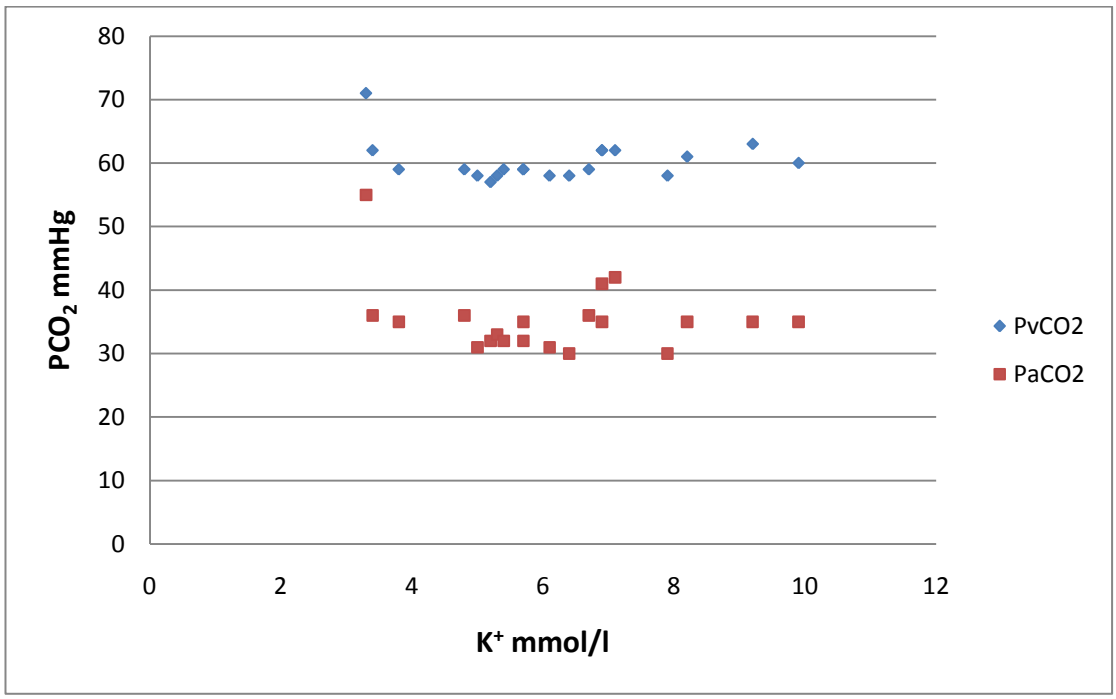

Figure 5.3 Effects of Haemolysis on PCO_2; There was no significant change in $PaCO_2$ ■ and P $\overline{V}$ CO_2 ♦ during haemolysis (p=0.298 and p=0.601, respectively). $PaCO_2$ was 35.00 ±5.19 mmHg and P $\overline{V}$ CO_2 was 60.50 ±2.93 mmHg.

There was no significant difference in $\dot{M}O_2$ (p=0.699 and p=0.605) or $\dot{M}CO_2$ (p=0.219 and p=0.153) during the water addition for these experiments although significant inter-run variation was noted. $\dot{M}O_2$ was 121.91 ±7.96 ml/min and 209.87 ±13.39 ml/min (inter-run p<0.0001) (Figure 5.4). $\dot{M}CO_2$ was 168.49 ±4.29 ml/min and 221.65 ±8.63 ml/min (inter-run p<0.001) (Figure 5.5).

Subsequently, no significant change was seen in DO_2 (p=0.588 and p=0.714) or DCO_2 (p=0.051 and p=0.128) during the water addition. DO_2 was 0.90 ±0.06 ml/min/mmHg and 1.60 ±0.12 ml/min/mmHg (Figure 5.6) while DCO_2 was 8.95 ±2.48 ml/min/mmHg and 3.24 ±0.54 ml/min/mmHg (Figure 5.7). Inter-run variation was significant for both DO_2 and DCO_2 (p<0.0001 and p<0.001).

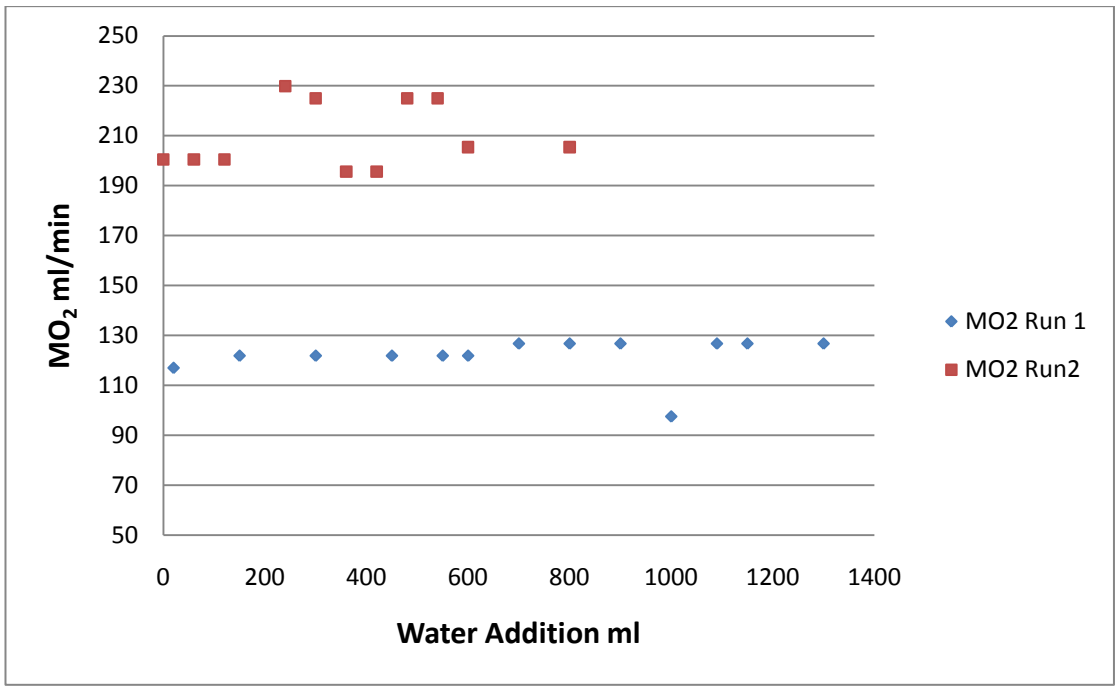

Figure 5.4 Effects of Haemolysis on $\dot{M}O_2$; $\dot{M}O_2$ averaged ♦ 121.91 ±7.96 ml/min and ■ 209.87 ±13.39 ml/min (inter-run p<0.0001) with no change during haemolysis (p=0.699 and p=0.605).

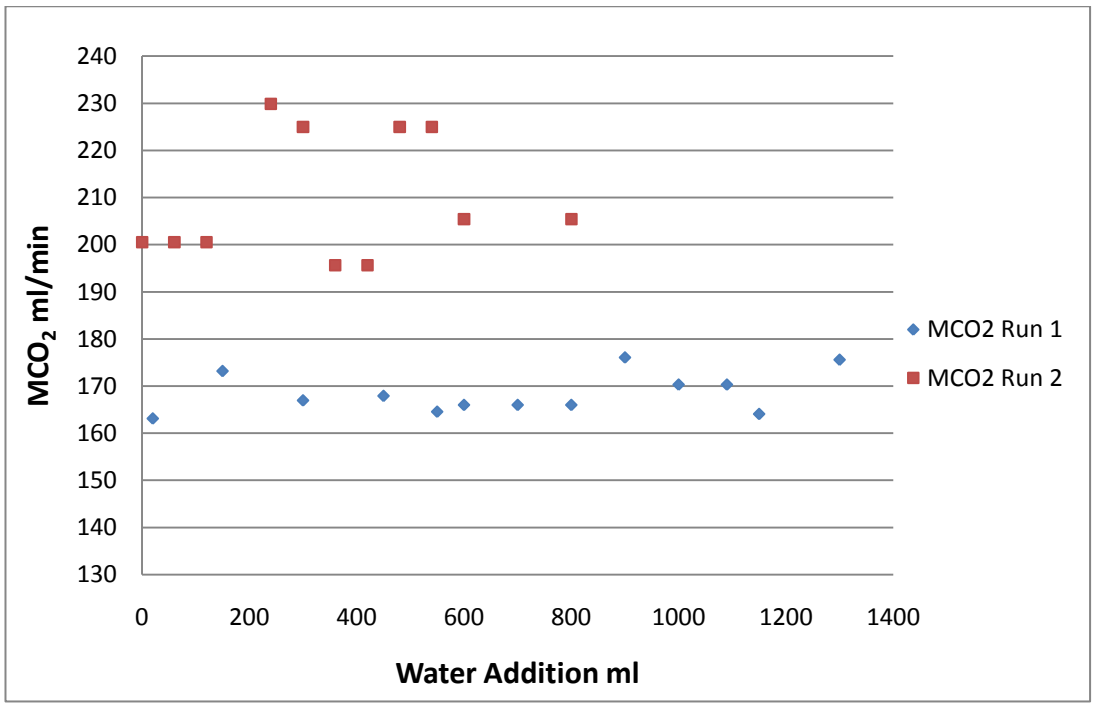

Figure 5.5 Effects of Haemolysis on $\dot{M}CO_2$; $\dot{M}CO_2$ was ♦ 168.49 ±4.29 ml/min and ■ 221.65 ±8.63 ml/min (inter-run p<0.001) with no change during haemolysis (p=0.219 and p=0.153).

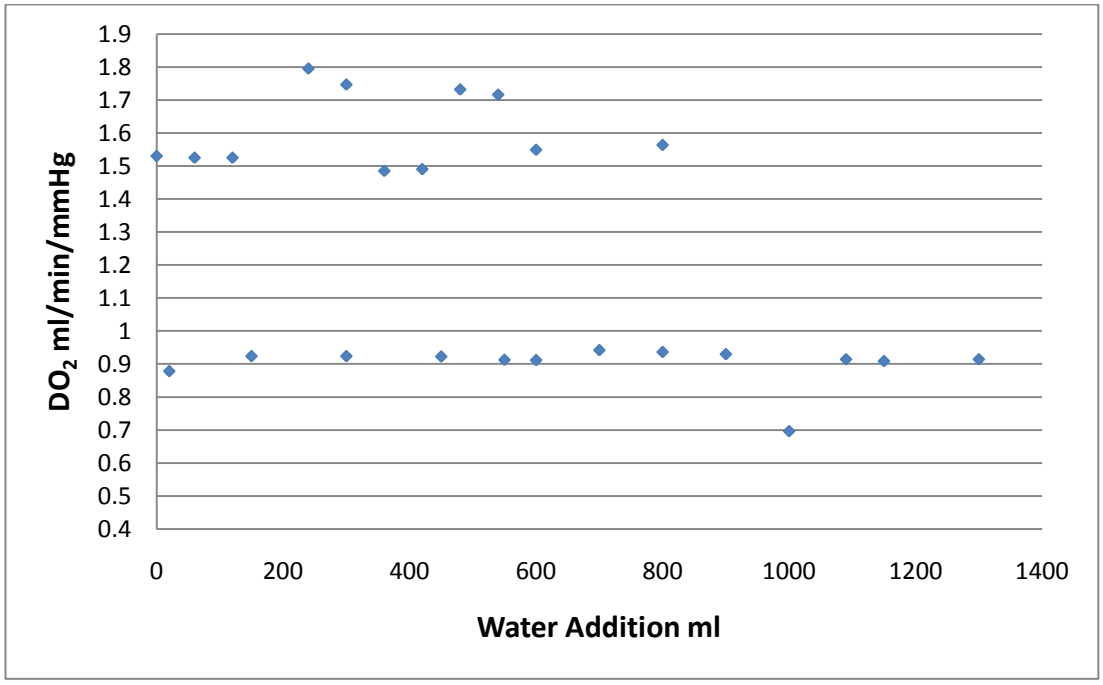

Figure 5.6 Effects of Haemolysis on DO_2; No significant change was observed in DO_2 (p=0.588 and p=0.714) averaging 0.90 ±0.06 ml/min/mmHg and 1.60 ±0.12 ml/min/mmHg.

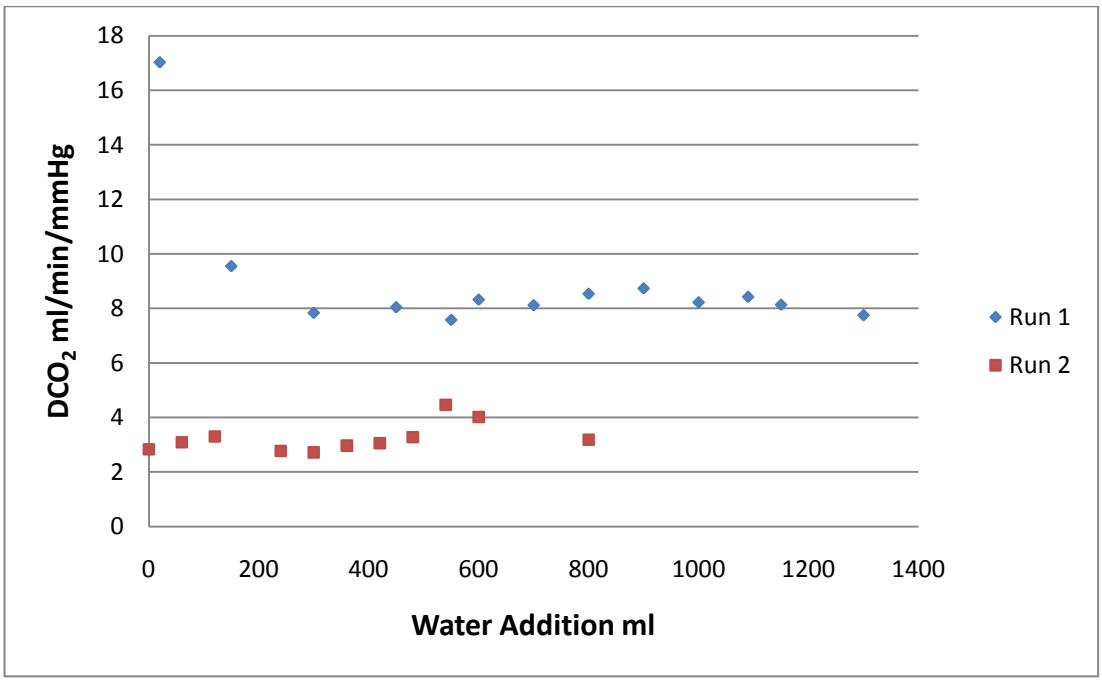

Figure 5.7 Effects of Haemolysis on DCO_2; No significant change was observed in DCO_2 during haemolysis (p=0.051 and p=0.128) averaging ♦ 8.95 ±2.48 ml/min/mmHg in run 1 and ■ 3.24 ±0.54 ml/min/mmHg in run 2.

Table 5.1 Increasing Gross Haemolysis Data Summary

Increasing Gross Haemolysis				
Parameter	***Trend***	***Statistical value***	***p value***	***d.f. or n***
K^+	Curvilinear increase	*r*=0.872	p<0.0001	n=20
pHa	Linear decrease	R^2=0.359	p=0.023	d.f.=19
pHv	Linear decrease	R^2=0.464	p=0.005	d.f.=19
PaO_2	No change	R^2=0.171	p=0.070	d.f.=19
$P\bar{v}O_2$	Slight decrease	R^2=0.203	p=0.046	d.f.=19
$\dot{M}O_2$	No change	R^2=0.014, 0.031	p=0.699, 0.605	d.f.=12, 10
DO_2	No change	R^2=0.027, 0.016	p=0.588, 0.714	d.f.=12, 10
$PaCO_2$	No change	R^2=0.060	p=0.298	d.f.=19
$P\bar{v}CO_2$	No change	R^2=0.016	p=0.601	d.f.=19
$\dot{M}CO_2$	No change	R^2=0.134, 0.213	p=0.219, 0.153	d.f.=12, 10
DCO_2	No change	R^2=0.304, 0.238	p=0.051, 0.128	d.f.=12, 10
Shunt Fraction	Curvilinear decrease	*r*=-0.985	p<0.0001	n=13

5.6.2 Effects of Free Hb Solution on O_2 Transfer

There was a linear increase in potassium levels with gradual addition of free Hb solution to the circuit blood (p=0.001). Potassium rose from 5.6 ±1.43 mmol/l to 8.3 ±1.57 mmol/l.

There was no change in pHa or pHv on addition of free Hb solution to the circuit (p=0.690 and p=0.080, respectively). pHa averaged 7.27 ±0.06 and pHv averaged 7.18 ±0.05 (Figure 5.8).

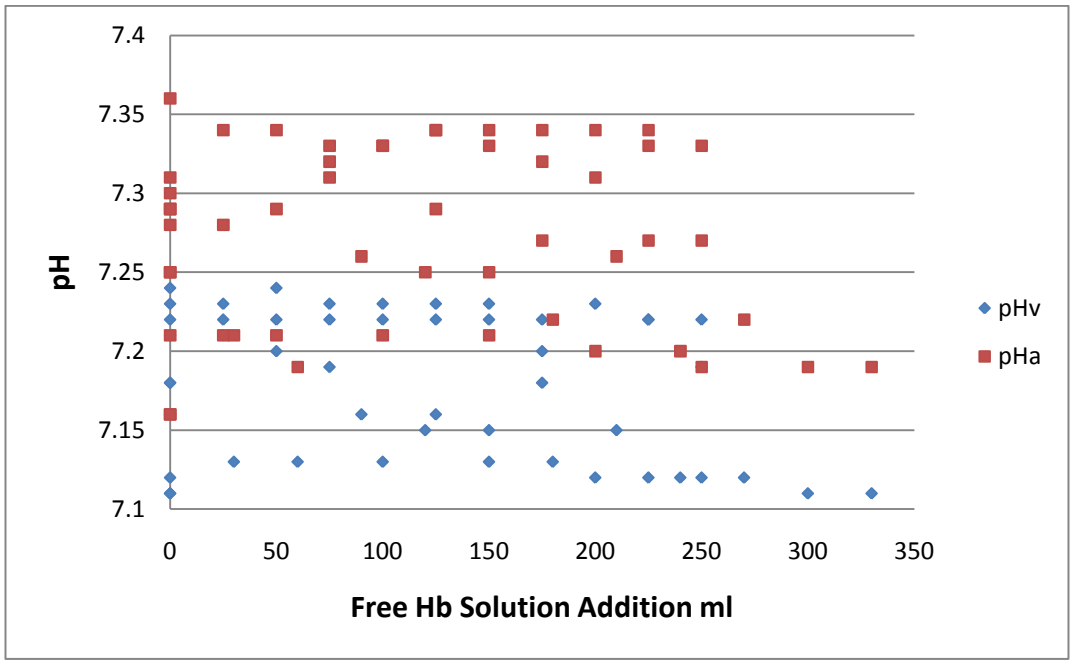

Figure 5.8 Effects of Free Hb Solution Addition on pH; pHa ■ averaged 7.27 ±0.06 and pHv ♦ averaged 7.18 ±0.05.

There was a slight decrease in both PaO_2 and $P\overline{v}O_2$ with addition of free Hb solution to the circuit (p=0.025 and p<0.001, respectively). The data distribution for $P\overline{v}O_2$ is small so a slight decrease gives rise to a more prominent statistical significance. PaO_2 averaged 78.10 ±5.85 mmHg and $P\overline{v}O_2$ averaged 35.88 ±2.22 mmHg (Figure 5.9).

$PaCO_2$ and P $\overline{V}$ CO_2 did not change with increasing addition of free Hb solution to the circuit (p=0.816 and p=0.778 respectively). $PaCO_2$ averaged 40.46 ±6.02 mmHg and P $\overline{V}$ CO_2 averaged 59.17 ±4.92 mmHg (Figure 5.10).

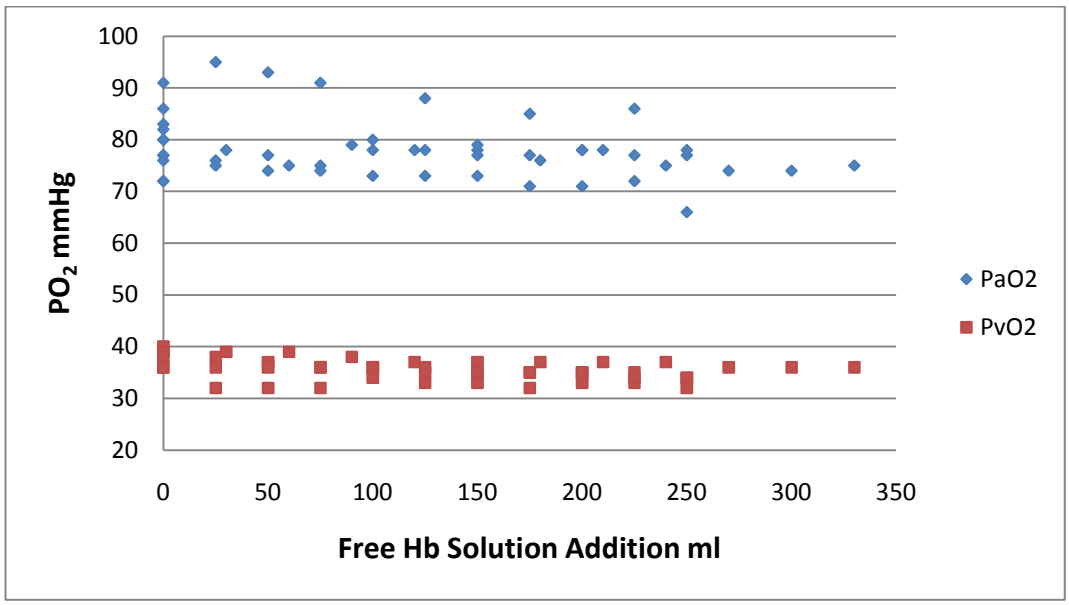

Figure 5.9 Effects of Free Hb Solution Addition on PO_2; There was a slight decrease in both PaO_2 and P $\overline{V}$ O_2 (p=0.025 and p<0.001) where PaO_2 ♦ averaged 78.10 ±5.85 mmHg and P $\overline{V}$ O_2 ■ averaged 35.88 ±2.22 mmHg.

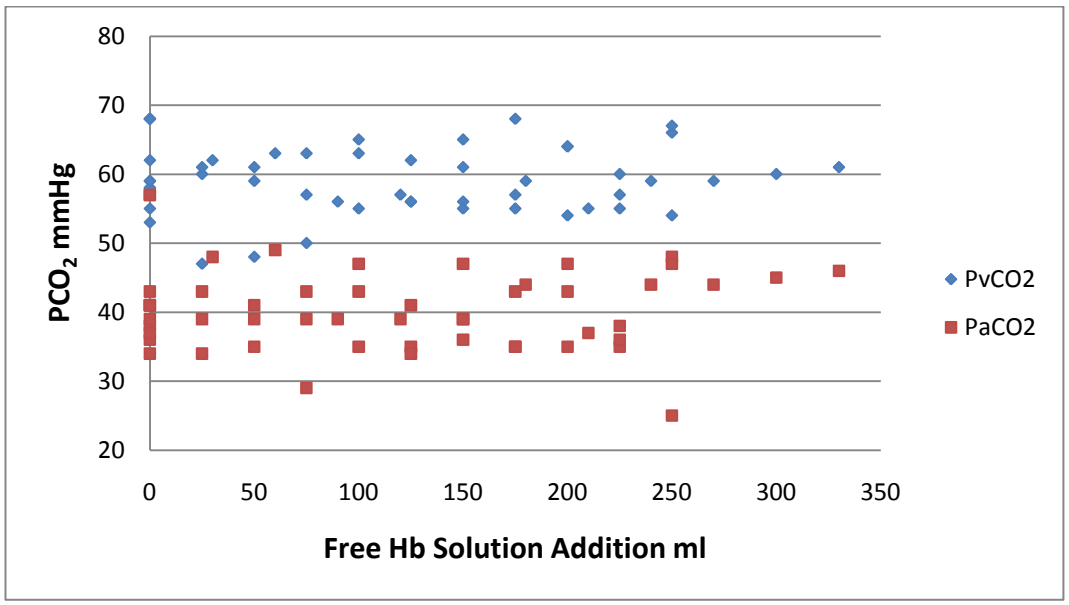

Figure 5.10 Effects of Free Hb Solution Addition on PCO_2; There was no change in $PaCO_2$ and P $\overline{V}$ CO_2 (p=0.816 and p=0.778) where $PaCO_2$ ■ averaged 40.46 ±6.02 mmHg and P $\overline{V}$ CO_2 ♦ averaged 59.17 ±4.92 mmHg.

$\dot{M}O_2$ and DO_2 remained stable when free Hb solution was added to the circuit blood (p=0.554 and p=0.792, respectively). $\dot{M}O_2$ averaged 164.87 ±17.63 ml/min (Figure 5.11) and DO_2 averaged 1.22 ±0.16 ml/min/mmHg (Figure 5.12).

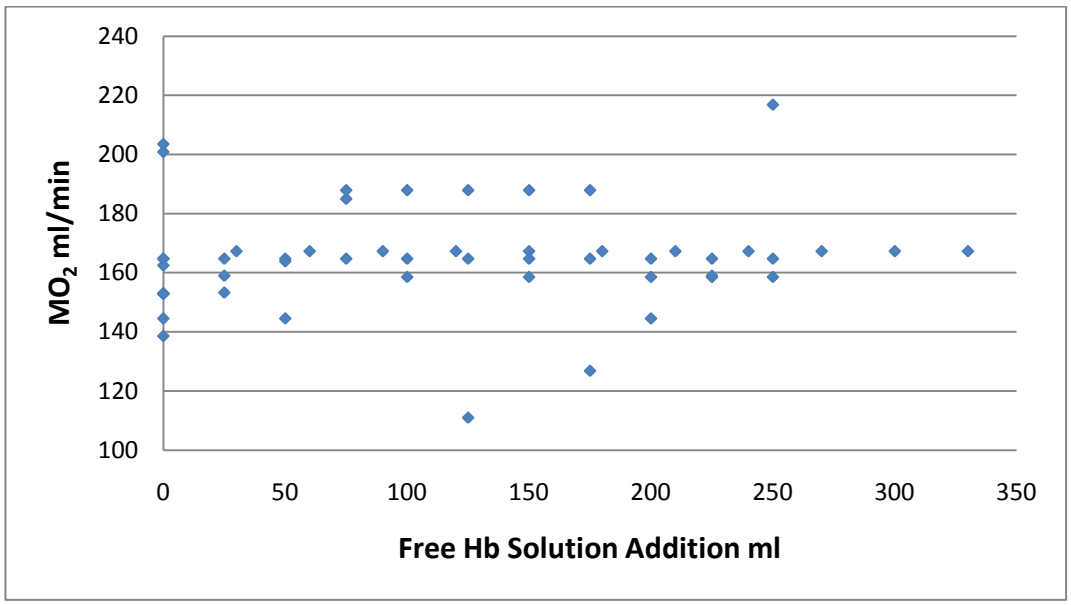

Figure 5.11 Effects of Free Hb Solution Addition on $\dot{M}O_2$; There was no change in $\dot{M}O_2$ (p=0.554) averaging 164.87 ±17.63 ml/min.

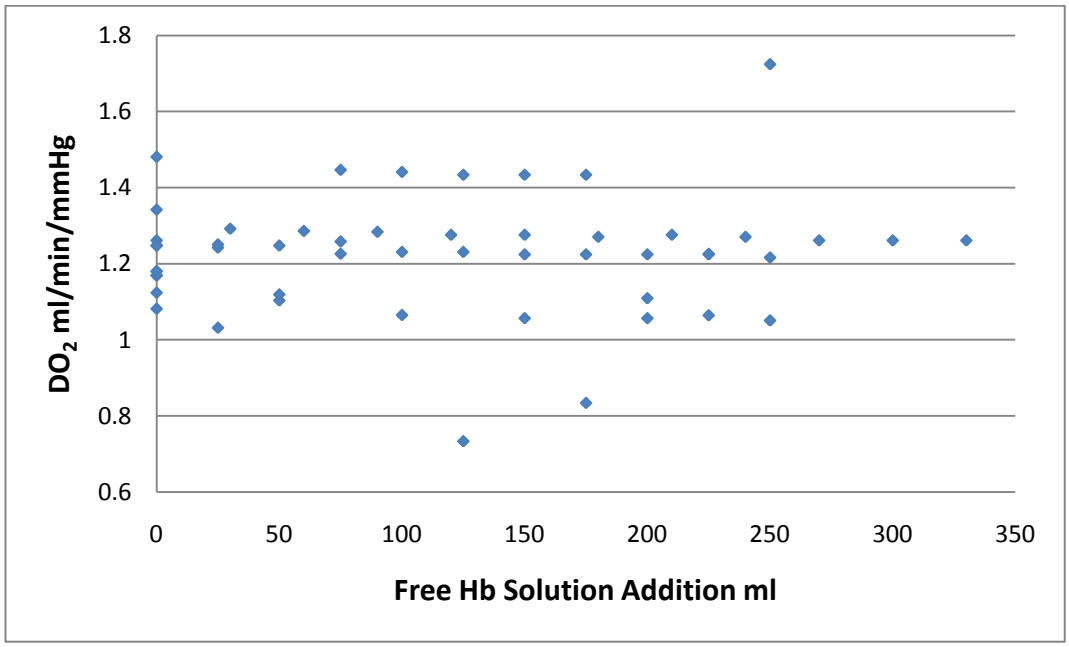

Figure 5.12 Effects of Free Hb Solution Addition on DO_2; There was no change in DO_2 (p=0.792) averaging 1.22 ±0.16 ml/min/mmHg.

5.6.3 Effects of Free Hb Solution on ODC

SO_2 was plotted against PO_2 for both the arterial and venous blood data to achieve the respective ODCs. The data underwent logarithmic transformation to achieve Hills plots for both arterial and venous ODCs. The arterial ODC showed a significant correlation between SaO_2 (S/1-S) and log PaO_2 ($p<0.0001$) and a left shift in the presence of 250 ml free Hb solution when compared to the control ($p<0.001$) (figures 5.13 and 5.14).

The venous Hills plot showed good linear correlation between the $S\bar{V}O_2$ (S/1-S) and log $P\bar{V}O_2$ ($p<0.0001$) and a significant left shift in the presence of 250 ml free Hb solution ($p<0.0001$) (Figures 5.15 and 5.16). P_{50} was calculated from the venous Hills plot data as 22.15 mmHg for the circuit equine blood and 15.50 mmHg after addition of 250 ml free Hb solution.

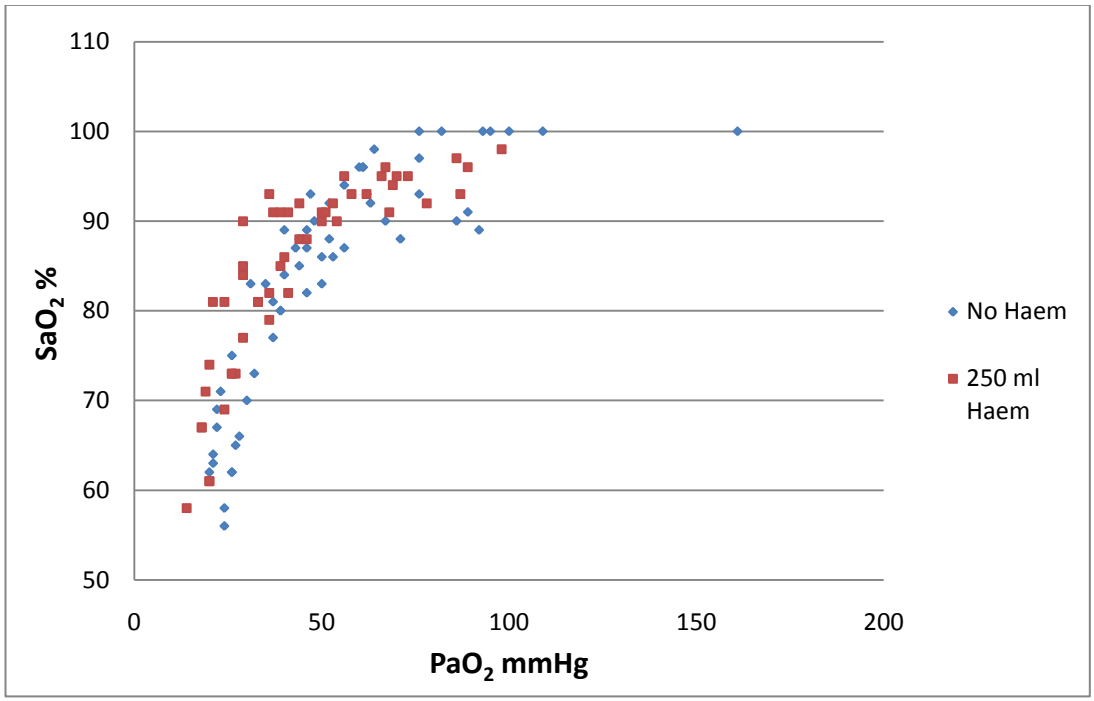

Figure 5.13 Effects of Free Hb Addition on the Arterial ODC; A left shift was apparent after 250 ml free Hb solution addition ■ compared to the control ♦.

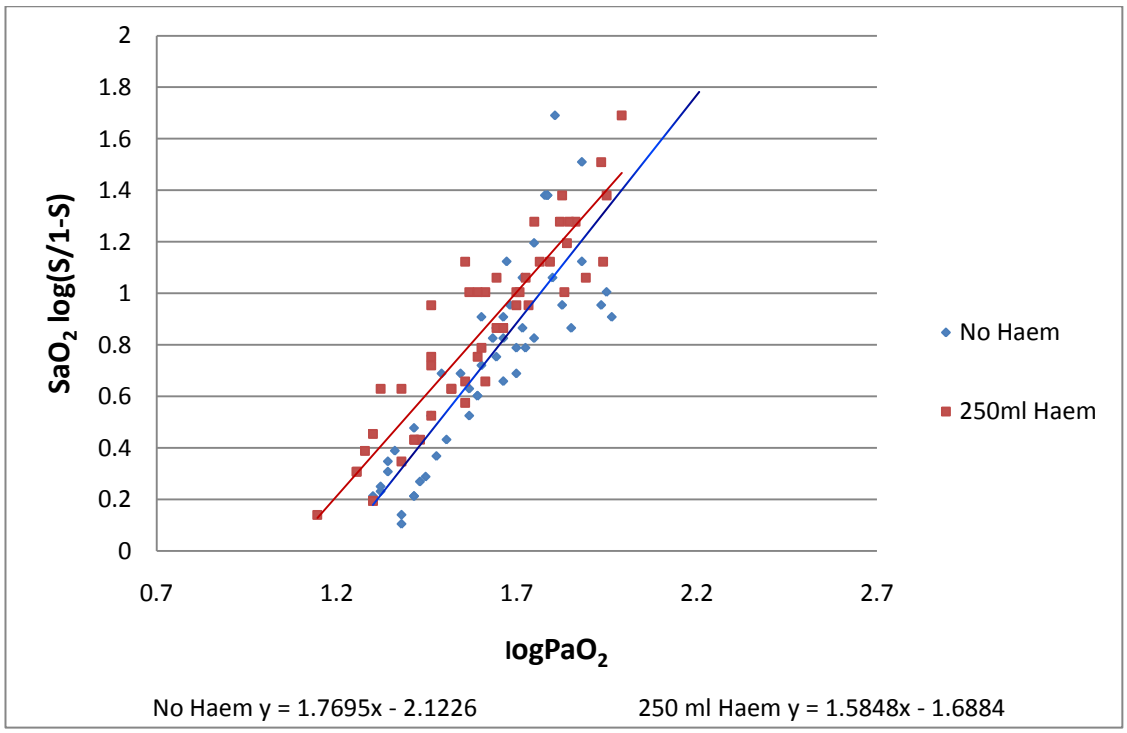

Figure 5.14 Effects of Free Hb Addition on the Arterial ODC – Hills plot; A significant correlation was observed between SaO_2 (S/1-S) and log PaO_2 ($p<0.0001$) and a left shift in the presence of 250 ml free Hb solution ■ when compared to the control ♦ ($p<0.001$).

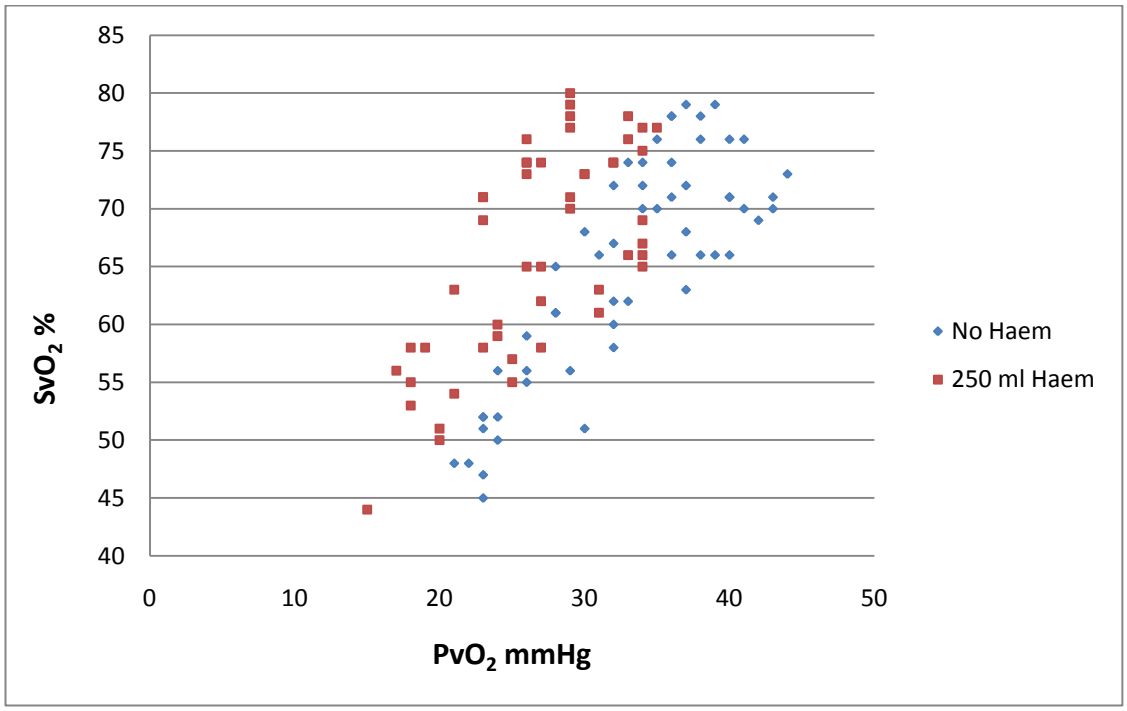

Figure 5.15 Effects of Free Hb Addition on the Venous ODC; A significant left shift in the presence of 250 ml free Hb solution ■ ($p<0.0001$) was evident compared to the control ♦.

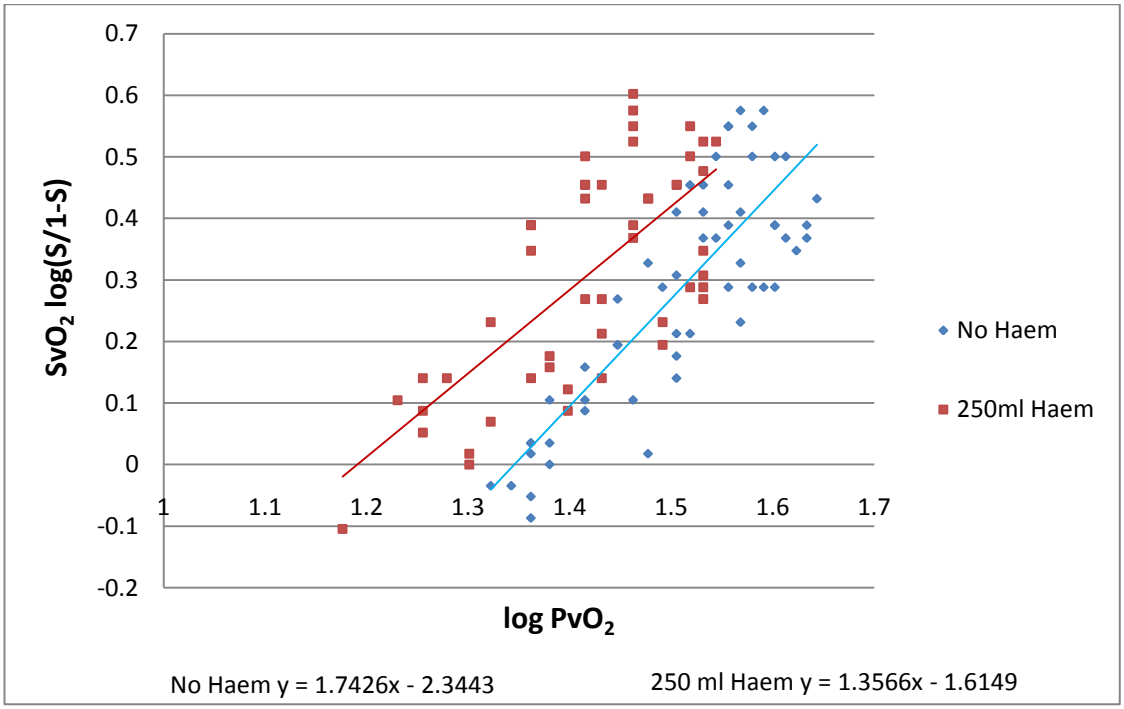

Figure 5.16 Effects of Free Hb Addition on the Venous ODC – Hills plot; A good linear correlation between the S $\overline{V}$ O_2 (S/1-S) and log P $\overline{V}$ O_2 ($p<0.0001$) and a significant left shift in the presence of 250 ml free Hb solution ■ ($p<0.0001$) was evident compared to the control ♦.

Table 5.2 Effects of Free Hb Solution Addition Data Summary

Effects of Free Hb Solution Addition				
Parameter	***Trend***	***Statistical value***	***p value***	***d.f. or n***
K^+	Linear increase	R^2=0.268	p=0.001	d.f.=37
pHa	No change	R^2=0.003	p=0.690	d.f.=51
pHv	No change	R^2=0.060	p=0.080	d.f.=51
PaO_2	Slight decrease	R^2=0.097	p=0.025	d.f.=51
P $\overline{V}$ O_2	Slight decrease	R^2=0.242	p<0.001	d.f.=51
$PaCO_2$	No change	R^2=0.001	p=0.816	d.f.=51
P $\overline{V}$ CO_2	No change	R^2=0.002	p=0.778	d.f.=51
$\dot{M}$ O_2	No change	R^2=0.007	p=0.554	d.f.=51
DO_2	No change	R^2=0.001	p=0.792	d.f.=51
Art Hills plot	Correlation Left Shift	R^2=0.783 *t*=3.925	p<0.0001 p<0.001	d.f.=102 d.f.=102
Ven Hills plot	Correlation Left Shift	R^2=0.594 *t*=6.611	p<0.0001 p<0.0001	d.f.=109 d.f.=109

5.6.4 Shunt Fraction in Gross Haemolysis

The shunt fraction significantly decreased in a curvilinear trend with increasing water addition to the circuit blood ($p<0.0001$). The shunt fraction reduced from 18.7% to 6.8% over the addition of 1300 ml water to the circuit blood (Figure 5.17).

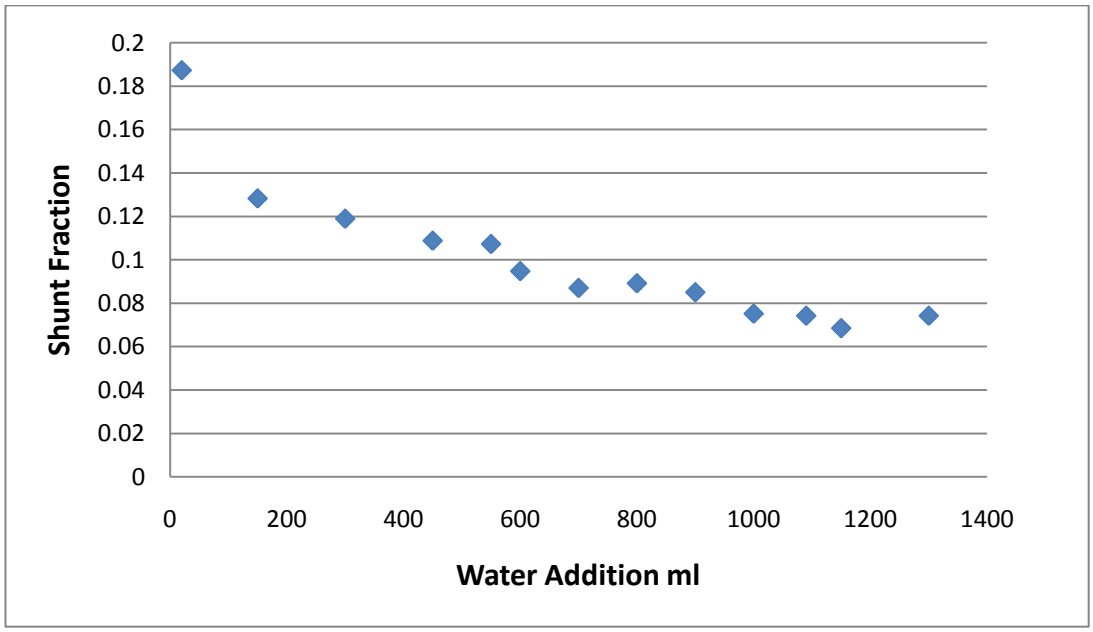

Figure 5.17 Effects of Haemolysis on Shunt Fraction; With increasing haemolysis, shunt fraction decreased curvilinearly from 18.7% to 6.8% ($p<0.0001$).

5.7 Effects of Haemolysis on DNO and DCO: Results

5.7.1 Effects of Gross Haemolysis on DNO and DCO

Haemolysing the circuit blood did not affect DCO ($p=0.052$). DCO averaged 1.17 ±0.21 ml/min/mmHg in run 1 and averaged 0.69 ±0.14 ml/min/mmHg in run 2 during haemolysis (Figure 5.18). There was a significant inter-run variation between the two circuits for DCO ($p<0.001$)

DNO was seen to significantly increase curvilinearly with water addition from 4.66 ml/min/mmHg to 24.24 ml/min/mmHg in run 1 and from 3.60 ml/min/mmHg to 9.98 ml/min/mmHg in run 2 ($p<0.001$) (Figure 5.19). There was a significant inter-run variation between the two circuits ($p<0.001$).

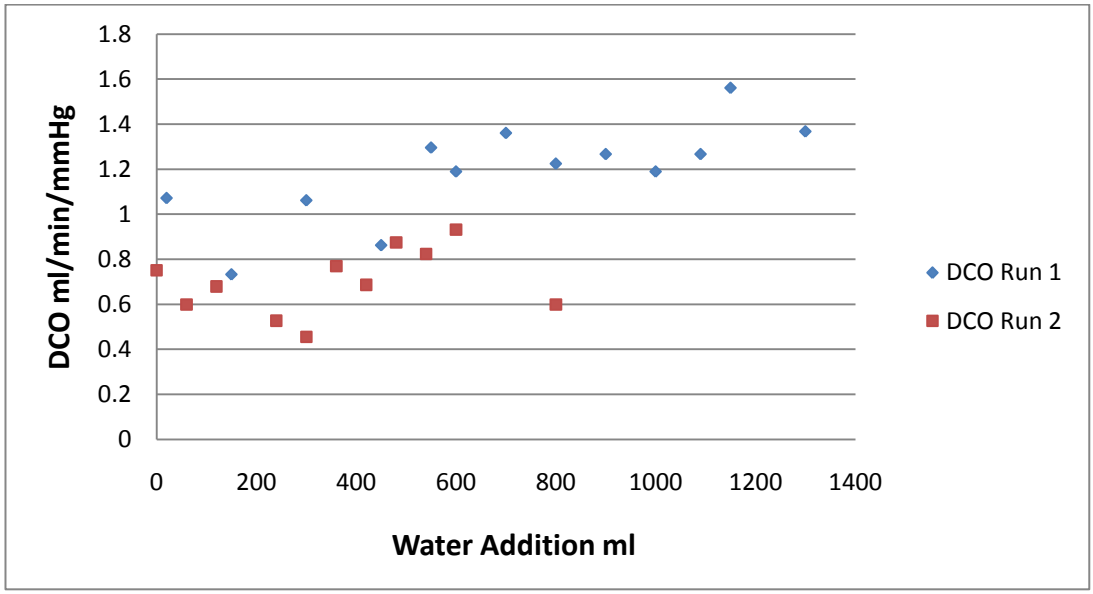

Figure 5.18 Effects of Haemolysis on DCO; DCO was unaffected by haemolysis ($p=0.052$) averaging 1.17 ±0.21 ml/min/mmHg in run 1♦ and 0.69 ±0.14 ml/min/mmHg in run 2 ■.

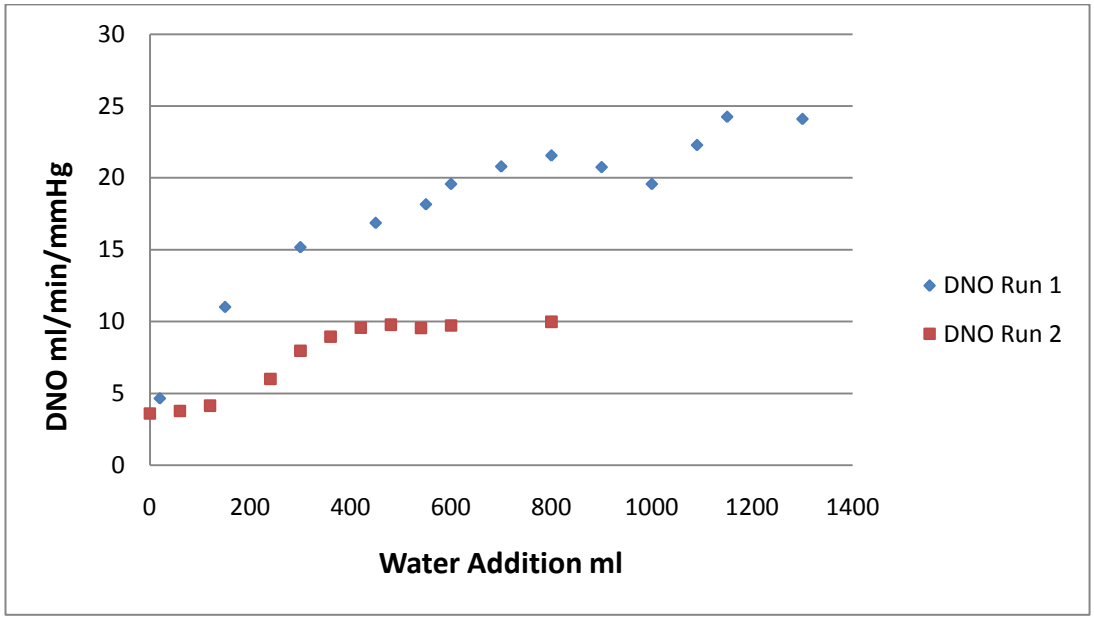

Figure 5.19 Effects of Haemolysis on DNO; DNO increased curvilinearly with haemolysis ($p<0.001$) from 4.66 ml/min/mmHg to 24.24 ml/min/mmHg in run 1 ♦ and from 3.60 ml/min/mmHg to 9.98 ml/min/mmHg in run 2 ■.

Table 5.3 Effects of Gross Haemolysis on DNO and DCO

DNO and DCO Increasing Gross Haemolysis				
Parameter	***Trend***	***Statistical value***	***p value***	***d.f. or n***
DCO	No change	R^2=0.293	p=0.052	d.f.=19
DNO	Curvilinear increase	*r*=0.881	p<0.001	d.f.=24
Inter-run Variation	Observed	DCO *t*=6.341 DNO *t*=5.980	p<0.001 p<0.001	d.f.=22 d.f.=22

5.7.2 Effects of Free Hb Solution on DNO and DCO

DCO was not affected by addition of free Hb solution to the circuit blood (p=0.061). DCO averaged 1.57 ±0.24 ml/min/mmHg throughout free Hb solution addition (Figure 5.20).

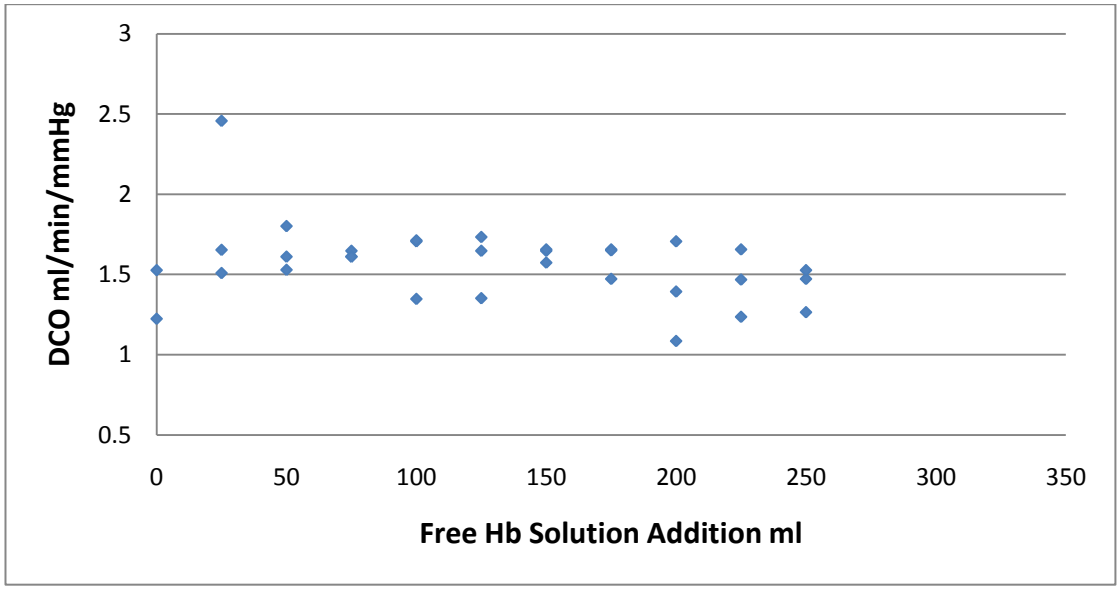

Figure 5.20 Effects of Free Hb Addition on DCO; DCO was unaffected by free Hb addition (p=0.061) averaging 1.57 ±0.24 ml/min/mmHg.

DNO increased curvilinearly with increasing addition of free Hb solution to the circuit blood (p<0.0001). DNO increased from 11.79 ±3.48 ml/min/mmHg with 0 ml free Hb solution up to 22.25 ±8.03 ml/min/mmHg after 250 ml free Hb solution addition (Figure 5.21), an overall increase of 91% compared to baseline. After just 25 or 30 ml free Hb

solution addition to the circuit blood, DNO had increased to 13.40 ±3.31 ml/min/mmHg, an increase of 14% compared to baseline. DNO showed some inter-run variation ($p<0.0001$).

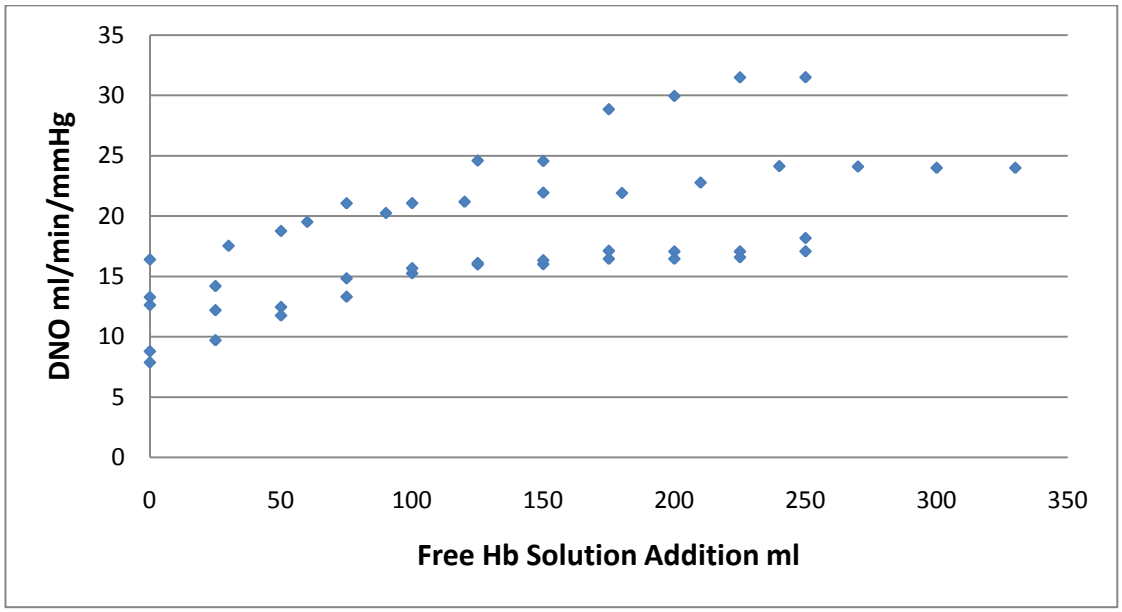

Figure 5.21 Effects of Free Hb Addition on DNO; DNO increased curvilinearly with free Hb addition ($p<0.0001$) increasing from 11.79 ±3.48 ml/min/mmHg with 0 ml free Hb up to 22.25 ±8.03 ml/min/mmHg after 250 ml free Hb solution.

5.7.3 Effects of NO on ODC

There were no significant effects of NO on the arterial ODC ($t=-1.176$, d.f.=14, $p=0.267$). The Hills plot demonstrated good correlation between log PaO_2 and SaO_2 (S/1-S) ($R^2=0.896$, d.f.=14, $p<0.0001$).

The Hills plot of the venous ODC demonstrated significant correlation between log $P\overline{v}O_2$ and $S\overline{v}O_2$(S/1-S) ($R^2=0.925$, d.f=29, $p<0.0001$). The venous ODC was shifted leftwards in the presence of NO when compared to the control ($t=7.425$, d.f.=19, $p<0.0001$). When free Hb solution was added in the presence of NO this further shifted the venous ODC to the left ($t=6.063$, d.f.=19, $p<0.0001$). P_{50} was calculated as 29.41 mmHg for the circuit blood, 26.12 mmHg for the circuit blood exposed to NO and

21.59 mmHg for the combined NO and free Hb addition to the circuit blood (Figures 5.22 and 5.23).

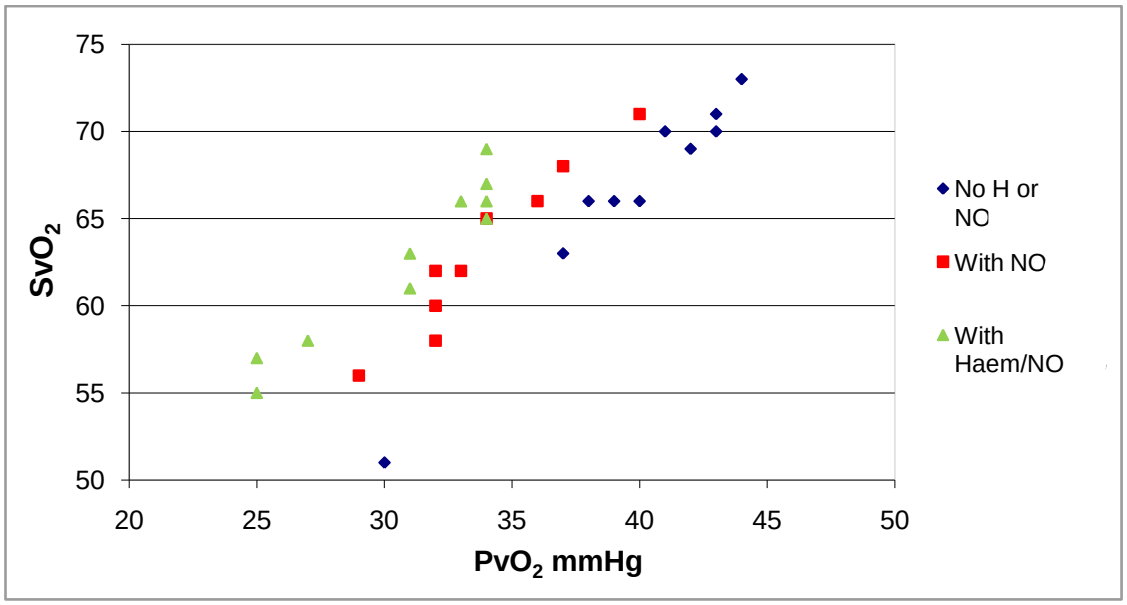

Figure 5.22 Effects of Free Hb and NO on the Venous ODC; A leftward ODC shift was observed following NO exposure ■ ($p<0.0001$) and a further left shift was seen with 250ml free Hb addition ▲ ($p<0.0001$) compared to equine blood ♦.

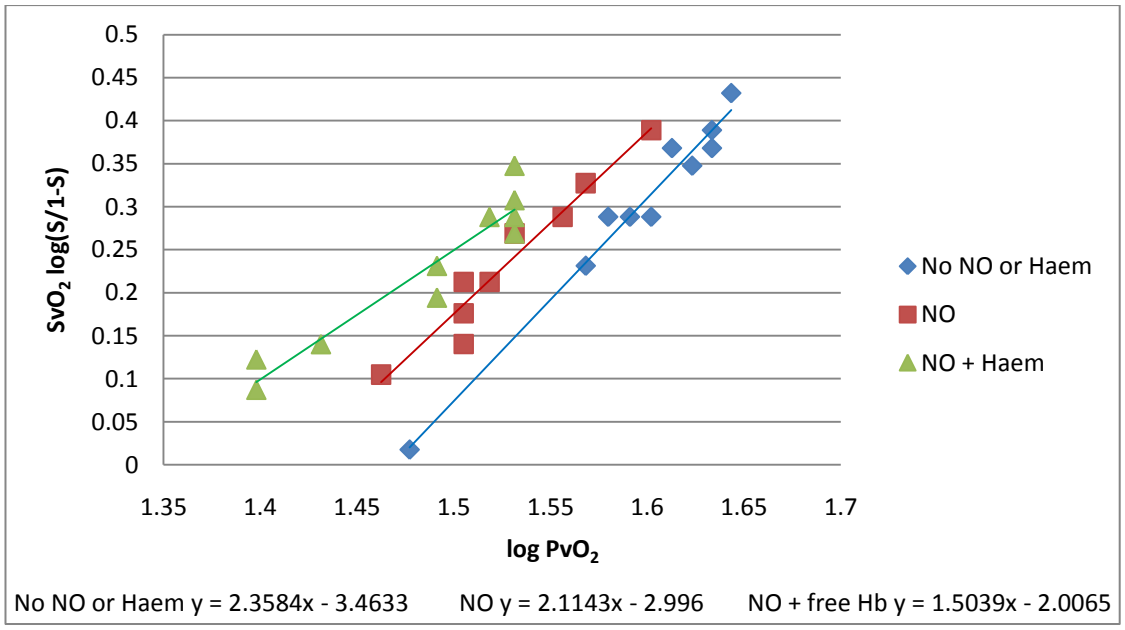

Figure 5.23 Effects of Free Hb and NO on the Venous ODC – Hills plot; P_{50} was calculated as 29.41 mmHg for equine blood ♦, 26.12 mmHg for equine blood exposed to NO ■ and 21.59 mmHg for the combined NO and free Hb addition ▲ to equine blood.

Table 5.4 Effects of Free Hb Solution on DNO and DCO

Effects of Free Hb Solution Addition on DNO and DCO				
Parameter	***Trend***	***Statistical value***	***p value***	***d.f. or n***
DCO	No change	R^2=0.112	p=0.061	d.f.=31
DNO	Curvilinear increase	*r*=0.654	p<0.0001	n=46
Inter-run variation	Observed for DNO	*t*=7.119, 5.411	p<0.0001, p<0.0001	d.f.=20, 19

5.8 Implications of Haemolysis on Gas Transfer in the Membrane Oxygenator: Discussion.

Adding water to the circuit induced gradual haemolysis indicated by increasing potassium levels leached out of ruptured RBCs. A curvilinear increase in potassium was detectable by the CDI 500 analyser (up to 10mmol). The pH decreased, but as the water was pH 7.1-7.9, the acidity was attributed to leaching of RBC contents further indicating successful haemolysis. Latterly, free Hb solution was added to the circuit giving levels encountered clinically by shear stress with long-term dialysis or ventricular assist devices. Haemolytic anaemia (i.e. Thalassemia, Sickle-cell anaemia, hereditary Spherocytosis) can cause elevated free Hb in plasma and resultant abdominal pain, pulmonary hypertension, systemic hypertension and renal dysfunction have been linked to nitric oxide scavenging by free Hb (Rother *et al* 2005).

From this data, haemolysing blood or addition of free Hb solution did not alter carbon dioxide partial pressures or uptake. It is concluded that plasma, red cell membrane and haemoglobin packing within the red cell have limited effect on carbon dioxide transfer. CO_2 is carried in the blood as dissolved CO_2, bound to haemoglobin and plasma protein

amino acids or as bicarbonate ions. Due to the complex way in which the gas is carried in plasma and red cells, the lack of effect of red cell disruption is unsurprising.

The transfer of oxygen comprises several components. Initially, oxygen diffuses across the membrane. It then moves through plasma before crossing the RBC membrane to bind with Hb. Free Hb reduces the distance between the alveolar membrane and Hb as the red cell is bypassed. In the membrane oxygenator, shunt fraction reduced with haemolysis indicating less boundary effect. An increased oxygen uptake would be expected. Several factors resulting from the haemolysis were considered to be limiting to $\dot{M}O_2$. Haemodilution of haemoglobin concentrations by water addition (minimum circuit Hb 6.4 g/dl) should reduce $\dot{M}O_2$ but work on varying Hb (Chapter 3) did not affect $\dot{M}O_2$ at concentrations >5g/dl. Decreasing pH should cause right ODC shifting, reducing Hb oxygen binding. In this data, a leftward venous ODC shift was observed after 250 ml free Hb solution addition to the circuit (P_{50} 22 to 15.5 mmHg). Stroma free Hb has a P_{50} of 12-14 mmHg (Grethlein *et al* 2007) compared to 26.5 mmHg (whole blood). This is because stroma free Hb dissociates into α and β chains which have a high oxygen affinity. A leftward ODC shift results in increased oxygen uptake but poor tissue offloading. It appears that the effects described above act in opposition so that there is no net effect of haemolysis on $\dot{M}O_2$.

In this circuit, NO caused a significant leftward shift of the venous ODC. When oxyHb is exposed to NO the O_2 is displaced by NO and the iron atom oxidises to form methaemoglobin. The iron oxidates to a ferric state (Fe^{+++}) which limits the Hb oxygen binding compared to the usual ferrous state (Fe^{++}) (normal oxygen binding). Bound-NO causes the Hb molecule to remain in the high oxygen affinity R-state conformation limiting oxygen offloading. NO therapy is a potential therapy for sickle cell crisis patients

where sickle RBCs have impaired oxygen carrying capacity resulting in arterial hypoxia. Low dose NO (80 ppm) can induce a leftward shift of the ODC, increasing oxygen uptake during a crisis (Head *et al* 1997, Martinez-Ruiz *et al* 2001).

Haemolysis did not affect DCO but DNO increased significantly during gross haemolysis and addition of free Hb solution suggesting that the RBC membrane, interior or its surrounding creates resistance to its transfer (Borland *et al* 2006, 2010). The level of DNO increase was less with low amounts of free Hb present in the circuit blood compared to that seen with gross haemolysis. This finding corresponds with uptake of NO via free Hb present in the circuit. The increase in DNO with low levels of free Hb present in the circuit blood has implication for D_LNO in lung function testing. Some authorities believe that D_LNO in patients is a measure solely of NO transport across the alveolar membrane (Heller and Schuster 1998). The specific conductance of NO with the blood (θ_{NO}) was thought to be infinite (Guenard *et al* 1987). Therefore due to the instantaneous reaction rate of NO with Hb, D_LNO would equal D_MNO. This experiment demonstrates that D_LNO does not reflect D_MNO as the RBC membrane, interior or its surrounding plays a significant role in DNO resistance and θ_{NO} is not infinite (Borland *et al* 2006). Increased DNO during haemolysis of the circuit blood or addition of free Hb solution can be attributed to three areas of resistance; RBC membrane, RBC interior and surrounding plasma. RBC membrane resistance to DNO is obviously lost when the RBC membrane is lysed. Release of tightly packed Hb within the RBC may also increase DNO on haemolysis. Free Hb within the circulating blood will reduce the diffusion distance and plasma resistance to DNO. This work (gross haemolysis or free Hb solution addition) does not differentiate between these three potential resistances to DNO. To establish if DNO resistance can be attributed to plasma, a Haemoglobin-Based-Oxygen-Carrier (HBOC) was added to the circulating blood to increase free Hb without disruption of the

RBCs. After gradual Oxyglobin addition to the circuit, haemolysis will be induced in the circuit to test for DNO resistance as a result of the RBC membrane and interior.

From this work, gross circuit haemolysis and addition of free Hb solution resulted in a significant DNO increase. Whilst gross haemolysis was not clinically representative, a similar increase in DNO was observed at lower levels of free Hb which could be more clinically attributed. Presence of free Hb in the circuit blood alters the carriage of oxygen via a leftward shift of the venous ODC. Further work will investigate the factors responsible for DNO resistance and to examine the potential for the HBOC Oxyglobin to scavenge NO from the circuit.

CHAPTER 6 Effects of Oxyglobin Solution Addition on DO_2 DNO and DCO

Aims

The aim was to determine if the Haemoglobin-Based-Oxygen-Carrier (HBOC) Oxyglobin affected DO_2, DNO and DCO in the membrane oxygenator circuit. Chapter 5 concluded that haemolysis and addition of free Hb solution to the circuit results in increased DNO. Whole blood resistance to DNO was attributed to one of three areas; the RBC membrane, the RBC interior or the plasma surrounding the RBC. To determine if plasma provided DNO resistance, Oxyglobin was added to the circuit blood. Oxyglobin is free bovine Hb modified to give a larger molecular weight (increasing half-life) and adjusted for oxygen affinity. The RBCs within the circuit blood would remain intact thus eliminating the influence of both RBC membrane and interior which were present in the haemolysis work (Chapter 5). Subsequently, the circuit blood was haemolysed post Oxyglobin addition to determine if further increases in DNO would occur consistent with RBC membrane or interior resistance to DNO. Concurrent with this work, the HBOC Oxyglobin was assessed for its NO scavenging potential, a potential contributing factor in HBOC related vasoconstriction.

6.1 Addition of Oxyglobin Solution to the Circuit Blood: Circuit Set-Up.

6.1.1 Oxyglobin

Oxyglobin is polymerised bovine Hb with a P_{50} 34 mmHg (Driessen *et al* 2001). The elevated P_{50} decreases oxygen affinity of Oxyglobin thus enhancing oxygenation of the tissues. During the experimental phase, Oxyglobin was the only licensed HBOC available for veterinary or human use. This product was licensed for use in dogs for improving the

clinical signs of anaemia independent of the underlying cause (Arnolds, Shrewsbury, UK). Oxyglobin solution was provided as a 130 mg/ml solution with a recommended dosage of 30 ml/kg. Each box contained two 125 ml intravenous infusion packs, totalling 250 ml per box. The Oxyglobin solution infusion packs accommodated a standard infusion giving set allowing removal into a syringe for repeated administration of known volume aliquots.

In dogs, Oxyglobin solution can cause mild to moderate discoloration of the mucous membranes and urine due to metabolism and excretion of free Hb. Advisory notes state that colorimetric tests may be affected by this discoloration. sO_2 monitoring in blood is determined by spectrophotometric techniques, typically infrared light. Infrared light of a known wavelength is directed at the blood which is refracted back at different wavelengths depending on the deoxyhaemoglobin and oxyhaemoglobin ratio. To determine if Oxyglobin affects sO_2 analysis, two different spectrophotometric analysers were compared. The Cobe Sat/Hct monitor utilises infrared light technology compared to the Spectrum Medical M2 which utilises white light technology.

6.1.2 Addition of Oxyglobin Solution to the Circuit

The circuit was set up and primed with equine blood (Chapter 3, section 3.1). The circuit was run for a minimum of 30 minutes at normoxic conditions while control data was collected. Oxyglobin solution was added via a Luer Lock connection on the top of the venous reservoir in syringed aliquots of 25 or 30 ml. A total transfusion volume of 240 ml (30 ml aliquots in run 1) or 250 ml (25 ml aliquots in subsequent runs) Oxyglobin solution was added to the circuit blood (2000 ml) giving a total circulating volume of 2240-2250 ml. The circuit Oxyglobin concentration achieved during the gradual addition was calculated as 1.60 to 14.44 mg/ml, added to a circuit Hb range 11.7 to 13.5 g/dl.

6.2 Pilot Experiments With Oxyglobin Solution

Based on the free Hb addition work (Chapter 5) no methodology related pilot studies were considered necessary for the Oxyglobin solution addition work. Experiments on sO_2 measurements were conducted concurrently with the first two experimental runs due to limited availability of Oxyglobin.

6.3 Effects of Oxyglobin Solution on O_2 Transfer: Methodology

Each circuit was set-up and primed with equine blood (Chapter 3, section 3.1). Each aliquot or change in circuit settings was allowed 5 minutes circulation for equilibrium to be achieved (Chapter 3, section 3.2). pH, PO_2 and PCO_2 values from the CDI 500 analyser were noted. Venous and arterial blood saturations were recorded from the Spectrum Medical M2 analyser and the Cobe Sat/Hct analyser. The oxygenator FiO_2 and FeO_2 were established for each change.

6.3.1 Effects of Oxyglobin Solution on sO_2 Analysis

The blood flow was set at 2.5 l/min. The oxygenator gases were set to 5 l/min air with 0.3 l/min O_2. The deoxygenator gases were set to 5 l/min CO_2 in balanced N_2 with 0.2 l/min CO_2. Oxyglobin solution was added to the circuit in ten 25 ml aliquots, totalling 250 ml. sO_2 were recorded on both the Spectrum Medical M2 and the Cobe Sat/Hct analysers for each 25 ml Oxyglobin aliquot. In the second run, blood flow was set at 2.5 l/min. The oxygenator gases were a mixture of N_2 and O_2 giving a FiO_2 range of 5.3 to 26.4 %. The deoxygenator gases were set to 5 l/min CO_2 in balanced N_2 with 0.2 l/min CO_2. sO_2 was recorded for the circuit blood at a range of FiO_2 and repeated post 250 ml Oxyglobin addition.

6.3.2 Effects of Oxyglobin Solution on O_2 Transfer

The circuit was run at a blood flow of 2.5 l/min. The oxygenator received 5 l/min air with 0.3 l/min O_2. The deoxygenator gases were set to 5 l/min 5% CO_2 in balanced N_2 with 0.1-0.3 l/min CO_2. At five minute intervals, 30 ml (run 1) or 25 ml (subsequent runs) aliquots of Oxyglobin Solution were added into the top of the venous reservoir, totalling 240 or 250 ml, respectively.

6.3.3 Effects of Oxyglobin Solution on ODC

The blood flow was set to 2.5 l/min. The oxygenator was ventilated with 5 l/min N_2 and O_2 at varying mixtures to give a FiO_2 ranging 9.1 to 35.2%. The deoxygenator gases were set to 5 l/min 5% CO_2 in balanced N_2 with 0.2 l/min CO_2. The ODC experiment was conducted with whole equine blood and repeated in the presence of 250 ml Oxyglobin solution.

6.3.4 Calculations

The calculations used for the data generated in this chapter are those detailed in Chapter 3, section 3.3.8. Hills plots are described in Chapter 2, section 2.1.

6.3.5 Statistical Analysis

The statistical analysis tests used for the data generated in this chapter are described in chapter 2, section 2.2.

6.4 Effects of Oxyglobin Solution on DNO and DCO: Methodology

Five minutes after each aliquot of Oxyglobin solution or water, the NOin, NOout, COin and COout were determined

6.4.1 Effects of Oxyglobin Solution on DNO and DCO

The same methodology as that described in section 6.3.2 was used. NO was added to the oxygenator gas at 4000, 6600 and 8000 ppb for each run to ensure that the inlet concentration exceeded that crossing the membrane. CO was added to the oxygenator gas at 0.03%.

6.4.2 Effects of Oxyglobin Solution combined with NO on ODC

The blood flow was set at 2.5 l/min. The oxygenator was ventilated with 5 l/min N_2 and O_2 at varying mixtures to give a FiO_2 ranging 5.3 to 34.7%. The deoxygenator gases were set to 5 l/min 5% CO_2 in balanced N_2 with 0.1-0.2 l/min CO_2. The ODC experiment was conducted with whole equine blood in the absence of Oxyglobin solution. 250 ml Oxyglobin solution was added to the circuit. The ODC experiment was repeated with whole equine blood in the presence of 250 ml Oxyglobin solution while being exposed to 6600 (run 1) or 8000 (run 2) ppb NO.

6.4.3 Effects of Haemolysis post Oxyglobin Solution Addition on DNO and DCO

The circuit was run at a blood flow of 2.5 l/min. The oxygenator received 5 l/min air with 0.3 l/min O_2 with NO 16000 ppb and CO 0.03%. The deoxygenator gases were set to 5 l/min 5% CO_2 in balanced N_2 with 0.2 l/min CO_2. At five minute intervals 25 ml aliquots of Oxyglobin Solution were added into the top of the venous reservoir, totalling 250 ml. Once 250 ml Oxyglobin solution had been added, the circuit was recirculated for a further

5 minutes. To haemolyse the circuit blood, tap water was added to the venous reservoir in 150ml aliquots (run 1) until 750 ml had been added and the K^+ had exceeded the analyser limit (>10 mmol/l). In subsequent runs, 100 ml aliquots of water were added to a total of 700 ml.

6.4.4 Calculations

The calculations for DNO and DCO are detailed in Chapter 3, section 3.4.3.

6.5 Effects of Oxyglobin Solution on O_2 Transfer: Results

6.5.1 Effects of Oxyglobin Solution on sO_2 Analysis

SaO_2 and $S\overline{v}O_2$ both decreased with a gradual addition of Oxyglobin to the circuit for both analysers. The M2 analyser decrease in SaO_2 and $S\overline{v}O_2$ were significant ($p<0.001$ and $p=0.0001$) but less pronounced graphically than the Cobe SaO_2 and $S\overline{v}O_2$ ($p<0.001$ and $p=0.049$) (Figure 6.1). SaO_2 and $S\overline{v}O_2$ achieved with the varying FiO_2 test showed a good linear correlation between the two analysers ($R^2=0.976$ and $R^2=0.920$, respectively) (Figure 6.2).

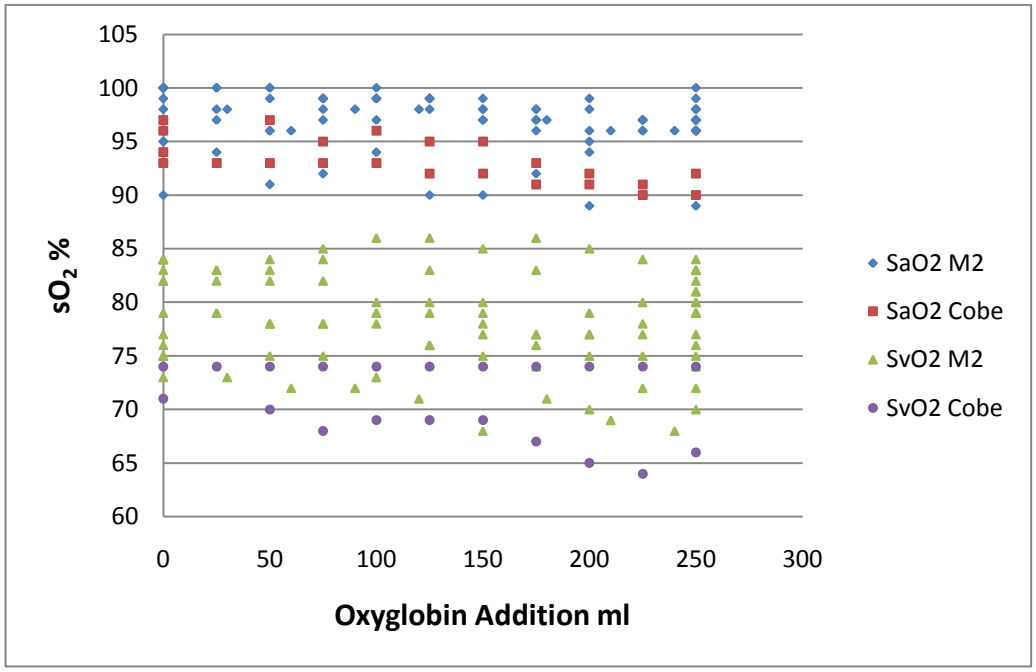

Figure 6.1 Effects of Oxyglobin Addition on sO_2 Analysers; SaO_2 and S $\overline{V}$ O_2 decreased for both the M2 (♦ SaO_2 p<0.001 and ▲ S $\overline{V}$ O_2 p=0.0001) and Cobe (■ SaO_2 p<0.001 and ● S $\overline{V}$ O_2 p=0.049) analysers.

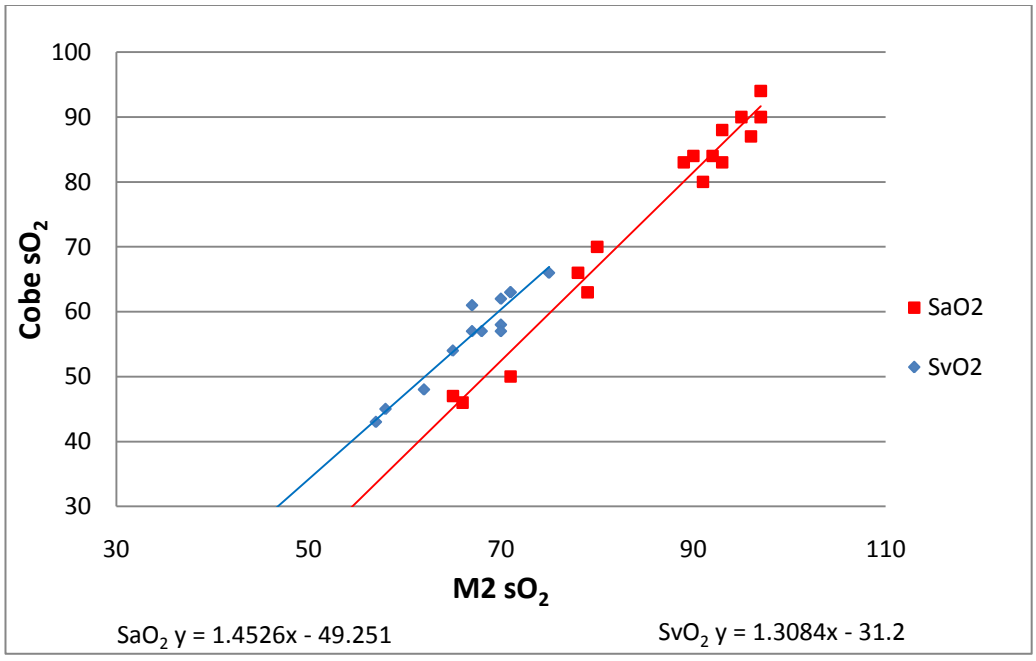

Figure 6.2 M2 versus Cobe sO_2 Correlation; Both SaO_2 ■ and S $\overline{V}$ O_2 ♦ showed good correlation between the two analysers (SaO_2 R^2=0.976 and S $\overline{V}$ O_2 R^2=0.920).

Table 6.1 Effects of Oxyglobin Solution Addition on sO_2

Effects of Oxyglobin Solution Addition on sO_2				
Parameter	***Trend***	***Statistical value***	***p value***	***d.f. or n***
M2 SaO_2	Decrease	R^2=0.134	p<0.001	d.f.=96
M2 S $\overline{v}$ O_2	Decrease	R^2=0.153	p=0.0001	d.f.=96
Cobe SaO_2	Decrease	R^2=0.450	p<0.001	d.f.=23
Cobe S $\overline{v}$ O_2	Decrease	R^2=0.165	p=0.049	d.f.=23
SaO_2 Analyser Correlation	Significant	R^2=0.976	p<0.001	d.f.=23
S $\overline{v}$ O_2 Analyser Correlation	Significant	R^2=0.920	p<0.001	d.f.=23

6.5.2 Effects of Oxyglobin Solution on O_2 Transfer

There was no change in potassium levels with gradual addition of Oxyglobin solution to the circuit blood (p=0.964). Potassium averaged 6.02 ±0.33 mmol/l.

There was no change in pHa or pHv on addition of Oxyglobin solution to the circuit blood (p=0.465 and p=0.766, respectively). pHa averaged 7.35 ±0.07 and pHv averaged 7.21 ±0.34.

There was no change in PaO_2 or P $\overline{v}$ O_2 with addition of Oxyglobin solution to the circuit blood (p=0.098 and p=0.591, respectively). PaO_2 averaged 79.33 ±6.91 mmHg and P $\overline{v}$ O_2 averaged 40.88 ±3.27 mmHg (Figure 6.3). $PaCO_2$ and P $\overline{v}$ CO_2 did not change with increasing addition of Oxyglobin solution to the circuit (p=0.605 and p=0.267,

respectively). $PaCO_2$ averaged 39.80 ±7.18 mmHg and P $\overline{V}$ CO_2 averaged 58.16 ±11.27 mmHg (Figure 6.4).

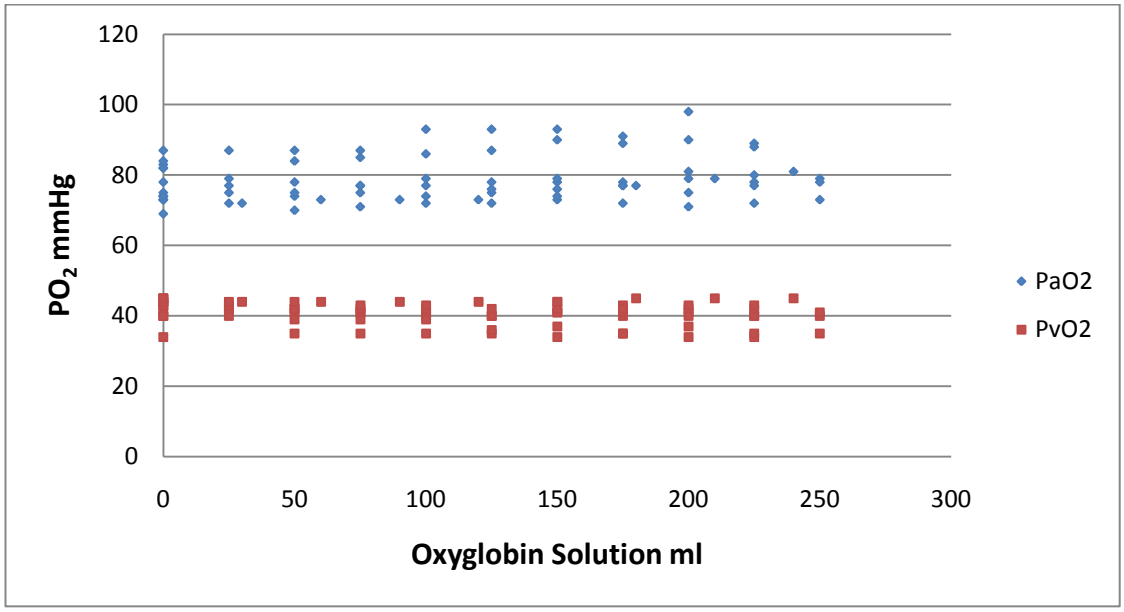

Figure 6.3 Effects of Oxyglobin Addition on PO_2; PaO_2 and P $\overline{V}$ O_2 were unaffected by Oxyglobin addition (p=0.098 and p=0.591). PaO_2 ♦ averaged 79.33 ±6.91 mmHg and P $\overline{V}$ O_2 ■ averaged 40.88 ±3.27 mmHg.

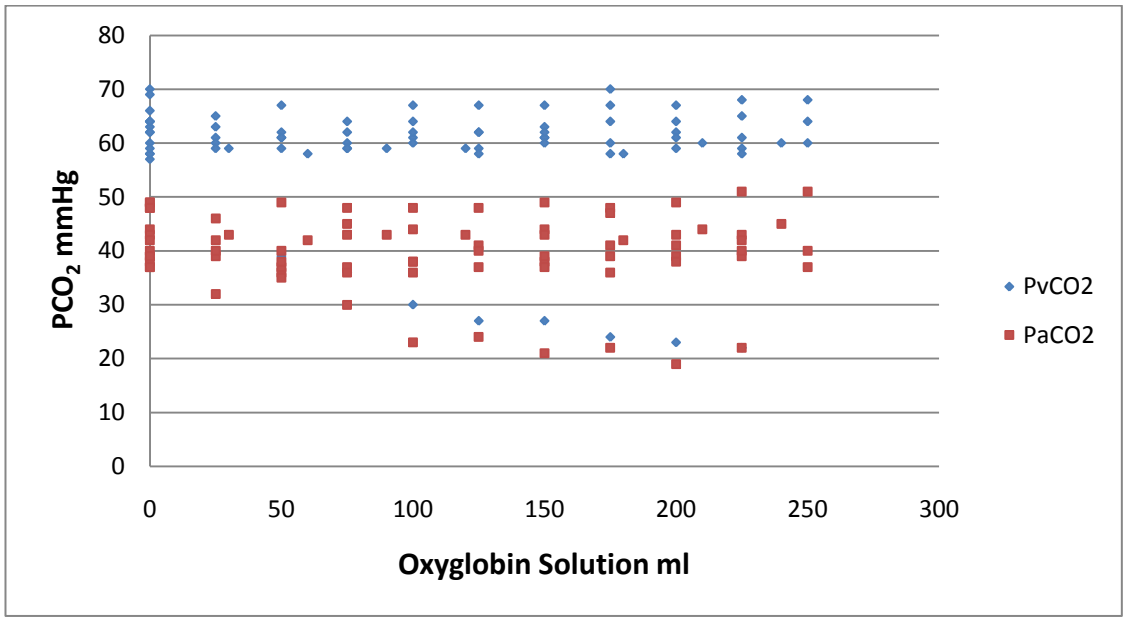

Figure 6.4 Effects of Oxyglobin Addition on PCO_2; $PaCO_2$ and P $\overline{V}$ CO_2 were unaffected by Oxyglobin addition (p=0.605 and p=0.267) where $PaCO_2$ ■ averaged 39.80 ±7.18 mmHg and P $\overline{V}$ CO_2 ♦ averaged 58.16 ±11.27 mmHg.

$\dot{M}O_2$ and DO_2 remained stable with gradual addition of Oxyglobin solution to the circuit (p=0.066 and p=0.051, respectively). $\dot{M}O_2$ averaged 196.10 ±64.11 ml/min (Figure 6.5) and DO_2 averaged 1.55 ±0.56 ml/min/mmHg (Figure 6.6). Inter-run variation was evident for both $\dot{M}O_2$ and DO_2 graphically and from the standard deviations presented.

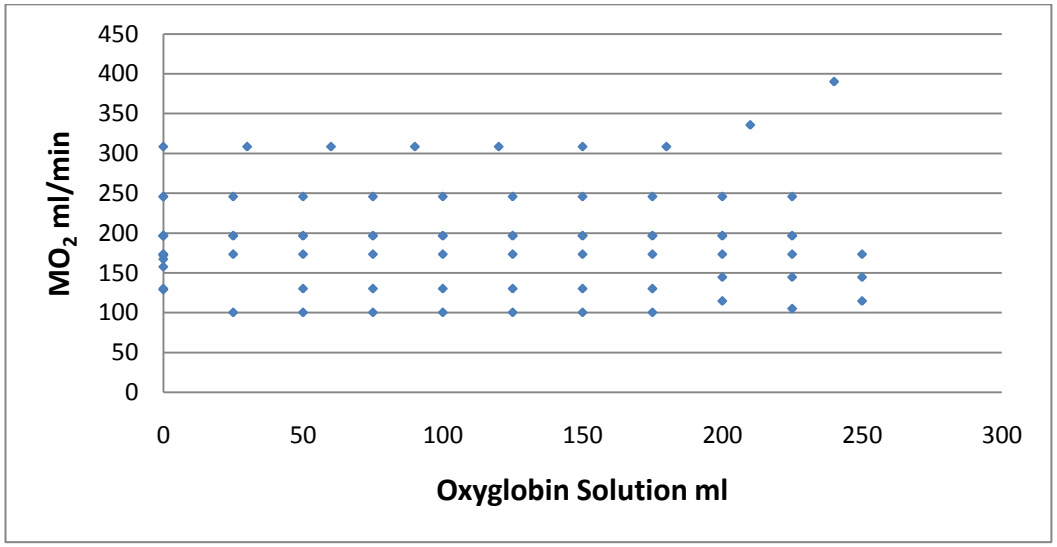

Figure 6.5 Effects of Oxyglobin Addition on $\dot{M}O_2$; $\dot{M}O_2$ was unaffected by Oxyglobin addition (p=0.066) averaging 196.10 ±64.11 ml/min.

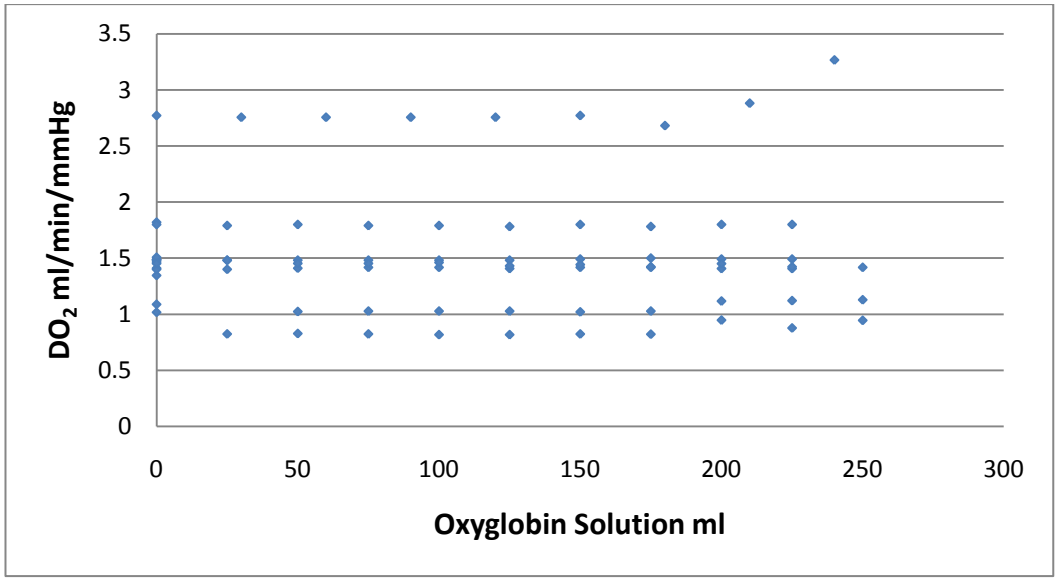

Figure 6.6 Effects of Oxyglobin Addition on DO_2; DO_2 was unaffected by Oxyglobin addition (p=0.051) averaging 1.55 ±0.56 ml/min/mmHg.

6.5.3 Effects of Oxyglobin Solution on ODC

The data demonstrated good curvilinear relationships between sO_2 and PO_2 for both the venous and arterial ODCs (Figures 6.7 and 6.9).

The Hills plot showed a good correlation between log PaO_2 and SaO_2 (S/1-S) ($p<0.0001$). A significant right shift of the arterial ODC in the presence of 250 ml Oxyglobin was evident when compared to the circuit blood ($p<0.0001$) (Figure 6.8).

The Hills plot of the venous ODC demonstrated significant correlation between log $P\overline{v}O_2$ and $S\overline{v}O_2$(S/1-S) ($p<0.0001$). The venous ODC was shifted to the right in the presence of 250 ml Oxyglobin when compared to the circuit blood ($p<0.0001$) (Figure 6.10).

P_{50} was calculated from the venous ODC data as 30.50 mmHg for the circuit blood and 35.20 mmHg for the 250 ml Oxyglobin solution addition to the circuit blood.

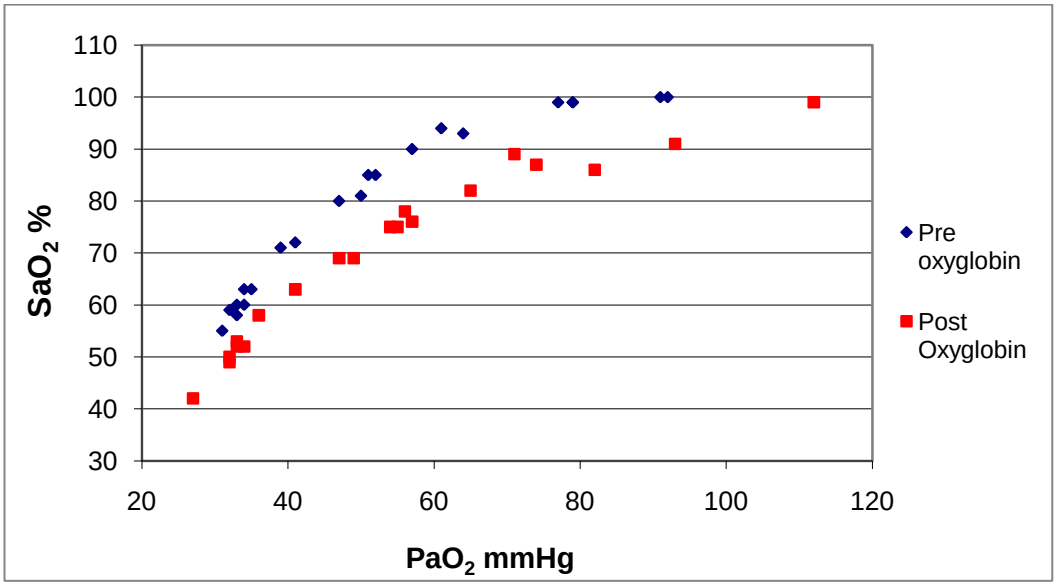

Figure 6.7 Effects of Oxyglobin Addition on the Arterial ODC; Oxyglobin ■ addition resulted in a right shift of the ODC ($p<0.0001$) compared to equine blood ♦.

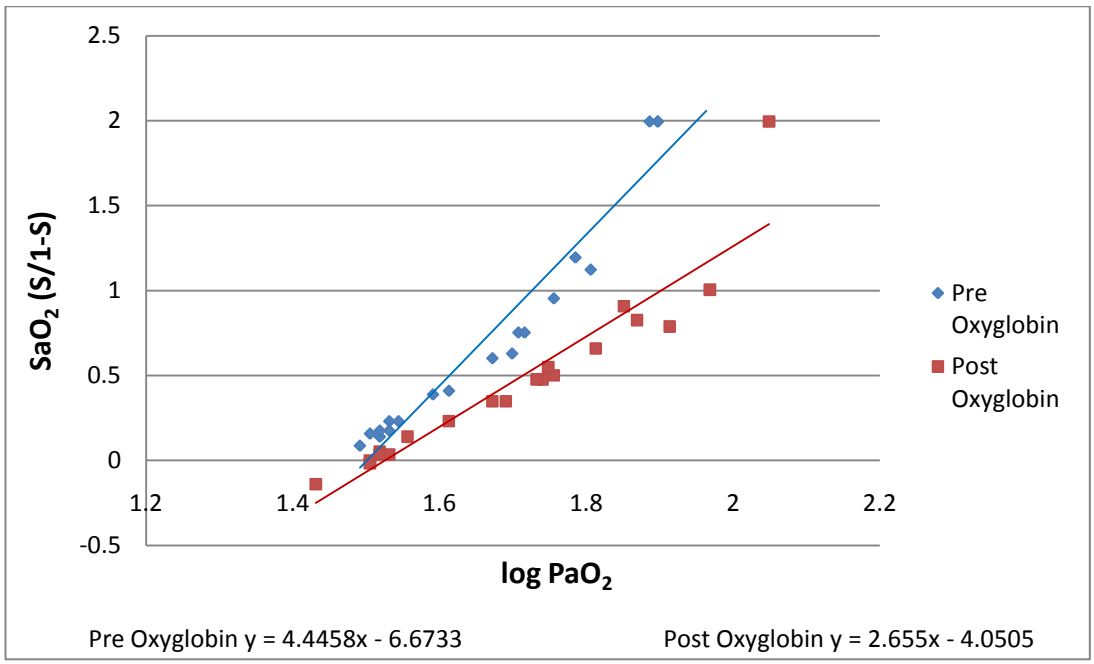

Figure 6.8 Effects of Oxyglobin Addition on the Arterial ODC – Hills plot; A significant right shift of the arterial ODC in the presence of 250 ml Oxyglobin ■ was evident when compared to equine blood ♦ ($p<0.0001$).

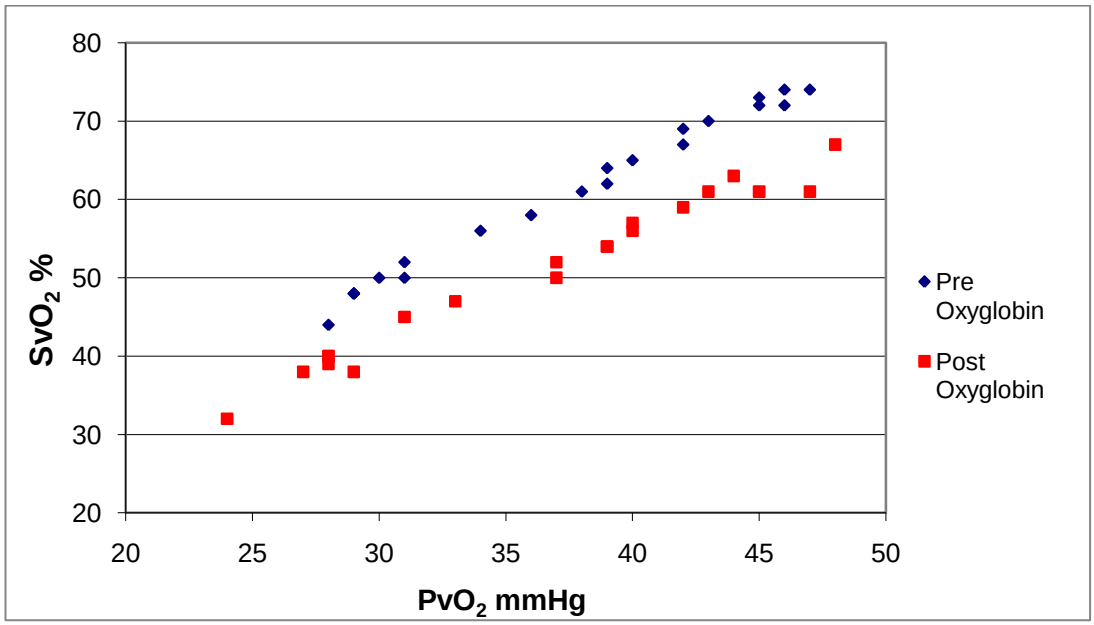

Figure 6.9 Effects of Oxyglobin Addition on the Venous ODC; A significant right shift of the ODC was observed after Oxyglobin ■ addition to equine blood ♦ ($p<0.0001$).

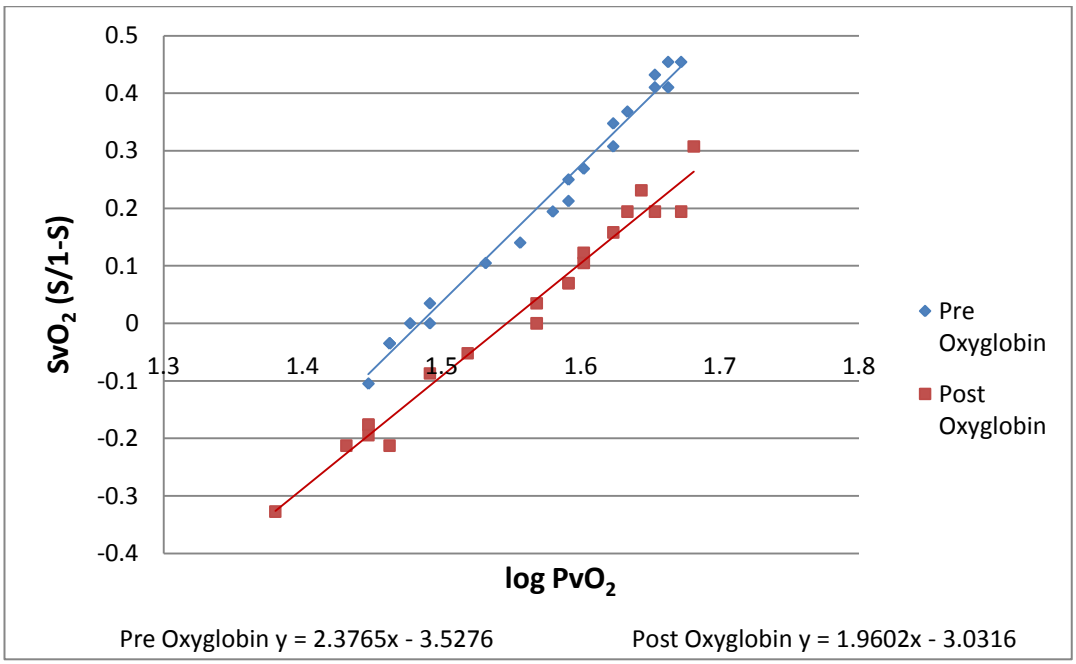

Figure 6.10 Effects of Oxyglobin Addition on the Venous ODC – Hills plot; Oxyglobin ■ addition to the equine blood ♦ resulted in a significant right ODC shift ($p<0.0001$).

6.6 Effects of Oxyglobin Solution on DNO and DCO: Results

6.6.1 Effects of Oxyglobin Solution on DNO and DCO

DNO increased curvilinearly with gradual addition of Oxyglobin solution to the circuit blood ($p<0.0001$) (Figure 6.11). DNO for the circuit blood averaged 7.41 ±2.77 ml/min/mmHg. After a 25 ml Oxyglobin solution aliquot to the circuit blood, DNO increased by 29% to a mean 9.59 ±3.90 ml/min/mmHg. After 250 ml Oxyglobin addition to the circuit blood, DNO had increased by 143% to an average 17.97 ±1.83 ml/min/mmHg.

DCO increased curvilinearly with gradual addition of Oxyglobin solution to the circuit blood ($p=0.005$) (Figure 6.12). DCO increased from 1.16 ±0.19 ml/min/mmHg prior to Oxyglobin addition up to 1.29 ±0.18 ml/min/mmHg after 225 ml Oxyglobin addition.

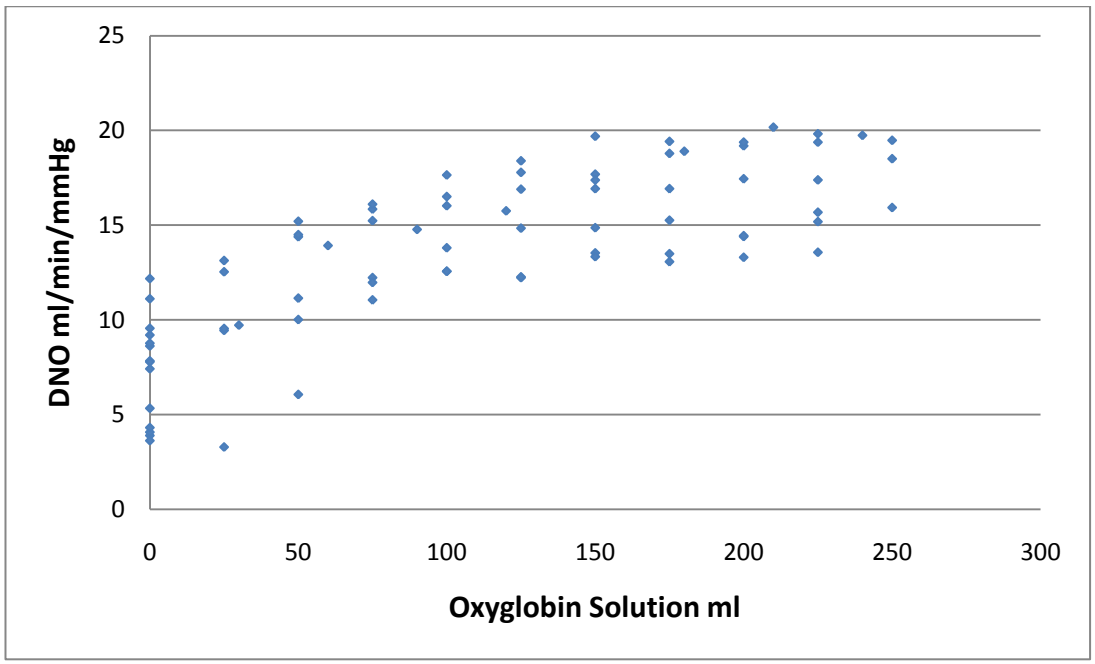

Figure 6.11 Effects of Oxyglobin Addition on DNO; DNO increased curvilinearly with Oxyglobin addition ($p<0.0001$) from 7.41 ±2.77 ml/min/mmHg (0 ml) to 17.97 ±1.83 ml/min/mmHg after 250 ml Oxyglobin.

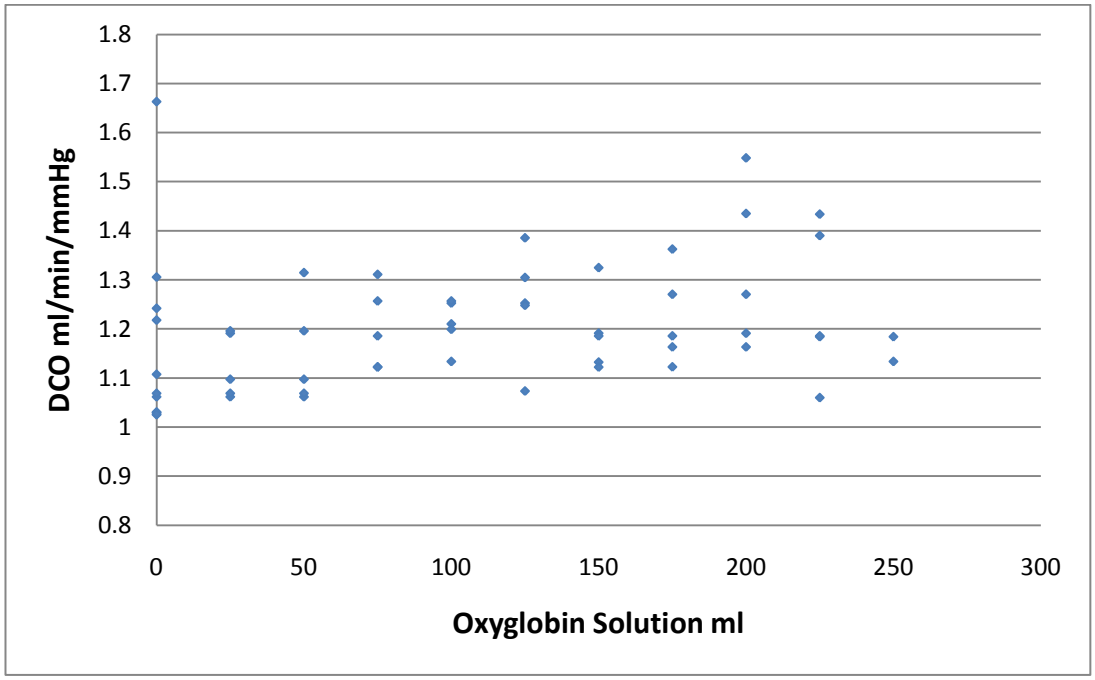

Figure 6.12 Effects of Oxyglobin Addition on DCO; DCO increased curvilinearly with Oxyglobin addition ($p=0.005$) from 1.16 ±0.19 ml/min/mmHg (0 ml) up to 1.29 ±0.18 ml/min/mmHg after 225 ml Oxyglobin.

6.6.2 Effects of Oxyglobin Solution combined with NO on ODC

The data demonstrated good curvilinear relationships between sO_2 and PO_2 for both the venous and arterial ODCs (Figures 6.13 and 6.15).

The Hills plot showed a good correlation between log PaO_2 and SaO_2 (S/1-S) ($p<0.0001$). A right shift of the arterial ODC in the presence of 250 ml Oxyglobin combined with NO was evident when compared to the circuit blood ($p=0.007$)(Figure 6.14).

Hills plot of the venous ODC demonstrated significant correlation between log P $\overline{v}$ O_2 and S $\overline{v}$ O_2(S/1-S) ($p<0.0001$). The venous ODC was shifted to the left in the presence of 250 ml Oxyglobin exposed to NO when compared to the circuit blood ($p=0.003$) (Figure 6.16). P_{50} was calculated from the venous ODC data as 25.34 mmHg for the circuit blood and 22.71 mmHg for the NO exposed Oxyglobin solution added to the circuit blood.

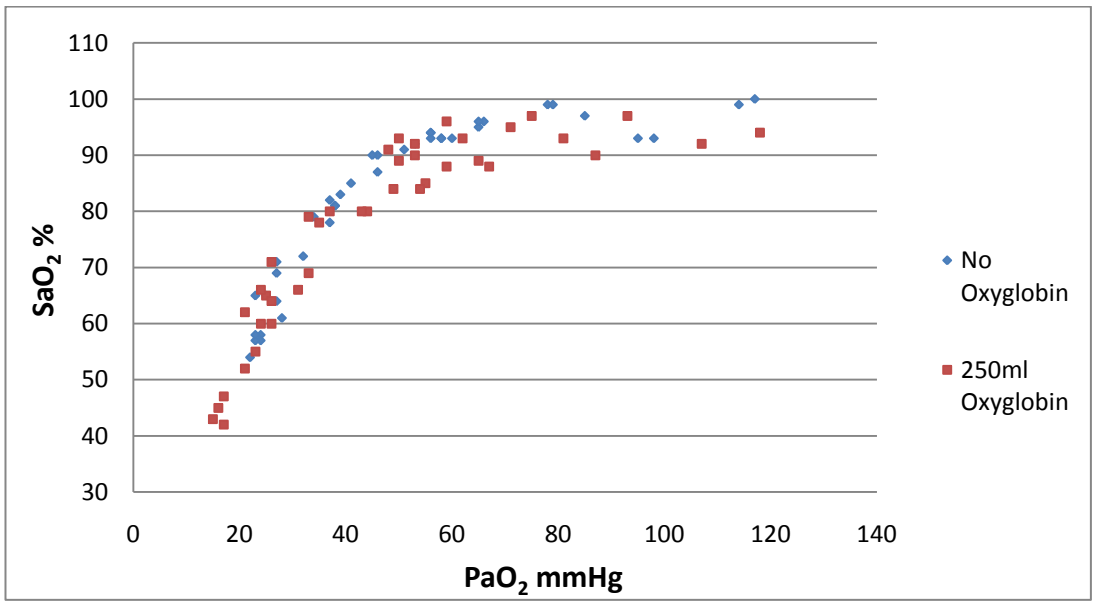

Figure 6.13 Effects of Oxyglobin and NO on the Arterial ODC; Oxyglobin combined with NO ■ resulted in a right shift of the arterial ODC compared to control ♦ ($p=0.007$).

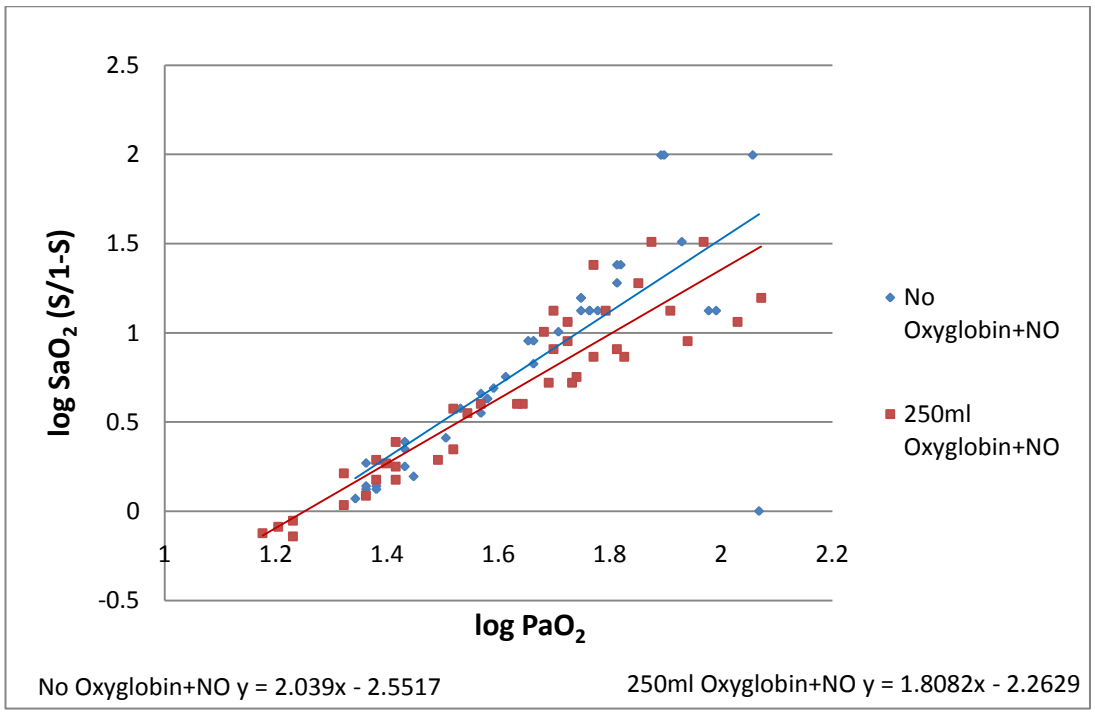

Figure 6.14 Effects of Oxyglobin and NO on the Arterial ODC – Hills plot; A right shift of the arterial ODC in the presence of 250 ml Oxyglobin combined with NO ■ was evident when compared to equine blood ♦ (p=0.007).

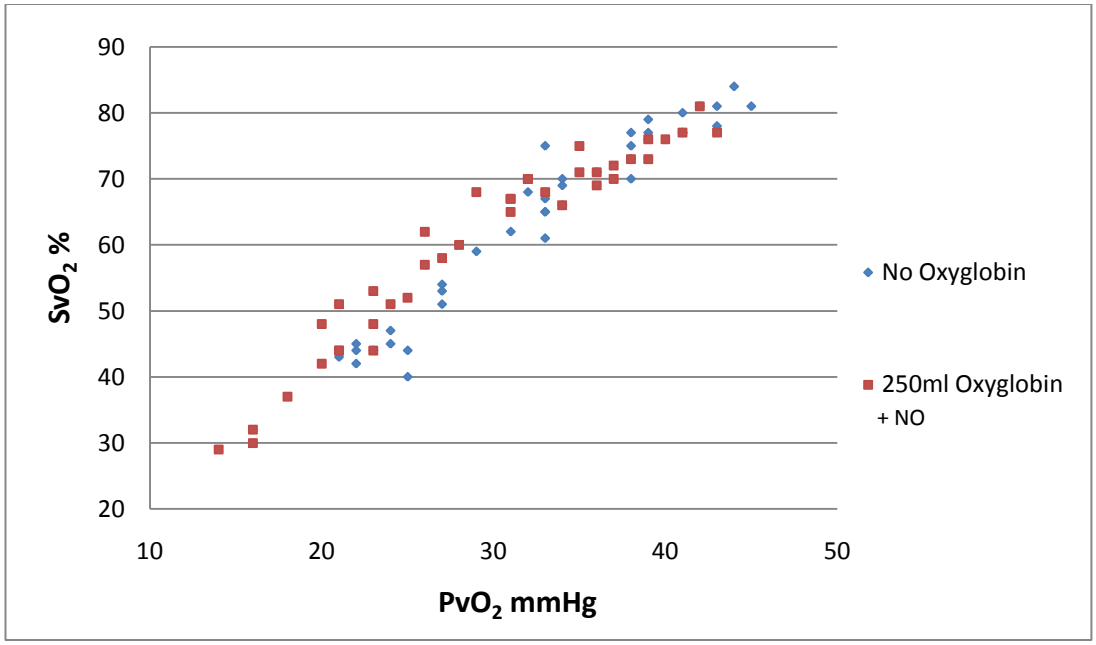

Figure 6.15 Effects of Oxyglobin and NO on the Venous ODC; 250 ml Oxyglobin combined with NO ■ resulted in a left venous ODC shift compared to equine blood ♦ (p=0.003).

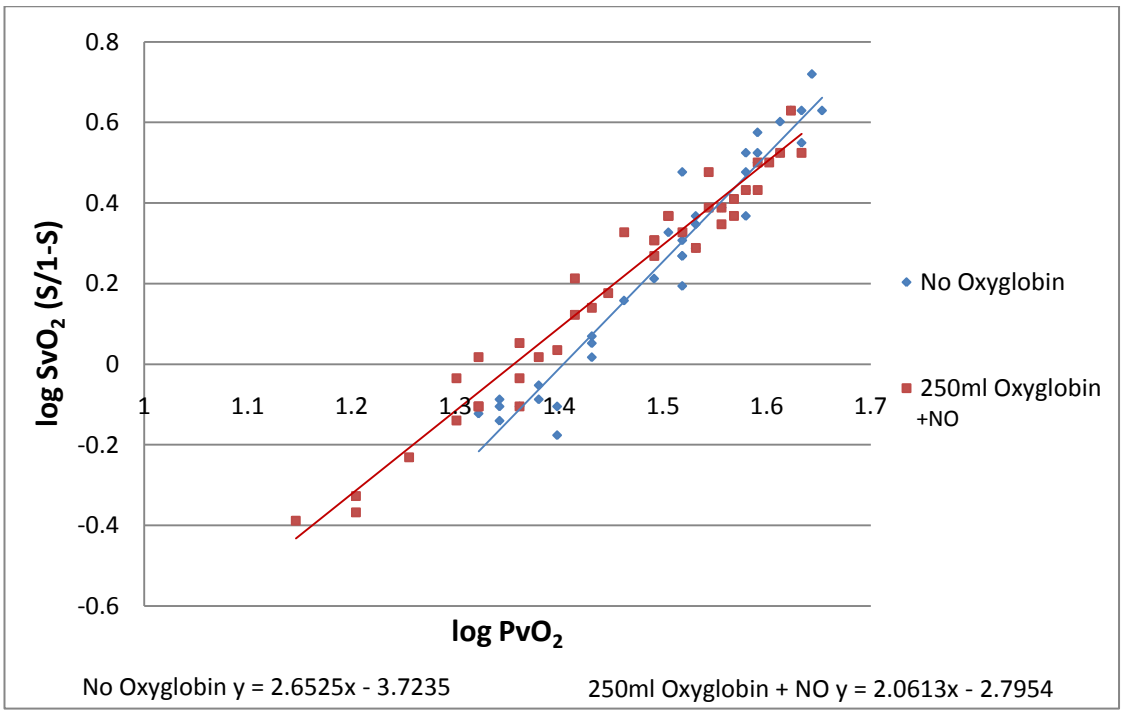

Figure 6.16 Effects of Oxyglobin and NO on the Venous ODC – Hills plot; The venous ODC was shifted to the left in the presence of 250 ml Oxyglobin exposed to NO ■ when compared to equine blood ♦ (p=0.003).

Table 6.2 Effects of Oxyglobin Solution on Gas Transfer

Effects of Oxyglobin Solution Addition on Gas Transfer				
Parameter	***Trend***	***Statistical value***	***p value***	***d.f. or n***
K^+	No change	R^2=0.000	p=0.964	d.f.=36
pHa	No change	R^2=0.007	p=0.465	d.f.=82
pHv	No change	R^2=0.001	p=0.766	d.f.=82
PaO_2	No change	R^2=0.033	p=0.098	d.f.=82
$P\overline{v}O_2$	No change	R^2=0.004	p=0.591	d.f.=82
$PaCO_2$	No change	R^2=0.003	p=0.605	d.f.=82
$P\overline{v}CO_2$	No change	R^2=0.015	p=0.267	d.f.=82
$\dot{M}O_2$	No change	R^2=0.041	p=0.066	d.f.=82
DO_2	No change	R^2=0.046	p=0.051	d.f.=82
Oxyglobin Art ODC Hills plot	Correlation Right Shift	R^2=0.865 *t*=14.689	p<0.0001 p<0.0001	d.f.=38 d.f.=38
Oxyglobin Ven ODC Hills plot	Correlation Right Shift	R^2=0.980 *t*=-16.235	p<0.0001 p<0.0001	d.f.=40 d.f.=40
DCO	Curvilinear increase	*r*=0.359	p=0.005	n=61
DNO	Curvilinear increase	*r*=0.704	p<0.0001	n=83
Oxygobin+NO Art ODC Hills plot	Correlation Right shift	R^2=0.853 *t*=-2.787	p<0.0001 p=0.007	d.f.=78 d.f.=78
Oxygobin+NO Ven ODC Hills plot	Correlation Left Shift	R^2=0.941 *t*=3.112	p<0.0001 p=0.003	d.f.=79 d.f.=79

6.6.3 Effects of Haemolysis post Oxyglobin Solution Addition on DNO and DCO

The results from this experiment were published and are presented in Appendix 9 (Borland *et al* 2010). Following publication, the calculations for DNO and DCO were modified to incorporate laboratory temperature and barometric pressure correction. Presented here are the modified results.

Addition of Oxyglobin to the oxygenator circuit increased DNO from 5.22 ±1.98 to 17.17 ±3.86 ml/min/mmHg ($p<0.0001$), while DCO increased from 1.02 ±0.05 to 1.37 ±0.19 ml/min/mmHg ($p<0.0001$). No significant further increase in DNO (mean 19.31 ±4.08 ml/min/mmHg) or DCO (mean 1.30 ±0.23 ml/min/mmHg) was observed after haemolysis was induced in the oxygenator circuit ($p=0.398$ and $p=0.600$, respectively) (Figures 6.17 and 6.18). Potassium levels rose from an average 6.03 ±0.33 (Oxyglobin phase) to >10 mmol/l during the haemolysis phase.

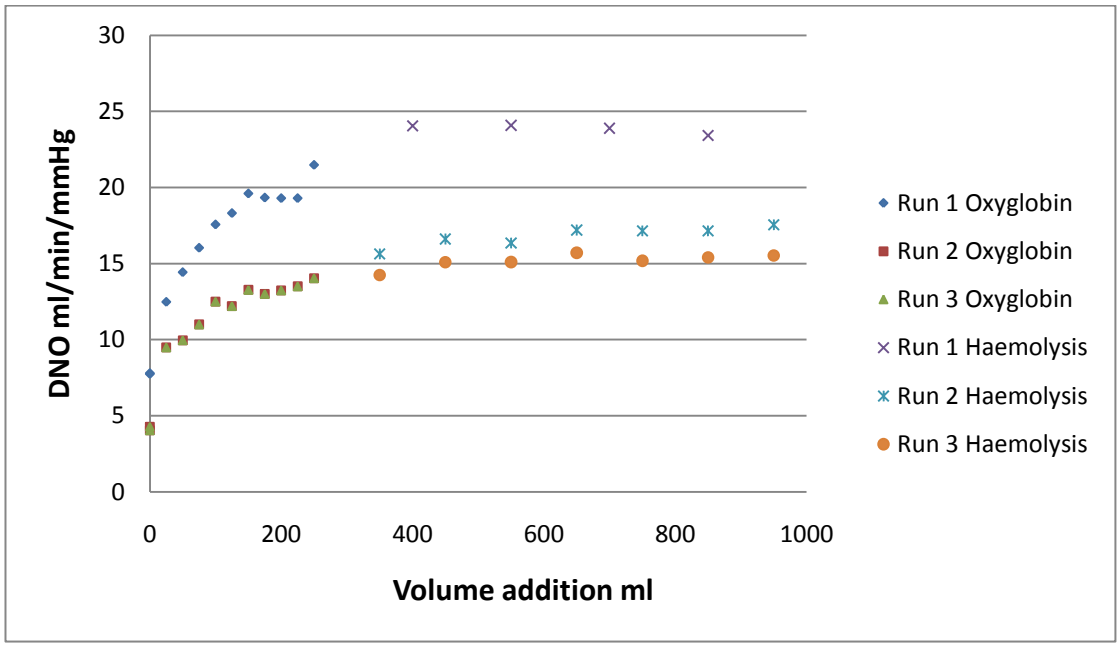

Figure 6.17 Effects of Oxyglobin and Subsequent Haemolysis on DNO; Addition of Oxyglobin ♦ ■ ▲ increased DNO from 5.22 ±1.98 to 17.17 ±3.86 ml/min/mmHg ($p<0.0001$) with no further increase in DNO during haemolysis X ✱ ● ($p=0.398$) (mean 19.31 ±4.08 ml/min/mmHg).

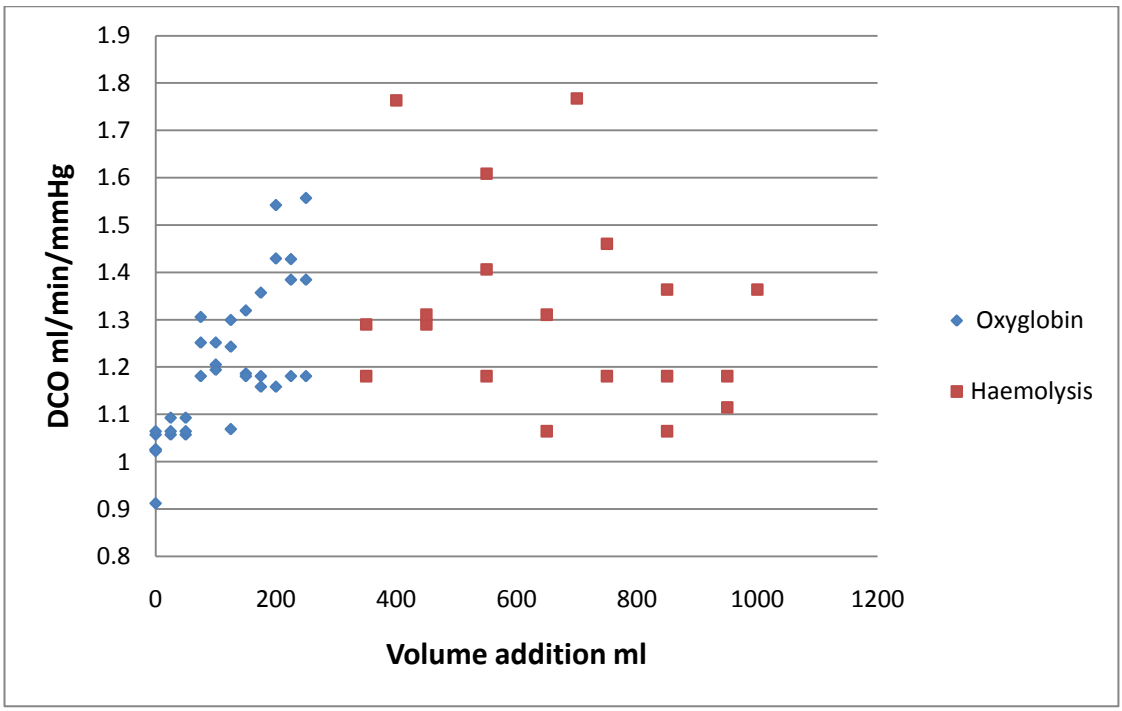

Figure 6.18 Effects of Oxyglobin and Subsequent Haemolysis on DCO; DCO increased from 1.02 ±0.05 to 1.37 ±0.19 ml/min/mmHg ($p<0.0001$) with Oxyglobin addition ♦ but no further increase was seen during the haemolysis ■ ($p=0.600$) (mean 1.30 ±0.23 ml/min/mmHg).

Table 6.3 Effects of Oxyglobin Solution Addition and Haemolysis on DNO and DCO

Effects of Oxyglobin Solution Addition and Haemolysis on DNO and DCO				
Parameter	***Trend***	***Statistical value***	***p value***	***d.f. or n***
Oxyglobin DNO	Curvilinear increase	$r=0.778$	$p<0.0001$	n=36
Oxyglobin DCO	Curvilinear increase	$r=0.712$	$p<0.0001$	n=36
Post Oxyglobin Haemolysis DNO	No change	$t=0.859$	p=0.398	d.f.=25
Post Oxyglobin Haemolysis DCO	No change	$t=-0.531$	p=0.600	d.f.=25

6.7 Implications of Oxyglobin Solution on Gas Transfer in the Membrane Oxygenator: Discussion

The aim was to determine if the Haemoglobin-Based-Oxygen-Carrier (HBOC) Oxyglobin affected DO_2, DNO and DCO in the membrane oxygenator circuit. It was previously concluded that haemolysis of circuit blood and addition of free Hb solution to the circuit resulted in an associated increase in DNO (Chapter 5). DNO resistance was attributed to one of three areas; RBC membrane, RBC interior or the plasma surrounding the RBC. To determine DNO resistance exerted by plasma, Oxyglobin was added to the circuit blood. Oxyglobin would reduce the boundary effect thus reducing plasma resistance. After HBOC addition, circulating RBCs were haemolysed to determine if the RBC membrane or interior was influential to DNO. The work in this chapter was extended to determine the NO scavenging potential of Oxyglobin. HBOCs have been linked to pulmonary hypertension, systemic hypertension, myocardial infarctions and strokes (Natanson *et al* 2008) due to the theoretical scavenging of endothelial NO in the vasculature (Irwin 2008).

Oxyglobin is a licensed HBOC for canine use and was the only available licensed product at the time of conducting this work. Oxyglobin can cause discolouration of blood during metabolism and excretion. Whilst Oxyglobin was not undergoing metabolic transformation within the circuit, an interference check was made of the spectrophotometric blood saturation analysers. A similar experiment in dogs pre and post Oxyglobin transfusion concluded that blood saturation equipment was unaffected by Oxyglobin (Jahr *et* al 2001). In this work, the Cobe Sat/Hct analyser (infrared light) and the Spectrum Medical M2 (white light) were comparably consistent in their results. There was no significant difference in sO_2 between the two analysers: a decrease in SvO_2 and SaO_2 was noted with gradual addition of Oxyglobin to the circuit blood. This was

considered an accurate result as it was evident in both analysers. The Oxyglobin manufacturing process increases P_{50} to enhance oxygen offloading to the tissues. The ODC experiments in this circuit showed a right ODC shift in the presence of Oxyglobin, increasing P_{50} from 32.50 mmHg for circuit blood to 35.20 mmHg. A right ODC shift would result in a reduction in SaO_2 and SvO_2 further supporting the Cobe and Spectrum Medical analyser results. Additionally, uptake of oxygen in the membrane would be reduced however in this circuit $\dot{M}O_2$ remained stable throughout the Oxyglobin. The lack of $\dot{M}O_2$ effect is due to the reduction in $\dot{M}O_2$ from the right ODC shift being masked by oxygen taken up by Oxyglobin.

DCO increased slightly with gradual addition of Oxyglobin to the circuit blood, whereas DNO increased up to 143%. This result confirms that RBC surroundings provide resistance to DNO. In flowing whole blood, a boundary layer effect occurs whereby the distance between the alveolar membrane and RBC is increased. Oxyglobin reduces the boundary effect as free Hb penetrates plasma surrounding the RBC and that between the RBC and the endothelial layer. Oxyglobin reduces DNO resistance by partaking in NO uptake which effectively bypasses the RBC membrane and interior. This finding was substantiated in three dogs undergoing D_LNO tests before and after three successive equal volume-exchange transfusions with Oxyglobin. D_LNO rose 57 ±16% after the Oxyglobin transfusions. The canine experiments were conducted and published in collaboration with this *in vitro* laboratory work (Borland *et al* 2010). Significant plasma resistance may also affect DNO at low Hb concentrations. In Chapter 3, a curvilinear increase in DNO was observed at lower Hb concentrations (<5 g/dl) which may be due to the spatial dispersion of RBC with increased unstirred RBC plasma layers or a lack of Hb availability. At clinical levels Hb has not affected D_LNO in anaemic patients' pre and post transfusion (van der Lee *et al* 2005).

To determine RBC membrane and interior resistance to DNO (post Oxyglobin addition), the RBCs were lysed by progressive water addition to the circuit. DNO did not significantly increase further with circuit haemolysis although a slight increase from a mean 17.17 ml/min/mmHg (250 ml Oxyglobin) to 19.31 ml/min/mmHg (haemolysis) was observed. It was considered that RBC membrane or interior resistance to DNO would result in a further DNO increase during the haemolysis phase. However, if the RBC membrane and interior effect was small it would be masked by the uptake of NO by Oxyglobin and liberated Hb. To clarify RBC membrane resistance, further work would need to be devised i.e. investigating DNO in normal compared to altered or reduced RBC membrane surface area. Despite this, the study has suggested that the traditional lung transfer equation for DNO, as detailed by Roughton and Forster (1957), may not be fully representative of the specific resistances encountered.

$$\frac{1}{D_L NO} = \frac{1}{D_M NO} + \frac{1}{\theta NO \times Vc}$$

In this equation (above) $D_L NO$ is the overall gas transfer for NO, $D_M NO$ is membrane transfer for NO, θNO is the blood conductance for NO and Vc is the pulmonary capillary blood volume. With data from this work, plasma has been isolated as an important source of DNO resistance. In patients with significant clinical haemolysis or post HBOC transfusion, lung function impairment may not be highlighted with current $D_L NO$ lung function testing. Presence of circulating free Hb or HBOC may enhance DNO in these patients. To rectify this, the calculation of DNO resistance should be modified to incorporate plasma resistance.

The combination of Oxyglobin and NO has not been documented. HBOCs scavenging endothelial NO have been widely accepted as the cause for HBOC induced pulmonary and systemic hypertension. The risk of HBOC associated MIs and increased mortality has halted licensing of such products for clinical use (Natanson *et al* 2008). The mechanism for HBOC induced MIs and increased mortality has been speculated as reduced coronary blood flow due to coronary vasoconstriction (Yu 2009) or inadequate organ perfusion due to systemic vasoconstriction (Winslow 2003). In this work, Oxyglobin has demonstrated NO scavenging potential and when Oxyglobin was administered to dogs, an increase in $D_L NO$ was observed (Borland *et al* 2010). Oxyglobin, as an HBOC example, readily binds NO supporting HBOC hypertension as a result of endothelial NO binding in the vasculature. To combat NO induced hypertension Yu *et al* (2009) suggested NO therapy prior to and during HBOC transfusion. In this study, Oxyglobin addition to the circuit blood when combined with NO resulted in a left venous ODC shift. Whole blood exposed to NO in this circuit also resulted in a left shift of the ODC (Chapter 5) so influence of Oxyglobin is unclear. Neya *et al* (1998) found that a Biopure HBOC oxidates to methaemoglobin readily over five hours in an extracorporeal circuit, associated with decreasing P_{50}. Oxyglobin in whole blood enhances P_{50} to increase oxygen offloading but when combined with NO, the P_{50} significantly reduced. Reduction in P_{50} results in poorer oxygen offloading in the tissues. It appears that HBOCs readily oxidate to methaemoglobin and NO enhances the oxidation rate. Oxidation rate was less with whole blood presence indicating antioxidant effects of whole blood upon HBOCs (Neya *et al* 1998). NO scavenging by the HBOC Oxyglobin could be coupled with a reduced P_{50} resulting in poorly perfused and poorly oxygenated organs. This work concludes that the HBOC Oxyglobin has NO scavenging properties with potential for increased oxygen affinity of the NO-bound HBOC.

CHAPTER 7 Discussion

In this work, a novel *in vitro* membrane oxygenator circuit was developed to test gas exchange. Circuit tests have shown that the RBC surroundings (plasma) provide significant resistance to nitric oxide diffusion, therefore in lung function testing $D_M NO$ cannot equal $D_L NO$ as the reaction rate of nitric oxide with blood does not equal infinity. The work has demonstrated a significant uptake of nitric oxide by the HBOC Oxyglobin, supporting its potential to scavenge endothelial nitric oxide *in vivo,* resulting in vasoconstriction. NO binding to Oxyglobin shifts the circuit blood ODC to the left resulting in poorer oxygen delivery to the tissues.

7.1 Circuit Design

The oxygenator circuit developed for this work is a unique model for testing gas exchange *in vitro* (Dunningham 2007). The circuit comprises two commercially available membrane oxygenators connected to form a continuous blood circuit resembling venous and arterial blood conditions. The work conducted in this circuit has demonstrated that particular elements of gas exchange can be examined whilst keeping other variables constant, so that the circuit can be manipulated to test theories previously devised. For example, in the diffusion resistance equation described by Roughton and Forster (1957), modified by Meade and Cotes (Cotes 1993), changes in gas exchange can be reliably attributed to specific resistance factors by changing each factor independently.

$$\frac{1}{D_L} = \frac{1}{D_M} + \frac{1}{\beta Q + \theta Vc}$$

In this equation, the overall resistance to lung diffusion (D_L) is made up of two components, the resistance of the membrane (D_M) and the resistance of the interaction of gas with the blood, where βQ is the influence of the ODC slope and blood flow and θVc is the specific conductance of the gas with 1 ml blood and the volume of pulmonary capillary blood.

This membrane oxygenator circuits allows examination of these individual diffusion resistances. The membrane oxygenator selected was a dual chamber device, enabling D_M and Vc to be tested by halving the membrane without altering blood flow. Blood flow could be adjusted from 0.1 to 2.5 l/min without affecting D_M. Varying FiO_2 experiments facilitated examination of β and θ elements of the reaction. Finally, varying Hct and haemolysis enabled diffusion resistances of the RBC to be investigated. In man, respiratory tests for gas exchange are subject to many clinical consequences i.e. a significant reduction in haematocrit results in increased cardiac output to compensate for reduced oxygen carrying capacity (Varat *et al* 1972). In this circuit, these consequences are not encountered so allowing for consistent experimental conditions. The scope of experiments undertaken for this work would not be suitable *in vivo* as some changing conditions would be detrimental to life i.e. hypoxia, low haematocrit and haemolysis. The experimental circuit has given insight into gas transfer for clinical and sub-clinical conditions. Such a circuit has not been developed previously for this type of investigation.

A commercial membrane oxygenator used as a deoxygenator is unusual as there is no clinical necessity. Several other researchers have cited varying deoxygenator unit numbers, membrane sizes and gas regimes (Gourlay *et al* 1990 and 1994, Van Meurs *et al* 1991, Rais-Bahrami *et al* 1992, Vocelka *et al* 1993, Griffiths *et al* 1994, Beckley *et al* 1996, Matsuda *et al* 2000, Kawahito *et al* 2001, Walczak *et al* 2005). This study used a

single deoxygenator unit with approximately 5 l/min (5.1-5.3 l/min) 8-10% CO_2 in N_2 to deoxygenate 2.5 l/min blood flow (Dunningham *et al* 2007). Similar deoxygenator circuits are now being described in Ex-Vivo-Lung-Perfusion (EVLP) circuits where harvested marginal donor lungs are maintained on a circuit for organ evaluation and re-conditioning prior to transplantation with good outcomes (Cypel *et al* 2009, Pego-Fernandes *et al* 2010, Okamoto *et al* 2010). These studies use 7% CO_2 in N_2 for the deoxygenator gas and ventilated lungs for arterialising the blood.

The blood used in this circuit was of equine origin rather than human due to ethical considerations. Several human donors of a compatible blood group would be required for each circuit (1500-2000 ml) leading to greater variation. Human blood from out-dated blood bank supply was considered inappropriate for gas transfer testing due to storage conditions that appear to induce 'storage lesion' of the blood. Red blood cells subjected to 'storage lesion' exhibit cell changes such as morphological changes, slowed metabolism, acidosis with decreased 2,3-DPG concentrations, decreased Hb nitric oxide binding, loss of functional pumps with loss of intracellular potassium and accumulation of sodium and loss of parts of the membrane (Liumbruno and Aubuchon 2010). All of these defects in stored RBC could have an impact on the results of this work. Previous use of alternative membrane oxygenator circuits have used vast quantities of blood obtained from abattoirs, typically of bovine origin (Vocelka *et al* 1993, Griffiths *et al* 1994, Gourlay and Taylor 1994, Beckley *et al* 1996). In this circuit, the quantities of blood required were much less due to the compact nature of the circuit. Equine blood was chosen as it is commercially available from horse donors where the age and gender can be specified. The blood is freshly withdrawn and used within a week of delivery to optimise gas transfer potential. Additionally, the haematocrit is kept within a consistent range (Hct 40-50 %) from the supplier. As the blood is commercially available it allows for reproduction of the

methodology. Alternative animal species were considered but the size of the horse enabled one donor to supply blood to complete a single circuit with haemolysed solution. There are differences between equine and human blood that have to be acknowledged. Clerbaux *et al* (1993) compared blood of horse with human blood. The equine RBC is slightly smaller at 5-6 µm compared to human (6-8 µm). The haemoglobin structure is the same comprising two alpha and two beta chains. There is slightly more 2,3 DPG present in equine RBCs compared to human RBCs, yet the P_{50} of equine blood is lower at 23.8 ±0.8 mmHg compared to human P_{50} 26.6 mmHg (Clerbaux *et al* 1986 and 1993). Equine blood has a higher affinity for oxygen compared to human blood resulting in a leftward ODC shift. The differences in equine and human ODC would not affect the ODC tests carried out in this work as control data was taken from the same circuit and donor as the 'treated' group. Calculations of DO_2 were based on Severinghaus which is related to human blood. When a correction factor was applied to the Severinghaus formula for equine blood (based on data from Clerbaux *et al* 1993) there was no significant difference in Severinghaus and Clerbaux corrected DO_2 calculations ($p=0.854$) (Appendix 2). Despite minor differences in equine and human blood, the use of equine blood does not detract from the results and conclusions so derived.

7.2 Effects of the Volatile Anaesthetic Isoflurane on Gas Transfer

The test circuit was used to determine the effects of Isoflurane on gas transfer in the membrane oxygenator. This volatile anaesthetic is routinely used during cardiopulmonary bypass, being administered via the membrane oxygenator. Manufacturers of membrane oxygenators do not advocate use of volatile anaesthetic agents in their devices as they have insufficient data supporting the relicensing requirements of regulatory authorities.

The literature review highlighted a lack of data demonstrating the effects of volatile anaesthetic agents on gas transfer in membrane oxygenators, although studies have been conducted in bubble type oxygenators (Price *et al* 1988, Henderson *et al* 1988, Nussmeier *et al* 1988 and 1989). Work in this circuit demonstrated adequate transfer of Isoflurane across the polypropylene membrane oxygenator which concurred with previous research by Henderson *et al* 1988, Stern *et al* 1989, Hickey *et al* 1996, Lockwood 1999 and Wiesenack *et al* 2002. The wash-out time observed in this circuit was substantially lower than that quoted in previous work. Those data were established in the clinical setting and were subjected to patient uptake of Isoflurane. This *in vitro* circuit was not influenced by patient distribution of Isoflurane, thus Isoflurane was rapidly removed from blood across the membrane. Preliminary data in this circuit supported an increased oxygen uptake ($\dot{M}O_2$) in the presence of Isoflurane without a change in PO_2 (Borland *et al* 2007b). No other research groups have reported such an effect. This observation led to the modification of the circuit equipment to facilitate simultaneous PO_2 and sO_2 monitoring at varying FiO_2 replicating the ODC. Early data showed a venous left ODC shift which is associated with poor oxygen offloading in the tissues but enhanced oxygen uptake in the lungs (Borland *et al* 2007b). This finding was supportive of the previous increase in $\dot{M}O_2$ but was not Isoflurane dose dependent casting doubts on the effects seen. Further investigations into the increased $\dot{M}O_2$ with Isoflurane highlighted the critical factor being the FiO_2-FeO_2 difference in the $\dot{M}O_2$ calculation. Exploration of the methodology found that the Isoflurane vaporiser positioning had a profound impact on the FiO_2 reading when it was switched on. With the FiO_2 analyser placed prior to the Isoflurane vaporiser there was an increase in FiO_2 readings when the vaporiser was used, thus an artificially elevated FiO_2 resulted. By repositioning the FiO_2 analyser post vaporiser, the actual FiO_2 delivered to the membrane oxygenator was observed. Repeating the experimental work with appropriate positioning of the Isoflurane vaporiser revealed that Isoflurane had no effect

on oxygen transfer in the membrane oxygenator. The venous and arterial ODCs were unaffected by Isoflurane administration to the circuit blood. The oxygen uptake finding was consistent with those reported by Muhle *et al* (2001). Muhle's study was limited by the 30 second exposure time not being adequate for an effect to occur when other groups have reported lengthier wash-in and wash-out times. Muhle's single-pass methodology was limiting to the length of time the circuit could be run. This work sought to address these issues by utilising a continuously run circuit over a longer time duration, to ensure equilibrium was reached between the blood and gas phases. No other research group have conducted experiments to show the effect of Isoflurane administered via the membrane oxygenator on the ODC (Borland *et al* 2007b). The experimental work conducted with this circuit design has developed ODC methodology and concluded that Isoflurane does not affect oxygen carriage in the blood.

By utilising a diffusion limited gas (NO) the impact of Isoflurane on membrane integrity was investigated in this circuit. The methodology used in this work was vastly different from previous approaches. Crosbie *et al* (1998) exposed samples of polypropylene membrane to Isoflurane for extended periods prior to light microscopic evaluation, which showed no structural changes. They concluded that Isoflurane would not affect oxygen transfer across a polypropylene membrane oxygenator. Lanquetot (2005) evaluated clinical data from patients undergoing cardiopulmonary bypass with oxygenator Isoflurane anaesthesia administration. The author determined that oxygen transfer data was not affected by Isoflurane anaesthesia in the membrane oxygenator. In this research, there were physical constraints in accessing the membrane material from the oxygenator housing once the unit had been exposed to equine blood. Drilling a hole in the outer oxygenator casing followed by sample extraction via cork borer was explored but there were concerns about damage sustained by the membrane material during the process. This

alternative approach was devised to assess membrane integrity during the Isoflurane administration. If the structure or efficiency of the membrane was affected by Isoflurane then an effect would be observed in a diffusion limited gas. In this work, DNO did not increase in the presence of Isoflurane concluding that Isoflurane does not affect the integrity of the polypropylene membrane.

7.3 Resistance of the Erythrocyte and Surroundings on DNO

The circuit enabled the effects of haemolysis on gas transfer to be investigated. Gross haemolysis is not feasible *in vivo* due to the detrimental affects sustained by the lungs and kidneys. Haemolysis occurs when the RBC membrane is disrupted, liberating its contents into the RBC surroundings (plasma). Clinical haemolysis occurs in infections (bacterial or parasitic), autoimmune conditions or genetic disorders. The importance of the RBC membrane in overall gas transfer can be investigated in a circuit such as this. Gas diffusion describes the transfer of gas from the alveolar membrane to binding with haemoglobin. The process involves gas moving across the alveolar membrane where it diffuses through plasma, crosses the RBC membrane before binding with haemoglobin. In diffusion limited gas such as carbon monoxide or nitric oxide there is no influence from blood flow or ODC so Roughton and Forster's (1957) equation reflects this.

$$\frac{1}{D_L NO} = \frac{1}{D_M NO} + \frac{1}{\theta NO \times Vc}$$

Where, D_L is the overall resistance to lung diffusion, D_M is the resistance of the membrane, Vc is the pulmonary capillary blood volume and θ is the specific conductance of the gas with 1 ml blood.

The importance of RBC resistance has been disputed with regards to lung function testing where NO is utilised. The current standards describe the test as a single breath procedure with CO (Forster 1983), but a more recent procedure has emerged that combines results of both NO and CO transfer across the lungs (Guenard *et al* 1987, Borland *et al* 1989). NO has a faster binding to haemoglobin and is independent of inspired oxygen concentrations that can affect carbon monoxide uptake. Limitations have prevented NO use in lung function testing due to concerns with the length of breath holding, equipment sensitivity and NO toxicity. RBC resistance to NO has implications for the use of NO in lung function testing. The overall D_LNO would not be reflective of D_MNO depending on the resistance proportion attributed to the RBC. Guenard *et al* (1987) speculated that D_LNO would equal D_MNO due to the rapid and irreversible nature of the binding between NO and haemoglobin. It was thought that θNO could be considered infinite. Heller and Schuster (1998) reported that the diffusion element (D_MNO) accounted for 98 ±6% of the overall resistance to alveolar-capillary NO transfer suggesting that any resistance exerted by the RBC would have minimal impact on D_LNO. Other groups have questioned the importance of the RBC on D_LNO, suggesting that D_LNO is not just NO transfer across the alveolar membrane but also includes the diffusion of NO within the capillary plasma and the RBC (Borland *et al* 2006 and 2010).

In this apparatus, the methodology was amended to investigate the effects of haemolysis on DNO. Initially, the circuit blood was gradually haemolysed by addition of water resulting in gross haemolysis but as this was not clinically representative, so a haemolysed (free Hb) solution was made and added to the circuit blood. These experiments (Chapter 5) concluded that haemolysis of the circuit blood and addition of free Hb solution to the circuit resulted in an associated increase in DNO. The cause of the DNO resistance was attributed to one of three areas; RBC membrane, RBC interior or the plasma surrounding

the RBC (Borland *et al* 2006). During gross haemolysis of the circuit blood, the RBC membrane and interior resistance was eradicated and the liberated Hb from the lysed RBCs also reduced the RBC surroundings resistance. Therefore, the initial work could not reliably conclude the source of DNO resistance. Free Hb solution addition to the circuit blood reduced the plasma resistance but further lysis induced by the free Hb solution addition could not be eliminated. To determine if resistance to DNO in the circuit blood was due to the RBC surroundings, an HBOC was added to the circuit blood. After HBOC addition, the circulating volume was haemolysed to determine if the RBC membrane or interior was influential in DNO.

DNO increased up to 143% (ranged 29 to 143 %) with gradual Oxyglobin addition to the circuit. This result concluded that the RBC surroundings (plasma) provide resistance to DNO in this *in vitro* circuit. The outcome of this work concurred with a study conducted by Liu (2002) whereby competition NO diffusion experiments previously conducted by Vaughn *et al* (2000) were mathematically modelled and analysed. Liu (2002) concluded that competition methodology of rocker mixing the blood did not remove the extracellular barrier and the predominant RBC resistance to DNO was due to the surrounding unstirred layer. When whole blood flows through pulmonary capillaries there is a boundary layer effect whereby the distance between the alveolar membrane and RBC is increased with flow. Oxyglobin reduces the boundary effect as free Hb penetrates the plasma surrounding the RBC and that between the RBC and endothelial layer. Oxyglobin reduces DNO resistance by partaking in NO uptake and bypassing the RBC membrane and interior. In the oxygenator model, the blood flow channel is much larger than the pulmonary capillaries which facilitates laminar flow characteristics and therefore may exhibit a larger boundary effect. However, these oxygenators have mixing structures within the blood channels to minimise the laminar flow characteristics. The resistance of

the RBC surroundings on DNO was also substantiated when three dogs underwent D_LNO tests before and after three successive equal volume-exchange transfusions with Oxyglobin. D_LNO rose 57 ±16% after Oxyglobin transfusions (Borland *et al* 2010).

Post Oxyglobin addition to the circuit blood, there was a progressive addition of water to lyse the RBCs. This methodology was to determine if the RBC membrane or interior provided resistance to DNO, based on the idea that if either provided resistance then a further DNO increase would be observed. Other groups have cited intracellular resistance (Sakai *et al* 2008) and/or transmembrane resistance (Vaughn *et al* 2000) to DNO in their work. In this experiment, DNO did not significantly increase further with haemolysis of the circuit blood although there was a small increase from a mean 17.17 ±3.86 ml/min/mmHg (250 ml Oxyglobin) compared to 19.31 ±4.08 ml/min/mmHg (haemolysis). This result would conclude that the RBC membrane and interior do not provide resistance to DNO, although the methodology presented here may not fully explore this theory. Firstly, Oxyglobin and free Hb liberated from the RBCs during lysis have shown an associated curvilinear increase in DNO. The DNO increase is apparent after a small addition of free Hb or Oxyglobin to the circuit reducing the boundary effect exerted by plasma. The subsequent observed DNO plateau indicates that the threshold of resistance exerted by the unstirred plasma layer has been achieved. Post Oxyglobin haemolysis removes the RBC membrane and releases intracellular Hb but the resistance of the RBC membrane will have no further impact on DNO as the overriding plateau caused by Oxyglobin and free Hb mask the membrane effect. Alternatively, if the RBC encapsulated outer Hb has bound NO during the Oxyglobin addition phase, this is thought to provide a barrier to further NO penetration of the RBC (as described by Sakai *et al* 2008). Upon haemolysis, Hb within the central area of the RBC not previously exposed to NO will be liberated and would essentially be partaking in NO uptake within the plasma where the

effect (if small by comparison to Oxyglobin) would be lost within the overall DNO. It must be acknowledged that the conclusion from this work regarding the RBC membrane and interior resistances is not robust. To define the resistance applied by the RBC membrane and its interior, alternative experiments need to be conducted to validate the findings from this work. It would be necessary to demonstrate that red cell deformation had no effect on DNO thus forming the basis of future experiments. Despite this, the study has suggested that the traditional lung transfer equation for DNO, as detailed by Roughton and Forster (1957), may not be fully representative of the specific resistances encountered, such as plasma.

$$\frac{1}{D_L NO} = \frac{1}{D_M NO} + \frac{1}{\theta NO \times Vc}$$

In this equation (above) $D_L NO$ is the overall gas transfer for NO, $D_M NO$ is membrane transfer for NO, θ is the blood conductance for NO and Vc is the pulmonary capillary blood volume. With the data and results from this work an important resistance to DNO by the RBC surroundings (plasma) has been isolated. In the collaborative work conducted in dogs with exchange transfusion of Oxyglobin, 37% of the overall resistance to $D_L NO$ was attributed to the erythrocyte-related barrier (Borland *et al* 2010). This finding demonstrates the potential impact of clinical haemolysis or HBOC transfusion on $D_L NO$. In patients with significant clinical haemolysis or post HBOC transfusion, lung function impairment may not be highlighted with the current $D_L NO$ lung function testing. Presence of free Hb or HBOC in the circulation may enhance DNO in these patients. To rectify this, the calculation of DNO resistance should be modified to incorporate plasma resistance.

7.4 NO Binding Potential of the HBOC Oxyglobin and the Implications

The membrane oxygenator circuit was used to determine if the Haemoglobin-Based-Oxygen-Carrier (HBOC) Oxyglobin affected gas transfer of DO_2, DNO and DCO. Principally, the methodology was devised to investigate DNO resistance of the RBC surroundings by adding an HBOC to reduce the boundary layer whilst maintaining intact circulating RBCs. HBOCs have been linked to pulmonary hypertension, systemic hypertension, myocardial infarction and stroke (Natanson *et al* 2008) due to the theoretical endothelial NO scavenging potential in the vasculature (Irwin 2008). Oxyglobin was assessed for its NO scavenging potential via the uptake of NO across the membrane. The use of a membrane oxygenator circuit to assess and quantify NO uptake by an HBOC is a unique and novel investigation. By simultaneously measuring blood sO_2 and PO_2, the circuit was used as a continuous tonometer enabling the affects of Oxyglobin on venous and arterial ODCs to be assessed.

The ability of Oxyglobin to bind NO was demonstrated and quantified. NO uptake increased by up to 143% on addition of Oxyglobin to the circuit blood. The NO binding potential of Oxyglobin via the membrane oxygenator is immense. In dogs, D_LNO increased after exchange transfusion of Oxyglobin of 57 ±16% (Borland *et al* 2010) further supporting NO scavenging of Oxyglobin. The hypothesis that HBOCs bind endothelial NO resulting in HBOC associated vasoconstriction is supported by this work. Yu *et al* (2009) corroborated this theory by demonstrating that NO synthase deficient mice do not exhibit hypertensive effects when transfused with HBOC, compared to non-deficient normal mice. The same authors have shown that inhaled NO treatment prior to and during an HBOC transfusion can reduce the vasoconstrictive effects (Yu *et al* 2008 and 2009). In the collaborative canine study (Borland 2010), systemic and pulmonary

blood pressures were unaltered during exchange transfusion of Oxyglobin with NO inhalation. Pre-treatment of patients with inhaled NO prior to HBOC transfusion is a novel approach. For cardiothoracic patients undergoing cardiopulmonary bypass, pre-treatment with inhaled NO would be via the membrane oxygenator of the cardiopulmonary bypass circuit as the lungs would be deflated during the procedure. Body *et al* (1999) demonstrated that NO does not affect the structural integrity of polypropylene membrane oxygenators. This work shows that NO readily passes across the microporous polypropylene membrane oxygenator.

The manufacturing process of Oxyglobin incorporates an increase in P_{50} to enhance oxygen offloading to the tissues. Previous theories linked enhanced HBOC P_{50} to hypertension via autoregulation of the blood vessels in response to increased arteriolar blood partial pressure of oxygen. Therefore a small number of HBOCs were developed with a lower than normal P_{50}. The study by Natanson *et al* (2008) associating HBOCs to increased mortality and MIs incorporated HBOCs with higher and lower oxygen affinities, rendering the autoregulation theory unlikely. The ODC work carried out in this circuit demonstrated a right ODC shift post Oxyglobin transfusion to the circuit. The $P\overline{v}O_2$ for a given SvO_2 is elevated thus increasing the oxygen partial pressure difference in the tissues orchestrating better oxygen delivery. Oxyglobin significantly shifted the P_{50} from 32.50 mmHg (circuit blood) to 35.20 mmHg (circuit blood combined with Oxyglobin). In a right shift of the ODC, uptake of oxygen across the membrane would be reduced however $\dot{M}O_2$ remained stable throughout the Oxyglobin addition. The lack of $\dot{M}O_2$ effect would be due to the reduction in $\dot{M}O_2$ from the right shift being masked by oxygen taken up by Oxyglobin.

As previously discussed Oxyglobin readily binds NO. The affects of NO-bound Oxyglobin on the ODC is understudied, so this area was investigated in this research. Pre-treatment of patients with NO prior to HBOC transfusion (Yu *et al* 2008 and 2009) may affect the ODC. This work has demonstrated that NO significantly shifted the ODC of circuit blood to the left due to irreversible binding of NO to haemoglobin. The P_{50} of NO-bound circuit blood was 26.12 mmHg compared to the non-NO exposed circuit blood P_{50} 29.41 mmHg. If NO can shift the ODC of the circuit blood to the left, but Oxyglobin has demonstrated a right shift of the circuit blood, concern was raised about the effects of NO-bound Oxyglobin on the circuit blood. Tests in this apparatus demonstrated a leftward shift in the venous ODC with NO-bound Oxyglobin. Oxyglobin has an enhanced P_{50} of 35 mmHg to increase oxygen offloading but when combined with NO, the P_{50} significantly reduced to 22.71 mmHg compared to 25.34 mmHg for the circuit blood. A reduction in P_{50} would result in poor oxygen offloading in the tissues. These tests cannot determine the cause of the reduced P_{50} i.e. as a result of NO-bound Oxyglobin or NO-bound whole blood, as NO was administered via the membrane prior to and during the Oxyglobin addition. The ODC effect may not be as significant in patients undergoing HBOC transfusion that binds endothelial NO compared to patients pre-treated with NO prior and during an HBOC transfusion. The beneficial effects of HBOCs with elevated P_{50} would be lost if patients undergo NO pre-treatment. Similarly, HBOCs with a low P_{50} coupled with NO binding may reduce the blood P_{50} to unacceptably low levels affecting oxygen carriage of the blood. To further address the ODC effects of NO-bound HBOCs, the circuit could be primed solely with HBOC and the ODC conducted with and without NO via the membrane. In conclusion, vasoconstriction as a result of NO scavenging by Oxyglobin may be coupled with a reduction in P_{50} resulting in poorly perfused and poorly oxygenated organs. This work has demonstrated a potential dual mechanism for increased risk of MI and mortality of endothelial NO scavenging and increased oxygen affinity of

NO-bound HBOCs. This finding has not been published and substantiated by any other group.

7.5 Limitations and Further Work

The circuit designed for this work is based upon a commercially available membrane oxygenator. Structurally, there are differences between the membrane oxygenator and lungs however such models can provide valuable diffusion data of gases in response to varying physiological parameters. The predominant differences between the membrane oxygenator and lungs are the surface area, pulmonary capillary volume, cross-sectional diameter of the blood pathway, blood transit time and non-pulsatile blood flow. Between run variations were attributed to the differences between membrane oxygenator batch productions which can be eliminated by the study design. In this case, comparison of control versus treatment group was made using the same apparatus and repeated as necessary with complete new circuits.

The methodology used in this work to determine the resistances exerted by the RBC membrane and interior to DNO was not robust in order to support the evident conclusion. To clarify DNO resistance of the RBC membrane, normal RBCs could be compared to altered RBCs with a reduced or increased RBC membrane surface area. Carlson and Camroe (1958) demonstrated that DNO was comparable between discoidal and spherical RBC of similar volume, which suggested that the RBC interior is not a limiting factor. In crenated RBCs they noted a decrease in DNO. This may be a result of the reduced RBC membrane surface area or an effect of a resultant thickened membrane. Similar work to that described by Carlson and Camroe (1958) could be explored in this apparatus.

The work encompassing NO scavenging effects of Oxyglobin in this circuit has given insight into the possible vasoreactive mechanisms seen clinically. The risks associated with clinical administration of HBOCs and the lack of licensed products available limits replication of this work for the foreseeable future. This type of circuit would be ideal to investigate the NO scavenging potential of HBOCs with differing P_{50} characteristics to determine if this affects NO scavenging capacity of the HBOC. The effects of NO on the ODC of HBOCs could be clarified as this may critically affect oxygen delivery. To avoid NO scavenging by HBOCs the optimal solution would be haemoglobin encapsulation. Sakai *et al* (2010) demonstrated reduced NO uptake by liposome encapsulated Hb compared to an HBOC and free Hb. The substance used to encapsulate the Hb would need to be developed with consideration of its permeability to NO and O_2. The circuit designed in this work would represent an ideal testing apparatus for such innovative products.

Conclusion

In this work, a novel *in vitro* membrane oxygenator circuit was developed to test gas exchange simulating arterial and venous blood gas parameters.

The circuit tests have shown that the RBC surroundings (plasma) provide significant resistance to nitric oxide diffusion. In lung function testing $D_M NO$ cannot equal $D_L NO$ as the reaction rate of nitric oxide with blood does not equal infinity.

The work has demonstrated a significant uptake of nitric oxide by the HBOC Oxyglobin supporting its potential to scavenge endothelial nitric oxide *in vivo*, resulting in vasoconstriction. Nitric oxide bound Oxyglobin shifts the circuit blood ODC to the left resulting in poorer oxygen delivery to the tissues.

Figures

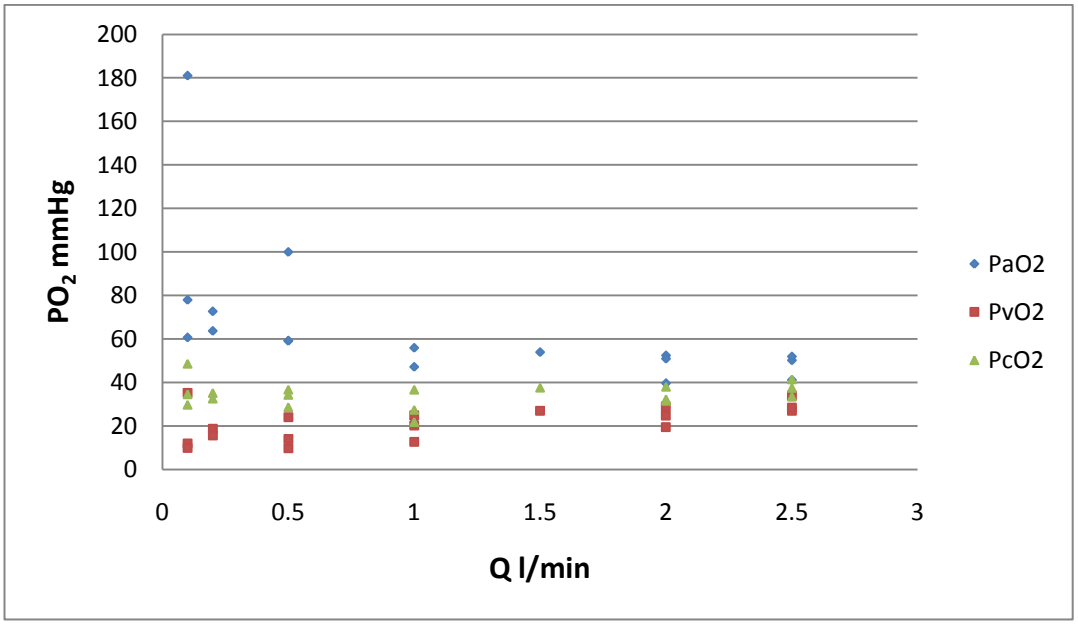

Figure 3.10 Effects of Blood Flow ($\dot{Q}$) with 1 Cell on PO_2; PaO_2 ♦ showed a very slight decrease over the blood flow range 0.1- 2.5 l/min whereas $P\bar{v}O_2$ ■ showed a very slight increase. The resultant $P_{\bar{c}}O_2$ ▲ remained static throughout the blood flow range. PaO_2 averaged 63.44 ±33.57 mmHg, $P\bar{v}O_2$ averaged 21.51 ±7.97 mmHg and $P_{\bar{c}}O_2$ was 34.37 ±5.83 mmHg for 1 cell.

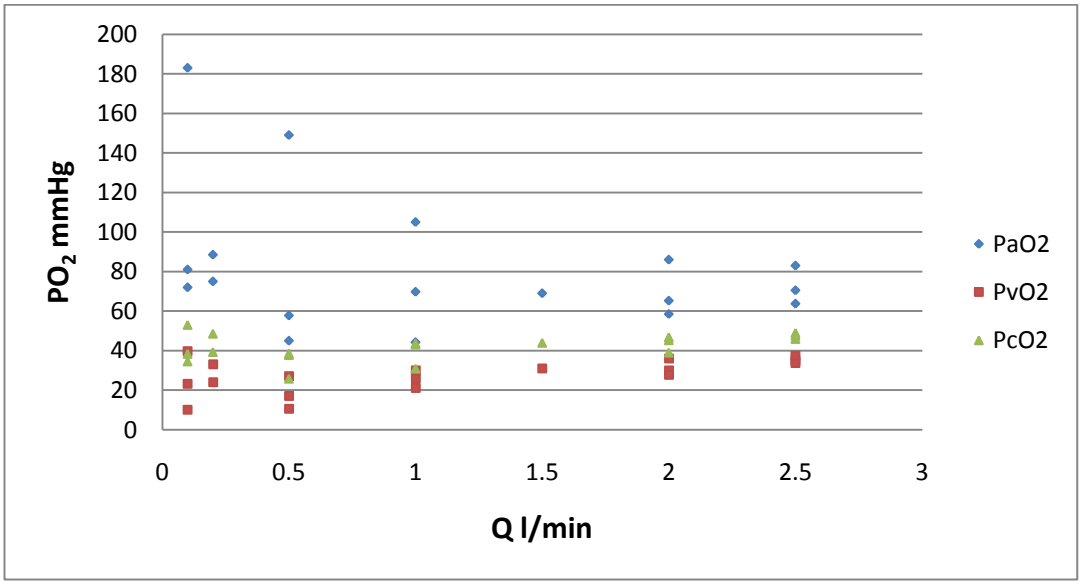

Figure 3.11 Effects of Blood Flow ($\dot{Q}$) with 2 Cells on PO_2; PaO_2 ♦ showed a very slight decrease over the blood flow range 0.1- 2.5 l/min whereas $P\bar{v}O_2$ ■ showed a very slight increase. The resultant $P_{\bar{c}}O_2$ ▲ remained static throughout the blood flow range. PaO_2 averaged 81.45 ±34.66 mmHg, $P\bar{v}O_2$ averaged 27.36 ±8.58 mmHg and $P_{\bar{c}}O_2$ was 41.75 ±6.85 mmHg for 2 cells.

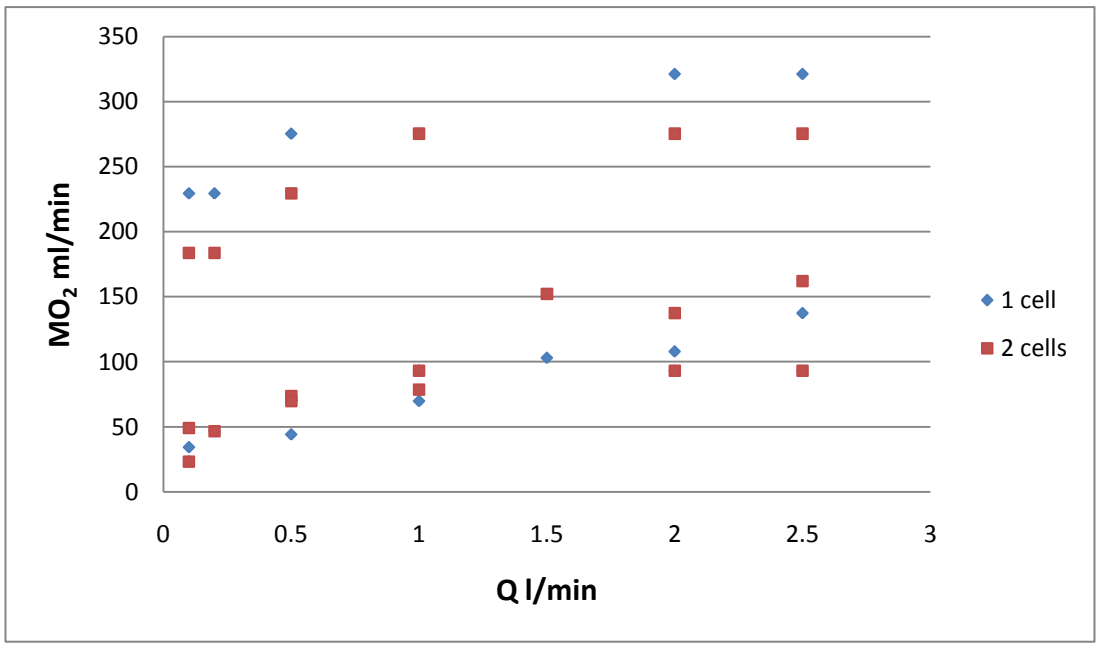

Figure 3.12 Effects of Blood Flow ($\dot{Q}$) with Surface Area (SA) on $\dot{M}O_2$; Increasing blood flow from 0.2 to 2.5 l/min for 1 cell ♦ and 2 cells ■ corresponded with a linear increase in $\dot{M}O_2$. $\dot{M}O_2$ for 1 cell ranged 23.28 to 93.11 ml/min (run 1, p=0.018), 229.46 to 321.24 ml/min (run 2, p=0.004) and 34.35 to 137.40 ml/min (run 3, p=0.002). $\dot{M}O_2$ ranged 23.28 to 93.11 ml/min (run 1, p=0.050), 183.57 to 275.35 ml/min (run 2, p=0.032) and 49.07 to 161.93 ml/min (run 3, p=0.006) for 2 cells.

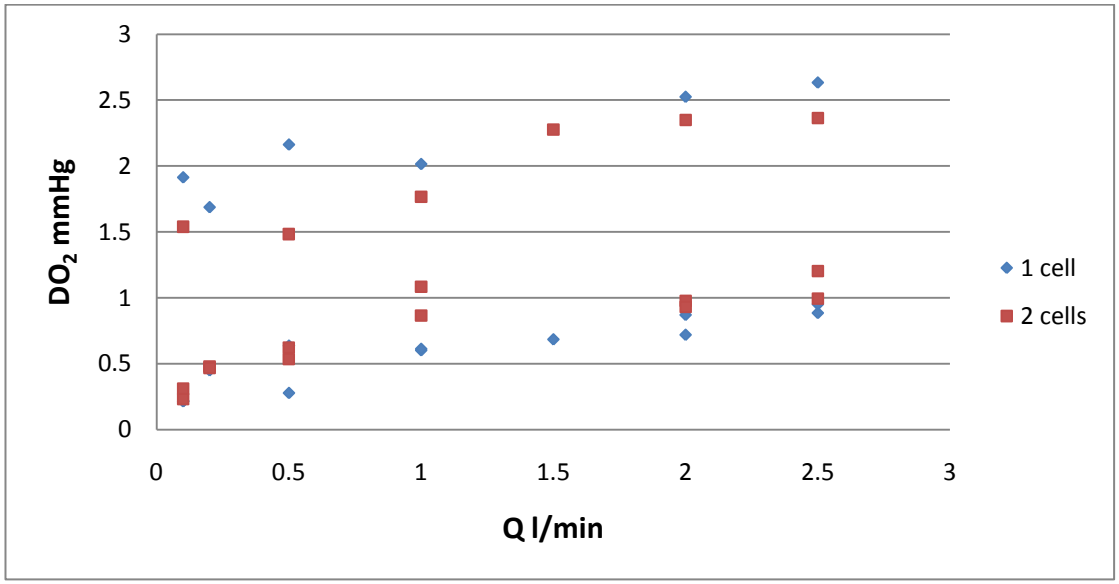

Figure 3.13 Effects of Blood Flow ($\dot{Q}$) and Surface Area (SA) on DO_2; Increasing blood flow from 0.2 to 2.5 l/min for 1 cell ♦ and 2 cells ■ corresponded with a linear increase in DO_2. DO_2 for 1 cell ranged 0.21 to 0.90 ml/min/mmHg (run 1, p=0.011), 1.91 to 2.63 ml/min/mmHg (run 2, p=0.008) and 0.22 to 0.95 ml/min/mmHg (run 3, p=0.002). DO_2 for 2 cells was calculated as 0.23 to 0.99 ml/min/mmHg (run 1, p=0.017), 1.54 to 2.36 ml/min/mmHg (run 2, p=0.014) and 0.31 to 1.20 ml/min/mmHg (run 3, p=0.005).

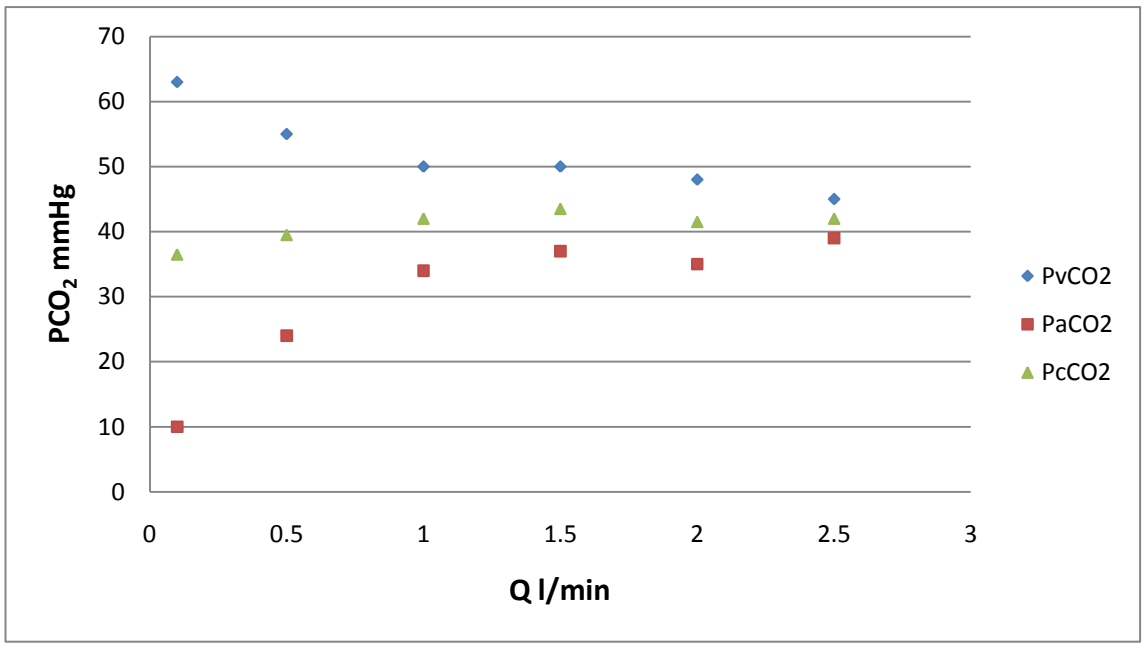

Figure 3.14 Effects of Blood Flow ($\dot{Q}$) with 1 Cell on PCO_2; $PaCO_2$ ■ increased curvilinearly with increasing blood flow from 10 mmHg at 0.1 l/min to a mean 36.25 ± 2.22 mmHg at 1.0-2.5 l/min. $P\bar{v}CO_2$ ♦ similarly decreased over the blood flow range from 63 mmHg at 0.1 l/min to a mean 48.25 ±2.36 mmHg over 1.0 – 2.5 l/min. $P\bar{c}CO_2$ ▲ (calculated from $P\bar{v}CO_2$ and $PaCO_2$) averaged 40.83 ±2.48 mmHg.

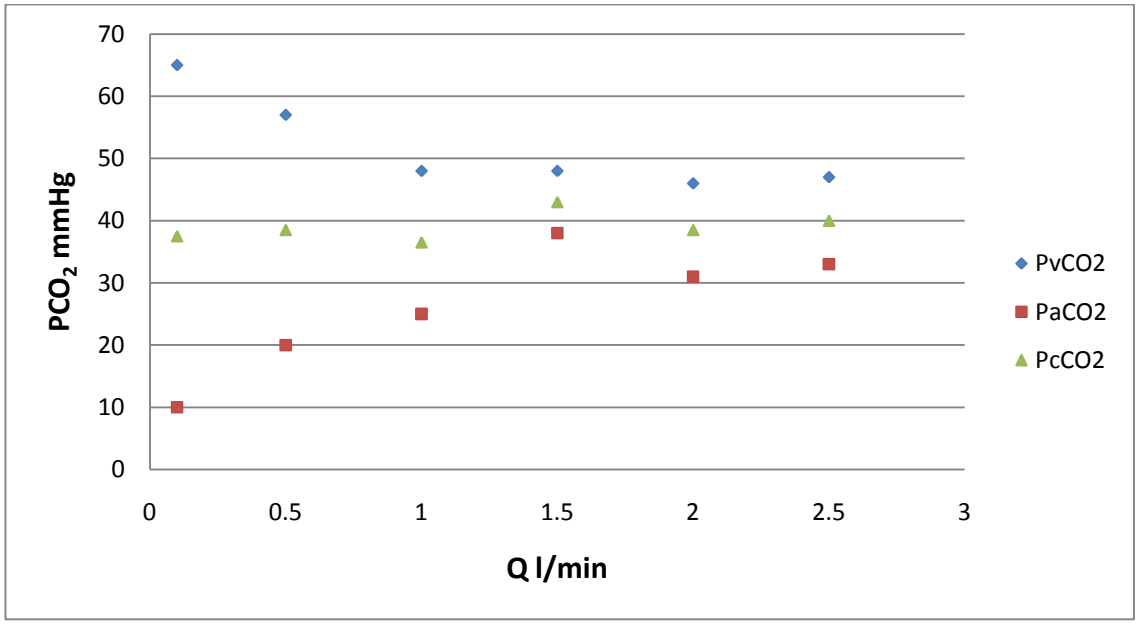

Figure 3.15 Effects of Blood Flow ($\dot{Q}$) with 2 Cells on PCO_2; $PaCO_2$ ■ increased curvilinearly with increasing blood flow from 10 mmHg at 0.1 l/min to a mean 31.75 ±5.38 mmHg at 1.0-2.5 l/min. $P\bar{v}CO_2$ ♦ similarly decreased over the blood flow range from 65 mmHg at 0.1 l/min to a mean 47.25 ±0.96 mmHg over 1.0-2.5 l/min. $P\bar{c}CO_2$ ▲ was calculated from $P\bar{v}CO_2$ and $PaCO_2$ and averaged 39.00 ±2.28 mmHg.

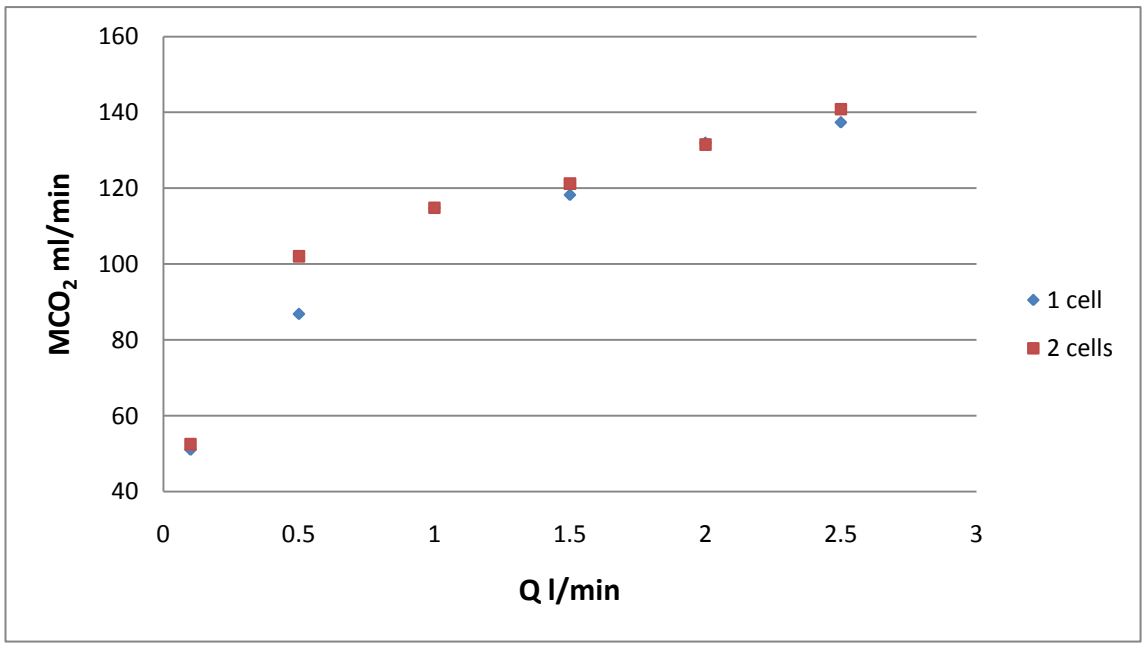

Figure 3.16 Effects of Blood Flow ($\dot{Q}$) and Surface Area (SA) on $\dot{M}CO_2$; $\dot{M}CO_2$ increased linearly from 51.03 to 137.40 ml/min for 1 oxygenator cell ♦ and 52.51 to 140.83 ml/min for 2 oxygenator cells ■.

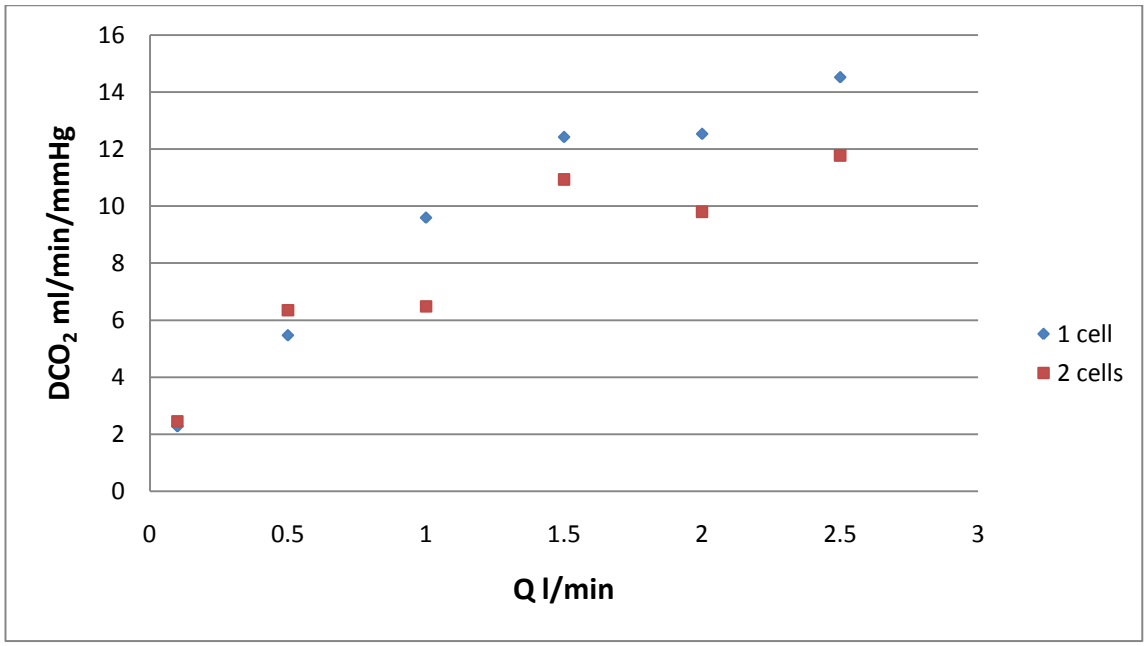

Figure 3.17 Effects of Blood Flow ($\dot{Q}$) and Surface Area (SA) on DCO_2; DCO_2 increased linearly from 2.28 to 14.52 ml/min/mmHg for 1 oxygenator cell ♦ and 2.46 to 11.78 ml/min/mmHg for 2 oxygenator cells ■.

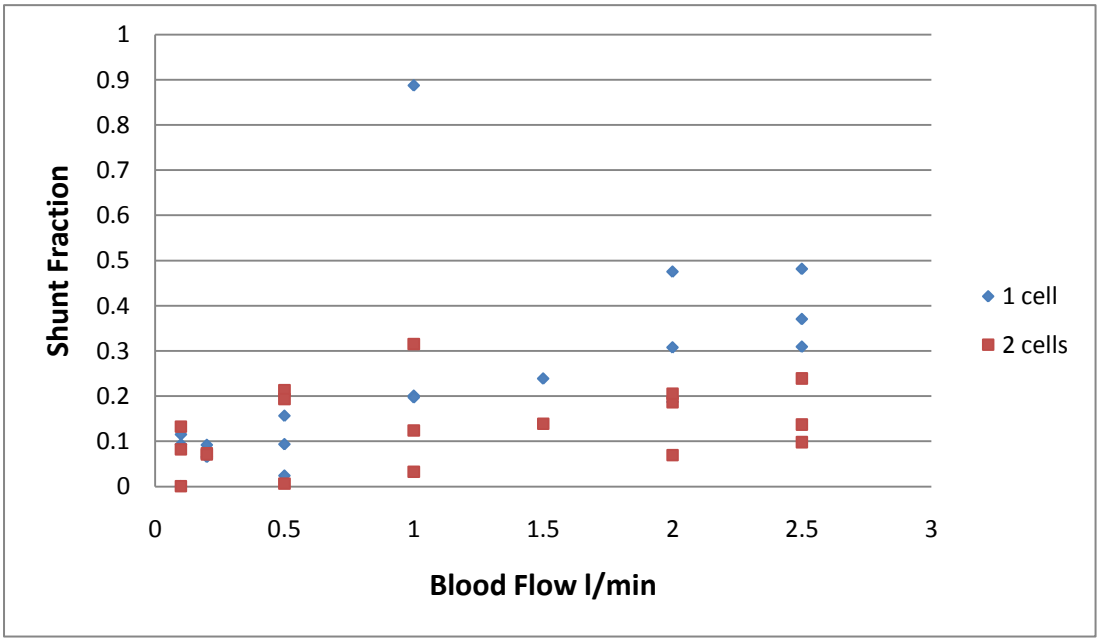

Figure 3.18 Effects of Blood Flow ($\dot{Q}$) and Surface Area (SA) on Shunt Fraction; where ♦ represents 1 cell and ■ represents 2 cells. Shunt fraction increased linearly with increasing blood flow (p=0.009). Shunt fraction ranged from 0.084% at 0.1 l/min up to 37% at 2.5 l/min. Shunt fraction for 1 cell and 2 cells was not significantly different (p=0.051).

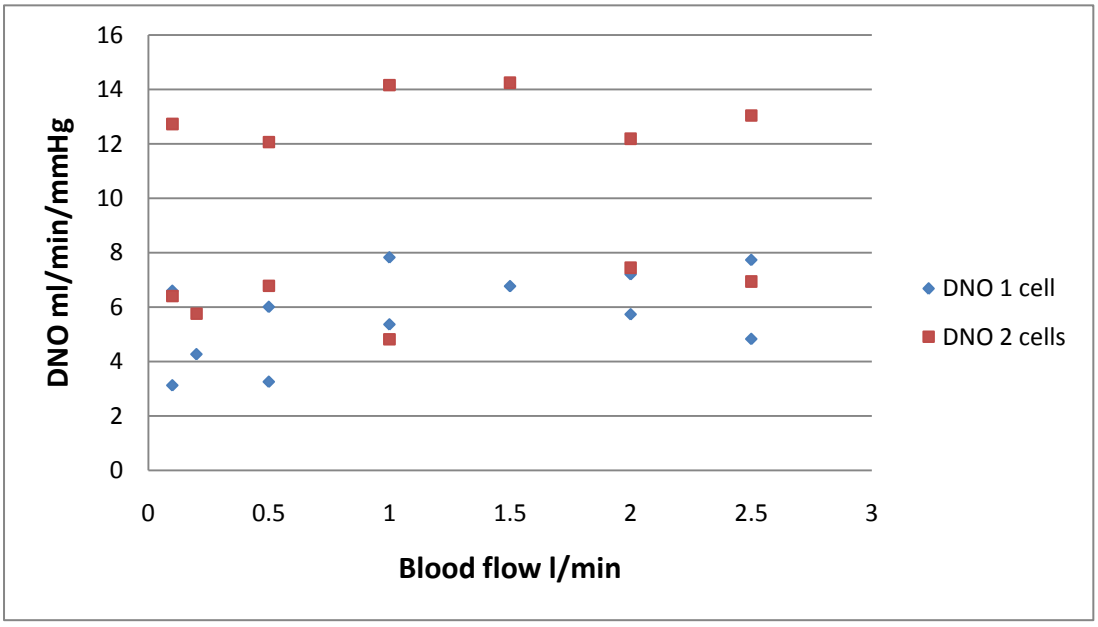

Figure 3.19 Effects of Blood Flow ($\dot{Q}$) and Surface Area (SA) on DNO; DNO was not affected by changes in blood flow from 0.1 to 2.5 l/min (p=0.333). Increasing surface area significantly increased DNO (p=0.002). DNO for 1 cell ♦ averaged 5.72 ±1.61 ml/min/mmHg and for 2 cells ■ averaged 9.71 ±3.62 ml/min/mmHg.

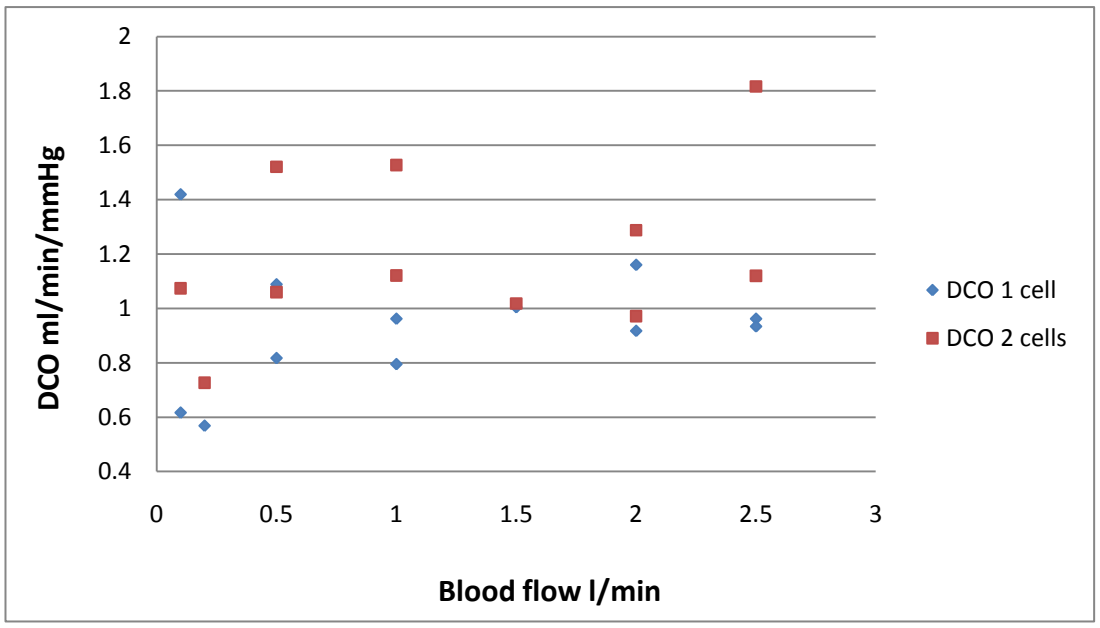

Figure 3.20 Effects of Blood Flow ($\dot{Q}$) and Surface Area (SA) on DCO; DCO was not significantly affected by changes in blood flow from 0.1 to 2.5 l/min (p=0.079). DCO was significantly affected surface area with 1 cell ♦ averaging 1.07 ±0.21 ml/min/mmHg and 2 cells ■ averaging 1.46 ±0.35 ml/min/mmHg for run 1 (p=0.039). In run 2 DCO for 1 cell ♦ averaged 0.81 ±0.17 ml/min/mmHg and for 2 cells ■ averaged 1.13 ±0.25 ml/min/mmHg (p=0.026).

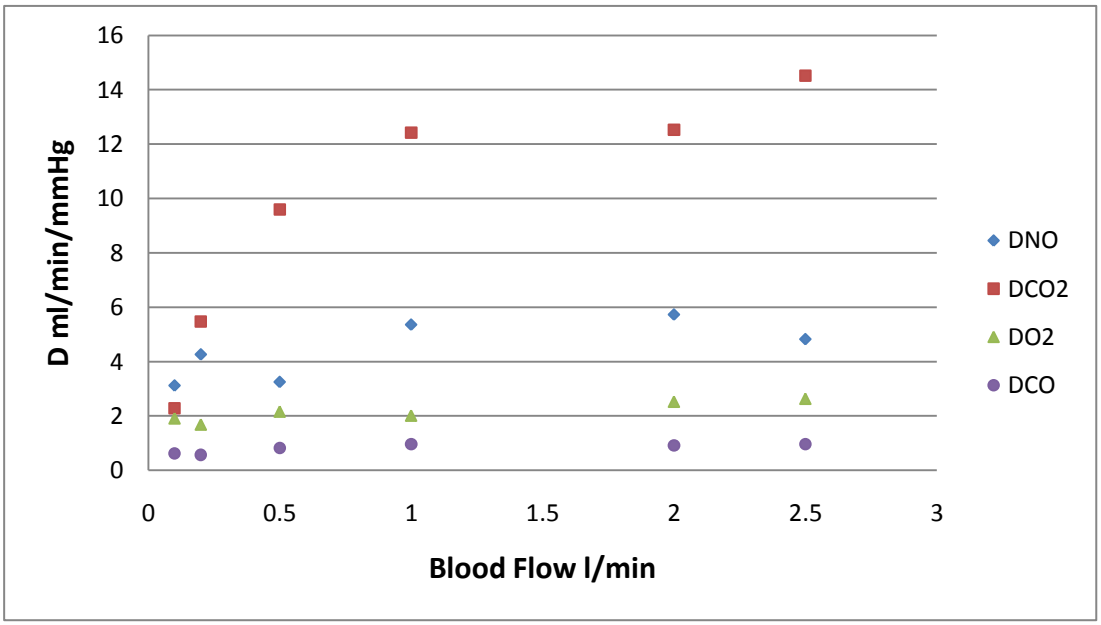

Figure 3.21 Effects of Blood Flow ($\dot{Q}$) on Diffusion (D); where ■ DCO_2 > ♦ DNO > ▲ DO_2 > ● DCO.

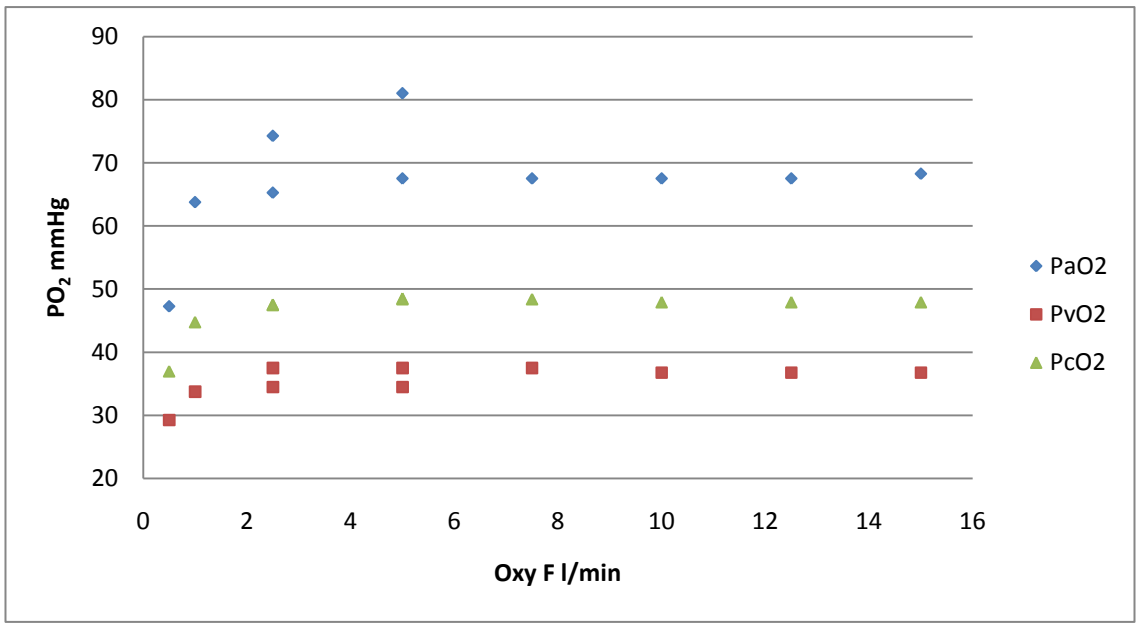

Figure 3.22 Effects of Oxygenator Gas Flow (F) on PO_2; PaO_2 ♦ increased initially from 47.25 mmHg (0.5 l/min) to 65.25 mmHg (2.5 l/min) after which the PaO_2 averaged 69.88 ±5.46 mmHg over the gas flow range 5 to 15 l/min. $P\bar{v}O_2$ ■ increased from 29.25 mmHg (0.5 l/min) to 37.5 mmHg (2.5 l/min) before averaging 36.63 ±1.10 mmHg over the 5 to 15 l/min gas flow range. $P\bar{c}O_2$ ▲ increased from 37.00 mmHg (0.5 l/min) to 47.48 mmHg (2.5 l/min) before averaging 48.19 ±0.29 mmHg for gas flows 5 to 15 l/min.

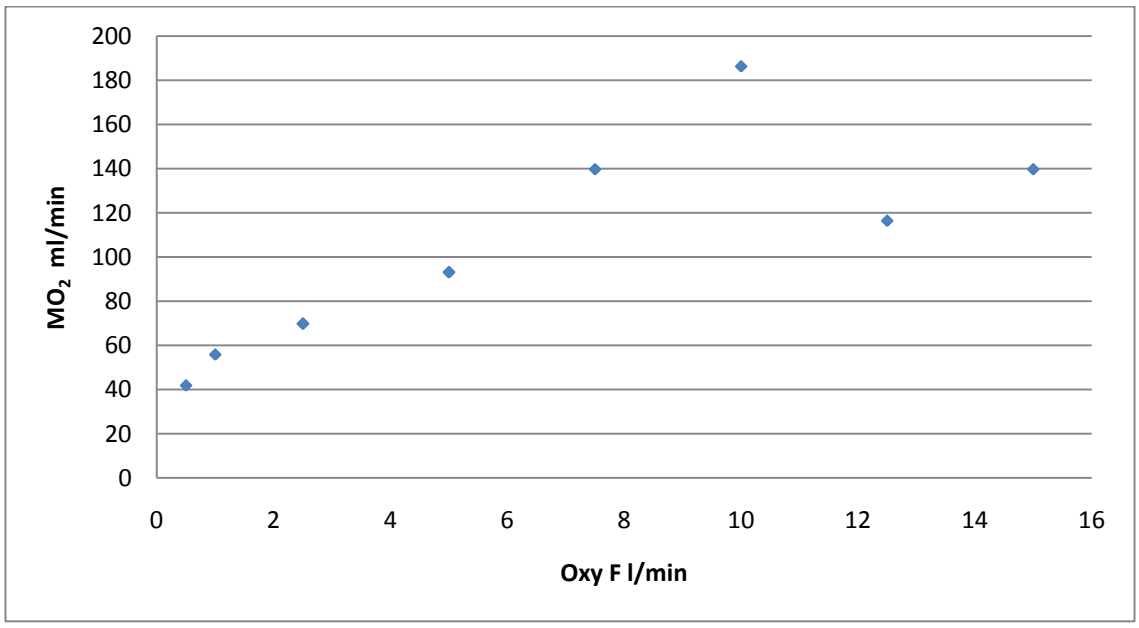

Figure 3.23 Effects of Oxygenator Gas Flow (F) on $\dot{M}O_2$; $\dot{M}O_2$ increased linearly with increasing oxygenator gas flow from 41.90 ml/min at 0.5 l/min to 139.67 ml/min at 15 l/min (p=0.004).

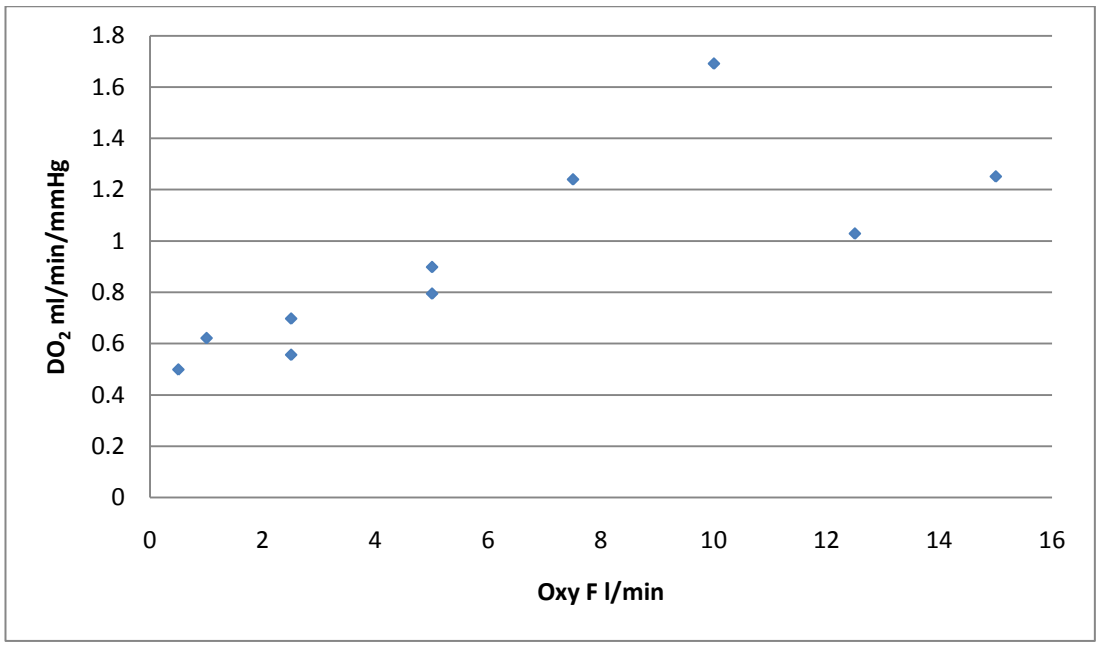

Figure 3.24 Effects of Oxygenator Gas Flow (F) on DO_2; DO_2 increased with increasing oxygenator gas flow from 0.50 ml/min/mmHg at 0.5 l/min to 1.25 ml/min/mmHg at 15 l/min (p=0.007).

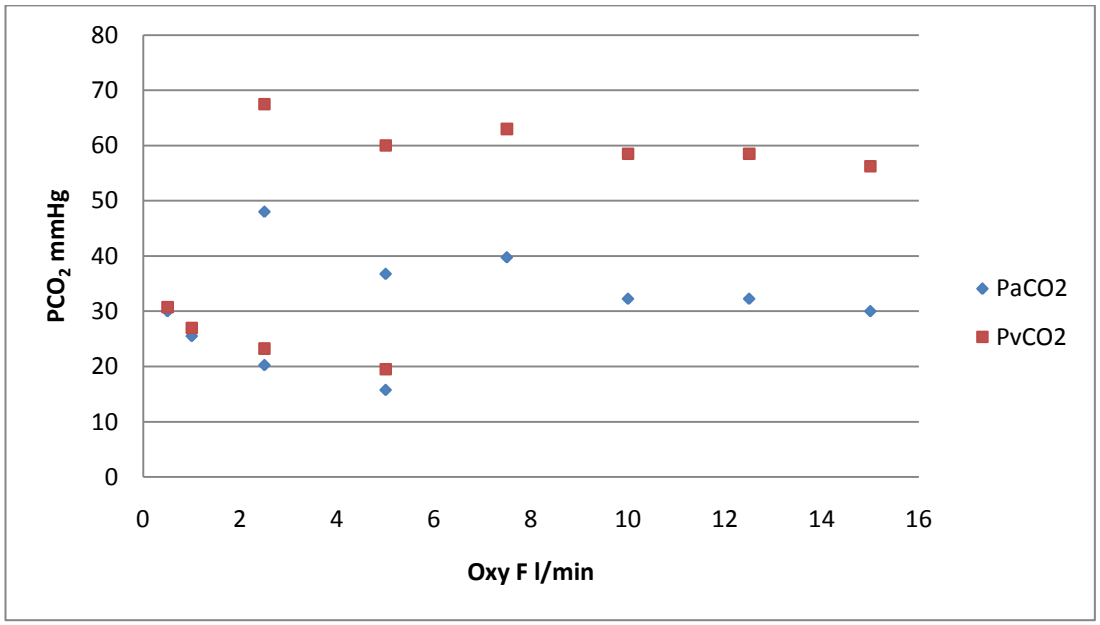

Figure 3.25 Effects of Oxygenator Gas Flow (F) on PCO_2; Increasing oxygenator gas flow would impact on the removal of CO_2 from the 'venous' blood. $PaCO_2$ ♦ slightly decreased with increasing oxygenator gas flow. In run 1, $PaCO_2$ reduced from 30 mmHg at 0.5 l/min to 15.75 mmHg at 5 l/min (p=0.042). In run 2, $PaCO_2$ reduced from 48 mmHg at 2.5 l/min down to 30 mmHg at 15 l/min (p=0.008). P $\overline{V}$ CO_2 ■ also decreased from 30.75 mmHg (0.5 l/min) to 19.50 mmHg (5 l/min) in run 1 and from 67.5 mmHg (2.5 l/min) to 56.25 mmHg (15 l/min) in run 2.

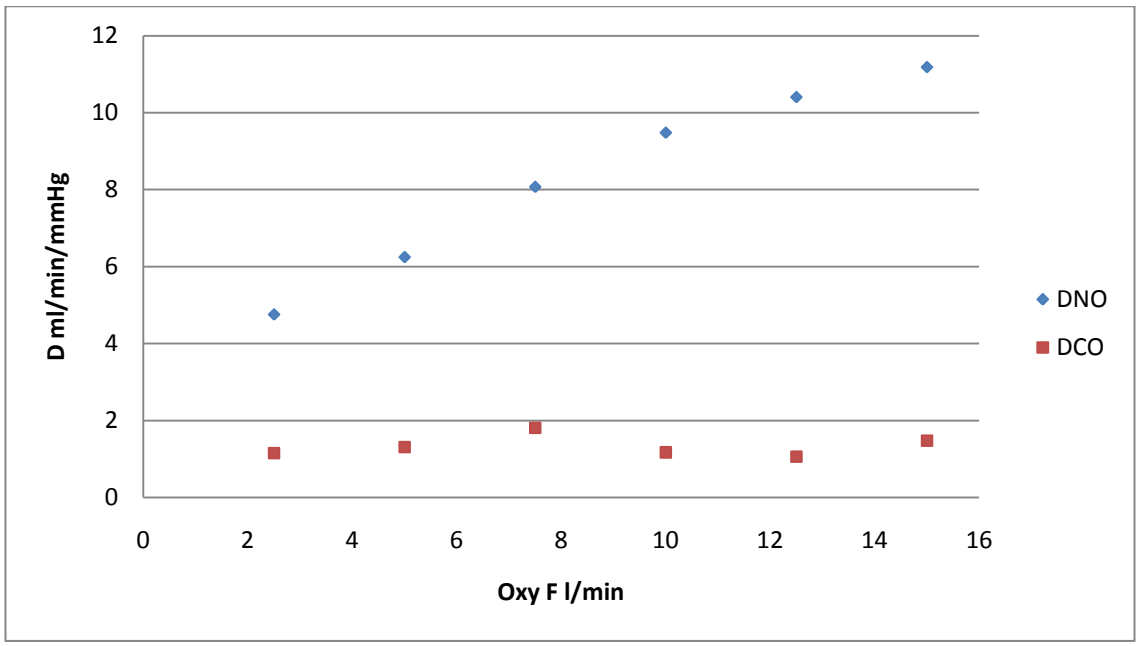

Figure 3.26 Effects of Oxygenator Gas Flow (F) on DNO and DCO; DNO ♦ increased linearly with increasing oxygenator gas flow 2.5 to 15.0 l/min ($p<0.001$) from 4.76 ml/min/mmHg (2.5 l/min) up to 11.19 ml/min/mmHg (15 l/min). DCO ■ showed no change with increasing oxygenator gas flow ($p=0.932$) averaging 1.36 ±0.28 ml/min/mmHg over the oxygenator gas flow range 2.5 to 15.0 l/min.

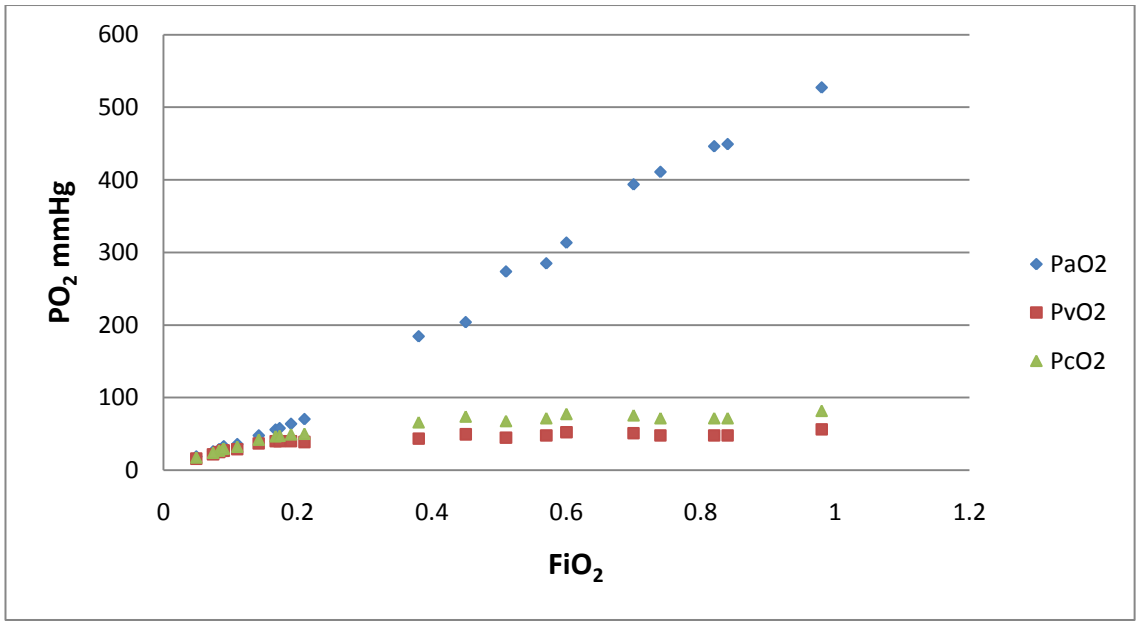

Figure 3.27 Effects of Oxygenator FiO_2 on PO_2; Over the FiO_2 range achieved, PaO_2 ♦ increased linearly from 19 mmHg up to 527 mmHg ($p<0.0001$). In contrast $P\bar{v}O_2$ ($p<0.0001$) and $P\bar{c}O_2$ ($p<0.0001$) increased curvilinearly. $P\bar{v}O_2$ ■ increased initially from 16 mmHg at FiO_2 4.9% up to 40 mmHg at a FiO_2 17.3% after which $P\bar{v}O_2$ averaged 48.98 ±3.64 mmHg. $P\bar{c}O_2$ ▲ increased from 17.5 mmHg at FiO_2 4.9% up to 50.1 mmHg at FiO_2 21%, after which $P\bar{c}O_2$ averaged 72.80 ±4.58 mmHg.

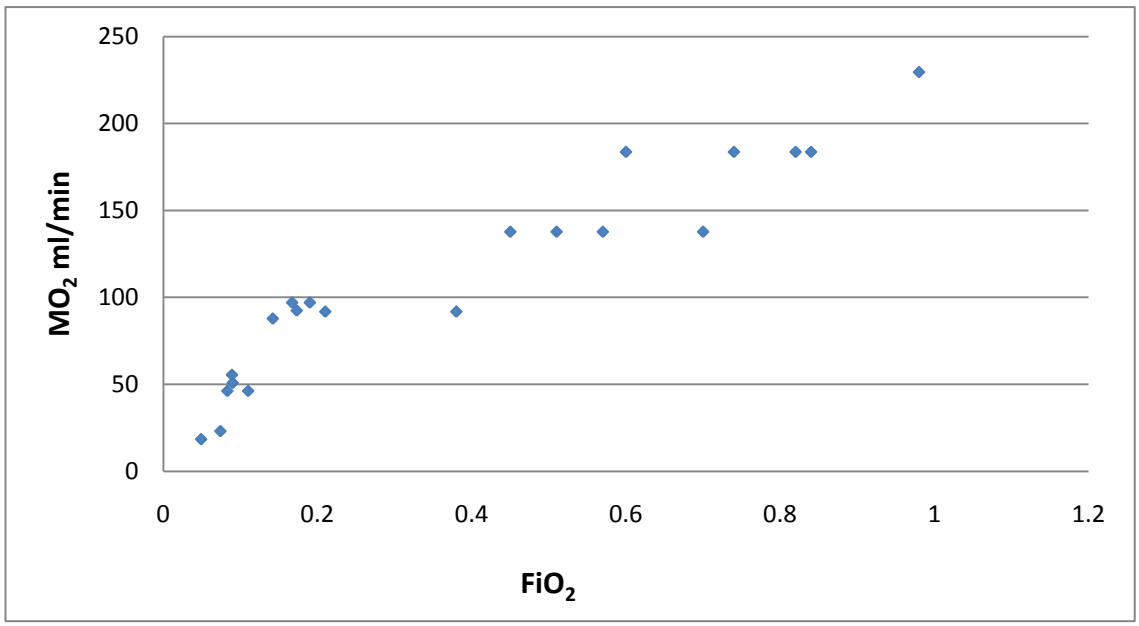

Figure 3.28 Effects of Oxygenator FiO_2 on $\dot{M}O_2$; $\dot{M}O_2$ increased linearly ($p<0.0001$) when plotted against FiO_2, from 18.48 ml/min at FiO_2 4.9% up to 229.46 ml/min at FiO_2 98%.

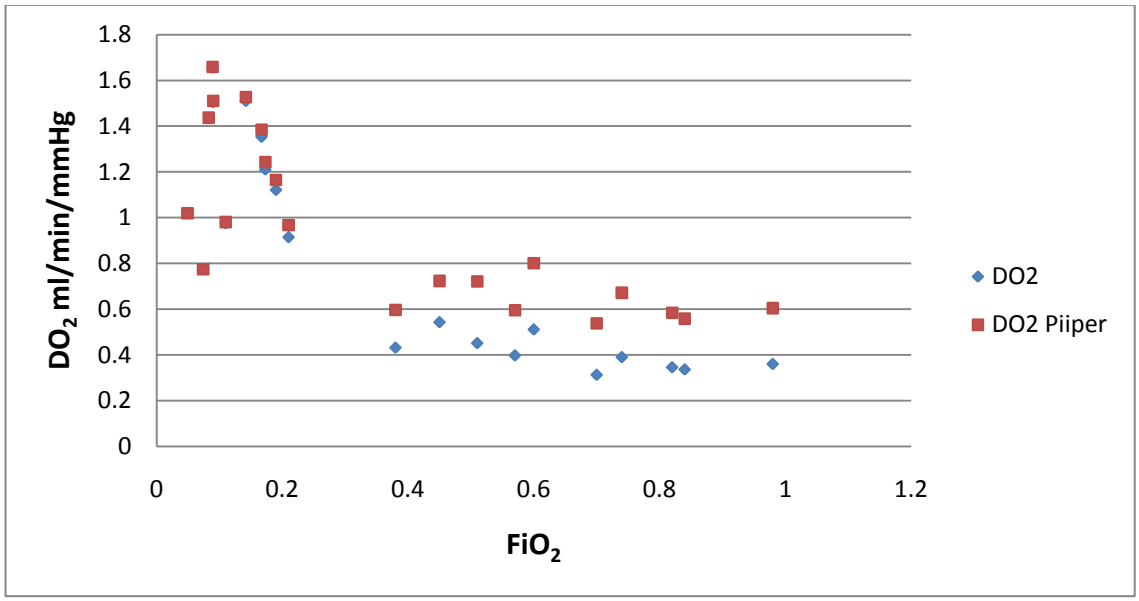

Figure 3.29 Effects of Oxygenator FiO_2 on DO_2; DO_2 showed a complex relationship with FiO_2. Lilienthal DO_2 ♦ increased sharply from 0.77 ml/min/mmHg at FiO_2 7.4% up to 1.66 ml/min/mmHg at FiO_2 8.9%. DO_2 then steeply decreased down to 0.91 ml/min/mmHg at FiO_2 21% before averaging 0.45 ±0.17 ml/min/mmHg at FiO_2 25 to 98%. Piiper's DO_2 ■ increased sharply from 0.77 ml/min/mmHg at FiO_2 7.4% up to 1.66 ml/min/mmHg at FiO_2 8.9%. The DO_2 then steeply decreased down to 0.97 ml/min/mmHg at FiO_2 21% before averaging 0.67 ±0.13 ml/min/mmHg at FiO_2 25 to 98%.

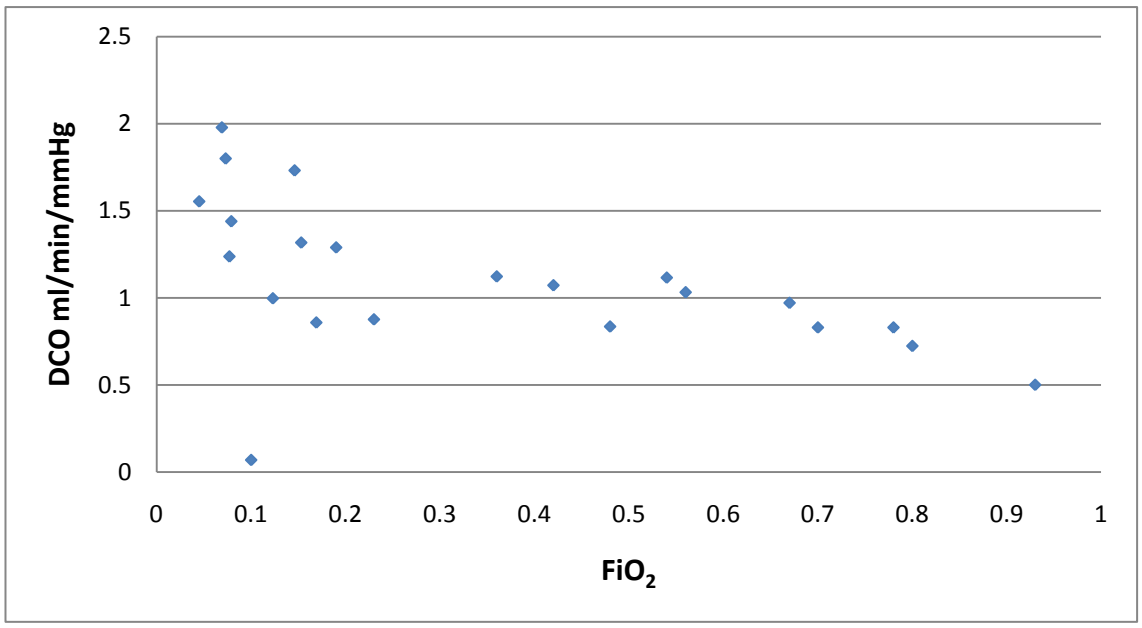

Figure 3.30 Effects of Oxygenator FiO_2 on DCO; DCO significantly decreased linearly from 1.98 ml/min/mmHg to 0.50 ml/min/mmHg with increasing FiO_2 over the range 4.9-98% (p=0.011)

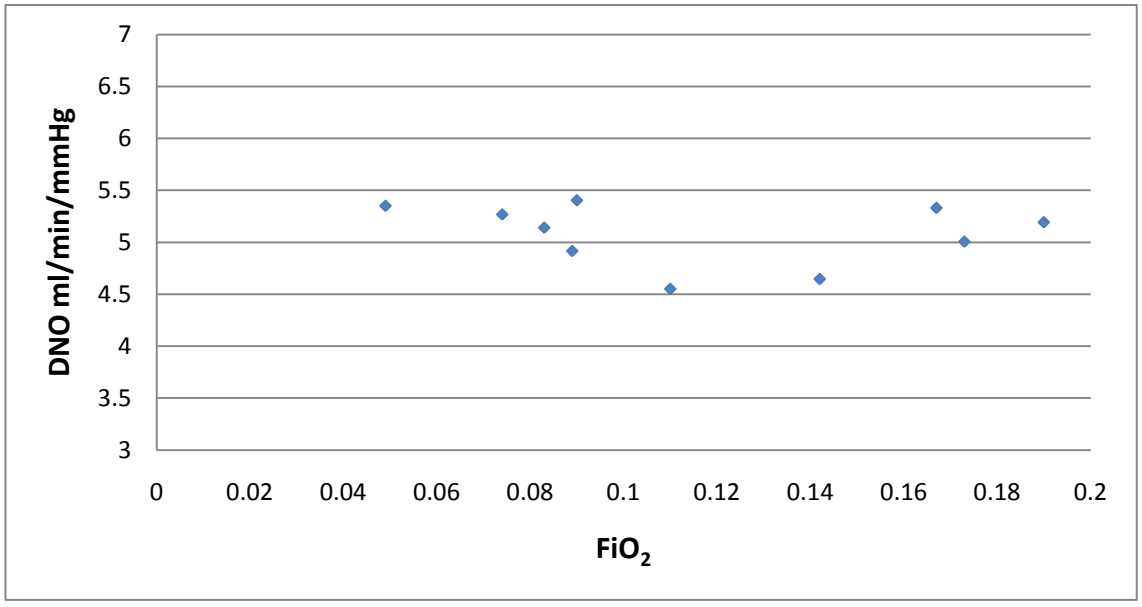

Figure 3.31 Effects of Oxygenator (Hypoxic) FiO_2 on DNO; DNO was unaffected by FiO_2 in the hypoxic range 4.9-20% with DNO averaging 5.08 ±0.30 ml/min/mmHg (p=0.617).

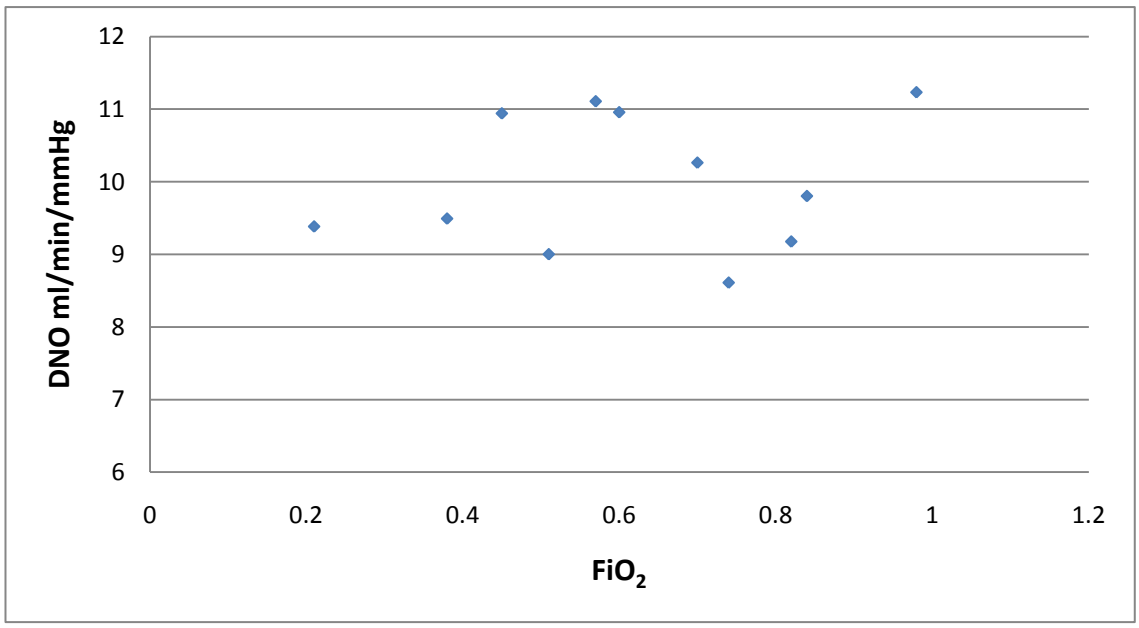

Figure 3.32 Effects of Oxygenator (Hyperoxic) FiO_2 on DNO; DNO was unaffected by increasing FiO_2 in the hyperoxic range 21-98% with DNO averaging 10.00 ±0.94 ml/min/mmHg (p=0.639)

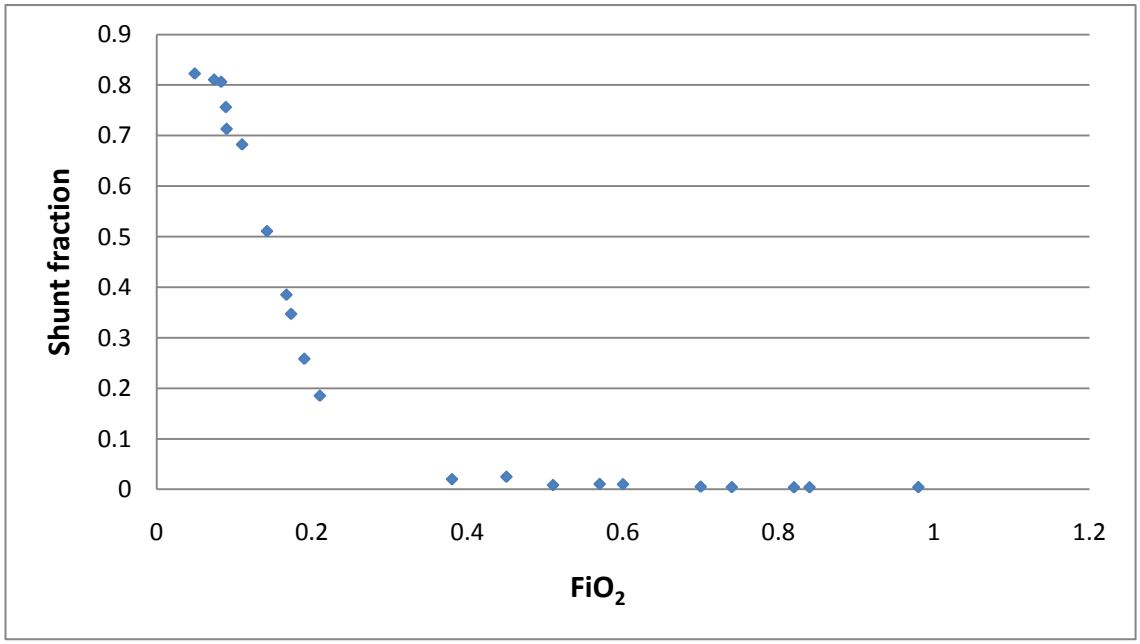

Figure 3.33 Effects of Oxygenator FiO_2 on Shunt Fraction; At a standard blood flow rate (2.5 l/min) the shunt fraction decreased curvilinearly with increasing FiO_2 ($p<0.0001$). At low FiO_2 (4.9%), the shunt was calculated as 82.2% reducing to 18.5% at FiO_2 21%. At higher FiO_2 (38-98%) the shunt fraction averaged 0.93 ±0.007%.

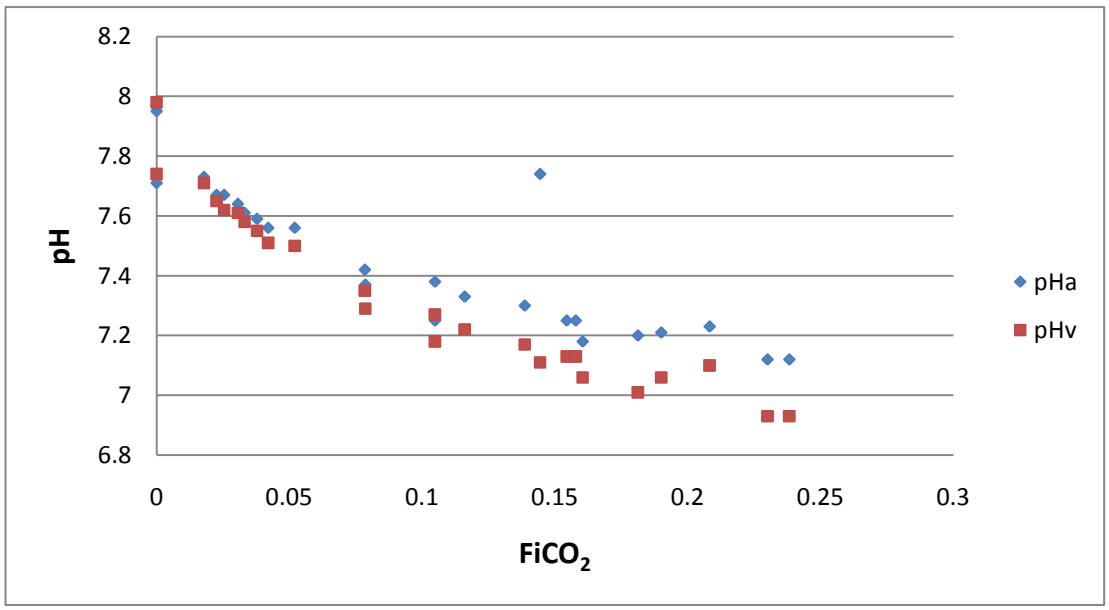

Figure 3.34 Effects of Deoxygenator $FiCO_2$ on pH; pH decreased with increasing $FiCO_2$ ♦ arterial pH decreased from 7.73 to 7.12 ($p<0.0001$) and ■ venous pH decreased from 7.71 to 6.93 ($p<0.0001$).

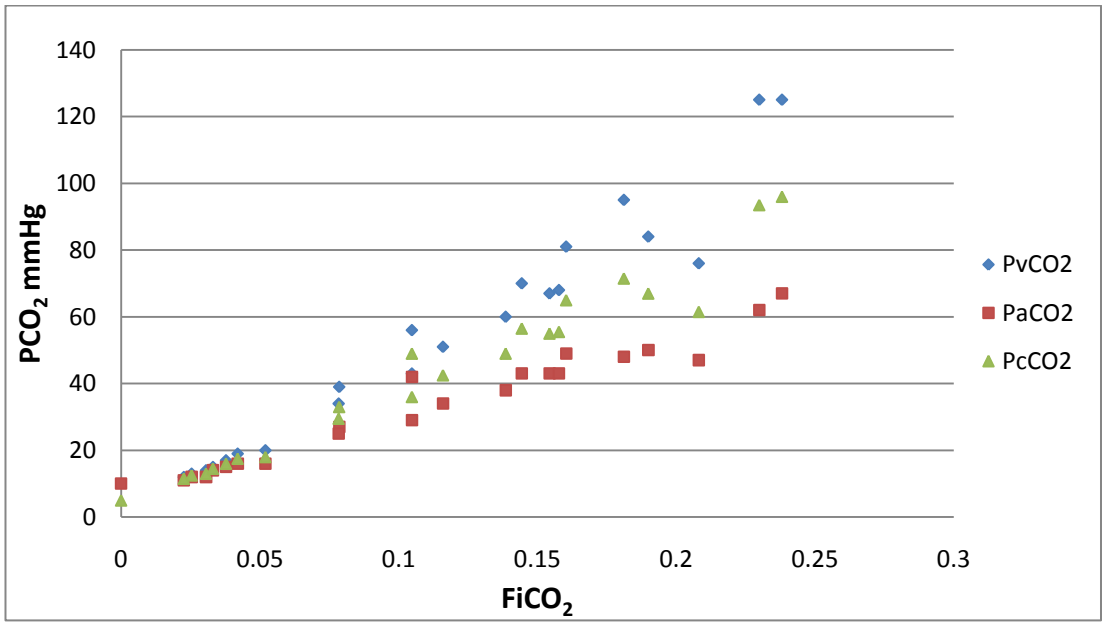

Figure 3.35 Effects of Deoxygenator $FiCO_2$ on PCO_2; Both $P\bar{v}CO_2$ ($p<0.0001$) and $PaCO_2$ ($p<0.0001$) increased linearly with increasing $FiCO_2$. For the $FiCO_2$ range 2.26 to 23.8% $P\bar{v}CO_2$ ♦ was 12 to 125 mmHg and $PaCO_2$ ■ ranged 11 to 67 mmHg. $P\bar{c}CO_2$ ▲ increased linearly from 11.5 to 96 mmHg ($p<0.0001$).

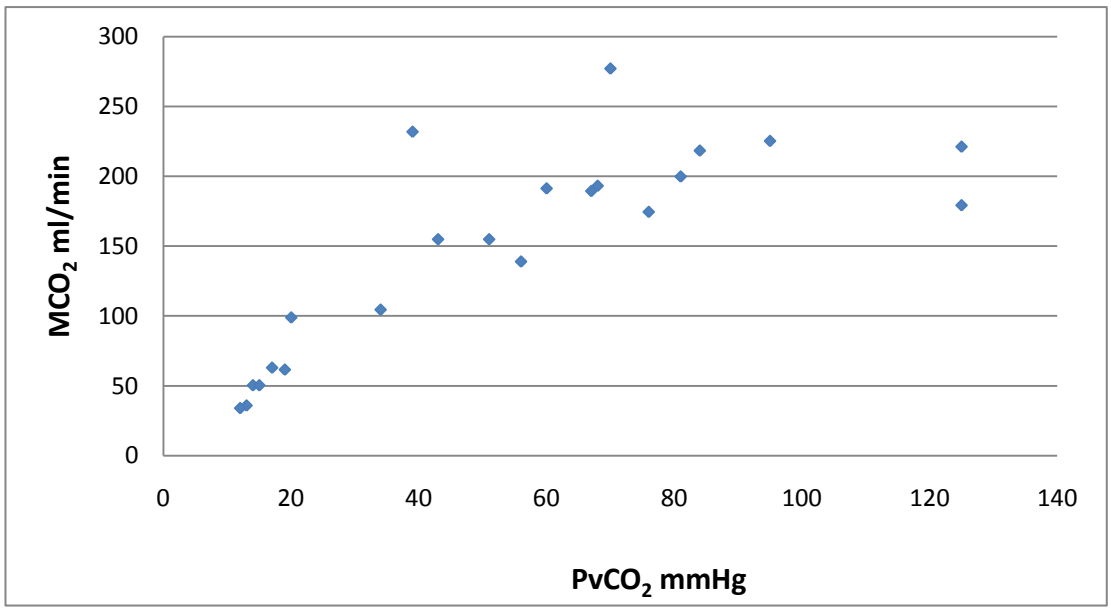

Figure 3.36 Effects of Deoxygenator $FiCO_2$ on $\dot{M}CO_2$; $\dot{M}CO_2$ increased linearly with increasing $FiCO_2$ from 34.06 ml/min (at 2.26%) to 221.16 ml/min (at 23.8%) ($p<0.0001$).

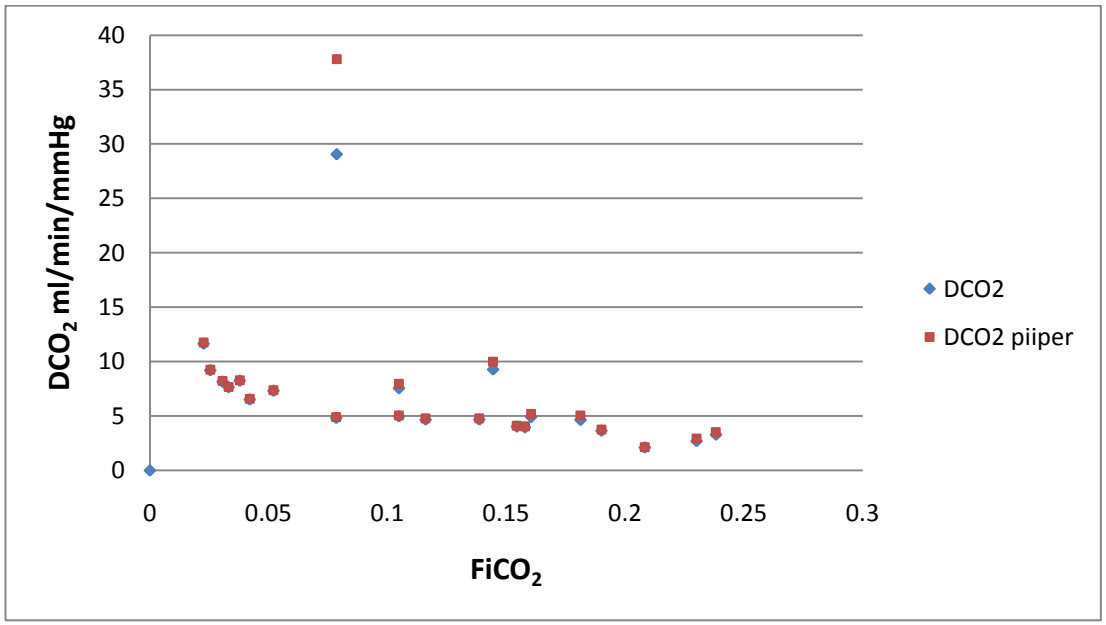

Figure 3.37 Effects of Deoxygenator $FiCO_2$ on DCO_2; DCO_2 ♦ started high at 11.65 ml/min/mmHg at $FiCO_2$ 2.26% and then decreased curvilinearly to 3.29 ml/min/mmHg at $FiCO_2$ 23.8% ($p=0.031$). Modified Piiper DCO_2 ■ started at 11.76 ml/min/mmHg at $FiCO_2$ 2.26% and gradually decreasing to 3.52 ml/min/mmHg at $FiCO_2$ 23.8%.

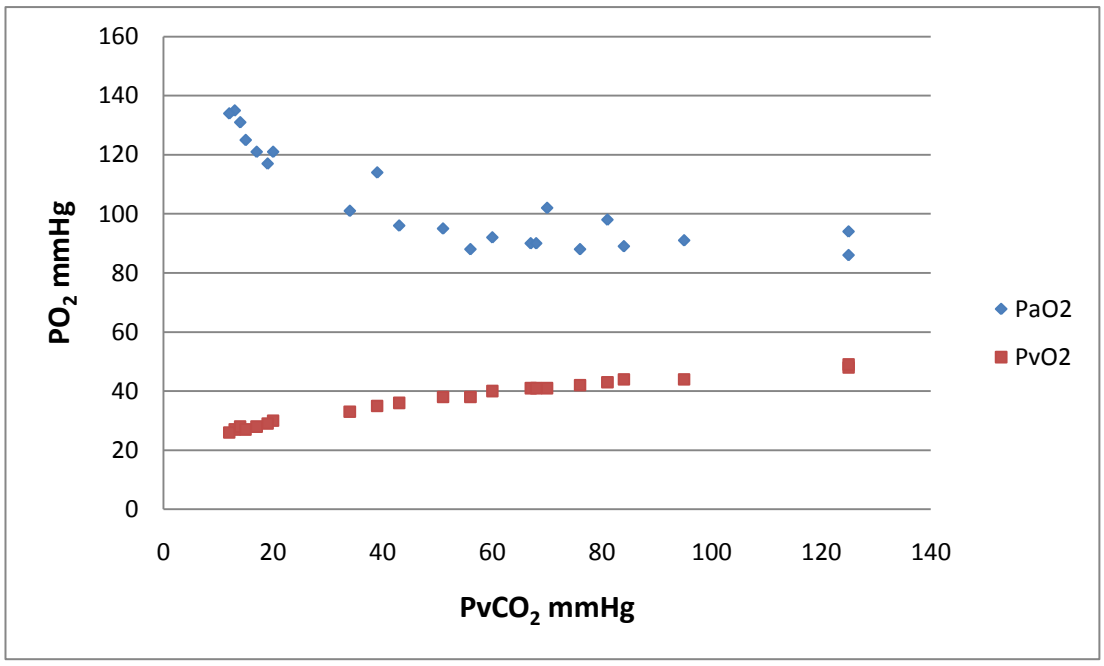

Figure 3.38 Effects of P $\bar{V}$ CO_2 on PO_2; PaO_2 ♦ curvilinearly ($p<0.0001$) decreased from 135 mmHg (P $\bar{V}$ CO_2 13 mmHg) to 96 mmHg (P $\bar{V}$ CO_2 43 mmHg) with increasing P $\bar{V}$ CO_2, plateauing at 90 ±2.89 mmHg (P $\bar{V}$ CO_2 43 to 125 mmHg). P $\bar{V}$ O_2 ■ increased curvilinearly ($p<0.0001$) from 26 mmHg (P $\bar{V}$ CO_2 12 mmHg) to 48 mmHg (P $\bar{V}$ CO_2 125 mmHg).

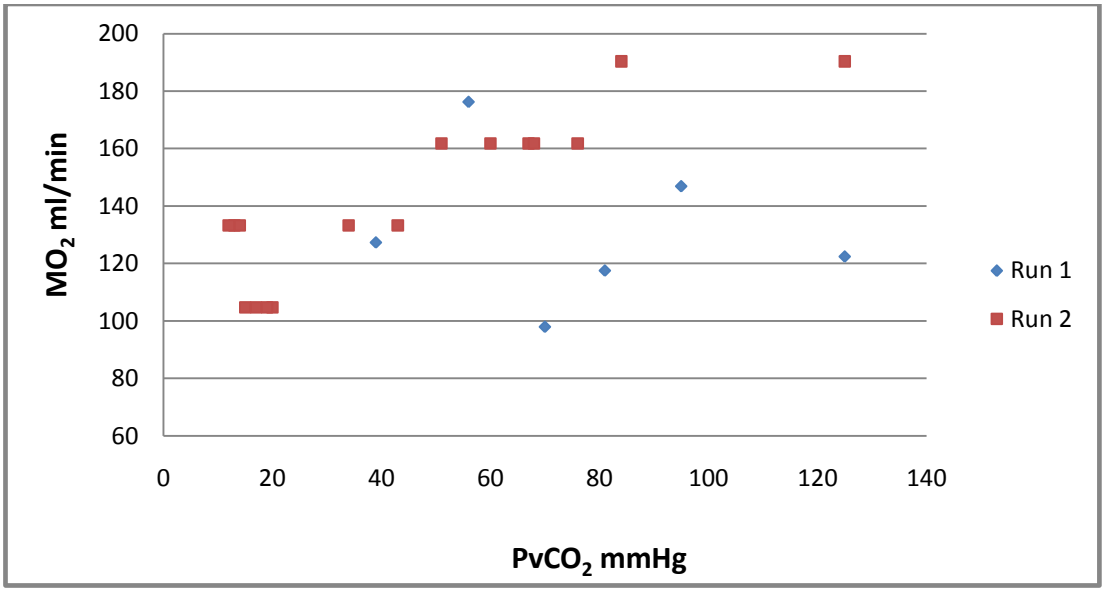

Figure 3.39 Effects of Deoxygenator $FiCO_2$ on $\dot{M}O_2$; where ♦ represents run 1 and ■ represents run 2. $\dot{M}O_2$ increased linearly with increasing P $\bar{V}$ CO_2 ($p<0.001$) from 104.7 ml/min (P $\bar{V}$ CO_2 15 mmHg) to 190.36 ml/min (P $\bar{V}$ CO_2 125 mmHg).

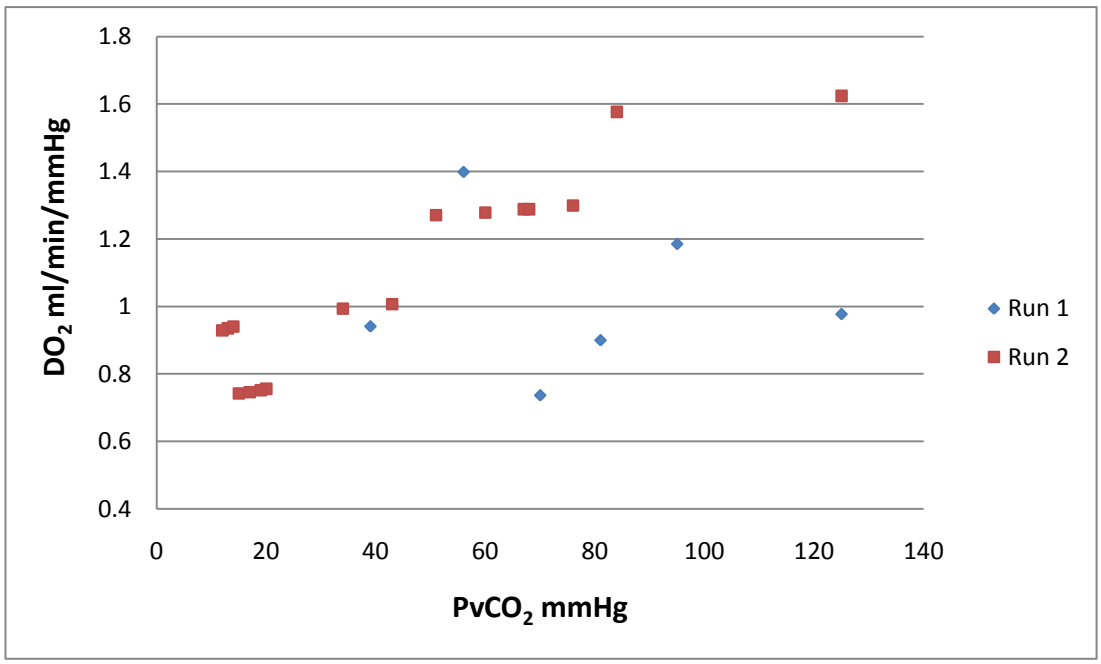

Figure 3.40 Effects of Deoxygenator FiCO_2 on DO_2; where ♦ represents run 1 and ■ represents run 2. DO_2 increased linearly with increasing P $\overline{V}$ CO_2 ($p<0.0001$) from 0.74 ml/min/mmHg (P $\overline{V}$ CO_2 15 mmHg) to 1.62 ml/min/mmHg (P $\overline{V}$ CO_2 125 mmHg).

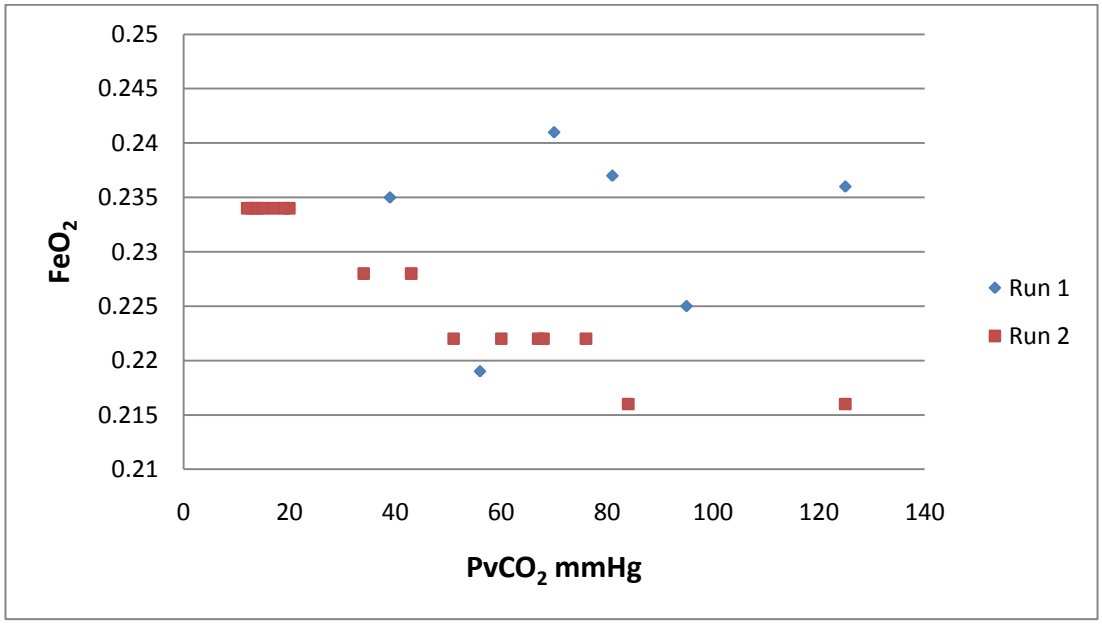

Figure 3.41 Effects of P $\overline{V}$ CO_2 on FeO_2; where ♦ represents run 1 and ■ represents run 2. To investigate the impact of P $\overline{V}$ CO_2 on PaO_2 the FeO_2 was plotted against P $\overline{V}$ CO_2. FeO_2 decreased linearly with increasing P $\overline{V}$ CO_2 ($p<0.0001$) from 23.4% (P $\overline{V}$ CO_2 12 mmHg) to 21.6% (P $\overline{V}$ CO_2 125 mmHg).

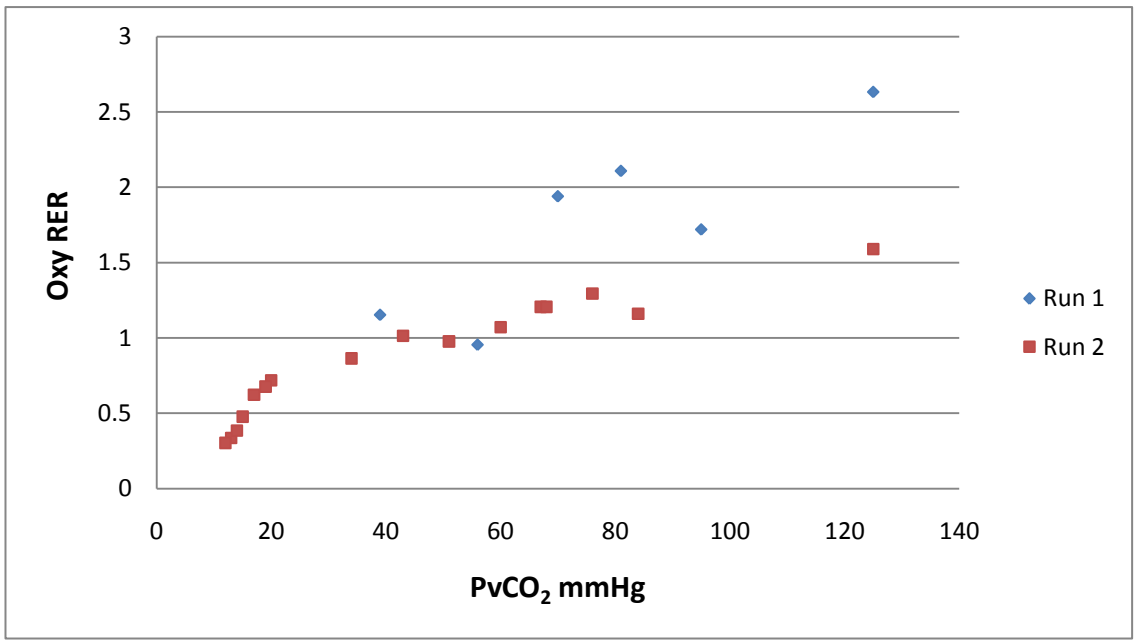

Figure 3.42 Effects of P $\bar{V}$ CO_2 on Oxygenator RER; where ♦ represents run 1 and ■ represents run 2. The RER increased from 0.30 (P $\bar{V}$ CO_2 12 mmHg) to 1.59 (P $\bar{V}$ CO_2 125 mmHg) in response to increasing P $\bar{V}$ CO_2 ($p<0.0001$).

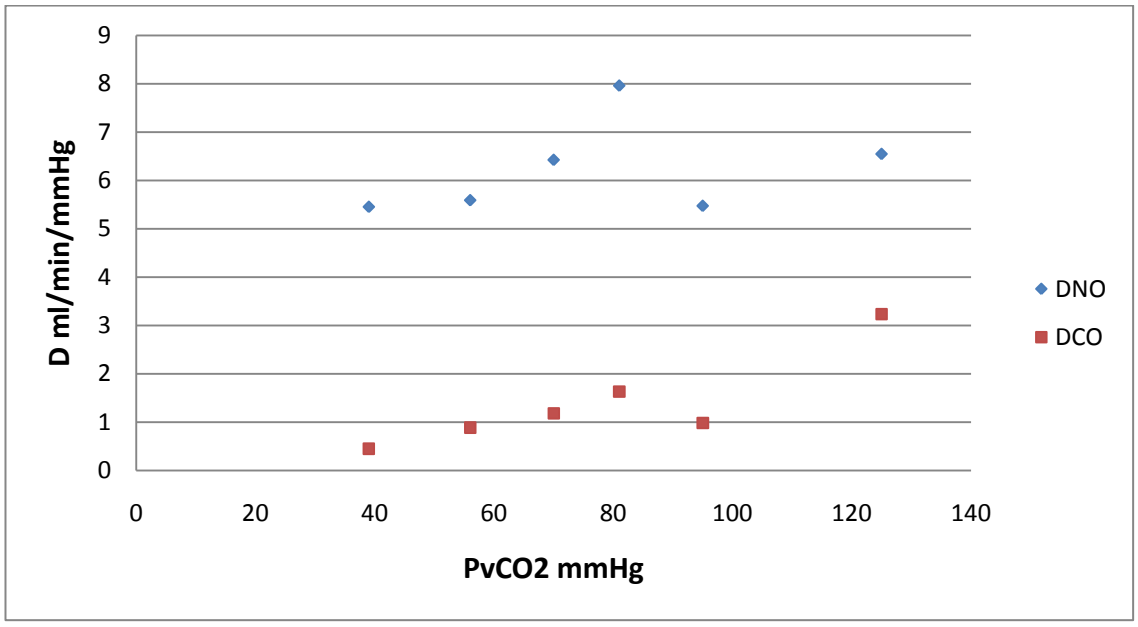

Figure 3.43 Effects of P $\bar{V}$ CO_2 on DNO and DCO; DNO ♦ was unaffected by increasing deoxygenator $FiCO_2$ ranging 7.8-23% with DNO averaging 6.19 ±0.89 ml/min/mmHg ($p=0.509$). DCO ■ increased linearly with increasing deoxygenator $FiCO_2$ ranging 7.8-23% with DCO increasing from 0.45 ml/min/mmHg to 3.24 ml/min/mmHg ($p=0.022$).

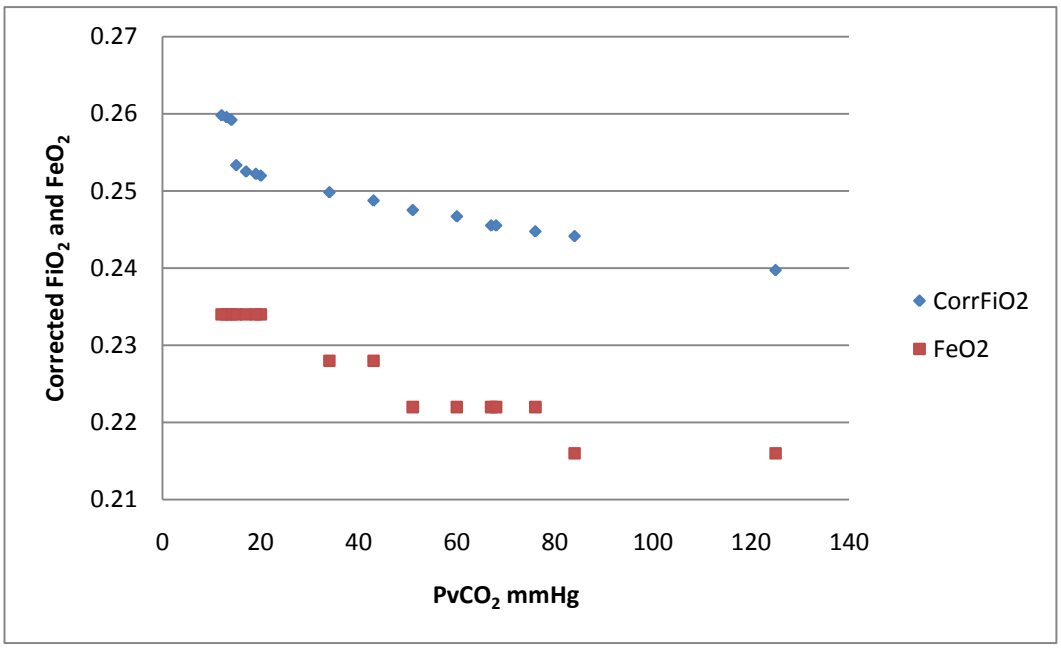

Figure 3.44 Effects of RER Correction Factor on Oxygenator FiO_2 with Varying Deoxygenator $FiCO_2$; With a correction factor applied to the FiO_2 values ♦, corresponding to the increasing oxygenator $FeCO_2$, the oxygenator FiO_2 significantly decreases with increasing $P\overline{v}\,CO_2$ (R^2=0.841, d.f.=14, p<0.0001). FiO_2 reduced from 0.26 ($P\overline{v}\,CO_2$ 13 mmHg) to 0.24 ($P\overline{v}\,CO_2$ 125).

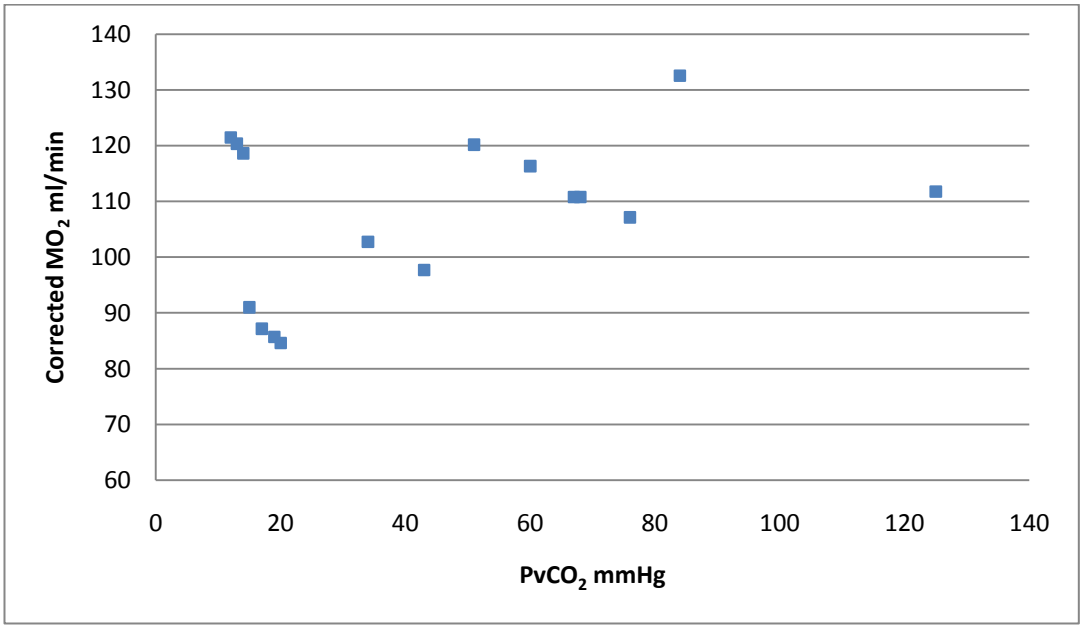

Figure 3.45 Effects of RER Correction Factor on MO_2 with Varying Deoxygenator $FiCO_2$; The resultant corrected $\dot{M}O_2$ shows no significant change with increasing $P\overline{v}\,CO_2$ (R^2=0.217, d.f.=14, p=0.080) averaging 106.50 ±14.52 ml/min.

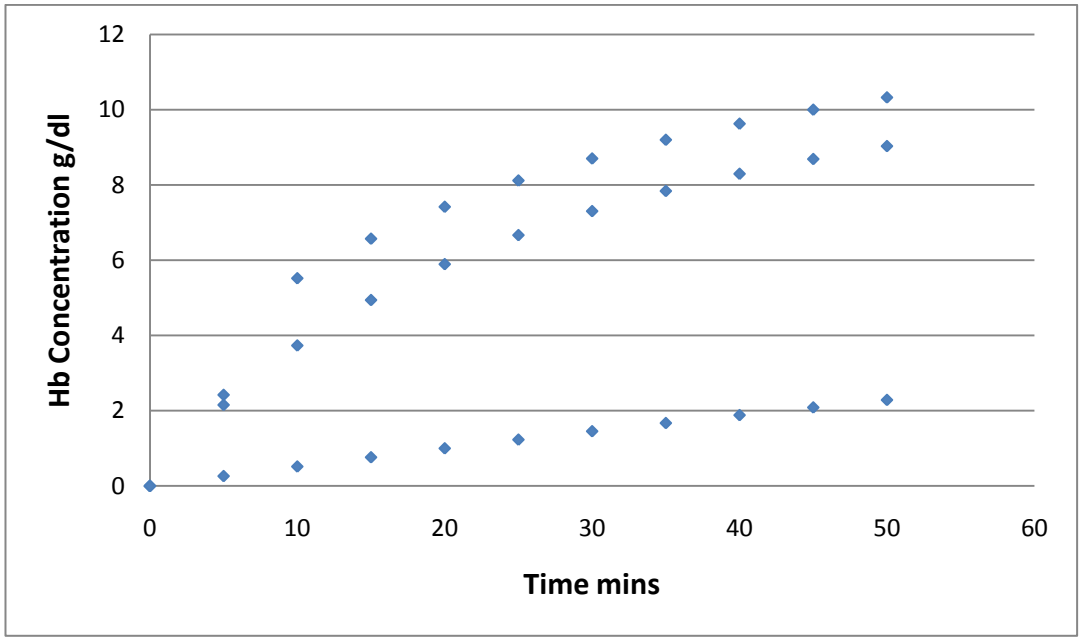

Figure 3.46 Circuit Hb Concentration Achieved During Hb Addition Over Time; The haematocrit ranges achieved were 7.3-31.0% (run 1), 6.5-27.1% (run 2) and 0.66-5.7% (run 3).

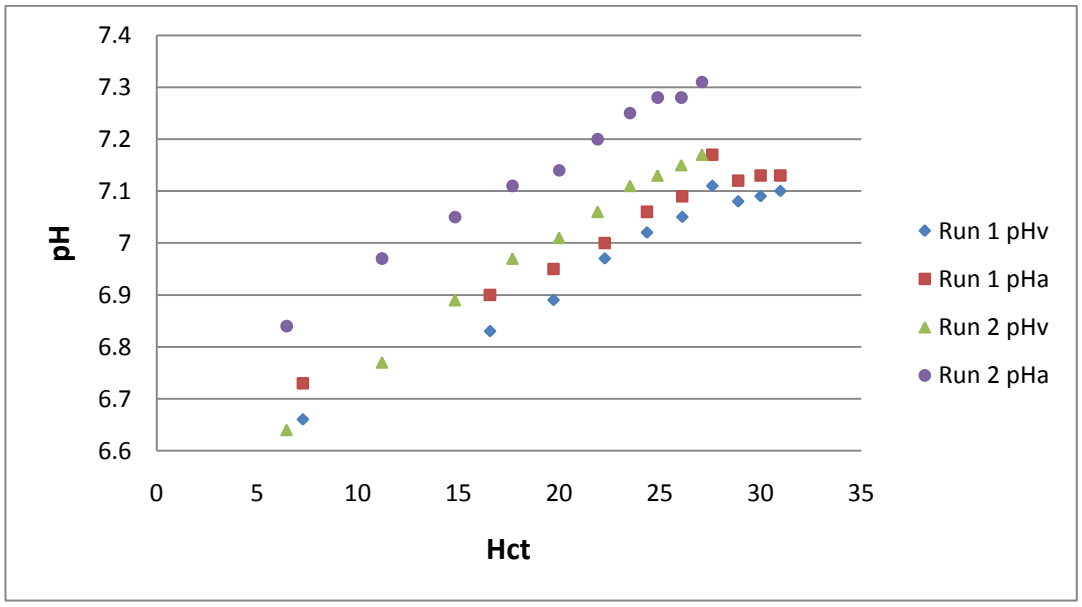

Figure 3.47 Effects of Hct on pH; pHv ($p<0.0001$) and pHa ($p<0.001$) were seen to increase linearly during the blood addition for the experimental runs encompassing Hb 6.5 to 31.0 g/dl. In run 1 ♦ pHv ranged 6.66-7.10 and ■ pHa ranged 6.73-7.13. Similarly in run 2 ▲ pHv ranged 6.64-7.17 and ● pHa ranged 6.84-7.31. For run 3 with lower Hct levels the pHv and majority of pHa values were below that detected by the analyser <6.5.

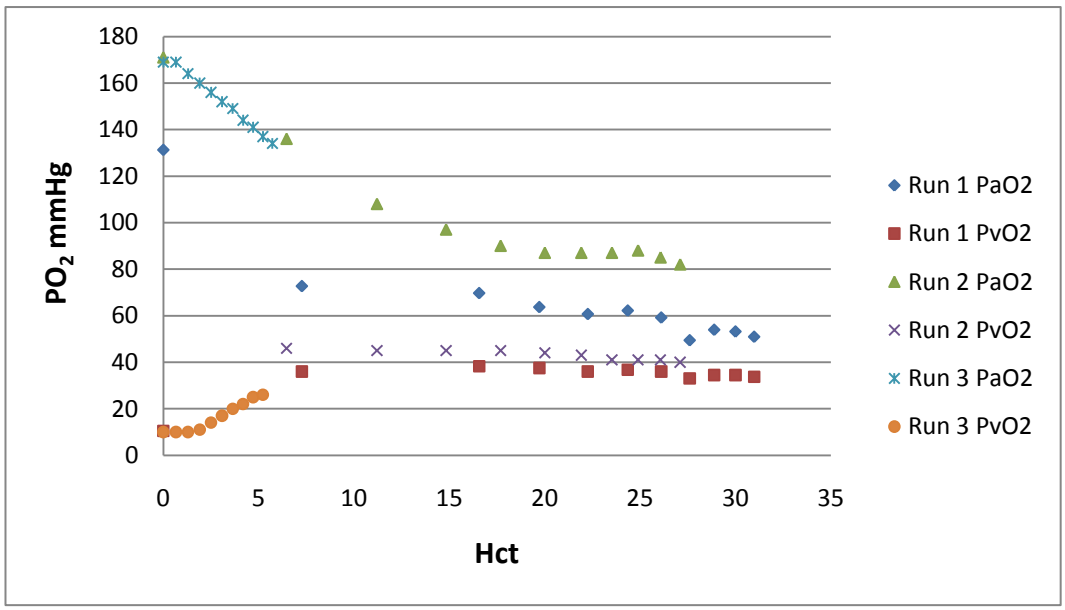

Figure 3.48 Effects of Hct on PO_2; PaO_2 ($p<0.0001$) and $P\bar{V}O_2$ ($p=0.023$) showed a curvilinear relationship when plotted against Hb concentration. The PaO_2 was high with the saline prime (X run 3 = 169mmHg) but reduced until the Hct was approximately 20% stabilising between 50 to 60 mmHg (♦ run 1) or 80-90 mmHg (▲ run 2). The $P\bar{V}O_2$ read low with saline prime at 10 mmHg (● run 3) but increased up to a Hct of 15% where $P\bar{V}O_2$ stabilised between 35-38 mmHg (■ run 1) and 40-45 mmHg (X run 2).

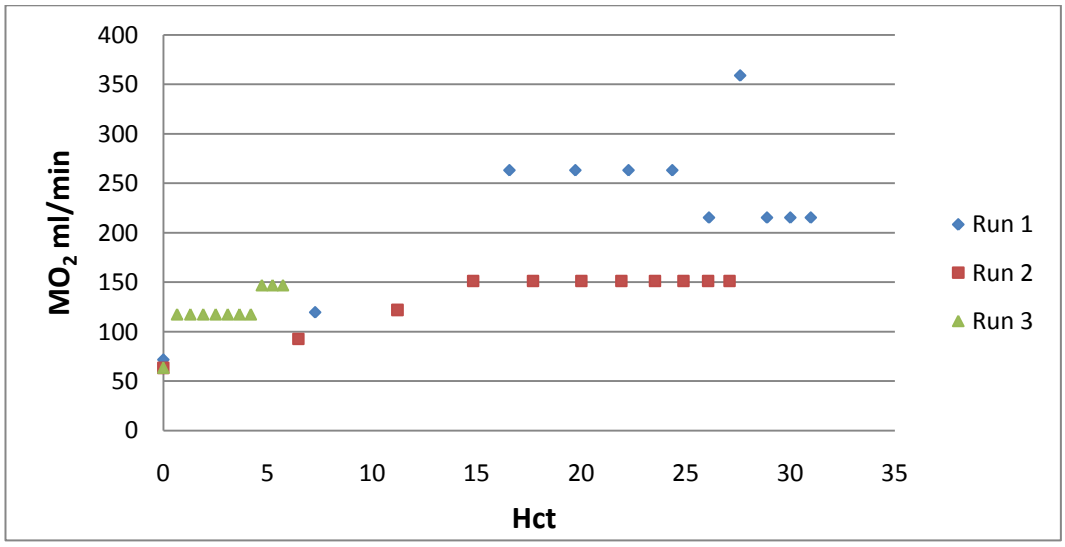

Figure 3.49 Effects of Hct on $\dot{M}O_2$; The $\dot{M}O_2$ ($p<0.0001$) increased curvilinearly over the Hct range with significant increase from Hct 0% to 15% before plateauing. In run 1 ♦ with FiO_2 21% $\dot{M}O_2$ rose from 71.7 ml/min (0%) to a mean of 252.43 ±46.47 ml/min. In run 2 ■ with FiO_2 26.3%, $\dot{M}O_2$ started at 63.39 ml/min at 0% increasing to a mean of 151.17 ±0 ml/min. Run 3 ▲ revealed a gradual increase in $\dot{M}O_2$ over the Hct range 0.66-5.71 rising from 63.66 ml/min to 146.92 ml/min with an oxygenator FiO_2 26.5%.

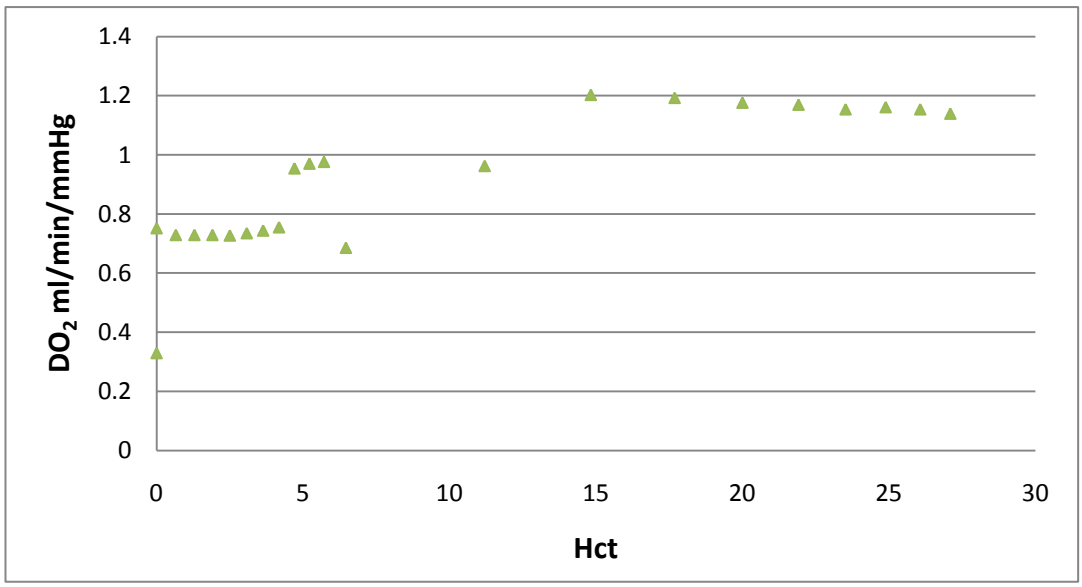

Figure 3.50 Effects of Hct on DO_2; DO_2 ($p<0.0001$) increased curvilinearly over the Hct range with significant rise from Hct 0 to 15% before plateauing. DO_2 started at 0.33 ml/min/mmHg at 0% increasing to a mean of 1.17 ±0.02 ml/min/mmHg. At lower Hct range (0.66-5.71) a gradual increase in DO_2 was observed rising from 0.75 ml/min/mmHg to 0.98 ml/min/mmHg.

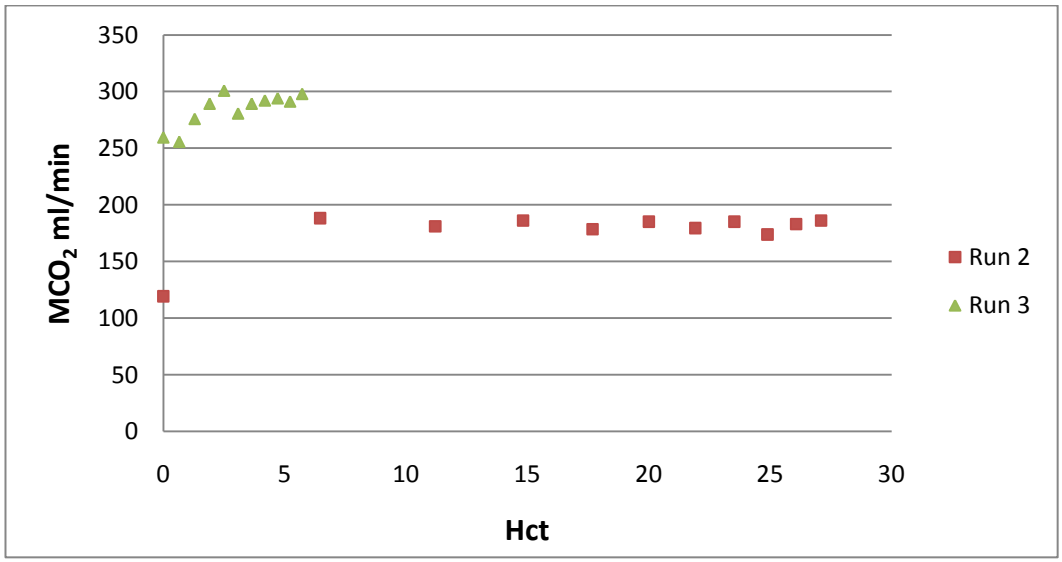

Figure 3.51 Effects of Hct on $\dot{M}CO_2$; At lower Hct range (▲) 0.66-5.71 $\dot{M}CO_2$ increased curvilinearly from 259.46 ml/min to 297.90 ml/min ($p=0.004$). At the higher Hct range (■) 6.5-27.1 $\dot{M}CO_2$ started at 119.34 ml/min (Hb=0) but maintained a mean $\dot{M}CO_2$ 182.71 ±4.43 ml/min thereafter in the presence of RBC.

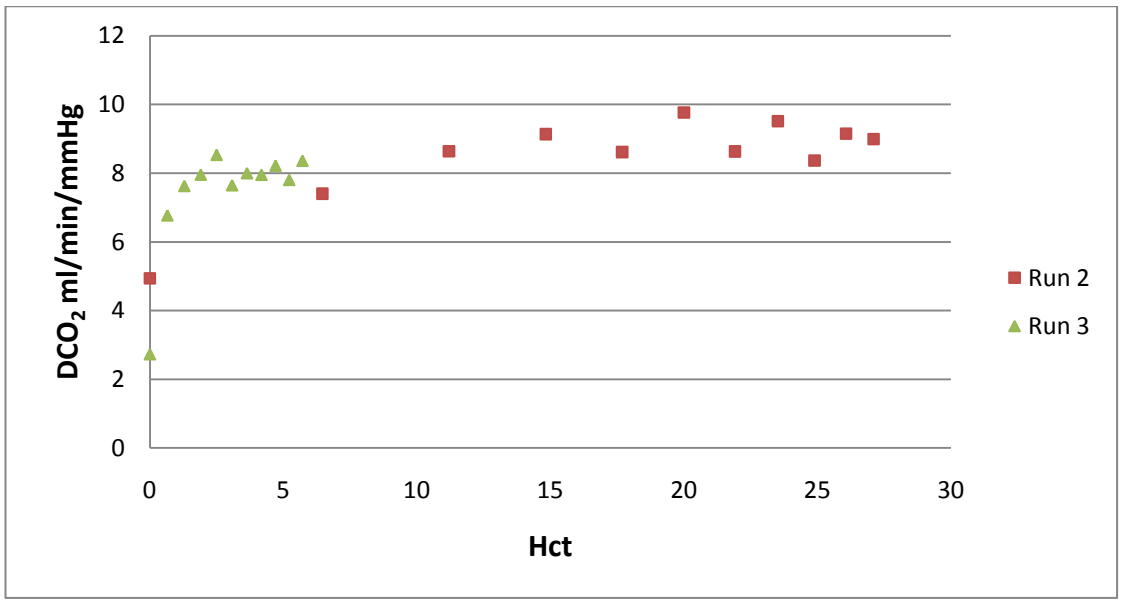

Figure 3.52 Effects of Hct on DCO_2; Across the whole Hct range 0.66-27.1 DCO_2 increased curvilinearly (p=0.002). DCO_2 increased from 6.77 ml/min/mmHg to 8.36 ml/min/mmHg over the Hct range 0.66-5.71 ▲. At the higher Hct range DCO_2 was 4.94 ml/min/mmHg with the saline prime and maintained a mean 8.82 ±0.66 ml/min/mmHg over the Hct range 6.45-27.1 ■.

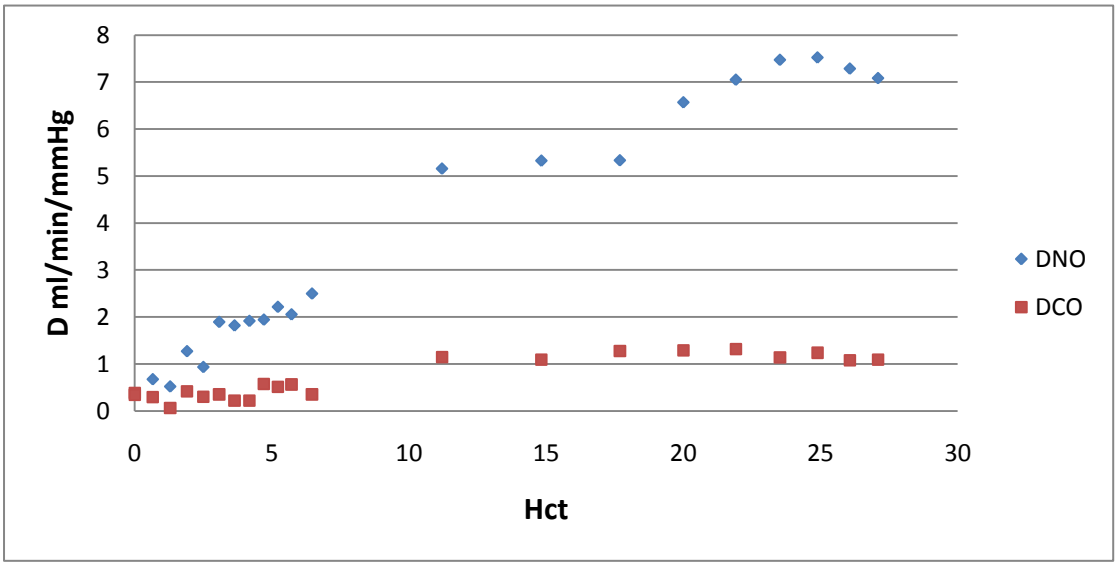

Figure 3.53 Effects of Hct on DNO and DCO; DNO ♦ significantly increased with rising Hct (p<0.0001) from 0.68 ml/min/mmHg at Hct 0.66 up to 7.08 ml/min/mmHg at Hct 27.1. DCO ■ increased curvilinearly with increasing Hct (p<0.0001) from 0.34 ml/min/mmHg (saline prime) up to 1.09 ml/min/mmHg at Hct 27.1.

References

AAMI, 2009. *Cardiovascular implants and artificial organs – Blood-gas exchangers (oxygenators), 2009.* AAMI ISO 7199:2009.

ALSTON, R.P., 1989. Vasodilating effect of Isoflurane during cardiopulmonary bypass. *Journal of Cardiothoracic Anesthesia,* **3**(5 Suppl 1), pp. 91.

AMBERSON, W.R., JENNINGS, J.J. and RHODE, C.M., 1949. Clinical experience with hemoglobin-saline solutions. *Journal of Applied Physiology,* **1**(7), pp. 469-489.

AnaesthesiaUK, 2004. *Isoflurane*. [online] AnaesthesiaUK. Available at: http://www.anaesthesiauk.com/article.aspx?articleid=275 [July 2010]

ARNAUD, F., SAILTETUS, A.H., KIM, B., HAQUE, A., SAHA, B., NIGAM, S., MOON-MASSAT, P., AUKER, C., MCCARRON, R., FREILICH, D., 2010. Dose response of sodium nitrite on vasoactivity associated with HBOC-201 in a swine model of controlled haemorrhage. *Artif Cells Blood Substit Immobil Biotechnol*, Dec 6.

BAUDIN-CREUZA, V., CHAUVIERRE, C., DOMINGUES, E., KIGER, L., LECLERC, L., VASSEUR, C., CELIER, C., MARDEN, M.C., 2008. Octomers and nanoparticles as hemoglobin based blood substitutes. *Biochim Biophys Acta Prot*, **1784**, pp. 1448-1453.

BECK, J.R., MONGERO, L.B., KROSLOWITZ, R.M., CHOUDHRI, A.F., CHEN, J.M., DEROSE, J.J., ARGENZIANO, M., SMERLING, A.J. and OZ, M.C., 1999. Inhaled nitric oxide improves hemodynamics in patients with acute pulmonary hypertension after high-risk cardiac surgery. *Perfusion,* **14**(1), pp. 37-42.

BECKLEY, P.D., MORRIS, S.M., SMITH, J.J., MCNAMARA, J.L. and NOVAK, J.A., 1996. Comparison of the performance characteristics of three generations of membrane oxygenators: Univox®, Univox® Gold™ and SpiralGold™. *Perfusion,* **11**(1), pp. 61-70.

BODY, S.C., FITZGERALD, D., VOORHEES, C., HANSEN, E., CROWLEY, C., VOORHEES, M.E. and SHERNAN, S.K., 1999. Effect of nitric oxide upon gas transfer and structural integrity of a polypropylene membrane oxygenator. *ASAIO*, **45**, pp. 550-554.

BOHR, C., 1909. Uber die speizifische tatigkeit der lungen bei der respiratorischen gasaufnahme und ihr verhalten zu der durch die alveolarwand stattfindenden gasdiffusion. *Skand Arch Physiol*, **22**, pp. 221-280.

BORLAND, C.D. and HIGENBOTTAM, T.W., 1989. A simultaneous single breath measurement of pulmonary diffusing capacity with nitric oxide and carbon monoxide. *The European Respiratory Journal: official Journal of the European Society for Clinical Respiratory Physiology,* **2**(1), pp. 56-63.

BORLAND, C., 1990. NO and CO transfer. *The European Respiratory Journal: official Journal of the European Society for Clinical Respiratory Physiology,* **3**(8), pp. 977-978.

BORLAND, C., CHANDLER, J., DUNNINGHAM, H., MISSO, S., VUYLSTEKE, A. and PROMNITZ, A., 2003. Using a membrane oxygenator for simultaneous measurement of nitric oxide and carbon monoxide diffusing capacity, *European Respiratory Society Annual Congress*, 2003.

BORLAND, C., DUNNINGHAM, H., BOTTRILL, F. and VUYLSTEKE, A., 2005. Modelling lung NO and CO transfer using a membrane oxygenator, *ATS International Conference*, 2005.

BORLAND, C., DUNNINGHAM, H., BOTTRILL, F. and VUYLSTEKE, A., 2006. Can a membrane oxygenator be a model for lung NO and CO transfer? *J. Appl. Physiol*, **100**(5), pp. 1527-1538.

BORLAND, C., DUNNINGHAM, H., BOTTRILL, F. and VUYLSTEKE, A., 2007. Can a membrane oxygenator be a model for lung oxygen and carbon dioxide transfer? *ATS International Conference*, 23 May 2007, 2007.

BORLAND, C.D., DUNNINGHAM, H., BOTTRILL, F., GORDON, D. and VUYLSTEKE, A., 2007b. Isoflurane increases oxygen uptake by a membrane oxygenator, *ATS International Conference*, 23 May 2007, 2007.

BORLAND, C.D., DUNNINGHAM, H., BOTTRILL, F., VUYLSTEKE, A., YILMAZ, C., DANE, M.D., and HSIA, C.C.W., 2010. Significant blood resistance to nitric oxide transfer in the lung. *J.Appl.Physiol.*, **108**, pp. 1052-1060.

Brown University, April 2005. *Haemoglobin-Based-Oxygen-Carriers*. [online] Homepage of brown.edu. Available at: http://biomed.brown.edu/Courses/BI108/BI108_2005_Groups/10/webpages/HBOClink.htm. [January, 2011]

CARLSEN, E. and CAMROE, J.H., 1958. The rate of uptake of carbon monoxide and nitric oxide by normal human erythrocytes and experimentally produced spherocytes. *The Journal of General Physiology*, **42**(1), pp. 83-107.

CHEN, J.Y., SCERBO, M. and KRAMER, G., 2009. A review of blood substitutes: examining the history, clinical trial results, and ethics of hemoglobin-based oxygen carriers. *Clinics (Sao Paulo, Brazil)*, **64**(8), pp. 803-813.

CLARK, I., 2007. Haemoglobin-Based Oxygen Carriers (HBOCs). *Perfusionist*, **31**(3), pp. 5-8.

CLERBAUX, T., GUSTIN, P., DETRY, B., CAO, M.L. and FRANS, A., 1993. A comparative study of the oxyhaemoglobin dissociation curve of four mammals: man, dog, horse and cattle. *Compendium Of Biochemical Physiology*, **106A**(4), pp. 687-694.

CLERBAUX, T., SERTEYN, D., WILLEMS, E. and BRASSEUR, L., 1986. Determination of standard oxyhaemoglobin dissociation curve in horses; effects of temperature, ph and diphosphoglycerate. *Can J Vet Res*, **50**(2), pp. 188-192.

COLE, R., VANDEGRIFF, K.D., SZERI, A.J., SAVAS, O., BAKER, D.A. and WINSLOW, R.M., 2007. A quantitative framework for the design of acellular haemoglobins as blood substitutes: implications of dynamic flow conditions. *Biophys Chem*, **128**, pp. 63-74.

COLE, R., VANDEGRIFF, K., SZERI, A., SAVAS, O. and WINSLOW, R., 2008. Targeted O_2 delivery by blood substitutes; *in vitro* arteriolar simulations of first- and second- generation products. *Microvascular Research*, **76**, pp. 169-179.

COLE, R.H., MALAVALLI, A. and VANDEGRIFF, K.D., 2009. Erythrocytic ATP release in the presence of modified cell-free hemoglobin. *Biophys Chem*, **144**, pp. 119-122.

COOPER, S. and LEVIN, R., 1987. Near catastrophic oxygenator failure. *Anesthesiology*, **66**, pp. 101-102.

COTES, J.E., 1993. *Lung function assessment and application in medicine.* 5th edn. London: Blackwell Scientific Publications.

COTES, J.E., CHINN, D.J. and MILLER, M.R., 2006. *Lung function: physiology, measurement and application in medicine.* 6 edn. Oxford: Blackwell Publishing.

CROSBIE, A.E., VUYLSTEKE, A. and LATIMER, R.D., 1998. Inhalation anaesthetics and the Medtronic Maxima plus membrane oxygenator. *Br.J.Anaesth*, **80**(6), pp. 878-878.

CYPEL, M., RUBACHA, M., YEUNG, J., HIRAYAMA, S., TORBICKI, K., MADONIK, M., FISCHER, S., HWANG, D., PIERRE, A., WADDELL, T.K., DE PERROT, M., LIU, M. and KESHAVJEE, S., 2009. Normothermic ex vivo perfusion prevents lung injury compared to extended cold preservation for transplantation. *Am J Transplant*, **9**, pp. 2262-2269.

DOHERTY, D.H., DOYLE, M.P., CURRY, S.R., VALI, R.J., FATTOR, T.J., OLSON, J.S. and LEMON, D.D., 1998. Rate of reaction with nitric oxide determines the hypertensive effect of cell-free hemoglobin. *Nature Biotechnology*, **16**(7), pp. 672-676.

DRIESSEN, B., JAHR, J.S., LURIE, F., GRIFFEY, S.M. and GUNTHER, R.A., 2001. Effects of haemoglobin-based oxygen carrier hemoglobin glutamer-200 (bovine) on intestinal perfusion and oxygenation in a canine hypovolaemic model. *Br.J.Anaesth.*, **86**(5), pp. 683-692.

DUNNINGHAM, H., BORLAND, C.D., BOTTRILL, F., GORDON, D. and VUYLSTEKE, A., 2007. Modelling lung and tissue diffusion using a membrane oxygenator circuit. *Perfusion*, **22**, pp. 231-238.

EGER, E.I., 2004. Characteristics of anesthetic agents used for induction and maintenance of general anesthesia. *American Society of Health System Pharmacists*, **61**, pp. S3-s10.

FDA, 2004. *1-19. Guidance for Industry: Criteria for safety and efficacy evaluation of oxygen therapeutics as red blood cell substitutes*. Washington D.C.: FDA

FORSTER, R.E., 1983. The single-breath carbon monoxide transfer test 25 years on: a reappraisal. *Thorax,* **38**, pp. 1-5.

FRIED, D.W. and MOHAMED, H., 1994. Use of the oxygen transfer slope and estimated membrane oxygen transfer to predict PaO_2. *Perfusion,* **9**, pp. 49-55.

GEDNEY, J.A. and GHOSH, S., 1995. Pharmacokinetics of analgesics, sedatives and anaesthetic agents during cardiopulmonary bypass. *Br.J.Anaesth,* **75**, pp. 344-351.

GIBSON, Q.H., 1954. Stopped-flow apparatus for the study of rapid reactions. *Discussions Faraday Soc*, **17**, pp. 137-139.

GLADWIN, M.T., GRUBINA, R., and DOYLE, M.P., 2009. The new chemical biology of nitrite reactions with hemoglobin: R-state catalysis, oxidative denitrosylation, and nitrite reductase/anhydrase. *Acc Chem Res*, **42**, pp. 157-167.

GOULD, S.A., MOORE, E.E., HOYT, D.B., NESS, P.M., NORRIS, E.J., CARSON, J.L., HIDES, G.A., FREEMAN, I.H., DEWOSKIN, R. and MOSS, G.S., 2002. The life-sustaining capacity of human polymerized hemoglobin when red cells might be unavailable. *Journal of the American College of Surgeons,* **195**(4), pp. 445-52; discussion 452-5.

GOURLAY, T., FLEMING, J., TAYLOR, K.M. and ASLAM, M., 1990. Evaluation of a range of extracorporeal membrane oxygenators. *Perfusion,* **5**, pp. 117-133.

GOURLAY, T. and TAYLOR, K.M., 1994. Pulsatile flow and membrane oxygenators. *Perfusion,* **9**, pp. 189-196.

GRETHLEIN, S., RAJAN, A., BARTZ, R.R., PRZYBELSKI, R., COURSIN, D. and WILLIAMS, E.C., November 2007, *Blood Substitutes.* [online] eMedicine. Available at: <http://emedicine.medscape.com/article/207801-overview> [17 November 2009].

GRIFFITHS, K.E., VASQUEZ, M.R., BECKLEY, P.D. and LALONE, B.J., 1994. Predicting oxygenator clinical performance from laboratory in vitro testing. *JECT.,* **26**(3), pp. 114-120.

GUENARD, H., VARENE, N. and VAIDA, P., 1987. Determination of lung capillary blood volume and membrane diffusing capacity in man by the measurements of NO and CO transfer. *Respiration physiology,* **70**(1), pp. 113-120.

GUYTON, A.C., 1976. *Textbook of medical physiology.* Philadelphia: WB Saunders.

HARE, G.M., HARRINGTON, A., LIU, E., WANG, J.L., BAKER, A.J., and MAZER, C.D, 2006. Effect of oxygen affinity and molecular weight of HBOCs on cerebral oxygenation and blood pressure in rats. *Can J Anaesth,* **53**(10), pp. 1030-1038.

HARTRIDGE, H. and ROUGHTON, F.J.W., 1923. The velocity with which carbon monoxide displaces oxygen from combination with haemoglobin, part I. *Proc. R. Soc. Lond. B*, **94**, pp. 336-367.

HARTRIDGE, H. and ROUGHTON, F.J.W., 1923b. The measurement of the rates of oxidation and reduction of haemoglobin. *Nature*, **111**, pp. 325-326.

HEAD, C.A., BRUGNARA, C., MARTINEZ-RUIZ, R., KACMAREK, R.M., BRIDGES, K.R., KUTER, D., BLOCH, K.D. and ZAPOL, W.M., 1997. Low concentrations of nitric oxide increase oxygen affinity of sickle erythrocytes in vitro and in vivo. *J. Clin Invest,* **100**(5), pp. 1193-1198.

HELLER, H. and SCHUSTER, K., 1998. Nitric oxide used to test pulmonary gas exchange in rabbits. *Pflugers Archiv: European Journal of Physiology,* **437**(1), pp. 94-97.

HENDERSON, J.M., NATHAN, H.J., LALANDE, M., WINKLER, M.H. and DUBE, L.M., 1988. Washin and washout of isoflurane during cardiopulmonary bypass. *Canadian Journal of Anaesthesia = Journal Canadien d'Anesthesie,* **35**(6), pp. 587-590.

HICKEY, S., GAYLOR, J.D. and KENNY, G.N., 1996. In vitro uptake and elimination of Isoflurane by different membrane oxygenators. *Journal of Cardiothoracic and Vascular Anesthesia,* **10**(3), pp. 352-355.

HILL, A.V., 1910. The possible effects of the aggregation of the molecules of haemoglobin on its dissociation curves. *The Journal of Physiology,* **40**(1), pp. iv-vii.

HU, D.X., KLUGER, R., 2008. Functional cross-linked haemoglobin bis-tetramers: geometry and cooperativity. *Biochemistry*, **47**, pp. 12551-12561.

HUGHES, J.M.B and BATES, D.V., 2003. Historical review: the carbon monoxide diffusing capacity (DL_{CO}) and its membrane (D_M) and red cell (θ,Vc) components. *Respir Physiol Neurobiol*, **138**, pp. 115-142.

IRWIN, D.C., FOREMAN, B., MORRIS, K., WHITE, M., SULLIVAN, T., JACOBS, R., MONNET, E., HACKETT, T., TISSOTVANPATOT, M.C., HAMILTON, K.L. and GOTSHALL, R.W., 2008. Polymerized bovine hemoglobin decreases oxygen delivery during normoxia and acute hypoxia in the rat. *American Journal of Physiology.Heart and Circulatory Physiology,* **295**(3), pp. H1090-H1099.

JAHR, J.S., LURIE, F., DRIESSEN, B., GUNTHER, R.A. and GOLKARYEH, M.S., 2001. Comparing arterial oxygen saturation (SaO2) from a Nellcor oxygen saturation monitor, IL Co-Oximeter and (LEXO2CON) with varying concentrations of Hemoglobin-Based Oxygen Carrier (HBOC) in a dog hemorrhage model. *Anesthesiology,* **95**, pp. A557.

JENKINS, T., 2007. The impact of HIV/AIDS on blood transfusion practice in South Africa: some ethical issues. *South African Medical Journal,* (November),.

KARIMOVA, A., ROBERTSON, A., CROSS, N., SMITH, L., O'CALLAGHAN, M., TULEU, C., LONG, P., BEETON, A., HAN, J., RIDOUT, D., GOLDMAN, A. and BROWN, K., 2005. A wet-primed extracorporeal membrane oxygenation circuit with hollow-fiber membrane oxygenator maintains adequate function for use during cardiopulmonary resuscitation after two weeks on standby. *Crit Care Med,* **33**(7), pp. 1572-1576.

KAWAHITO, S., MAEDO, T., MOTOMURA, T., TAKANO, T., NONAKA, K., LINNEWEBER, J., MIKAMI, M., ICHIKAWA, S., KAWAMURA, M., GLUEK, J., SATO, K. and NOSE, Y., 2001. Development of a new hollow fiber silicone membrane oxygenator: in vitro study. *Artif Org*, **25**(6), pp. 494-498.

KAWAHITO, S., MOTOMURA, T., GLUECK, J. and NOSE, Y., 2002. Development of a new hollow fiber silicone membrane oxygenator for ECMO: the recent progress. *Ann Thorac Cardiovasc Surg*, **8**(5), pp. 268-274.

KAWAK, A.M., GAYLOR, J.D., SIMPSON, K. and KIRKLAND, M., 1991. An in vitro technique to assess oxygenator potential for respiratory failure techniques. *Int J Artif Organs*, **14**(4), pp. 234-238.

KEH, D., GERLACH, M., KURER, I., SPIELMANN, S., KERNER, T., BUSCH, T., HANSEN, R. and FALKE,K.,GERLACH,H., 1999. Nitric oxide diffusion across membrane lungs protects platelets during simulated extracorporeal circulation. *European Journal of Clinical Investigation*, **29**, pp. 344-350.

KROGH, M., 1915. The diffusion of gases through the lungs of man. *The Journal of Physiology*, **49**(4), pp. 271-300.

LANQUETOT, H., 2005. Practical use of isoflurane during cardiac surgery with extracorporeal circulation. *ITBM-RBM*, **26**, pp. S19-S25.

LILIENTHAL, J.J., RILEY, R.L., PROEMMEL, D.D. and FRANKE, R.E., 1946. An experimental analysis in man of the oxygen pressure gradient from alveolar air to arterial blood during rest and exercise at sea level and at altitude. *Am J Physiol*, **147**, pp. 199-216.

LIU, E.H. and DHARA, S.S., 2005. Monitoring oxygenator expiratory isoflurane concentrations and the bispectral index to guide isoflurane requirements during cardiopulmonary bypass. *Journal of Cardiothoracic and Vascular Anesthesia*, **19**(4), pp. 485-487.

LIU, X., MILLER, M.J.S., JOSHI, M.S., SADOWSKA-KROWICKA, H., CLARK, D.A. AND LANCASTER, J.R., 1998. Diffusion-limited reaction of free nitric oxide with erythrocytes. *J. Biol. Chem.* **273**(30), pp. 18709–18713.

LIU, X., SAMOUILOV, A., LANCASTER, J.R. and ZWEIER, J.L., 2002. Nitric oxide uptake by erythrocytes is primarily limited by extracellular diffusion not membrane resistance. *The Journal of Biological Chemistry*, **277**(29), pp. 26194-26199.

LIUMBRUNO, G.M. and AUBUCHON, J.P., 2010. Old blood, new blood or better stored blood? *Blood Transfusion*, **8**, pp. 217-219.

LOCKWOOD, G.G., SAPSED-BYRNE, S.M. and ADAMS, S., 1999. A comparison of anaesthetic tensions in arterial blood and oxygenator exhaust gas during cardiopulmonary bypass. *Anaesthesia*, **54**(5), pp. 434-436.

LOOMIS, C.W., BRUNET, D., MILNE, B., CERVENKO, F.W. and JOHNSON, G.D., 1986. Arterial Isoflurane concentration and EEG burst suppression during cardiopulmonary bypass. *Clinical Pharmacology and Therapeutics*, **40**(3), pp. 304-313.

LOWE, K.C., 2006. Blood Substitutes: from chemistry to clinic. *Journal of Materials Chemistry,* **16**, pp. 4189-4196.

MAEDA, T., IWASAKI, A., KAWAHITO, S., NAKATA, K., NONAKA, K., LINNEWEBER, J., SCHULTE-EISTRUP, S., TAKANO, T., YOSHIKAWA, M., SATO, K., KUWANA, J., MURABAYASHI, S. and NOSE, Y., 2000. Preclinical evaluation of a hollow fiber silicone membrane oxygenator for extracorporeal membrane oxygenator application. *ASAIO J.,* **46**, pp. 426-430.

MALTRY, D.E. and EGGERS, G.W.N., 1987. Isoflurane-induced failure of the Bentley-10 oxygenator. *Anesthesiology,* **66**, pp. 100-101.

MARKS, R.R.D., 2003. Which anaesthetic agent for maintenance during normothermic cardiopulmonary bypass? *Br.J.Anaesth,* **90**(2), pp. 118-121.

MARTINEZ-RUIZ, R., MONTERO-HUERTA, P., HROMI, J. and HEAD, C.A., 2001. Inhaled nitric oxide improves survival rates during hypoxia in a sickle cell (SAD) mouse model. *Anesthesiology,* **94**(6), pp. 1113-1118.

MATSUDA, N. and SAKAI, K., 2000. Blood flow and oxygen transfer rate of an outside blood flow membrane oxygenator. *Journal of Membrane Science,* **170**, pp. 153-158.

MCCARTHY, M., VANDEGRIFF, K. and WINSLOW, R., 2001. The role of facilitated diffusion in oxygen transport by cell-free hemoglobins: implications for the design of hemoglobin-based oxygen carriers. *Biophys Chem*, **92**, pp. 103-117.

MOORE, E.E., MOORE, F.A., FABIAN, T.C., BERNARD, A.C., FULDA, G.J., HOYT, D.B., DUANE, T.M., WEIRETER, L.J.,JR, GOMEZ, G.A., CIPOLLE, M.D., RODMAN, G.H.,JR, MALANGONI, M.A., HIDES, G.A., OMERT, L.A., GOULD, S.A. and POLYHEME STUDY GROUP, 2009. Human polymerized hemoglobin for the treatment of hemorrhagic shock when blood is unavailable: the USA multicenter trial. *Journal of the American College of Surgeons,* **208**(1), pp. 1-13.

MOTOMURA, T., MAEDA, T., KAWAHITO, S., MATSUI, T., ICHIKAWA, S., ISHITOYA, H., KAWAMURA, M., SHINOHARA, T., SATO, K., KAWAGUCHI, Y., TAYLOR, D., OESTMANN, D., GLUECK, J. and NOSE, Y., 2003. Development of silicone rubber hollow fiber membrane oxygenator for ECMO. *Artif Org,* **27**(11), pp. 1050-1053.

MUHLE, M.L., STAMMERS, A.H., TREMAIN, K.D., NIIMI, K.S., GLOGOWSKI, K.R., TROWBRIDGE, C.C. and YANG, T., 2001. An in vitro study of the effects of isoflurane on oxygen transfer. *Perfusion,* **16**(4), pp. 293-299.

NATANSON, C., KERN, S.J., LURIE, P., BANKS, S.M. and WOLFE, S.M., 2008. Cell-free hemoglobin-based blood substitutes and risk of myocardial infarction and death. *Journal of American Medical Association,* **299**(19), pp. 2304-2312.

NEYA, K., LEE, R. and VLAHAKES, G.J., 1998. Hemoglobin based oxygen carrying solution stability in extracorporeal circulation: an in vitro evaluation and implications for clinical use. *ASAIO,* **44**(3), pp. 166-170.

NIIMI, Y., UEYAMA, K., YAMAJI, K., YAMANE, S., TAYAMA, E., SUEOKA, A., KUWANA, K., TAHARA, K. and NOSÉ, Y., 1997. Effects of ultrthin silicone coating on porous membrane on gas transfer and haemolytic performance. *Artif Org,* **21**(10), pp. 1082-1086.

NUSSMEIER, N.A., MOSKOWITZ, G.J., WEISKOPF, R.B., COHEN, N.H., FISHER, D.M. and EGER, E.I., 1988. In vitro anesthetic washin and washout via bubble oxygenators: influence of anesthetic solubility and rates of carrier gas inflow and pump blood flow. *Anesthesia and Analgesia,* **67**, pp. 982-987.

NUSSMEIER, N.A., LAMBERT, M.L., MOSKOWITZ, G.J., COHEN, N.H., WEISKOPF, R.B., FISHER, D.M. and EGER, E.I.,2ND, 1989. Washin and washout of Isoflurane administered via bubble oxygenators during hypothermic cardiopulmonary bypass. *Anesthesiology,* **71**(4), pp. 519-525.

OKAMOTO, T., CHEN, F., ZHANG, J., YAMADA, T., NAKAYAMA, E., MORIKAWA, H., BANDO, T. and DATE, H., 2010. Establishment of an ex vivo lung perfusion model using non-heart beating large pigs. *Transplantation Proceedings*, **42**, pp. 1598-1601.

OLSON, J.S., FOLEY, E.W., ROGGE, C., TSAI, A.L., DOYLE, M.P. and LEMON, D.D., 2004. NO scavenging and the hypertensive effect of haemoglobin-based blood substitutes. *Free Rad Biol Med*, **36**, pp. 685-697.

Oxyglobin Datasheet, 2006. Arnolds Veterinary Products/Dechra Veterinary Products.

PEGO-FERNANDES, P.M., DE MEDEIROS, I.L., MARIANI, A.W., FERNANDES, F.G., UNTERPERTINGER, F.D.V., SAMANO, M.N., WEREBE, E.D.C., CANZIAN, M. and JANTENE, F.B., 2010. Ex vivo lung perfusion: early report of Brazilian experience. *Transplantation Proceedings*, **42**, pp. 440-443.

PHILIPP, A., WIESENACK, C., BEHR, R., SCHMID, F.X. and BIRNBAUM, D.E., 2002. High risk of intraoperative awareness during cardiopulmonary bypass with isoflurane administration via diffusion membrane oxygenators. *Perfusion,* **17**(3), pp. 175-178.

PIIPER, J. and SCHEID, P., 1980. Blood-gas equilibration in lungs. In: J.B. West, ed *Pulmonary Gas Exchange Ventilation, Blood Flow and Diffusion*. New York: Academic.

PRICE, S.L., BROWN, D.L., CARPENTER, R.L., UNADKAT, J.D. and CROSBY, S.S., 1988. Isoflurane elimination via a bubble oxygenator during extracorporeal circulation. *Journal of Cardiothoracic Anesthesia,* **2**(1), pp. 41-44.

RABINER, S.F., HELBERT, J.R., LOPAS, H. and FRIEDMAN, L.H., 1967. Evaluation of a stroma-free hemoglobin solution for use as a plasma expander. *The Journal of Experimental Medicine,* **126**(6), pp. 1127-1142.

RAIS-BAHRAMI, K., MIKESELL, G., SEALE, W.R., RIVERA, O., HEARTY, J.P. and SHORT, B.L., 1992. In vitro evaluation of the Mera Silox-S 0.5 and 0.8 m^2 silicone hollow-fibre membrane oxygenator for use in neonatal ECMO. *Perfusion,* **7**(4), pp. 315-320.

RILEY, R.L. and PERMUTT, S., 1973. Venous admixture component of the $AaPO_2$ gradient. *J.Appl.Physiol.,* **35**(3), pp. 430-431.

Rhodia New Zealand Ltd, January 1999. *Datasheet: Isoflurane.* [online] Information for Health Professionals. Available at: <http://www.medsafe.govt.nz/Profs/datasheet/i/Isofluraneliqgas.htm> [July 1, 2005].

ROHLFS, R.J., BRUNER, E., CHIU, A., GONZALES, A., GONZALES, M., MAGDE, D., MAGDE, M.D., VANDEGRIFF, K.D. and WINSLOW, R.M., 1998. Arterial blood pressure responses to cell-free hemoglobin solutions and the reaction with nitric oxide. *J. Biol. Chem.,* **273**, pp. 12128-12134.

ROTHER, R.P., BELL, L., HILLMEN, P. and GLADWIN, M.T., 2005. The clinical sequelae of intravascular hemolysis and extracellular plasma hemoglobin: a novel mechanism of human disease. *Journal of the American Medical Association,* **293**(13), pp. 1653-1662.

ROUGHTON, F.J. and FORSTER, R.E., 1957. Relative importance of diffusion and chemical reaction rates in determining rate of exchange of gases in the human lung, with special reference to true diffusing capacity of pulmonary membrane and volume of blood in the lung capillaries. *J. Appl. Physiol.,* **11**(2), pp. 290-302.

ROUGHTON, F.J., FORSTER, R.E., and CANDER, L., 1957. Rates at which carbon monoxide replaces oxygen from combination with human haemoglobin in solution and in the red cell. *J. Appl. Physiol*., **11**, pp. 269-276.

SAKAI, H., OKUDA, N., SATO, A., YAMAUE, T., TAKEOKA, S., and TSUCHIDA, E., (2010). Hemoglobin encapsulation in vesicles retards NO and CO binding and O_2 release when perfused through narrow gas-permeable tubes. *Am J Physiol Heart Circ Physiol*, **298**, H956-965.

SAKAI, H., SATO, A., MASUDA, K., TAKEOKA, S. and TSUCHIDA, E., 2008. Encapsulation of concentrated hemoglobin solution in phospolipid vesicles retards the reaction with NO, but not CO, by intracellular diffusion barrier. *The Journal of Biological Chemistry,* **283**(3), pp. 1508-1517.

SEGERS, P.M., HEIDA, J.F., DE VRIES, I., MAAS, C., BOOGAART, A.J. and EILANDER, S., 2001. Clinical evaluation of nine hollow-fibre membrane oxygenators. *Perfusion,* **16**, pp. 95-106.

SOKOL, G.M., VAN MEURS, K.P., WRIGHT, L.L., RIVERA, O., THORN, W.J., CHU, P.M. and SAMS, R.L., 1999. Nitrogen dioxide formation during inhaled nitric oxide therapy. *Clinical Chemistry,* **45**(3), pp. 382-387.

STANDL, T., 2004. Artificial oxygen carriers: hemoglobin-based oxygen carriers - current status 2004. *Transfusion Medicine And Hemotherapy,* **31**, pp. 262-268.

STERN, R.C., WEISS, C.I., STEINBACH, J.H. and EVERS, A.S., 1989. Isoflurane uptake and elimination are delayed by absorption of anesthetic by the Scimed membrane oxygenator. *Anesthesia and Analgesia,* **69**(5), pp. 657-662.

STOLLINGS, J.L. and OYEN, L.J., 2006. Oxygen therapeutics: oxygen delivery without blood. *Pharmacotherapy,* **26**(10), pp. 1453-1464.

TSAI, A.G., VANDEGRIFF, K.D., INTAGLIETTA, M. and WINSLOW, R.M., 2003. Targeted O_2 delivery by low-P_{50} hemoglobins: a new basis for O_2 therapeutics. *Am J Physiol*, **285**, H1411-H1419.

TSAI, A.G., CABRALES, P., MANJULA, B.N., ACHARYA, S.A., WINSLOW, R.M. and INTAGLIETTA, M., 2006. Dissociation of local nitric oxide concentration and vasoconstriction in the presence of cell-free hemoglobin oxygen carriers. *Blood,* **108**(10), pp. 3603-3610.

VANDEGRIFF, K.D., MALAVALLI, A., WOOLRIDGE, J., LOHMAN, J. and WINSLOW, R.M., 2003. MP4: a new nonvasoactive PEG-Hb conjugate. *Transfusion*, **43**, pp. 509-516.

VAN DER LEE, I., ZANEN, P., BIESMA, D.H. and VAN DEN BOSCH, J.M.M., 2005. The effect of red cell transfusion on nitric oxide diffusing capacity. *Respiration,* **72**, pp. 512-516.

VAN MEURS, K.P., MIKESELL, G.T., HEARTY, J.P., SCALE, W.R., RIVERA, O. and SHORT, B.L., 1991. In vitro testing of the $0.6m^2$ SciMed membrane oxygenator for use in neonatal extracorporeal membrane oxygenation. *JECT,* **23**(2), pp. 49-53.

VARAT, M.A., ADOLPH, R.J. and FOWLER, N.O., 1972. Fundamentals of clinical cardiology; cardiovascular affects of anaemia. *Am Heart J,* **83**(3), pp. 415-426.

VAUGHN, M., HUANG, K., KUO, L. and LIAO, J.C., 2000. Erythrocytes possess an intrinsic barrier to nitric oxide consumption. *The Journal of Biological Chemistry,* **275**(4), pp. 2342-2348.

VAUGHN, M.W., HUANG, K.T., KUO, L. and LIAO, J.C., 2001. Erythrocyte consumption of nitric oxide: competition experiment and model analysis. *Nitric Oxide : Biology and Chemistry / official Journal of the Nitric Oxide Society,* **5**(1), pp. 18-31.

VISSER, C. and DE JONG, D.S., 1997. Clinical evaluation of six hollow-fibre membrane oxygenators. *Perfusion,* **12**(6), pp. 357-368.

VOCELKA, C.R., BURDGE, E.C., KUNZELMAN, K.S., THOMAS, R. and VERRIER, E.D., 1993. An *in vitro* protocol for evaluation and comparison of membrane oxygenators. *JECT,* **25**(4), pp. 161-166.

VOCELKA, C.R., THOMAS, R., VERRIER, E. and KUNZELMAN, K., 1997. An *in vitro* comparison of gas transfer and pressure drop of the Bentley Duraflo Coated Spiral Gold and the Medtronic Carmeda Coated Maxima hollow fiber membrane oxygenators. *JECT.*, **29**(4), pp. 185-188.

WALCZAK, R., LAWSON, D.S., KAEMMER, D., MCROBB, C., MCDERMOTT, P., SMIGLA, G., SHEARER, I., LODGE, A. and JAGGERS, J., 2005. Evaluation of a preprimed microporous hollow-fiber membrane for rapid response neonatal extracorporeal membrane oxygenation. *Perfusion,* **20**, pp. 269-275.

WALLS, J.T., CURTIS, J.J., MCCLATCHEY, B.J. and WOOD, D., 1988. Adverse effects of anesthetic agents on polycarbonate plastic oxygenators. *The Journal of Thoracic and Cardiovascular Surgery*, **96**(4), pp. 667-668.

WEINBERGER, B., LASKIN, D.L., HECK, D.E. and LASKIN, J.D., 2001. The toxicology of inhaled nitric oxide. *Toxicological Sciences,* **59**, pp. 5-16.

WEISKOPF, R.B., VIELE, M.K., FEINER, J., KELLEY, S., LIEBERMAN, J., NOORANI, M., LEUNG, J.M., FISHER, D.M., MURRAY, W.R., TOY, P. and MOORE, M.A., 1998. Human Cardiovascular and Metabolic Response to Acute, Severe Isovolemic Anemia. *JAMA,* **279**, pp. 217-221.

WIESENACK, C., WIESNER, G., KEYL, C., GRUBER, M., PHILIPP, A., RITZKA, M., PRASSER, C. and TAEGER, K., 2002. In vivo uptake and elimination of isoflurane by different membrane oxygenators during cardiopulmonary bypass. *Anesthesiology,* **97**(1), pp. 133-138.

WINSLOW, R.M., GONZALES, A., GONZALES, M.L., MAGDE, M., MCCARTHY, M., ROHLFS, R.J. and VANDEGRIFF, K., 1998. Vascular resistance and the efficacy of red cell substitutes in a rat hemorrhage model. *J. Appl. Physiol,* **85**, pp. 993-1003.

WINSLOW, R.M., 2003. Current Status of Blood Substitute Research: Towards a New Paradigm. *J Intern Med,* **253**, pp. 508-517.

WINSLOW, R.M., KEIPERT, P., WINSLOW, N., OLOFSSON, N., FAGRELL, B., AHL, T., JOHANSSON, T., LARSSON, S., NELLGARD, P., PONZER, S., *et al*, 2005. A multi-center study of the safety and efficacy of MP4 (Hemospan (R)) in orthopedic surgery patients. *Crit Care Med* **33**, A6.

YANG, H., HOMI, M., SMITH, B.E. and GROCOTT, H.P., 2004. Cardiopulmonary Bypass Reduces the Minimum Alveolar Concentration for Isoflurane. *Journal of Cardiothoracic and Vascular Anesthesia,* **18**(5), pp. 620-623.

YU, B., BLOCH, K.D. and ZAPOL, W.M., 2009. Hemoglobin-based red blood cell substitutes and nitric oxide. *Trends in Cardiovascular Medicine,* **19**(3), pp. 103-107.

YU, B., RAHER, M.J., VOLPATO, G.P., BLOCH, K.D., ICHINOSE, F. and ZAPOL, W.M., 2008. Inhaled nitric oxide enables artificial blood transfusion without hypertension. *Circulation,* **117**(15), pp. 1982-1990.

YU, B., SHAHID, M., EGORINA, E.M., SOVERSHAEV, M.A., RAHER, M.J., LEI, C., WU, M.X., BLOCH, K.D. and ZAPOL, W.M., 2010. Endothelial dysfunction enhances vasoconstriction due to scavenging of nitric oxide by a hemoglobin-based oxygen carrier. *Anesthesiology,* **112**(3), pp. 586-594.

APPENDIX 1

Checklist of Circuit Hardware and Disposable Items.

Circuit Hardware Checklist
Stockert Roller Pump
Medtronic Heater/Cooler
Pressure Gauge
8 Tubing Clamps
CDI 500 Analyser with Calibration Gases
Spectrum Medical M2 Saturation Monitor with 3/8" wraparound sensors.
Cobe Sat/Hct Saturation Monitor
100% Oxygen Cylinder with Regulator
Air Cylinder with Regulator
N_2 Cylinder with Regulator
1000ppm NO in N_2 Cylinder with Regulator
CO (0.3%) in oxygen (19%) and Helium (11%) Cylinder with Regulator
5% CO_2 in balanced N_2 Cylinder with Regulator
100% CO_2 Cylinder with Regulator
Deoxygenator Gas Line
Oxygenator Gas Line
Deoxygenator Gas Exhaust Line
Oxygenator Gas Exhaust Line
2 x Gas line O_2 Analyser Teledyne X300

Disposable Items for Circuit
PVC tubing 3/8"
PVC tubing 1/2"
2 x Fluid Administration Line
Pressure Dome
2 x Cobe Duo Oxygenators with Integral Reservoirs
2 x CDI 500 'Arterial' pH, PO_2 and PCO_2 Sensors
3/8"x3/8" Luer Lock Connector
3/8"x1/2" Connector with Luer Lock
3/8" Cobe Sat/Hct sensor connector
2 litres 0.9% NaCl
Horse Blood (donated within 21 days)

APPENDIX 2

Bohr Integration Procedure via Excel Spreadsheet. Methodology devised by Dr. C. Borland (2010).

Bohr Integration Procedure via Excel Spreadsheet
Methodology devised by Dr. C. Borland (2010) via personal email communication dated 6th September 2010.

A computer based calculation of DO2 using Bohr's integration method
"How Bohr's integration works."

In calculus the area under the curve of a function between two points equals the area of a rectangle. This has height equal to the mean value of the function and length the distance between the points (19.0-16.3). Rearranging: the mean value equals the area divided by the distance between the two points. Bohr obtained the area between Pv(Sv) and Pa(Sa) by planimetry and plotted PO_2 (or rather 1/(PA-p) on the y axis and O_2 saturation (expressed as content) on the x axis (opposite to usual practice fig 1.).The average 1/(PA-p) = 0.02 is shown from Pv(Sv) 45.9(16.3) and 74.7 (19).

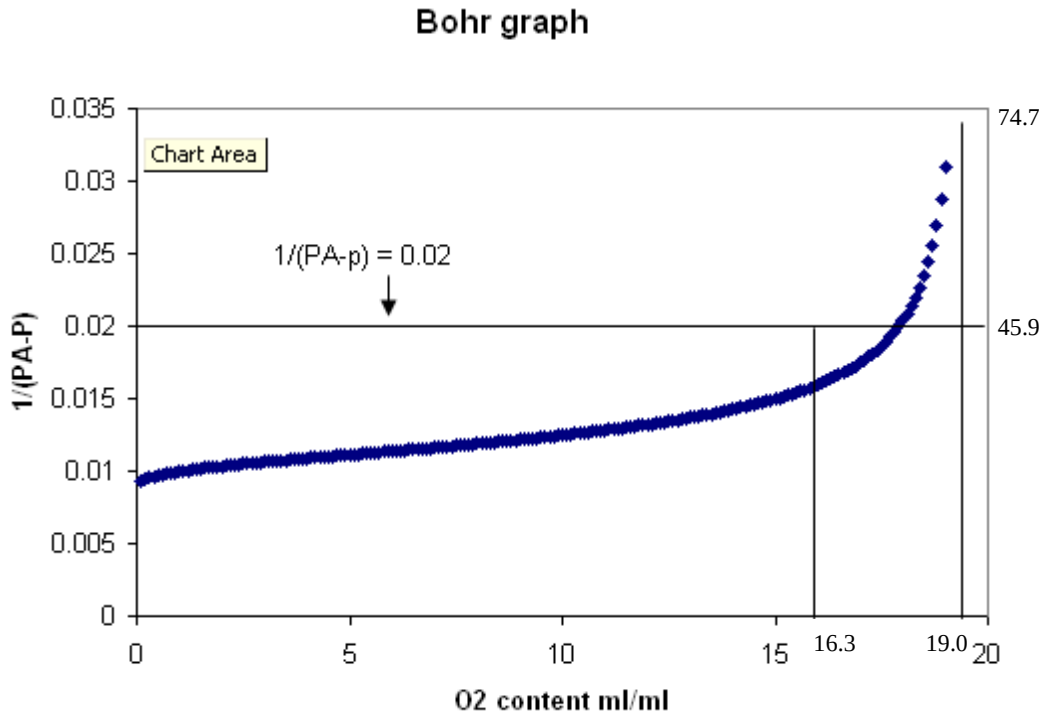

A computer spreadsheet makes integration (estimating the area under the curve) of a complex function very straightforward provided a formula for the function is available. The spreadsheet "counts the squares" to estimate area. An infinitesimal unit of oxygen content (we used 0.1) forms the side of the square while the base is the change in PO_2 or rather, 1/PA-Pc. The integral is the value for each "square" added onto the value of the previous. The area of Sv is subtracted from Sa and then divided by (Sa-Sv) to give $P\bar{c}O_2$

P(KpA)	vol%	Saturation	P (severinghaus mmHg)	1/P-p	vol%	Integral
6.105115	16.3	81.5	45.78836	0.016337	16.3	0.199218041
9.965414	19	95	74.7406	0.030999	19	0.254687079

Where:

Severinghaus' formula gives PmmHg from saturation=EXP(0.385*LN((((S/100)^-1)-1)^-1)+3.32-((72*(S/100))^-1)-(0.17*(S/100)^6))

1/(PA-p) = subtracts P Severinghaus from estimated "alveolar" PO_2.

Integral =0.1*1/(P-p) +∑1/(P-p) multiplies each estimate of 1/(P-p) by the infinitesimal change in oxygen content (0.1) and adds it to the value from the row above. This process goes from 0.1 to 20ml/ml.

So that using $\dot{M}O_2$ of 400ml/min alveolar PA 104 mmHg, Pv of 46 mmHg and Pa of 77mmHg and hence 1/(PA- $P\bar{c}O_2$) of (0.255-0.199)/(19-16.3)= 0.021 multiplied by 400 = 8.30 ml/min/Hg and Mean Pc = 107 – 1/.0207=58.8mmHg. It will be noted that the average 1/(PA-Pc) can also be obtained as average of 1/(PA- $P\bar{c}O_2$) over all the rows corresponding to Sv to Sa eg =AVERAGE(E183:E210) =0.021. This is not the same as the average of 0.1992 and 0.25468 = 0.227.

Initially we obtained 1/(PA- $P\bar{c}O_2$) by scrolling down the array to find the rows corresponding to Pa and Pv and entering them into the formulae. The excel command

VLOOKUP speeds up the process by finding the value for the integrals corresponding to Pa and Pv.

We were working with horse blood and here the relevant algorithm is from Clerbaux *et al* which gives saturation if pressure is known:

$SO_2 = 100 \times (3.103\times10^{-2} \times PO_2 + 2 \times 8.451\times10^{-4} \times PO_2^2 + 3\times1.447\times10^{-5} \times PO_2^3 + 4\times3.961 \times 10^{-6} \times PO_2^4)/(4 \times (1+3.103\times10^{-2} \times PO_2 + 8.451\times10^{-4} \times PO_2^2 + 1.447 \times 10^{-5} \times PO_2^3 + 3.961 \times 10^{-6} \times PO_2^4$

Instead of starting with increments of oxygen content we start with increments of PO_2 of 0.1mmHg, then in the next column display saturations using Clerbaux's formula. The integration is identical, multiplying the saturation by 0.1mmHg and adding to the value in the cell above.

Pv	Corresponding sat	Pa	Corresponding sat	integralv	Integral	Av sat	Av P
45.8	85.66113012	74.7	95.19345636	2045.44904	4695.820712	91.70836237	58.3
Using averages						91.68750984	58.3

Columns e.g. Pv and Pa can then be copied and pasted from the experimental results worksheet directly and the column of $P\bar{c}O_2$ pasted back.

The following table shows comparison of the calculations using the Severinghaus and Clerbaux *et al* algorithms. Bohr and Piiper calculations agree extremely well and the difference between Severinghaus and Clerbaux DO_2 are negligible. Independent t test on the DO_2 data comparing Severinghaus and Clerbaux with an assumed equal variance t=0.184, n=93 and p=0.855 (two-tailed) or 0.427 (one-tail).

PaO_2 mmHg	FAO_2 %	PAO_2 mmHg	$P\bar{v}O_2$ mmHg	$P\bar{c}O_2$ mmHg	Gas flow l/min	FeO_2 %	FiO_2 %	$\dot{M}O_2$ ml/min
71.25	19.4	145.9	34.50	49.20	5	18	21	137.6
71.25	19.4	145.9	39.75	53.00	5	18	21	137.6
70.50	19.4	145.9	45.00	56.20	5	18	21	137.6

$P\bar{c}O_2$ (Severinghaus) mmHg	$P\bar{c}O_2$ (Clerbaux) mmHg	DO_2 (Severinghaus) ml/min/mmHg	DO_2 (Clerbaux) ml/min/mmHg
48.7	49.2	1.41	1.42
52.8	53	1.48	1.48
56.9	56.2	1.54	1.53

APPENDIX 3

Borland CDR, Dunningham H, Bottrill F, Vuylsteke A. Modelling Lung NO and CO Transfer using a Membrane Oxygenator. ATS 2005, San Diego.

Rationale: The diffusing capacity for nitric oxide (D_{NO}) is generally accepted to reflect alveolar-capillary diffusion alone but debate remains whether this includes diffusion within the pulmonary capillary and whether the value for θ_{NO} is infinity or 4.5 ml ml^{-1} min^{-1} $torr^{-1}$ ie approximately sixfold θ_{CO} in normoxia .To help resolve this debate we have modelled lung nitric oxide and carbon monoxide gas transfer using a membrane oxygenator (Cobe Duo CML.)

Methods: the oxygenator was primed with freshly drawn horse blood.A mixture of 5 parts per million nitric oxide (NO), 0.02% carbon monoxide (CO) and 19% oxygen was directed into the gas inlet port at a flow rate of 5 L min^{-1} and the diffusing capacity (D) calculated from inlet and outlet NO and CO concentrations and gas flow rate.

Results: D_{NO} = 10.98 (SD 0.193) $ml.min^{-1}$ $torr^{-1}$ and D_{CO} = 0.452 (SD 0.042) $ml.min^{-1}$ $torr^{-1}$ .D_{NO} and D_{CO} increased ($p<0.001$) with blood volume and haemoglobin concentration. D_{NO} but not D_{CO} increased with haemolysis ($p<0.001$) indicating NO dependence on diffusive resistance associated with the red cell. D_{CO} but not D_{NO} fell with increasing oxygen tension ($p<0.05$).Both D_{NO} and D_{CO} fell with increasing gas flow rate ($p<0.01$).No statistically significant change in D_{NO} or D_{CO} occurred with changing blood flow rate.

Conclusion: Using the Roughton and Forster relationship ($1/D = 1/Dm + 1/\theta Vc$) and the post haemolysis value of D_{NO} to estimate the membrane diffusing capacity (Dm), we estimate that θ_{NO} exceeds θ_{CO} by at least twenty five fold.

Conclusions: It is possible to model NO and CO gas transfer using a membrane oxygenator and investigate variables such as haemoglobin concentration in isolation. Our data suggest a higher value for θ_{NO} than previous laboratory estimates.

APPENDIX 4

Borland CDR, Dunningham H, Bottrill F, Vuylsteke A. Can a membrane oxygenator be a model for lung NO and CO transfer? JAP 2006; 100:1527-1538.

J Appl Physiol 100: 1527–1538, 2006.
First published January 5, 2006; doi:10.1152/japplphysiol.00949.2005.

Can a membrane oxygenator be a model for lung NO and CO transfer?

Colin Borland,[1] Helen Dunningham,[2] Fiona Bottrill,[3] and Alain Vuylsteke[3]

[1]*Department of Medicine, Hinchingbrooke Hospital, Huntingdon; and* [2]*Cambridge Perfusion Services and* [3]*Department of Anaesthetic Research, Papworth Hospital, Cambridge, United Kingdom*

Submitted 3 August 2005; accepted in final form 19 December 2005

Borland, Colin, Helen Dunningham, Fiona Bottrill, and Alain Vuylsteke. Can a membrane oxygenator be a model for lung NO and CO transfer? *J Appl Physiol* 100: 1527–1538, 2006. First published January 5, 2006; doi:10.1152/japplphysiol.00949.2005.—To model lung nitric oxide (NO) and carbon monoxide (CO) uptake, a membrane oxygenator circuit was primed with horse blood flowing at 2.5 l/min. Its gas channel was ventilated with 5 parts/million NO, 0.02% CO, and 22% O_2 at 5 l/min. NO diffusing capacity (D_{NO}) and CO diffusing capacity (D_{CO}) were calculated from inlet and outlet gas concentrations and flow rates: D_{NO} = 13.45 ml·min^{-1}·Torr^{-1} (SD 5.84) and D_{CO} = 1.22 ml·min^{-1}·Torr^{-1} (SD 0.3). D_{NO} and D_{CO} increased (P = 0.002) with blood volume/surface area. 1/D_{NO} (P < 0.001) and 1/D_{CO} (P < 0.001) increased with 1/Hb. D_{NO} (P = 0.01) and D_{CO} (P = 0.004) fell with increasing gas flow. D_{NO} but not D_{CO} increased with hemolysis (P = 0.001), indicating D_{NO} dependence on red cell diffusive resistance. The posthemolysis value for membrane diffusing capacity = 41 ml·min^{-1}·Torr^{-1} is the true membrane diffusing capacity of the system. No change in D_{NO} or D_{CO} occurred with changing blood flow rate. 1/D_{CO} increased (P = 0.009) with increasing P_{O_2}. D_{NO} and D_{CO} appear to be diffusion limited, and D_{CO} reaction limited. In this apparatus, the red cell and plasma offer a significant barrier to NO but not CO diffusion. Applying the Roughton-Forster model yields similar specific transfer conductance of blood per milliliter for NO and CO to previous estimates. This approach allows alteration of membrane area/blood volume, blood flow, gas flow, oxygen tension, red cell integrity, and hematocrit (over a larger range than encountered clinically), while keeping other variables constant. Although structurally very different, it offers a functional model of lung NO and CO transfer.

nitric oxide; carbon monoxide; diffusing capacity; membrane diffusing capacity

BECAUSE OF ITS EXTREMELY RAPID and virtually irreversible reaction with oxyhemoglobin (12), nitric oxide (NO) is theoretically a better gas than oxygen (O_2) or carbon monoxide (CO) for measuring lung diffusing capacity (D_L) (4, 16, 22). The diffusing capacity for NO (D_{NO}) is generally accepted to be entirely diffusion limited and independent of capillary perfusion (18, 23). It is also believed to be independent of the rate of reaction with oxyhemoglobin (in contrast to CO). Debate continues as to whether NO transfer is solely limited to diffusion across the alveolar capillary membrane, or whether it includes diffusion within the capillary plasma or red cell (5, 23), as predicted by the finite rate of reaction of NO with the red cell in vitro (7).

In this study, we have used a flat-sheet polypropylene membrane oxygenator to model NO (and also CO) gas exchange. Altogether, we set out to answer five questions.

1) Are D_{NO} and CO diffusing capacity (D_{CO}) solely diffusion limited? Diffusion-limited gas transport is directly related to membrane surface area and thickness [membrane diffusing capacity (Dm)], capillary blood volume (Vc), and specific blood conductance (θ); by contrast, perfusion-limited gas transport is dependent on blood flow ($\beta\dot{Q}$, where β is the capacitance coefficient of blood) and independent of the membrane and Vc. The relationship is described mathematically by Cotes and Meade's extension of the Roughton-Forster equation (9):

$$1/D_L = 1/Dm + 1/(\beta\dot{Q} + \theta Vc) \quad (1)$$

With a dual-chamber membrane oxygenator, it is possible to halve Dm and Vc by clamping off blood lines to one-half of the unit without altering total blood flow. It is also possible to vary blood flow 25-fold without altering Dm and Vc, merely by altering the pump settings. This experiment directly addresses whether or not D_{NO} and D_{CO} are diffusion or perfusion limited and also tests whether it is legitimate to apply the Roughton-Forster relationship to the oxygenator.

2) Do D_{NO} and D_{CO} vary with gas flow? In preliminary experiments with the oxygenator, they appeared to do so; this can be further studied by varying gas flow while keeping blood flow constant.

3) Are D_{NO} and D_{CO} reaction limited? Varying O_2 tension alters D_{CO} in vitro and in vivo by altering the rate of combination of CO with oxyhemoglobin and hence θCO (26). Replicating this observation in the oxygenator is a further check on the validity of D_{CO} measurements and the Roughton-Forster relationship. It also allows estimation of Dm and, more importantly, Vc, whereby θ could be calculated for both CO and NO. Varying O_2 tension should not affect D_{NO} and does not in vivo (6).

4) Does the hematocrit and integrity of the red cell affect D_{NO} and D_{CO}? One approach to the debate of whether D_{NO} = Dm or includes intracapillary diffusion has been to examine the effect of anemia. Unfortunately, the results in humans have been conflicting (5, 23), no doubt because it is difficult to find a group of anemic patients with otherwise normal lung function. By contrast, the effect of anemia on D_{CO} is well documented (10). An even more radical approach would be to examine the effect of hemolysis, which would instantly abolish erythrocyte and plasma diffusive resistance. This would be difficult in vivo or in an isolated lung model, because the osmolarity change could permanently alter the alveolar-capillary membrane integrity, as occurs in fresh water drowning.

5) What happens to D_{NO} under conditions of zero flow? This should give information on the volume of distribution of NO and the contribution of reaction and diffusion limitation.

Address for reprint requests and other correspondence: C. Borland, Dept. of Medicine, Hinchingbrooke Hospital, Huntingdon, Cambridgeshire PE18 8NT, United Kingdom (e-mail: colin.borland@hinchingbrooke.nhs.uk).

The costs of publication of this article were defrayed in part by the payment of page charges. The article must therefore be hereby marked "*advertisement*" in accordance with 18 U.S.C. Section 1734 solely to indicate this fact.

Glossary

A	Surface area (cm^2)
a_c	Blood channel surface area (cm^2)
CI_{CO}	Inlet CO concentration (%)
CI_{NO}	Inlet NO concentration (ppb)
CO_{CO}	Outlet CO concentration (%)
CO_{NO}	Outlet NO concentration (ppb)
D	Diffusing capacity ($ml \cdot min^{-1} \cdot Torr^{-1}$)
DCO	Diffusing capacity for carbon monoxide ($ml \cdot min^{-1} \cdot Torr^{-1}$)
Dm	Diffusing capacity of oxygenator membrane ($ml \cdot min^{-1} \cdot Torr^{-1}$)
$Dm_{NO\ react}$	NO reaction conductance of polypropylene membrane ($ml \cdot min^{-1} \cdot Torr^{-1}$)
DNO	Diffusing capacity for nitric oxide ($ml \cdot min^{-1} \cdot Torr^{-1}$)
DNO_{diff}	Diffusing capacity for nitric oxide (excluding chemical reaction with membrane) ($ml \cdot min^{-1} \cdot Torr^{-1}$)
DO_2	Diffusing capacity for oxygen ($ml \cdot min^{-1} \cdot Torr^{-1}$)
f	Gas flow rate (l/min)
[Hb]	Hemoglobin concentration (g/dl)
k_{CO}	Diffusion coefficient of CO in water at 37°C (cm^2/s)
$K_{M_{NO}}$	Permeation coefficient of NO in oxygenator membrane at $37° \cdot cm^{-2} \cdot min^{-1} \cdot Torr^{-1}$
k_{NO}	Diffusion coefficient of NO in water at 37°C (cm^2/s)
l	Path length (cm)
L	Length of blood-carrying channel within oxygenator (cm)
m′c	Third-order rate constant of reaction of CO with oxygenated red cells (s^{-1})
MO_2	Rate of uptake of oxygen by oxygenator (ml/min)
NO	Nitric oxide [parts per billion (ppb)]
P_{ANO}	Partial pressure of NO in gas channel (Torr)
$P_{A_{O_2}}$	Partial pressure of oxygen in gas channel (Torr)
P_B	Barometric pressure (Torr)
$P_B - H_2O$	Barometric pressure less saturated vapor pressure of water (Torr)
$P_{C_{NO}}$	Partial pressure of nitric oxide in blood-carrying channel within oxygenator (Torr)
$P_{C_{O_2}}$	Average partial pressure of oxygen in blood-carrying channel within oxygenator (Torr)
$P_{V_{O_2}}$	Partial pressure of oxygen in blood channel entering oxygenator (Torr)
S	Cross-sectional surface area of blood-carrying channel within oxygenator (cm^2)
S'	Membrane surface area per unit length (cm)
Vc	Pulmonary capillary blood volume (ml)
α	Specific diffusion resistance of blood per milliliter for CO ($min^{-1} \cdot Torr^{-1}$)
β	Specific reaction resistance of blood per milliliter per Torr P_{O2} for CO (min)
θCO	Specific transfer conductance of blood per milliliter for CO ($min^{-1} \cdot Torr^{-1}$)
θNO	Specific transfer conductance of blood per milliliter for NO ($min^{-1}/Torr^{-1}$)
τ_m	Membrane thickness (cm)

METHODS

Gas Mixtures

Stock cylinders (British Oxygen Manufacturers' certificate of analysis, BOC gases, Worsley, Manchester, UK) of NO (1,000 ppm) in nitrogen and CO (0.3%), O_2 (19%), and helium (11%) were connected to a therapeutic NO mixing device (Nomius 305, MTA Sahlgrewska Goteborg Sweden and Bronkhorst Hi Tech, Ruurlo, Netherlands). The helium was present because the mixture is the standard used in our laboratory for single-breath CO gas transfer. The mixing device was adjusted to give 5 ppm of NO and 0.02% of CO. The NO and CO mix was diluted with compressed air and O_2 via a side arm downstream of the mixing device (Fig. 1) to give a flow rate of 5 l/min and O_2 concentration ($[O_2]$) as required (~22% for all except *experiment 3*, where the $[O_2]$ was varied).

Gas Analyzers

NO was analyzed using a chemiluminescent analyzer (Logan LR 2000, Logan Research, Rochester, Kent, UK) to which a custom-built CO analyzer was bolted on in series "upstream." O_2 was analyzed using a digital oxygen meter (5120, Datex Ohmeda, Louisville, KY), calibrated with 19, 21, and 100% O_2.

Blood Analysis

O_2 tension, CO_2 tension, potassium, and pH were measured using an inline optical fluorometric analyzer (CDI 500 Terumo Cardiovascular Systems UK, Egham, Surrey, UK). Hemoglobin, methemoglobin (metHb), and carboxyhemoglobin (HbCO) concentration were measured using a blood-gas analyzer (Rapidlab 800, Bayer, Newbury, Berks, UK). Specimens (1.5 ml) were withdrawn from the arterial sampling port (whole unit) or directly from the blood line (half unit) and placed on ice before analysis at the end of the experiment.

Oxygenator

The oxygenator consists of a microporous polypropylene membrane separating a gas stream and bloodstream moving at similar flow rates (1). Gas exchange takes place by diffusion down partial pressure gradients.

The device (Cobe Duo CML, Cobe Cardiovascular, Arvada, CO) used was of flat-sheet membrane design. It allows either half or whole unit operation. According to the manufacturer's information, the surface area is 1.3 m^2 (half) and 2.6 m^2 (whole), and the maximum O_2 transfer rate is 400 ml/min at 8 l/min. The priming blood volume is 260 ml (half unit) and 460 ml (full unit) so that the transit time at a flow rate of 2,500 ml/min is $260/2{,}500 \times 60 = 6.24$ s for the half unit and 12.5 s the for the full unit. To optimize gas exchange, the Cobe CML series uses extruded polypropylene mesh spacers between the membrane layers on both the gas and blood sides that reduce volume, maximize surface area, and promote turbulent flow (14). Unfortunately, we have no specific information on membrane thickness, blood path width, or length. The oxygenator was maintained at 37°C using a water bath for zero-flow experiments and using the inbuilt heat exchanger for the remainder. It was primed with 0.3 liter for zero flow and 1–1.5 liter horse blood for the remaining experiments. The blood inlet and outlet lines were joined to a polyvinyl chloride reservoir (Polystan, Jostra, Bellshill, UK) using polyvinyl chloride tubing to form a closed circuit. A second deoxygenator circuit scrubbed the oxygenated blood with 8.3% CO_2 in nitrogen to create normoxia and normocapnia (Fig. 1).

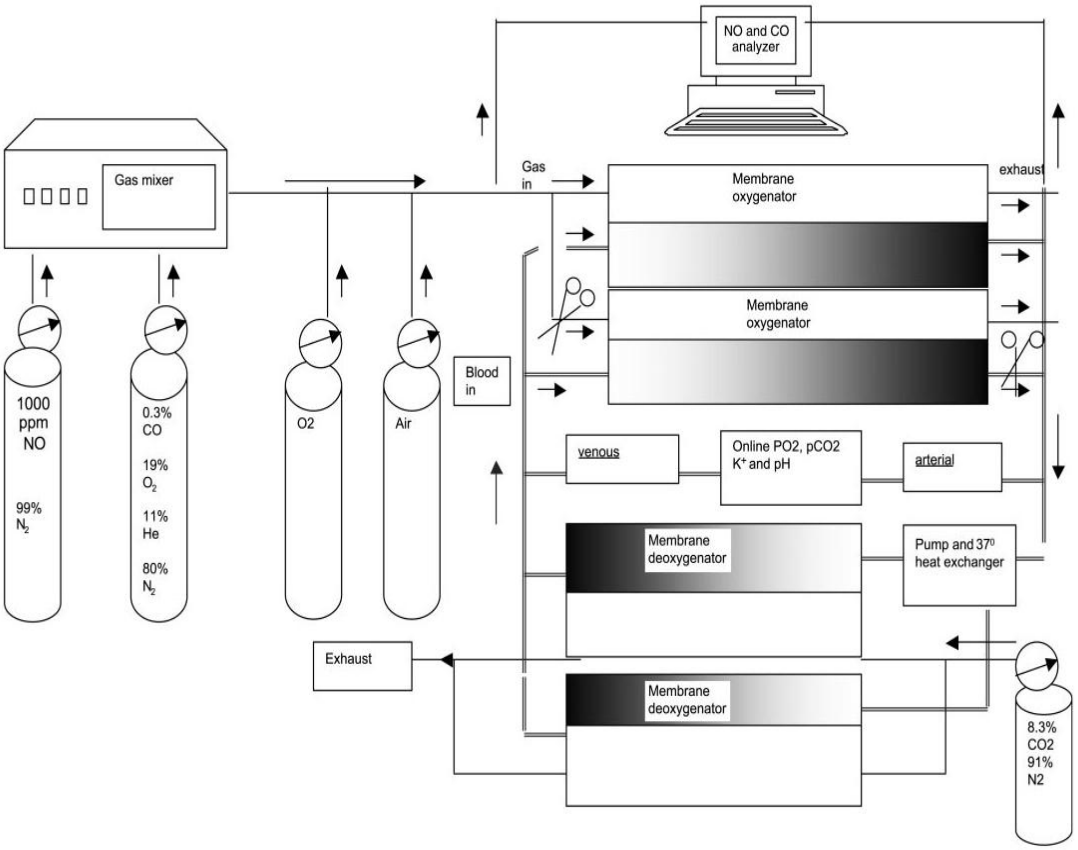

Fig. 1. Circuit for measurement of nitric oxide diffusing capacity (D_{NO}) and carbon monoxide diffusing capacity (D_{CO}) under standard conditions. Closure of the Spencer-Wells forceps allows perfusion and ventilation of the half unit only.

Blood

Commercial horse blood (TCS Biosciences, Buckingham, UK) was used within 28 days of collection. It was adjusted by the manufacturers to a hematocrit of 40–46% by adding and withdrawing serum. It was refrigerated at 4°C before use.

Experimental Protocol

Experiment 1: Varying blood flow, surface area, and Vc. To investigate the effect of varying blood flow, the oxygenator was set up in the usual manner and connected to the gas mixer and analyzers. A gas flow rate of 5 l/min was used. The blood flow rate was set at 0.1, 0.2, 0.5, 1, 1.5, 2, and 2.5 l/min using the variable flow rate on the bypass machine. The membrane surface area and blood channel volume were halved by cross clamping the arterial and venous unions. One estimate was made per blood flow rate for whole and for half units, allowing 5 min between measurements. The order of study was randomized.

Experiment 2: Variable gas flow. The bypass machine was used in the usual manner at a blood flow rate of 2.5 l/min.

The rotameters on the compressed air cylinders were adjusted to give flow rates of 2.5, 5, 7.5, 10, 12.5, and 15 l/min in random order. After 5-min equilibration, diffusing capacity (D) was measured.

Experiment 3: Varying [O_2]. The bypass machine was used in the usual manner and at a blood flow rate of 2.5 l/min and gas flow rate of 5 l/min. The effect of hyperoxia was studied by varying the [O_2] of the gas inlet mixture (Fig. 1). [O_2] of 19, 25, 32, 38, 44, 50, 57, 63, 71, and 84% (measured by oxygen meter on the inlet side) were created by varying the gas flow rate on the rotameters on the O_2 and compressed air cylinder heads. Five-minute equilibration took place between changes in gas concentrations. The blood O_2 tension was measured by the inline probe.

Experiment 4: Effects of altering hemoglobin concentration and inducing hemolysis. To alter hemoglobin concentration from ~1 to 10 g/dl, the circuit was preprimed with normal saline, and blood was progressively added at a rate of 60 ml/min using an additional oxygenator pump for two experimental runs. For a third run, to achieve a range of very low Hb concentration ([Hb]), 25-ml aliquots were added at 5-min intervals by hand to the saline-primed circuit using a plastic syringe. The inline hemoglobinometer gave erroneous results at <6 g/dl, so the hemoglobin was calculated from the concentration in the supplied stock blood, multiplied by the volume of blood added, divided by the system volume. To achieve hemolysis, tap water was pumped into the circuit previously primed with 1.5 liters of blood at a rate of 60 ml/min. Hemolysis was monitored by observation of increasing potassium concentration using the inline monitor.

Experiment 5: Zero blood flow. To investigate the effect of zero blood flow, a static system was used incorporating one-half the Cobe Duo unit. The arterial and venous unions were clamped, and sampling ports were all capped to give a single gas exchange unit, which was primed with 250-ml blood and immersed in a water bath at 37°C. The standard gas mixture (but omitting CO) was passed through the oxygenator at 5 l/min for 35 min, and D_{NO} was estimated each minute.

Experimental Organization

Each of the above experiments was carried out at least twice. No more than one of each type of experiment was performed on a given day. A fresh circuit was used each day, and, if hemolysis had been induced as part of the experiment, the oxygenator was discarded and a fresh one used for any subsequent experiments that day. Temperature was obtained over the course of the experimental day as maximum and minimum mercury thermometer and barometric pressure (P_B) by telephoning the local airforce weather station. Humidity was measured by wet and dry bulb thermometer (Met-check, Milton Keynes, UK) entrained in the gas outlet line emerging from the oxygenator.

Measurement of Back Tension

The NO and CO supplies were abruptly stopped by switching off the gas mixer at the end of a session, and the fall in concentration was observed continuously for a period of 60 s while ventilating the oxygenator with air alone.

Calculations

Consider oxygenator mass balance in a small length dx of volume δV, cross-sectional area S, and gas flow rate f.

Mass balance. Rate of change of mass = mass in − mass out − mass consumed.

$$\delta V \times dC_{NO}/dt = fC_{NO}(x) - fC_{NO}(x + \delta x) - D_{NO}' \times P_B \times C_{NO}(x)$$

where $C_{NO}(x)$ is gas NO concentration at distance x, P_B is barometric pressure less vapor pressure of water, and D_{NO}' is the diffusing capacity of an infinitesimally small length dx/L, i.e., $D_{NO}' = D_{NO}$ dx/L.

Let

$$dC_{NO}/dx = [C_{NO}(x + \delta x) - C_{NO}(dx)]/dx$$

$\delta V = S \times dx$, and L is the total length of the oxygenator, so dividing by dx $S \times dC_{NO}/dt = -f\ dC_{NO}/dx - D_{NO}/L \times P_B \times C_{NO}$.

At steady state, the left-hand side = 0

$$f \times dC_{NO}/dx = -D_{NO}/L \times P_B \times C_{NO}$$

Integrating over length of oxygenator, $Co_{NO} = Ci_{NO} \exp(-D_{NO} \times P_B/f)$, where Ci_{NO} and Co_{NO} are C_{NO} values at the inlet and outlet ports, respectively.

$$D_{NO} = f/P_B \log_e(Ci_{NO}/Co_{NO}) \quad (2)$$

Implicit in this calculation is that the volume of gas emerging from the oxygenator is identical to that entering. This should be the case if blood channel and gas channel O_2 are in equilibrium and using the very low NO and CO gas flows we employed. Likewise, back tension was ignored. Since D_{NO} is expressed in ml STPD·min^{-1}·Torr^{-1}, *Eq. 1* becomes D_{NO} = f × 273/[(273 + laboratory temperature) × (P_B in millibars)/1,000 × 750 − (saturated vapor pressure × relative humidity)/760 × $\log_e$ (Ci_{NO}/Co_{NO}). The equation for CO is identical but substituting Ci_{CO}/Co_{CO}.

If it is presumed that all of the NO or CO that diffuses across the microporous membrane ligands with hemoglobin within the red cell, then it is legitimate to apply the Roughton-Forster relationship [which is, after all, a simple mass-transfer equation (11)] (see APPENDIX for proof).

$$1/D_L = 1/Dm + 1/\theta Vc \quad (3)$$

One exception to this relationship would be if there was chemical reaction with the membrane; this is considered in *Eq. 4* below. Another exception would occur if there was significant uptake of gas physically dissolved in blood; this is addressed in *experiment 1*. Because the Krogh diffusion coefficient for NO (k_{NO}) is twice that for CO (k_{CO}) (16)

$$1/D_{CO} = 1/0.5Dm_{NO} + 1/\theta CO\ Vc \quad (4)$$

where Dm_{NO} is NO Dm. Because there has been concern that NO may react with polypropylene within membrane oxygenators (2), which could occur as it traverses the gaseous pores within the membrane, we have included this as an ohmic resistance in parallel to diffusion, hence

$$\text{Overall } D_{NO} = Dm_{NO\ react} + D_{NO_{diff}} \quad (5)$$

where $Dm_{NO\ react}$ is reaction Dm_{NO} and $D_{NO_{diff}}$ is diffusion D_{NO}. (Hereafter, for clarity we use D_{NO} to mean $D_{NO_{diff}}$, although in the calculations we have subtracted $Dm_{NO\ react}$ from D_{NO} in *Eq. 1*).

Equations 2 and *3* can be combined in various ways to yield different variables:

$$D_{NO}/D_{CO} = (2Vc/Dm_{NO} + 1/\theta CO)/(Vc/Dm_{NO} + 1/\theta NO) \quad (6)$$

$$\theta CO = 1/[Vc(1/D_{CO} - 2/Dm_{NO})] \quad (7)$$

$$\theta NO = 1/[Vc(1/D_{NO} - 1/Dm_{NO})] \quad (8)$$

The specific blood resistance to CO transfer can be written (9, 21) as follows:

$$1/\theta CO = \alpha + \beta(O_2) \quad (9)$$

where α is the specific diffusion resistance for CO per milliliter of blood, and β is the specific reaction resistance per milliliter of blood for CO per Torr average partial pressure of O_2 in blood-carrying channel within oxygenator (Pc_{O_2}).

$$1/D_{CO} = 2/Dm_{NO} + \alpha/Vc + \beta[O_2]/Vc \quad (10)$$

so that, if $1/D_{CO}$ is plotted against $[O_2]$:

$$(\text{intercept} - 2/Dm_{NO}) \times Vc = \alpha$$

and slope × Vc = β. Finally as previously described in reference (6)

$$Dm_{NO} = (\theta NO - 2\theta CO)/(\theta NO/D_{NO} - \theta CO/D_{CO}) \quad (11)$$

$$Vc = 1/(\theta CO/D_{CO} - 2\theta CO/Dm_{NO}) \quad (12)$$

Statistical Analysis

Variables were recorded on a spreadsheet in Microsoft excel and were further analyzed using the linear regression option in SPSS, inserting D or 1/D as the dependent variable and gas flow rate, blood flow rate, Po_2, 1/Hb, and whole or half unit as the independent variables to generate a series of univariate regression models. Where quoted, standard deviations (SD) include within- and between-experiment variation. Independent t-test was used to compare D_{CO} and D_{NO} pre- and posthemolysis.

RESULTS

Analyzer Performance

The time to 90% response of the NO analyzer measured by balloon burst (9) was 5 s for NO and 30 s for CO. The signal-to-noise ratio was ~100 for both inlet NO concentration (Ci_{NO}) and inlet CO concentration (Ci_{CO}), 5 for outlet NO concentration (Co_{NO}), and 6 for outlet CO concentration (Co_{CO}). The CO and NO analyzers were collinear to serial dilution in air (9) over the range of concentrations used.

Comparing Full Unit and Half Unit

Average D_{NO} and D_{CO} using the full unit was D_{NO} = 13.45 ml·min^{-1}·Torr^{-1} (SD 5.84) and D_{CO} = 1.22 ml·min^{-1}·

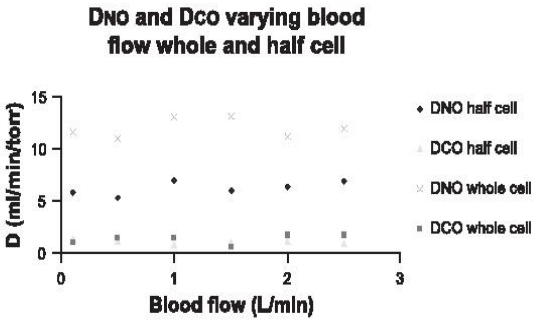

Fig. 2. The relationship between D_{NO}, D_{CO}, and blood flow rate for whole and half unit. Data are shown for a single experiment for clarity. D, diffusing capacity.

$Torr^{-1}$ (SD 0.30). There was a dramatic reduction in D_{NO} ($P = 0.002$) and D_{CO} ($P = 0.002$) when only one-half the unit was perfused with D_{NO} = 7.57 $ml \cdot min^{-1} \cdot Torr^{-1}$ (SD 3.28) and D_{CO} = 0.86 $ml \cdot min^{-1} \cdot Torr^{-1}$ (SD 0.21) (Fig. 2) ($n = 18$). Ratio of D_{NO} to D_{CO} = 10.79 (SD 6.14) (data from three experiments, $n = 18$).

Experiment 1: Variable blood flow. D_{NO} ($P = 0.999$) and D_{CO} ($P = 0.154$) were independent of blood flow over a 25-fold variation (Fig. 2) (data from three experiments, $n = 36$).

Experiment 2: Variable gas flow. Both D_{NO} ($P = 0.01$) and D_{CO} ($P = 0.004$) declined with increasing gas flow rates following a semilogarithmic pattern (Fig. 3) (data from three experiments, $n = 18$).

Experiment 3: Varying O_2. Increasing [O_2] was associated with a linear rise in $1/D_{CO} = 0.0011\ [O_2] + 0.6488$ ($P = 0.009$), but no significant change in D_{NO} ($P = 0.203$) (Fig. 4) (data from two experiments, $n = 21$).

Experiment 4: Varying hemoglobin and hemolysis. There was a significant increase in the uptake of both gases with hemoglobin concentration and more significantly between 1/D and 1/Hb for D_{NO} ($P < 0.001$) and D_{CO} ($P < 0.001$) (data from three experiments, $n = 30$). A significant rise in D_{NO} ($P = 0.001$) but not D_{CO} ($P = 0.928$) occurred with hemolysis (Figs. 5, 6, and 7) (data from four experiments, $n = 10$).

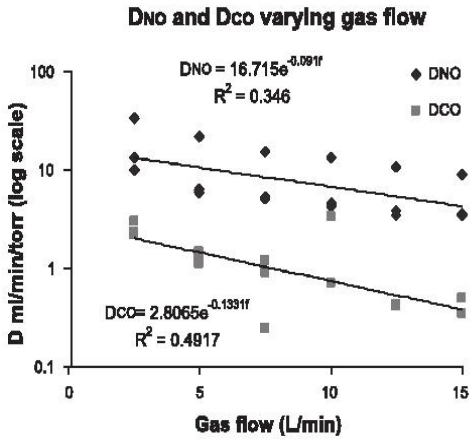

Fig. 3. The relationship between D_{NO}, D_{CO}, and gas flow rate for whole unit. Data shown are for the three experiments combined.

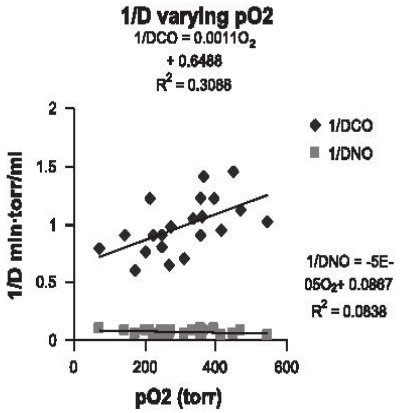

Fig. 4. The relationship between $1/D_{NO}$, $1/D_{CO}$, and P_{O_2} for the whole unit. Data shown are for the two experiments combined.

Experiment 5: Zero blood flow. There was a semilogarithmic decline in D_{NO} with time of exposure to the NO mixture (Fig. 8) with a mean half-life of 26.3 min (SD 1.7) (data from two experiments). From *Eq. 13* (APPENDIX), the uptake of NO was 0.53 ml over the half-time, implying a blood volume saturated with NO of 2.7 ml for the half-unit (5.4 ml for the whole unit).

Back Tension

For NO, there was a rapid decline to 0 ppb (Fig. 9). For CO there was a more gradual decline to 0.04%, which we did not regard as significantly different from the noise (0.03%) (Fig. 10). No back tension adjustment was therefore made to calculations of D for either gas (*Eq. 1*).

Other Variables

The concentration of metHb was <3% and HbCO <7.5% in all experiments. In general, the metHb concentration did not vary, and HbCO increased on average by 0.2% in each exper-

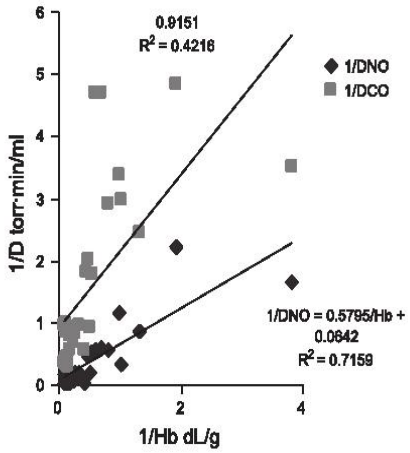

Fig. 5. The relationship between $1/D_{NO}$, $1/D_{CO}$, and 1/hemoglobin (Hb) during addition of whole blood to normal saline in a whole unit. Because our inline hemoglobinometer was unreliable at low Hb concentrations ([Hb]), [Hb] was measured as [Hb] supplied blood × volume of blood added/(volume of blood + priming volume). Data shown are for the three experiments combined.

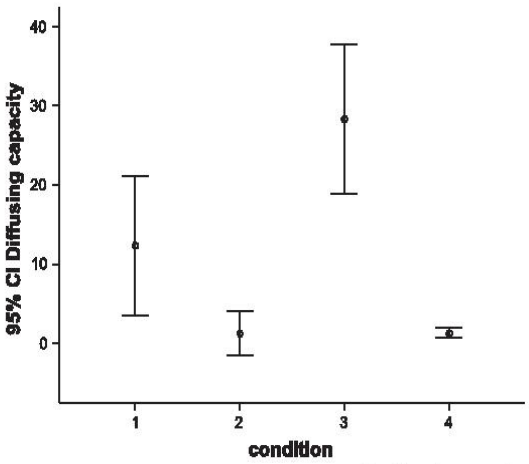

Fig. 6. The effect of hemolysis on D_{NO} and D_{CO}. *Condition 1* is D_{NO}, *2* is D_{CO}, *3* is posthemolysis D_{NO}, and *4* is posthemolysis D_{CO}. Data shown are from four experiments combined. CI, confidence interval.

iment; no consistent association was found between metHb, HbCO, and D. The average inlet [O_2] was 22.1% (SD 4.5), arterial P_{O_2} (Pa_{O_2}) 76.8 Torr (SD 37.6), P_{CO_2} 31.0 Torr (SD 9.22), and pH 7.36 (SD 0.16). The outlet relative humidity was 66%.

DISCUSSION

Main Findings

D_{NO} but not D_{CO} increased significantly following hemolysis: both altered with [Hb], with a significant linear association between 1/D and 1/Hb. These experiments support the argument that diffusion across plasma, the red cell membrane, and within the red cell is a component of D_{NO}. These experiments show that both D_{NO} and D_{CO} appeared to increase with membrane surface area and/or volume and appeared to fall with increasing gas flow rate. D_{CO} but not D_{NO} fell with increasing O_2 tension.

Relationship to the Work of Others

No previous group has measured D_{NO} or D_{CO} using a membrane oxygenator. One group reported values for O_2 diffusing capacity (D_{O_2}) for six hollow-fiber membrane oxygenators, ranging from 2.5 to 5 $ml \cdot min^{-1} \cdot kpA^{-1}$ (0.33–0.66 $ml \cdot min^{-1} \cdot Torr^{-1}$) (28). However, because they calculated $D_{O_2} = M_{O_2}/(PA_{O_2} - Pv_{O_2})$ rather than $D_{O_2} = M_{O_2}/(PA_{O_2} - Pc_{O_2})$, where M_{O_2} is rate of O_2 uptake by oxygenator, PA_{O_2} is partial pressure of O_2 in gas channel, and Pv_{O_2} is partial pressure of O_2 in blood channel entering oxygenator, this is likely to be an underestimate. In support of this view, our preliminary calculations of D_{O_2} using an oxygenator (C. Borland and H. Dunningham, unpublished observations; see APPENDIX for methodology), estimating P_{CO_2} by Bohr integration, give values of 0.2 to 1 $ml \cdot min^{-1} \cdot Torr^{-1}$, depending on blood flow.

No previous group has studied the effect of hemolysis on D_{NO} or D_{CO}, but Geiser and Betticher (15) found increased D_{O_2} when isolated rabbit lungs were perfused with hemoglobin solution compared with whole blood.

D_{NO}/D_{CO}

One striking finding from this work is that the D_{NO}-to-D_{CO} ratio is significantly greater than in vivo, either in animals (22) or humans (3, 4, 6, 16) where it is 4 to 5. Three possible explanations are advanced: hemolysis, a chemical reaction with the membrane, or a different Vc-to-Dm ratio compared with in vivo. It is conceivable that free hemoglobin in stored blood occurring as a result of hemolysis or hemolysis as the blood is recycled through the oxygenator could explain the higher D_{NO}/D_{CO} than we have observed in vivo and the major variation and corresponding increased SD between experiments. However, if that were the case, we might expect greater variation in D_{NO} compared with Dm_{NO}, and that is not apparent (Fig. 6). A rapid chemical reaction accounting for the higher D_{NO}/D_{CO} than observed in vivo is a less likely explanation. Minimal reaction was observed with the membrane oxygenator or tap water under zero-flow circumstances. Applying the Roughton-Forster model, it can be seen from *Eqs. 2* and *3* that D_{NO}/D_{CO} would vary from 2, if θNO and θCO were infinite, to a maximal value of $\theta NO/\theta CO$, if Dm were infinite. The ratio of 10.8 observed must, therefore, be regarded as the lower limit for $\theta NO/\theta CO$ under our experimental conditions. From *Eq. 5*, it can be seen how D_{NO}/D_{CO} crucially depends on the ratio Vc/Dm_{NO} for given values of θNO and θCO. In the oxygenator, in contrast to in vivo, θNO Vc might appear to limit D_{NO} to a greater degree than Dm. We believe that a reduced Vc/Dm_{NO} in the oxygenator compared with in vivo is the explanation of the increased D_{NO}/D_{CO} observed, and the calculations in *Values for θCO and θNO* and *The Physiological Significance* support this.

Factors Affecting D_{NO} and D_{CO}

Blood flow rate. The lack of effect of blood flow rate on D_{NO} and D_{CO} is not unexpected; since NO and CO are relatively water insoluble and of high D, they will be diffusion limited compared with soluble gases, such as acetylene and O_2 in normoxia, which are regarded as perfusion limited (24). We have not yet studied soluble gases in this setup, but our preliminary unpublished studies of D_{O_2} in normoxia show an increase with blood flow up to a plateau (C. Borland and H. Dunningham, unpublished observations). From this experiment, it is likely that the increases in D_{NO} and D_{CO} that have been observed on exercise in vivo (3, 4, 20) are due to increases in Dm and Vc rather than $\beta\dot{Q}$.

Half and whole unit. The approximate halving of D_{NO} and D_{CO} when half the unit is clamped off could be because the surface area or the volume is halved. The arguments of the second paragraph of this discussion relating to Vc/Dm strongly favor this reduction being due to change in blood volume rather than surface area. Normally, in vivo Dm and Vc will vary together (Hughes' "coupling") (21); for example, considering a pulmonary capillary to be a cylinder if its diameter increases, the increase in surface area and hence Dm will be proportionate to the square of the diameter and the volume proportional to the cube. Using an oxygenator with greatly increased Dm/Vc has "uncoupled" Dm and Vc so that the blood phase can effectively be examined in isolation.

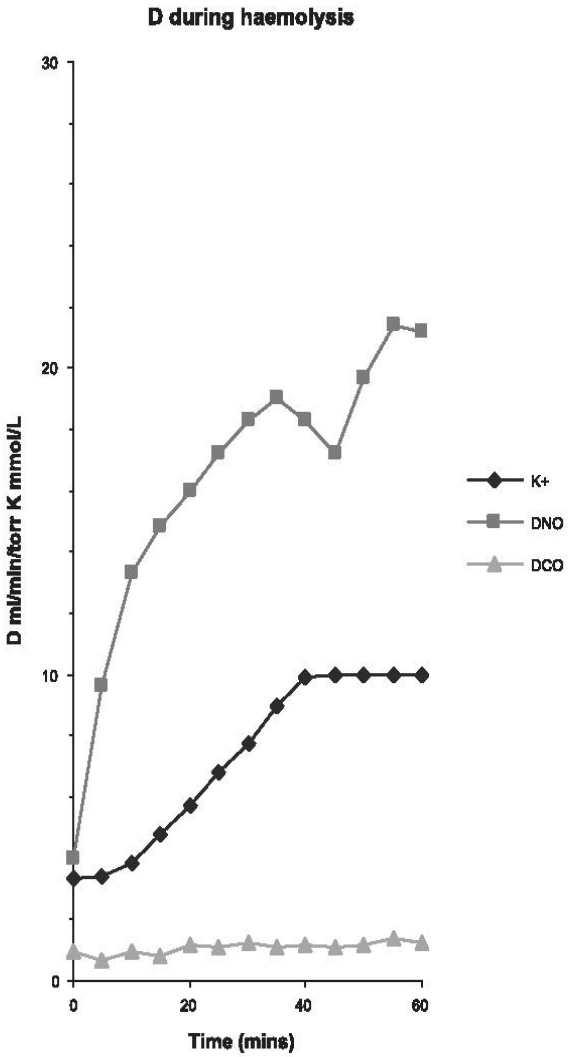

Fig. 7. The effect of hemolysis on D_{NO}, D_{CO}, and K^+ in a single experiment. The upper limit of detection of K^+ for the inline analyzer is 10 mmol/l.

Varying gas flow rate. From Fig. 3, there appears to be a decline in D_{NO} and D_{CO} with increasing gas flow rate. At any one point in the gas channel in the oxygenator, D_{NO}/f will, from *Eq. 1*, equal $1/P_B \log_e (C_{INO}/C_{ONO})$, where C_{INO} is the C_{NO} of fresh gas arriving at that point, and C_{ONO} the C_{NO} leaving. The magnitude of $1/P_B \log_e (C_{INO}/C_{ONO})$ will depend on the balance of bulk flow and diffusion. At high flow rates, the rate of arrival of fresh gas will be substantially greater than its removal by diffusion, and C_{ONO} will approximate C_{INO}, and D_{NO} will approach zero. At low-flow rates, diffusion will predominate, and C_{ONO} will approach zero. This caused us some pragmatic difficulties: if we employed too rapid flow rates, we could not obtain a detectable D_{CO}, but at too low flow rates C_{ONO} approached the lower detectable limit (30 ppb) of the analyzer on therapeutic mode. Using higher NO or CO concentrations raised metHb and HbCO blood concentrations unacceptably. A compromise of 5 ppm NO and 0.02% CO at a rate of 5 l/min was employed, but it is plausible that the true value for D_{NO} is the intercept of Fig. 3. A significant contribution of bulk flow of dry gas almost certainly explains why the humidity is <100%. Variation in gas flow rate and the essential need for accurately knowing the flow rate has a major impact on the measured and derived variables.

O_2 tension. For D_{CO}, altering O_2 tension and thereby the reaction rate with oxyhemoglobin had a major effect, indeed second only to gas flow on D_{CO}. For NO, the effect was negligible, as expected from its extremely rapid reaction with hemoglobin and from experiments in vivo (6). The reaction dependence of CO on O_2 is predicted from:

$$d[HbCO]/dt = m'c[CO][HbO_2]/[O_2] \qquad (13)$$

where $m'c$ is the third-order velocity constant, and [HbCO], [CO], $[HbO_2]$, and $[O_2]$ are the blood concentrations of HbCO, CO, oxyhemoglobin, and O_2, respectively (26, 27). From the slopes and intercepts of the relationship between

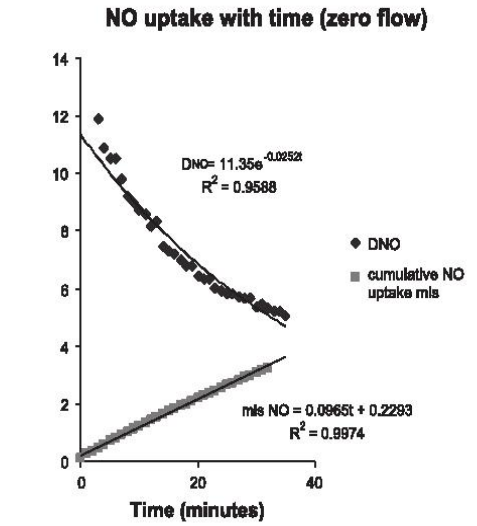

Fig. 8. Fall in D_{NO} with time (half unit). Data are shown for a single experiment for clarity.

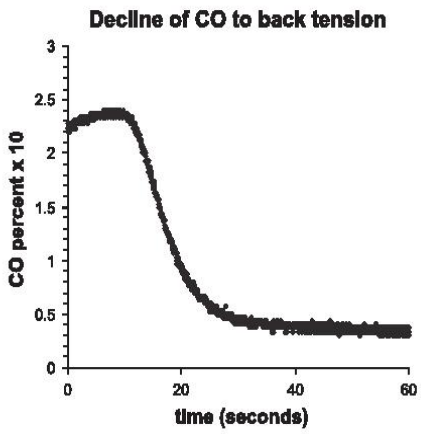

Fig. 10. Back tension for CO (single experiment).

1/D_{CO} and P_{O_2}, α and β are calculated (*Eq. 9*) in *Values for θCO and θNO*.

The Red Cell

Hemoglobin concentration. The limitation of D_{NO} and D_{CO} by hemoglobin concentration and the significant relationships between 1/D and 1/Hb for both gases lend support to applying the Roughton-Forster relationship to the oxygenator and to θNO being less than infinity. However, it must be acknowledged that the highly significant relationships we have demonstrated are over a unphysiological range, which is also largely outside clinical practice (0.26–9.73 g/dl) (Fig. 5).

Red cell integrity. There is a major effect of hemolysis on D_{NO} but not D_{CO}. The major effect of hemolysis, like the effect of altering [Hb] on D_{NO}, lends support to those who believe θNO is finite rather than equivalent to the effectively infinite rate with oxyhemoglobin solution. The posthemolysis figure should, given the extremely rapid reaction of NO with oxyhemoglobin, be a measure of Dm_{NO} alone. The difference between the pre- and posthemolysis figures will reflect the contribution of membrane immediately adjacent to red cell (20), plasma, and red cell interior to diffusion, and it is not possible to distinguish between them from this part of the experiment. For D_{CO}, however, the diffusion resistance of membrane, plasma, and within the erythrocyte appears negligible in contrast to the classic observations of Roughton et al. (26) using a continuous flow rapid reaction apparatus. It is difficult to reconcile this difference; in support of our findings, Reeves and Park (25) obtained a low-diffusion resistance for the red cell-to-CO transfer using a thin-film technique, and Chakraborty et al. (8) have advanced strong theoretical arguments for rapid reaction apparatuses, creating stagnant layers, leading to underprediction of θCO. It is plausible that highly turbulent mixing conditions due to the mesh spacers within the blood channel of the oxygenator (14, 29) within an oxygenator reduce the stagnant layer effect. In support of this view, we have found no effect of hemolysis or hematocrit on D_{O_2} (C. Borland and H. Dunningham, unpublished observations).

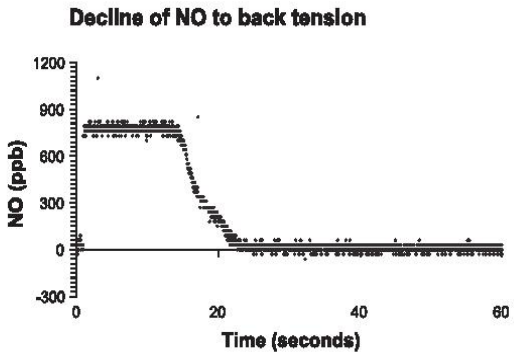

Fig. 9. Back tension for NO (single experiment). ppb, Parts per billion.

Limitation of D_{NO} at Zero Flow

With zero blood flow, there is a semilogarithmic decline in D_{NO} with time. What is limiting D_{NO} during this time? It cannot be perfusion limitation in the classic sense, as the blood is not physically or chemically saturated with NO (free oxyhemoglobin is still available, as demonstrated by a sample aspirated close to the membrane that showed an oxyhemoglobin content of 97.5%). For the same reason, it cannot be reaction limitation, given the extremely rapid reaction of oxyhemoglobin with NO. We believe that the observed decline is due to diffusion limitation: as the surface molecules of oxyhemoglobin become irreversibly oxidized to metHb, then the path length for NO diffusion within the erythrocyte steadily increases. If this explanation is correct, then Fig. 8 is a visual depiction of Hill's "advancing front" (21).

Is There Heterogeneity?

From the above, it would be anticipated that both D_{NO} and D_{CO} would be altered by heterogeneity of gas flow, membrane surface area, accessible blood volume, and hematocrit within and between gas and blood channels. Both should be independent of varying blood flow between blood channels. D_{CO} could

be altered by differing P_{O_2} between channels. It is certainly plausible that the decrease in D with gas flow is greater in some channels than others. Provided both units are completely filled with blood and because they are semitransparent, this appeared to be so, thus Dm and Vc heterogeneity are unlikely, although heterogeneity of D_{CO} could explain the 30% fall in D_{CO} compared with the 44% fall in D_{NO}. From the equation, it will be noted that D_{NO}/D_{CO} crucially depends on Vc/Dm. A greater fall in Dm than Vc when one-half the unit is clamped off would lead to a greater fall in D_{NO} than D_{CO}. Heterogeneity of Dm, Vc, and hematocrit may well occur in *experiment 4* due to uneven filling of the chambers, where blood is gradually added to the circuit preprimed with saline. Heterogeneity within blood channels should also be considered due to stagnant layers effect. As indicated above, such layers would instantly be abolished by hemolysis, and their existence might contribute to the increase in D_{NO} with hemolysis. However, as already mentioned, one would anticipate that a change in D_{CO} might also be seen with hemolysis, if there were stagnant layers.

Contribution of the Resistances to NO and CO Transfer

The reciprocal of our average D_{NO} value 1/13.45 = 0.074 $min \cdot Torr^{-1} \cdot ml^{-1}$ is the overall resistance to NO transfer. $1/Dm_{NO}$ = 0.024 $min \cdot Torr^{-1} \cdot ml^{-1}$ is the membrane resistance. In theory, the difference = 0.05 $min \cdot Torr^{-1} \cdot ml^{-1}$ is due to the resistance of the plasma and red cell membrane and interior. However, it may include some membrane resistance, if only the membrane directly adjacent to a red cell is available for gas transfer (20). Another expression of the membrane resistance is the intercept of Fig. 5. The value for $1/D_{NO}$ when 1/Hb is zero, i.e., infinite hemoglobin concentration. This value (=0.064 $min \cdot Torr^{-1} \cdot ml^{-1}$) is twice the posthemolysis value. The resistance of the plasma may account for some of this difference; however, some plasma resistance may be hematocrit dependent, since, as the number of red cells falls, the distance between them and hence the plasma resistance rises. For CO, the picture is more complex: the intercept of $1/D_{CO}$ and 1/Hb is 0.92 $min \cdot Torr^{-1} \cdot ml^{-1}$, which is substantially greater than 2 × 0.024 = 0.05 $min \cdot Torr^{-1} \cdot ml^{-1}$ predicted from the posthemolysis value for D_{NO} and more than twice the intercept for $1/D_{NO}$ (2 × 0.064 = 0.13 $min \cdot Torr^{-1} \cdot ml^{-1}$). Another expression of the membrane resistance for D_{CO} is the intercept of $1/D_{CO}$ and $[P_{O_2}]$ = 0.65 $min \cdot Torr^{-1} \cdot ml^{-1}$. The only explanation for these greater values for $1/D_{CO}$ is that they contain terms for the reaction resistance to CO transfer. At infinite Hb, *Eq. 12* does not become infinity but pseudo-second-order proportional to $[CO]/[O_2]$. Likewise, at zero P_{O_2}, *Eq. 12* becomes pseudo-second-order proportional to [CO][Hb]. If the intercept of $1/D_{CO}$ and $[P_{O_2}]$ contains a term for the reaction resistance, then CO diffusing capacity of membrane (Dm_{CO}) will always be underestimated by Roughton and Forster's method using two or more O_2 tensions.

Value for Vc. Unfortunately, it is very difficult to accurately estimate the volume of blood in contact with the membrane available for NO and CO uptake. Clearly, it will be considerably less than the priming volume of 460 ml using the oxygenator conventionally or 250 ml for the zero-flow experiments. Two approaches are outlined in the APPENDIX. It is also possible to draw up an estimate of Vc using our data and measures of θCO and θNO (Table 1) using *Eqs. 2* and *11*. It is clear that methods based on D_{NO}/D_{CO} give the lowest values for Vc followed by D_{CO} at more than one O_2 tension, but that even these estimates are lower then the likely true Vc value of the oxygenator. Using the estimate for Vc based on the half-life of D_{NO} under zero perfusion conditions assumes that Vc is the same, irrespective of perfusion rate. Using the estimate based on a boundary layer of 10 μm (17) assumes, almost certainly incorrectly, that NO and CO exchange with the same volume of blood as O_2 and CO_2. It is likely that low concentrations of these two diffusion-limited gases barely penetrate the outer layer of blood, whereas O_2 will fully saturate it, particularly if intraerythrocytic gas transport is aided by facilitated diffusion. This consideration has not been emphasized when extrapolating in vitro estimates of θ, which are generally made using gas concentrations substantially in excess of in vivo experiments. Whether the same situation holds in vivo requires further study. The Roughton-Forster model assumes even distribution of gas throughout the plasma and red cells.

Values for Dm

It seems reasonable to use one-half the posthemolysis value for D_{NO} for the whole unit = 41/2 = 20.5 $ml \cdot min^{-1} \cdot Torr^{-1}$ as the "gold standard" value for Dm_{CO}. From Table 1, it is clear that the negative values for Dm using Forster's estimate for θCO from 1987 and Borland and Cox's method imply overestimation of Dm. By contrast, using D_{CO} at more than one

Table 1. *Values for specific conductance of blood and derived variables*

α, $min \cdot Torr^{-1} \cdot ml^{-1}$	β, min/ml	θCO at 67.5 Torr*	Dm_{CO}‡	Vc†	Reference
0.7	0.0061	0.77*	1.34	7.6	Roughton et al. (26)
1.08	0.0065	0.49*	1.5	8.1	Holland (19)
1.30	0.0041	0.47*	2.00	5.1	Forster (13)
0.0156	0.008	1.36*	1.18	10	Reeves and Park (25)
		θNO			
0.7	0.0061	∞	6.73	1.94	Guenard et al. (16)
1.30	0.0041	3.26*	−16.24	2.41	Borland and Cox (6)
			20.5		Posthemolysis value of $D_{NO}/2$ × 2
				5.8	From semilogarithmic decline in D_{NO}
				13	From literature (17)

α, Specific diffusion resistance of blood per milliliter for carbon monoxide (CO); β, specific reaction resistance of blood per milliliter per Torr P_{O_2} for CO; θCO, specific transfer conductance of blood per milliliter for CO; Dm_{CO}, CO membrane diffusing capacity; Vc, pulmonary capillary blood volume; θNO, specific transfer conductance of blood per milliliter for nitric oxide (NO); Dm, diffusing capacity of oxygenator membrane; D_{NO}, NO diffusing capacity. *Corrected for average Hb of 11.3 g/dl, carboxyhemoglobin 1.5%, and methemoglobin 3.8%. †Vc = β/0.0011 (where 0.0011 = slope of Fig. 4). ‡Dm = 1/(0.6488 − α/Vc, where 0.6488 = intercept of Fig. 4).

[O_2] tends to underestimate Dm_{CO}. Guenard's method of estimating Dm_{CO} as 0.5 D_{NO} appears to give the closest measure to presumed Dm_{CO} but remains an underestimate.

Values for θCO and θNO

It is theoretically possible to calculate θCO, θNO, α, and β using *Eqs. 6–9*. From Table 1, we can very empirically take a median figure of ~5 ml for the whole unit for the blood volume that actually exchanges with CO and NO using *Eqs. 2* and *3*: θCO Vc = 1/(1/1.22 − 2/41) = 1.3 ml·min^{-1}·Torr^{-1} (where 1.22 is the overall average for D_{CO} and 41 is the posthemolysis value for $D_{NO} = Dm_{NO}$); θNO Vc = 1/(1/13.45 − 1/41) = 20 ml·min^{-1}·Torr^{-1} (where 13.45 is the overall average for D_{NO} and 41 is the posthemolysis value for $D_{NO} = Dm_{NO}$). This gives values for θCO (67.5 Torr) = 0.26 ml·min^{-1}·Torr^{-1}, θNO = 4 ml·min^{-1}·Torr^{-1}, α = 3 min/Torr, and β = 0.0055 min. Despite the many assumptions, these figures are reassuringly close to those obtained by others using rapid reaction apparatus and thin-layer techniques. Although we did not specifically examine this issue, it would be anticipated that θNO and θCO would be independent of flow rate, given that D_{NO} and D_{CO} are completely independent of flow rate.

Implications

We believe that this model allows testing of factors that affect NO and CO exchange in a way that would be impossible in vivo or in an isolated lung preparation. It would be impossible, for example, to generate [Hb] of <1 g/dl in an intact animal without also altering blood volume, cardiac output, and hence Vc and Dm. Likewise, hemolysis or infusion of hemoglobin solutions would irreparably damage the circulation. Nonetheless, the oxygenator is a reasonable model of lung gas exchange, and it is reassuring that values for θCO and θNO obtained half a century ago under unphysiological conditions in a rapid reaction apparatus appear to apply. However, given all of the above limitations, our laboratory's previous recommendations (3) to calculate Dm and Vc from simultaneous D_{NO} and D_{CO}, both assuming θNO is infinity and assuming it is 4.5 min^{-1}·Torr^{-1}, must remain.

The Physiological Significance

Structurally, there is no doubt that the oxygenator is very different from the lung. The polypropylene membrane is thicker but is interrupted by frequent pores, giving a direct air-liquid interface. The total area is smaller (1.3–2.6 m^2 compared with, say, 50–100 m^2 for the lung). There is probably a greater transverse and longitudinal blood path length. The transit time is ~10-fold greater for the half unit and 20-fold greater for the whole unit. The gas flow is not tidal but constant in the oxygenator; likewise, the blood flow is not pulsatile but constant. The journey taken by a red cell in the lung is of progressive oxygenation as it passes along the capillary; in an oxygenator, the balance between turbulent flow (29) and a growing boundary layer (17) may result in red cells moving between areas of low and high O_2 tension in a random fashion. Functionally, the oxygenator is very much more like the lung. It delivers up to 400 ml/min of O_2 and removes up to 450 ml/min of CO_2 at physiological pH, temperature, hematocrit, and O_2 and CO_2 tensions by diffusion down partial pressure gradients. Importantly for NO and CO transfer, we have shown (APPENDIX) that the classic Roughton-Forster equation is applicable to the oxygenator. The value for D_{NO} in a healthy adult is 125 ml·min^{-1}·Torr^{-1}, and we calculate Dm_{NO} to be 300 ml·min^{-1}·Torr^{-1}. These values are, therefore, ~9-fold and 7.5-fold greater, respectively, perhaps implying that the oxygenator "membrane", while 20- to 40-fold smaller in area, is functionally thinner than the alveolar-capillary membrane. Our result for D_{NO} and D_{CO} and O_2 (*experiment 3*) is entirely expected and identical to what is found in humans. Likewise, the major effect of surface area/volume on D_{NO} and D_{CO} transfer and lack of effect of blood flow is what is entirely predicted but never before directly demonstrated. The effect of gas flow is probably specific to an oxygenator, since lung gas flow is very different. The effect of hemoglobin on D_{CO} is similar to D_{CO} and Hb in humans. For Hb and D_{NO} in the oxygenator, there is undoubtedly a marked effect. Since hemolysis of this degree would be fatal to humans or animals and deleterious to an isolated lung, it is not physiological. Could the effect of hematocrit and hemolysis and D_{NO} occur in the oxygenator but not in vivo? This could occur if there were a significant stagnant plasma layer in the oxygenator that would increase the diffusion resistance of the blood (14). Another possibility would be if there were significant facilitated diffusion due to convective transport within the red cell in vivo but not the oxygenator (8): this would increase the blood resistance to NO transfer in the oxygenator. Were either of these to be the case, we might expect hemolysis to increase D_{CO} and not just D_{NO}. We should concede that, because of its far faster reaction with hemoglobin, a reduction in blood resistance would have greater impact on NO than CO. However, we have also found D_{O_2} to be independent of hemolysis (C. Borland and H. Dunningham, unpublished observations), and the reaction rates of O_2 and NO with hemoglobin are comparable (8).

Limitations

Clearly, our results were obtained with horse blood, whereas the major interest is human blood. Our calculated values need to be interpreted with some caution, given the sensitivity of D_{NO} and D_{CO} to gas flow rate. Both the D_{CO} and, in particular, D_{NO} values are highly variable between experiments due perhaps to gas flow variation, the low signal-to-noise ratio, and, in the case of D_{NO}, hemolysed blood in the stock solution. Other sources of variation could be between oxygenator variability and metHb and HbCO, which rise during the course of the experiment. Unfortunately, we have no information on effective membrane thickness, blood path width, or length for the Cobe Duo. We do not have details of laminar or turbulent flow for our device for differing blood and gas flows. Clearly, the relationship of D_{NO} and Hb is not only of theoretical interest, but also of concern to clinical physiologists wishing to know whether it is necessary to adjust D_{NO} for Hb. Given that many of our observations were made outside a clinical range and without a low-reading hemoglobinometer, we cannot advocate such an adjustment derived from our regression equation at present.

Directions for Future Work

If the value of the oxygenator volume could be accurately determined, this work suggests that, for the first time, θCO and θNO could be measured under physiological conditions using

an "off-the-shelf" commercial oxygenator and gas mixtures and analyzers that are part of the equipment of many modern respiratory laboratories. We hope that others will be stimulated to test our conclusions. It would be possible to adapt the apparatus to measure D_{O_2} and hence perhaps D_{CO_2} also.

APPENDIX

Oxygenator Blood Volume

The accessible volume of the oxygenator can be calculated in two ways.

1) The static boundary layer of blood in oxygenators where diffusion takes place is regarded as 10 μm (10^{-3} cm) thick for O_2 and CO_2 (17). The surface area of a single cell of the Cobe Duo is 1.3 m^2 = 1.3×10^4 cm^2. Therefore, the accessible volume of each cell is 13 ml.

2) There is a semilogarithmic decline in D_{NO} with time. Let the half time for this decline be $t_{1/2}$. Let total volume NO transferred between t_0 and $t_{1/2}$ = f $t_0 \int t_{1/2}$ ($C_{I_{NO}} - C_{O_{NO}}$) dt. Because NO ligands to Hb in exactly the same proportion as O_2, the volume of blood saturated with

$$NO = 5 \times f\, t_0 \int t_{1/2}(C_{I_{NO}} - C_{O_{NO}})dt \qquad (14)$$

(The accessible volume is likely to be less than this figure.)

Proof of Application of Roughton-Forster Relationship to NO (and CO) Transfer in a Membrane Oxygenator

Ignoring any reaction with the membrane or NO dissolved in plasma, a balance exists between the mass of NO diffusing from the air channel across the membrane and that reacting with Hb/HbO_2 within the red cell, i.e.

$$S' K_{M_{NO}}/T_m(P_{A_{NO}} - P_{C_{NO}})dl/dt = \theta NO\ P_{C_{NO}} a_c dl/dt\ ml \qquad (15)$$

This equation is entirely analogous to *Eq. 9* in Ref. 27, excepting that we have applied it to NO as well as CO, and the notation has been updated (the original Roughton and Forster symbols are in parentheses): S' (S) is the surface area of a single blood channel per unit length (cm), $P_{A_{NO}}$ ($P_{A_{CO}}$) is the instantaneous NO partial pressure in the gas channel (Torr), $K_{M_{NO}}$ (d) is the membrane permeation coefficient for NO ($cm^2 \cdot min^{-1} \cdot Torr^{-1}$), τ_m (x) is membrane thickness (cm), $P_{C_{NO}}$ (Pco) is instantaneous plasma NO partial pressure (Torr), and a_c (a) is cross-sectional area of a single blood channel (cm^2).

Rearranging the equation in parentheses

$$P_{c_{NO}} = P_{A_{NO}}(1 + \theta NO a_c \tau_m / S' K_{M_{NO}})$$

Integrating the equation in parentheses over n blood channels and total length L on the left-hand side becomes:

$$n S' K_{M_{NO}}/\tau_m \int_0^L [(P_{A_{NO}} - P_{C_{NO}})dl]dt$$

Substituting for $P_{C_{NO}}$ gives:

$$n L S' K_{M_{NO}}/\tau_m\, P_{A_{NO}}[1 - 1/(1 + \theta NO a_c \tau_m / S' K_{M_{NO}})]dt$$

But $n\ LS' = A_m$ (A) the membrane surface area (cm^2), $Dm_{NO} = A_m K_{M_{NO}}/\tau_m$, and $Vc = a_c\ n\ L$. The left-hand side of the part of the equation in parentheses = $Dm_{NO}\ P_{A_{NO}}\ dt\ (1 + Dm_{NO}/\theta NO\ Vc)$ and is also = $D_{NO}\ P_{A_{NO}}\ dt$. Dividing through by $P_{A_{NO}}\ dt$ and rearranging:

$$1/D_{NO} = 1/Dm_{NO} + 1/\theta NO\ Vc$$

Identical arguments apply to D_{CO}.

Calculation of D_{O_2}

D_{O_2} was measured from gas inlet and outlet [O_2] and blood inlet and outlet gas tensions. $D_{O_2} = M_{O_2}/(P_{A_{O_2}} - P_{C_{O_2}})$, where $P_{A_{O_2}}$ is the logarithmic mean of the inlet and outlet O_2 gas tensions, and $P_{C_{O_2}}$ is the average blood channel O_2 tension calculated by Bohr integration from the inlet to outlet blood gas tensions (9). Similar values were obtained from the simpler calculation $D_{O_2} = M_{O_2}/(P_{A_{O_2}} - P_{V_{O_2}}) \times \log_e [(P_{A_{O_2}} - P_{V_{O_2}})/(P_{A_{O_2}} - P_{a_{O_2}})]$, where $P_{a_{O_2}}$ is the blood outlet O_2 gas tension (24).

ACKNOWLEDGMENTS

We are grateful to Professor J. M. B. Hughes and Dr. N. M. Tsoukias for helpful comments and to Drs. Sonia Misso and Jim Chandler for help with the initial experiments.

REFERENCES

1. **Bidani A, Tao W, and Zwischenberger JB.** Testing and performance evaluation of artificial lungs. In: *The Artificial Lung*, edited by Vaslef SN and Anderson RW Georgetown, TX: Landes Bioscience, 2002.
2. **Body SC, Fitzgerald D, Voorhees C, Hansen E, Crowley C, Voorhees ME, and Shernan SK.** Effect of nitric oxide upon gas transfer and structural integrity of a polypropylene membrane oxygenator. *ASAIO J* 45: 550–554, 1999.
3. **Borland C, Mist B, Zammit M, and Vuylsteke A.** Steady-state measurement of NO and CO lung diffusing capacity on moderate exercise in men. *J Appl Physiol* 90: 538–544, 2001.
4. **Borland CDR and Higenbottam TW.** A simultaneous single breath measurement of pulmonary diffusing capacity with nitric oxide and carbon monoxide. *Eur Respir J* 2: 56–63, 1989.
5. **Borland C.** NO and CO transfer. *Eur Respir J* 3: 977–978, 1990.
6. **Borland CDR and Cox Y.** Effect of varying alveolar oxygen partial pressure on diffusing capacity for nitric oxide and carbon monoxide, membrane diffusing capacity and lung capillary blood volume. *Clin Sci (Lond)* 81: 759–765, 1991.
7. **Carlsen E and Comroe JH.** The rate of uptake of nitric monoxide by normal erythrocytes and experimentally produced spherocytes. *J Gen Physiol* 42: 83–107, 1958.
8. **Chakraborty S, Balakotaiah V, and Bidani A.** Diffusing capacity reexamined: relative roles of diffusion and chemical reaction in red cell uptake of O_2, CO, CO_2, and NO. *J Appl Physiol* 97: 2284–2302, 2004.
9. **Cotes JE.** *Lung Function: Assessment and Application in Medicine.* Oxford, UK: Blackwell Scientific, 1993, p. 297–301.
10. **Cotes JE, Dabbs JM, Elwood PC, Hall AM, McDonald A, and Saunders MJ.** Iron deficiency anaemia: its effect on transfer of the lung (diffusing capacity) and ventilation and cardiac frequency during submaximal exercise. *Clin Sci* 42: 325–335, 1972.
11. **Coulson JM and Richardson JF.** Mass transfer. In: *Coulson and Richardson's Chemical Engineering. Fluid Flow, Heat Transfer, and Mass Transfer* (6th ed.). Amsterdam: Elsevier, 1999, vol I. chapt. 10.
12. **Doyle MP and Hoekstra JW.** Oxidation of nitrogen oxides by bound dioxygen in haemoproteins. *J Inorg Biochem* 14: 351–358, 1981.
13. **Forster RE.** Diffusion of gases across the alveolar membrane. In: *Handbook of Physiology. The Respiratory System. Gas Exchange.* Bethesda, MD: Am. Physiol. Soc., 1987, sect. 3, vol. IV, chapt. 5, p. 71–88.
14. **Gaylor JDS, Hickey S, Bell G, and Pei JM.** Membrane oxygenators: influence of design on performance. *Perfusion* 9: 173–180, 1994.
15. **Geiser J and Betticher DG.** Gas transfer in isolated lungs perfused with red cell suspension or haemoglobin solution. *Respir Physiol* 77: 31–40, 1989.
16. **Guenard H, Varene N, and Vaida P.** Determination of lung capillary blood volume and membrane diffusing capacity in man by the measurements of NO and CO transfer. *Respir Physiol* 70: 113–120, 1987.
17. **Hattler BG and Federspiel WJ.** Gas exchange in the venous system. In: *The Artificial Lung*, edited by Vaslef SN and Anderson RW. Georgetown, TX: Landes Bioscience, 2002.
18. **Heller H and Schuster KD.** Role of reaction resistance in limiting carbon monoxide uptake in rabbit lungs. *J Appl Physiol* 84: 2066–2069, 1998.
19. **Holland RAB.** Rate at which CO replaces O_2 from oxyhaemoglobin in red cells of different species. *Respir Physiol* 7: 43–63, 1969.
20. **Hsia CCW.** Recruitment of lung diffusing capacity: update of concept and application. *Chest* 122: 1774–1783, 2002.

21. **Hughes JM and Bates DV.** Historical review: the carbon monoxide diffusing capacity (DLCO) and its membrane component (DM) and red cell (Θ.Vc) components. *Respir Physiol Neurobiol* 138: 115–142, 2003.
22. **Meyer M, Schuster KD, Schulz H, Mohr M, and Piiper J.** Pulmonary diffusing capacities for nitric oxide and carbon monoxide determined by rebreathing in dogs. *J Appl Physiol* 68: 2344–2357, 1990.
23. **Moinard J and Guenard H.** Membrane diffusion of the lungs in patients with chronic renal failure. *Eur Respir J* 6: 225–230, 1999.
24. **Piiper J and Scheid P.** Blood-gas equilibration in lungs. In: *Pulmonary Gas Exchange Ventilation, Blood Flow And Diffusion*, edited by West JB. New York: Academic, 1980.
25. **Reeves RB and Park HK.** CO uptake kinetics of red cells and carbon monoxide diffusing capacity. *Respir Physiol* 88: 1–21, 1992.
26. **Roughton FJW, Forster RE, and Cander L.** Rate at which carbon monoxide replaces oxygen from combination with human hemoglobin in solution and in the red cell. *J Appl Physiol* 11: 269–276, 1957.
27. **Roughton FJW and Forster RE.** Relative importance of diffusion and chemical reaction in determining the rate of exchange of gases in the human lung. *J Appl Physiol* 11: 290–302, 1957.
28. **Visser C and de Jong DS.** Clinical evaluation of six hollow-fibre membrane oxygenators. *Perfusion* 12: 357–368, 1997.
29. **Wegner JA.** Oxygenator anatomy, and function. *J Cardiothorac Vasc Anesth* 11: 275–281, 1997.

APPENDIX 5

Borland CDR, Dunningham H, Bottrill F, Vuylsteke A. Can a Membrane Oxygenator be a Model for Lung Oxygen and Carbon Dioxide Transfer? ATS 2007, San Francisco.

We have previously developed a membrane oxygenator model to study lung nitric oxide and carbon monoxide gas exchange (Borland C, Dunningham H, Bottrill F and Vuylsteke A J Appl Physiol 2006;100:1527-1538.)To investigate a membrane oxygenator as a model of oxygen and carbon dioxide gas exchange two oxygenators were connected to form a circuit continuously perfused with horse blood at a flow of 2.5 L min^{-1}. The "lung" oxygenator was ventilated by 28% oxygen with the remainder nitrogen and the "tissue" deoxygenator by 7% carbon dioxide in nitrogen to achieve normoxia and normocapnoea. The oxygen diffusing capacity measured by modified Bohr's integration was 1.87 ml min^{-1} $torr^{-1}$ and carbon dioxide diffusing capacity was 19.3 ml min^{-1} $torr^{-1}$.DO_2 and DCO_2 were minimally affected by haemoglobin concentration, haemolysis, surface area or blood volume.DO_2 increased in hypoxia whereas DCO_2 was only affected by the addition of carbonic anhydrase.DCO_2 was unaffected by blood flow whereas DO_2 increased to a plateau. By applying Cotes and Meade's extension of Roughton and Forster's relationship $1/D = 1/Dm + 1/(\beta Q + \theta Vc)$ and using previously estimated values for Dm and Vc θ_{O2} = 4.94 ml min^{-1} $torr^{-1}$ ml^{-1} and θ_{CO2} = 4.03 ml min^{-1} $torr^{-1}$ ml^{-1}

In this model DO_2 appears limited by chemical reaction and blood flow and minimally diffusion limited even in hypoxia. Conversely DCO_2 appears entirely reaction limited.

APPENDIX 6

Borland CDR, Dunningham H, Bottrill F, Vuylsteke A. Isoflurane Increases Oxygen Uptake by a Membrane Oxygenator. ATS 2007, San Francisco.

We have previously developed a membrane oxygenator model to study lung gas exchange (Borland C, Dunningham H, Bottrill F and Vuylsteke A J Appl Physiol 2006;100:1527-1538.)We wished to see whether a volatile anaesthetic altered oxygen exchange. Two oxygenators were connected to form a circuit continuously perfused with horse blood at a flow rate of 2.5 litres/minute. The "lung" oxygenator was ventilated by 26% oxygen with the remainder nitrogen and the "tissue" deoxygenator by 7% carbon dioxide in nitrogen to achieve normoxia and normocapnoea. Increasing concentrations of isoflurane 1-5% were added to the inlet of the "lung" oxygenator in random order. Addition of isoflurane was associated with an increase in oxygen uptake from 82.85 (SD 15.17) ml/min to 174.75 (SD 29.01) ml/min. To further investigate this phenomenon the system was used as a tonometer by simultaneously measuring partial pressure (PO_2) using an in line optical fluorometric analyser (CDI 500 Terumo systems) and saturation (sO_2) using a Cobe saturation meter with probes in the "arterial" and "venous" blood lines. Addition of isoflurane had no significant effect ($p > 0.05$) on "arterial" blood PO_2 or sO_2 or on "venous" PO_2 but a highly significant ($p = 0.007$), dose related effect on venous sO_2 due to a leftward shift of the venous, but not arterial oxygen dissociation curve. A volatile anaesthetic appears to have the potential to increase tissue oxygen delivery and could be of benefit in the severely hypoxic patient.

APPENDIX 7

Dunningham H, Borland C, Bottrill F, Gordon D, Vuylsteke A. Modelling Lung and Tissue Perfusion Using a Membrane Oxygenator Circuit. Perfusion 2007; 22:231-238.

Perfusion 2007; **22**: 231–238

Modelling lung and tissue diffusion using a membrane oxygenator circuit

H Dunningham[1], C Borland[2], F Bottrill[3], D Gordon[4] and A Vuylsteke[3]

[1]*Cambridge Perfusion Services, Papworth Hospital, Papworth Everard, Cambridge, CAMBS;*
[2]*Department of Medicine, Hinchingbrooke Hospital, Huntingdon, CAMBS;*
[3]*Department of Anaesthetic Research, Papworth Hospital, Papworth Everard, Cambridge, CAMBS;*
[4]*Anglia Ruskin University, East Road, Cambridge, CAMBS*

A simple model lung has been designed using a membrane oxygenator circuit comprising two membrane oxygenators primed with one to two litres of equine blood, giving reproducible results over several hours. Normoxia and normocapnia were achieved consistently over the duration of the test with a blood flow of 2.5 l/min, oxygenator ventilation gas flow of 5 l/min air with 0.3 l/min O_2 and deoxygenator ventilation gas flow of 5 l/min 5% CO_2 in N_2 with 0.2 l/min CO_2. The measured PaO_2 was 81.3 (SD 3.35 mmHg), $P\bar{v}O_2$ 38.3 (SD 1.38 mmHg), $P\bar{v}CO_2$ 60.6 (SD 1.13 mmHg) and $PaCO_2$ 36.1 (SD 0.69 mmHg). MO_2 and MCO_2 were 116 ml/min and 169 ml/min, respectively. An increasing linear relationship was observed for FiO_2 and the corresponding PaO_2 and, similarly, with $FiCO_2$ and $P\bar{v}CO_2$, providing reference ranges for this model. *Perfusion* (2007) **22**, 231–238.

Introduction

Literature searches suggest that testing and comparison of membrane oxygenators is generally performed using *ex vivo* methods or during cardiopulmonary bypass in anaesthetised patients.[1] *In vitro* testing is less widely performed and has often utilised several oxygenators and large volumes of blood, adding to the expense of the procedure.[2–4] In order to further investigate oxygen and carbon dioxide gas exchange in a range of physiological conditions, we have designed a simple model lung, using a continuous flow membrane oxygenator circuit including a deoxygenator to mimic normoxia, normocapnia and physiological pH.

Methods

Gas mixtures

All gases were obtained from British Oxygen, Manchester, UK. For the oxygenator, stock cylinders of air and oxygen were connected via Y gas tubing to produce a hyperoxic gas mix. For hypoxic gas mixtures, cylinders of nitrogen (99.9%) and oxygen were used.

For the deoxygenator, a cylinder containing 5% CO_2 in N_2 and a stock cylinder of CO_2 were connected via Y gas tubing to provide adequate CO_2 concentration. For varying the $FiCO_2$ experiment, stock cylinders of N_2, CO_2 and 5% CO_2 in N_2 were used.

The gas flow of each gas was controlled by individual gas rotameters.

Gas analysers

Oxygen levels in the inlet (FiO_2) and exhaust (FeO_2) gases were analysed using a medical oxygen analyser (AX300, Teledyne analytical instruments, Cambridge, UK). The oxygen analyser was calibrated in accordance with the manufacturer's recommendations at the beginning of each experimental run.

Carbon dioxide levels in the inlet ($FiCO_2$) and exhaust ($FeCO_2$) gases were analysed using a chemiluminescent analyser (Logan LR2000, Logan Research, Kent, UK) to which a custom-built infrared CO_2 analyser was added in series upstream (accuracy 0.1%).

Blood

Commercially available defibrinated horse blood (TCS Biosciences, Buckingham, UK) was used within twenty-eight days of collection. It was guaranteed free of haemolysis and adjusted by adding and withdrawing serum to a constant haematocrit of between 40 to 43% by the manufacturers. The blood was refrigerated at 4°C prior to the day of use.

Address for correspondence: H Dunningham, Cambridge Perfusion Services, Papworth Hospital, Papworth Everard, Cambridge, Cambridgeshire CB23 3RE, UK.
Tel: 01480 364415; Fax: 01480 831226

10.1177/0267659107083240

The measured circuit Hb during the experimental phase was 9-11 g/dl.

Circuit design

The circuit comprised two commercially available Cobe Duo CML membrane oxygenators (Cobe Cardiovascular, Arvada, USA) with one acting as an oxygenator and the other as a deoxygenator. A Cobe hardshell venous reservoir (Cobe Cardiovascular) was connected to the oxygenator via 3/8″ PVC tubing running through a calibrated Stockert roller pump (Cobe Cardiovascular). From the oxygenator, 3/8″ PVC tubing carried blood to the deoxygenator and, from this the tubing, was stepped up from 3/8″ to 1/2″ tubing for connection back into the venous reservoir. Sample shunt lines from the oxygenator and deoxygenator outlets were utilised for continuous blood gas analysis, with both lines returning blood back to the venous reservoir. The circuit was initially primed with 1.5 litres 0.9% saline (Baxter Healthcare, Norfolk, UK) and then flushed out on addition of equine blood to the circuit.

The temperature of the circuit was maintained at 36–37°C, using a Medtronic heater/cooler unit (Medtronic, M-N, USA) connected to the inbuilt heat exchanger on the deoxygenator. The temperature was checked continuously via temperature probes within the CDI500 sensors located on the venous and arterial blood shunt lines.

To obtain normoxic blood oxygen and carbon dioxide partial pressures (pO_2 and pCO_2) the oxygenator was ventilated with 5 l/min air and 0.3 l/min oxygen to give a FiO_2 of 25.5% and the deoxygenator was ventilated with 5 l/min 5% CO_2 in N_2 and 0.2 l/min CO_2 giving a $FeCO_2$ of 8.2% . The oxygenator and deoxygenator gases were carried to the respective device via 1/4″ PVC tubing. The exhaust from each device was carried away via 3/8″ PVC tubing. Inlet or exhaust gas analysis was made by incorporating the O_2 and CO_2 analysers within the ventilating gas tubing or exhaust gas tubing, as appropriate.

FiO_2, FeO_2, $FiCO_2$ and $FeCO_2$ measurements were documented throughout the experiments. The temperature and barometric pressure were recorded for each experimental session. The temperature was measured over the experimental run by a minimum and maximum mercury thermometer and ranged 18–24°C. The barometric pressure was determined by the local weather station located at the Royal Air Force base, Wittering, and ranged 763.5–795 mmHg. The humidity of the oxygenator outlet was determined as 66% by a wet and a dry bulb thermometer (Met-check, Milton Keynes, UK).

Blood gas analysis

Blood gas analysis was made using the CDI Blood Parameter Monitoring System 500, an in-line optical Fluorometric analyser which requires a minimum blood flow rate of 35 ml/min (Terumo Cardiovascular Systems, Surrey, UK). The blood sample shunt lines exiting the deoxygenator and the oxygenator were each connected to a calibrated shunt sensor which continually monitored pH, pO_2, pCO_2 and potassium (K), with values temperature corrected to 37°C. The blood gas tensions exiting the oxygenator and deoxygenator for each experimental change to the circuit were allowed to equilibrate before documenting these values.

Haemoglobin concentrations were measured using a bench-top analyser, Rapidlab 800 (Bayer, Berks, UK). Blood samples 1.5 ml were withdrawn from the arterial shunt line (also used for the CDI500 sensor) into heparinised syringes and either analysed immediately or kept refrigerated prior to analysis at the end of the experiment.

Experimental protocol

The circuit was assembled and primed as described above. Each experiment was run in duplicate with a different circuit each time.

Consistency of circuit over time

On each experimental day, a single circuit was used for various tests (e.g. varying blood flow, varying gas flow and varying FiO_2) over several hours. To check the circuit for consistency, the circuit was returned to normoxic parameters as previously determined i.e. blood flow of 2.5 l/min, oxygenator ventilation gas of 5 l/min air with 0.3 l/min O_2 and deoxygenator ventilation gas of 5 l/min 5%CO_2 in N_2 with 0.2 l/min CO_2. The venous and arterial blood gas partial pressures were noted and subsequently carbon dioxide uptake and oxygen uptake ($\dot{M}CO_2$ and $\dot{M}O_2$values) were calculated and compared to those at the beginning of the run.

Varying oxygenator FiO_2

To achieve hypoxic gases, nitrogen was mixed with oxygen to provide a range of hypoxic FiO_2 to the oxygenator whilst maintaining a total gas sweep of 5 l/min. The FiO_2 used during the test run were 4.9, 7.4, 8.3, 8.9, 9.0, 11.0, 14.2, 16.7, 17.3 and 19.0% and were tested in a random order. To achieve hyperoxia, the oxygenator was run with a total gas sweep of 5 l/min made up of varying quantities of air and oxygen to give a range of FiO_2 at 21, 38, 45,

51, 57, 60, 70, 74, 82, 84 and 98%, which were tested in a random order. The deoxygenator received 5 l/min 5% CO_2 in N_2 and 0.2 l/min CO_2 and the blood flow of the circuit was maintained at 2.5 l/min throughout hypoxia and hyperoxia testing.

Varying deoxygenator $FiCO_2$

To vary the $FiCO_2$, the deoxygenator was ventilated with varying quantities of N_2, CO_2 and 5% CO_2 in N_2, but aiming for a total gas sweep of approximately 5 l/min (4.7–5.3 l/min). The $FiCO_2$ achieved were 0, 0.38, 1.18, 1.53, 1.77, 1.98, 2.23, 2.43, 2.88, 3.08, 5.6, 7.2, 7.8, 8.3, 9.7, 9.8, 10.5, 10.7, 11.4, 11.4, 11.6, 12.4, 13.0, 13.1, 13.3, 14.3, 14.4, 16.0, 18.1, 21.1, 23.0 and 23.8%, which were tested in a randomised order. The blood flow was maintained at 2.5 l/min and the oxygenator ventilated with 5 l/min air with 0.3 l/min O_2.

Calculations (5)

$$\dot{M}O_2 = f \times (FiO_2 - FeO_2) \times 273/(273+t) \times (P_B - H_2O)/760$$

where f is gas flow rate in ml/min, t is ambient temperature, P_B-H_2O is barometric pressure less saturated vapour pressure at ambient temperature in mmHg

$\dot{M}CO_2$ was calculated using the $\dot{M}O_2$ equation above, but substituting FiO_2 and FeO_2 for $FiCO_2$ and $FeCO_2$, respectively.

Statistics

For linear correlations, linear regression was used and for curvilinear relationships, Spearman's Rank was utilised. Statistical significance is expressed as $p < 0.05$, $p < 0.005$ and $p < 0.001$.

Results

Consistency of circuit over time

Over the course of three hours, the PaO_2 and $P\bar{v}O_2$ averaged 81.3 mmHg (SD 3.35) and 38.3 mmHg (SD 1.38), respectively. The $P\bar{v}CO_2$ was seen to reduce very slightly over the time, although not significantly, averaging 60.6 mmHg (SD 1.13). The $PaCO_2$ averaged 36.1 mmHg (SD 0.69) (Figure 1). $\dot{M}O_2$ was calculated as 148 ml/min in the first 10 minutes and, thereafter, $\dot{M}O_2$ stabilised at approximately 115.9 ml/min (SD 5.04). $\dot{M}CO_2$ remained at an average of 168.7 ml/min (SD 4.43) (Figure 2).

Varying oxygenator FiO_2

Over the range of FiO_2, 4.9–98%, there was a close linear correlation with the resultant PaO_2, ranging

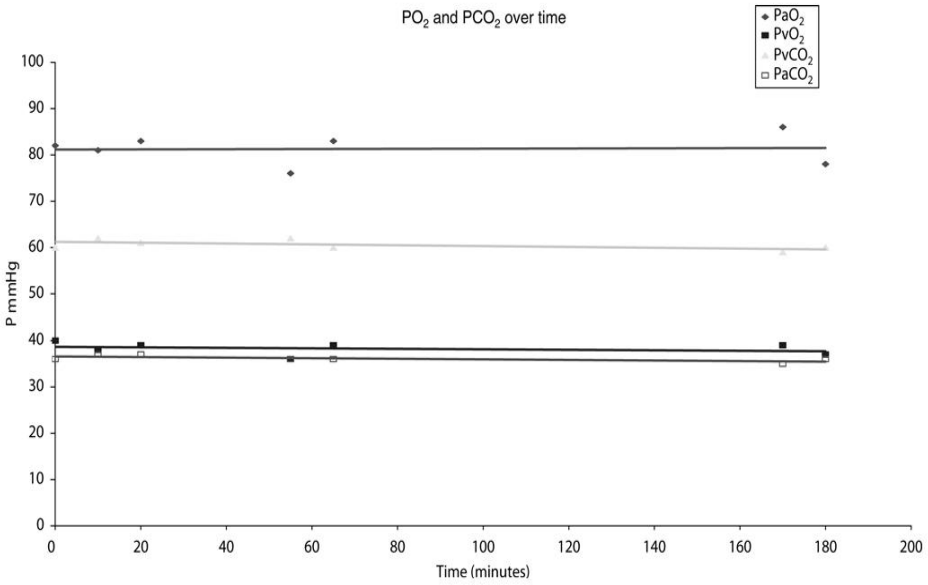

Figure 1 Over the course of three hours the PaO_2 and $P\bar{v}O_2$ averaged 81.3 mmHg (SD 3.35) and 38.3 mmHg (SD 1.38), respectively. The $P\bar{v}CO_2$ averaged 60.6 mmHg (SD 1.13) and $PaCO_2$ averaged 36.1 mmHg (SD 0.69).

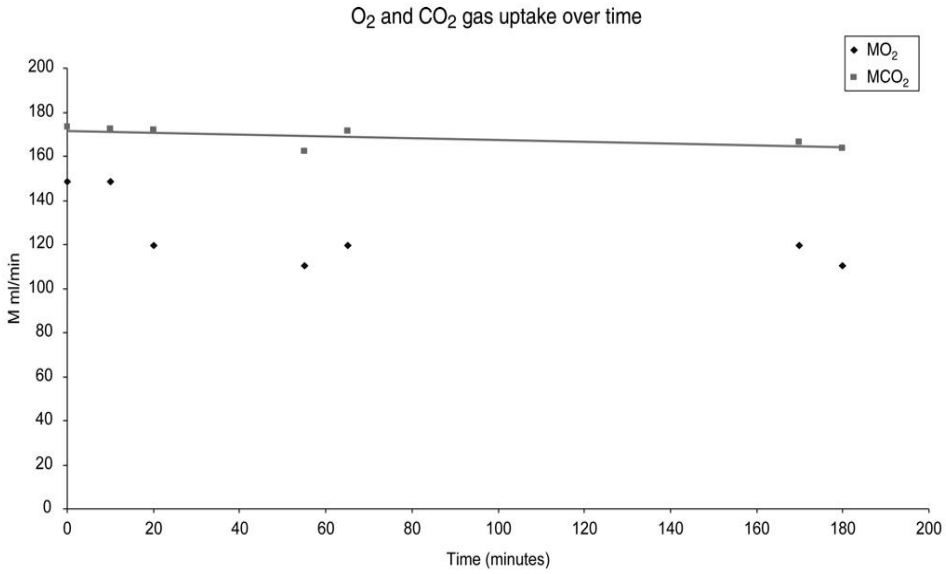

Figure 2 $\dot{M}O_2$ was calculated as 148 ml/min in the first 10 minutes and thereafter $\dot{M}O_2$ stabilised at approximately 115.9 ml/min (SD 5.04). $\dot{M}CO_2$ remained at approximately 168.7 ml/min (SD 4.43).

from 26.0 to 527.3 mmHg (Figure 3, r = 0.996). $\dot{M}O_2$ was plotted against FiO_2 and revealed a curvilinear relationship (Figure 4, $p < 0.005$) with $\dot{M}O_2$ increasing from 18.5 to 122.4 ml/min over the FiO_2, 7.4% to 25.5% (corresponding PaO_2 range 19 to 89 mmHg). In hyperoxia, $\dot{M}O_2$ averaged 170 ml/min.

Varying deoxygenator $FiCO_2$

$FiCO_2$, range 0-23%, was plotted against the resultant $P\bar{v}CO_2$ (Figure 5) and a close linear relationship was seen with $P\bar{v}CO_2$ ranging from 10 to 125 mmHg (r = 0.975). $\dot{M}CO_2$ was plotted against $P\bar{v}CO_2$, revealing a curvilinear relationship ($p < 0.005$, Figure 6), with $\dot{M}CO_2$ increasing from 28.0 ml/min at $PvCO_2$ 10 mmHg to 225.3 ml/min at $PvCO_2$ 95 mmHg.

Discussion

Main findings

From the data, it is evident that a reliable *in vitro* model of lung and tissue gas exchange over physiological blood partial pressure ranges can be achieved with two commercially available oxygenators. This model has demonstrated that a membrane surface area of 2.6 m^2 is adequate to provide deoxygenation. Over extended periods of time, there is consistency within the experimental model with respect to PaO_2, $P\bar{v}O_2$, $PaCO_2$, $P\bar{v}CO_2$ and the resultant $\dot{M}O_2$ and $\dot{M}CO_2$. The oxygenators used have been rated for up to six hours usage by the manufacturer so there is potential to investigate the consistency of this model over a longer time period. The CDI500 sensors have no specified time limit from the manufacturer, but, clinically, they have been used for six or more hours without failure.

With increasing FiO_2, a close linear correlation with increasing PaO_2 was observed, which is also expected in life. This study provides a reference guide for the required FiO_2 needed to give any desired PaO_2. In this model, the data suggested that a FiO_2 of 26% was required to give $P\bar{v}O_2$ and PaO_2 within a clinical range compared to 21% required in life. This is probably attributed to the differences between the membrane oxygenator and the lungs, such as smaller membrane surface area, larger diameter 'pulmonary capillaries', thicker membrane and heterogeneity of blood and gas flow, which all contribute to resistance to gas exchange.

The $\dot{M}O_2$ value for the consistency test conducted over three hours was comparable to the data achieved in the increasing FiO_2 test. These tests were conducted using different circuits, set up as detailed in the methods. The curvilinear relationship seen between increasing FiO_2 and the resultant $\dot{M}O_2$ showed a steeper increase in oxygen transfer

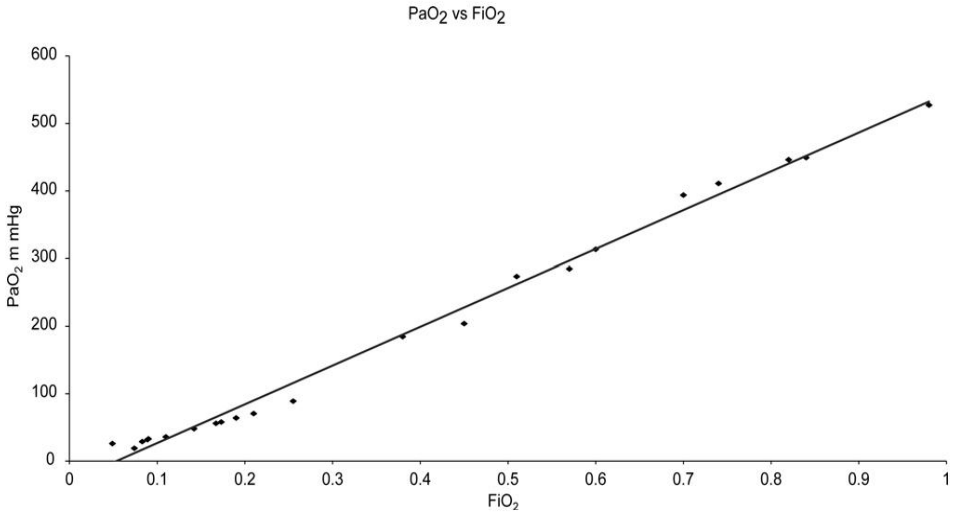

Figure 3 Over the range of FiO_2 4.9-98% there was a close linear correlation with the resultant PaO_2 ranging from 26.0 to 527.3 mmHg (R = 0.996).

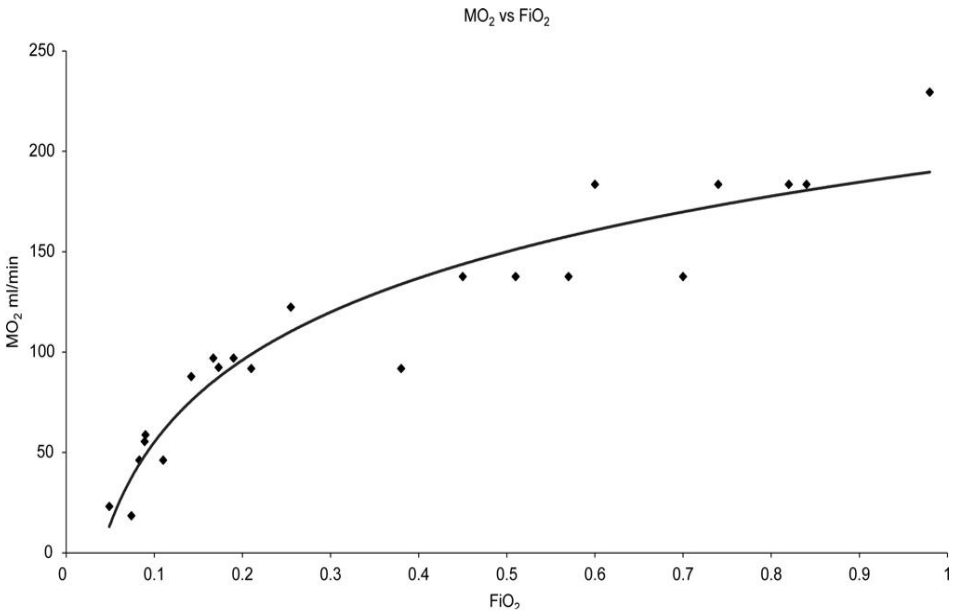

Figure 4 $\dot{M}O_2$ vs FiO_2 revealed a curvilinear relationship ($p < 0.005$) with $\dot{M}O_2$ increasing from 18.5 to 122.4 ml/min over the FiO_2 range 7.4% to 25.5% (corresponding PaO_2 range 19 to 89 mmHg).

during hypoxia, with the low inspired gas oxygen tensions limiting the amount of oxygen transfer. As more oxygen was available in the gas phase, the oxygen transfer was seen to increase until the blood was approximately 100% saturated (approximately 175 mmHg achieved with FiO_2 38%) where a plateau effect was evident.

Carbon dioxide transfer across the membrane oxygenator is less widely investigated, probably due to the complex way in which carbon dioxide is

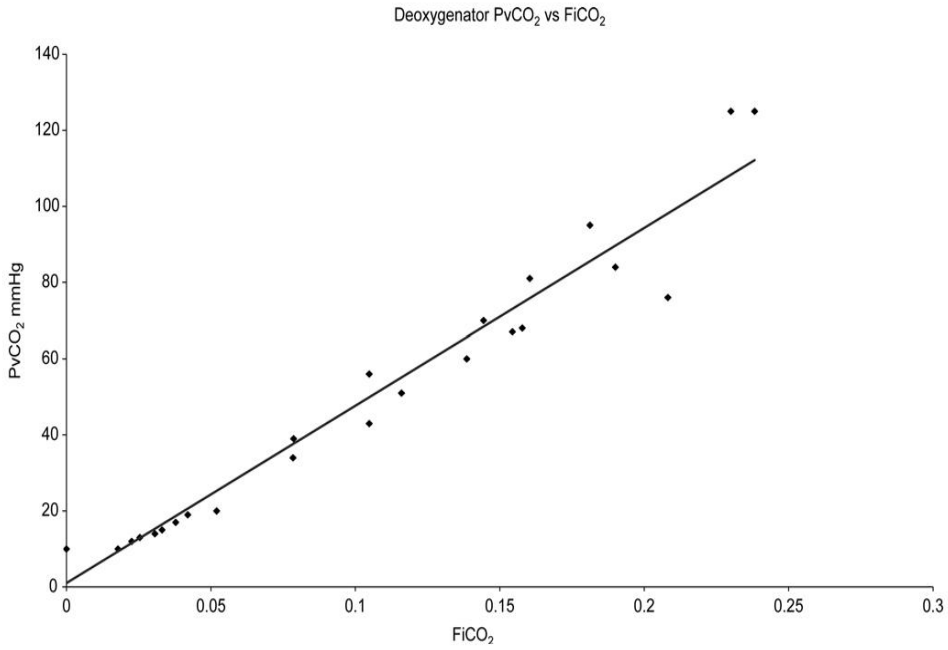

Figure 5 A linear relationship was seen with $FiCO_2$ range 0–23% resulting in $P\bar{v}CO_2$ from 10 to 125 mmHg ($R = 0.975$).

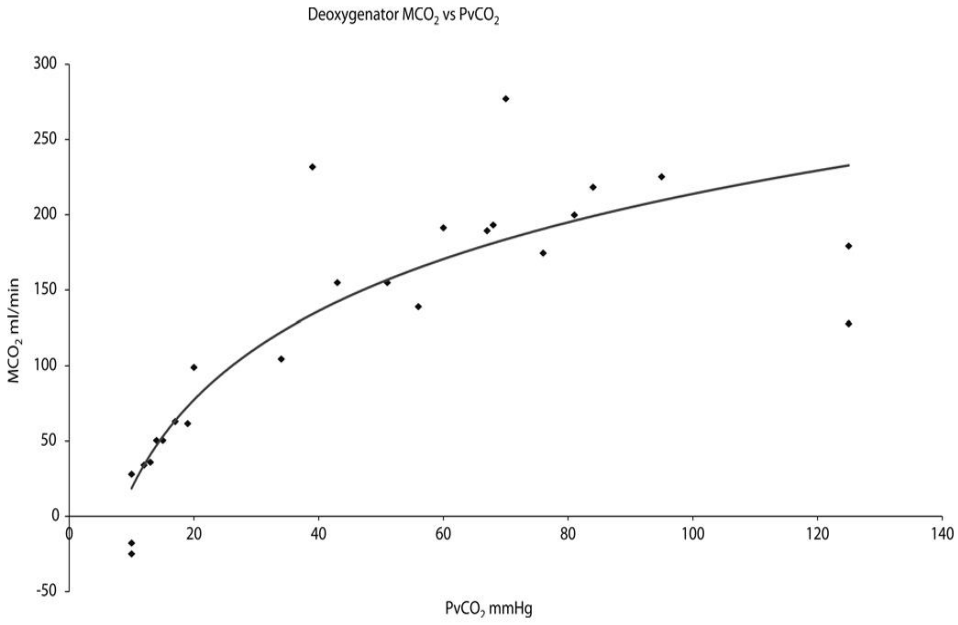

Figure 6 $\dot{M}CO_2$ was plotted against $PvCO_2$ revealing a curvilinear relationship ($p < 0.005$) with $P\bar{v}CO_2$ increasing from 27.99 ml/min at $P\bar{v}CO_2$ 10 mmHg to 225.27 ml/min at $P\bar{v}CO_2$ 95 mmHg.

present within the blood and red blood cell. In this model, carbon dioxide is actively added to the blood via a membrane deoxygenator in order to mimic tissue gas exchange. The $P\bar{v}CO_2$ was seen to increase linearly with increasing $FiCO_2$, which provides a reference range for this model. $\dot{M}CO_2$, when plotted against $P\bar{v}CO_2$, exhibited a curvilinear relationship, indicating a steep increase in carbon dioxide

transfer up to approximately 20 mmHg, followed by a less steep, but continuing rise, thereafter.

A wide range of gas exchange data can be extrapolated from this model and adaptations of this method can be made for investigating both clinical and non-clinical parameters. This circuit has previously been used to model gas exchange in the presence of nitric oxide and carbon monoxide[6,7] and we are using the technique to test the effect of volatile agents[8] and blood-borne substances on gas exchange. In recent experiments conducted in our laboratory[9] the membrane oxygenator circuit has been successfully utilised to study gas exchange relating to nitric oxide diffusion (DNO) and carbon monoxide diffusion (DCO) with varying physiological parameters such as blood flow, gas flow, haemoglobin and haemolysis, which would not be feasible in animal or human models. It has also been modified as a tonometry circuit by incorporating venous and arterial blood saturation probes to investigate the effects of isoflurane on the oxygen dissociation curve.[8]

A model such as this could also be used in the testing of oxygenator gas exchange performance as required by the 'Association for the Advancement of Medical Instrumentation'.[10] The AAMI specification aids the classification of oxygenator performance by stipulating venous inlet parameters, but does not reflect the type of circuit to be used, the outlet blood partial pressures to be achieved or that test conditions should reflect clinical situations such as low haemoglobin states. The manufacturers are responsible for the testing of their products and the wide variations within the AAMI criteria leads to confusion in product comparison. Publications by the authors Fried,[11] Bethune[12] and Ueyama[13] have all questioned the validity of such testing guidelines and perhaps a more suitable benchmark is required.

Comparison to the work of others

Previous *in vitro* testing of oxygenators has utilised a range of circuit designs. However, the incorporation of a deoxygenator within a circuit is less widely used and literature review indicates that a single pass system rather than a continuously running circuit is often employed.[2–4] In single pass circuits, a large quantity (18–40 litres) of heparinised bovine blood is held in a reservoir, which is then recirculated via a centrifugal or roller pump through a deoxygenator ventilated with carbon dioxide and nitrogen until the partial pressures of oxygen and carbon dioxide resemble that of venous blood. The blood is then diverted from the venous circuit to the test circuit by an additional pump, where the blood is used in a single-pass technique through the test oxygenator to an arterial reservoir. Once all of the venous blood has been utilised, the arterialised blood is returned to the venous system for further reconditioning. For this experiment, previously published designs, as described above, were considered unsuitable as this circuit needed to be kept compact with minimal components, minimal blood usage and the ability to be run continuously over an extended period of time.

Limitations of study

Structurally, there are many differences between the membrane oxygenator and lungs. However, a model such as this can still provide data on trends relating to the varying physiological parameters and their impact on gas exchange. It must be noted that the maximal oxygen transfer capacity of the Cobe Duo oxygenator is only 15% of that of the lungs, which is achieved with only approximately 5% of the minimal surface area of the lungs.

The blood used in this experiment was equine blood which has some variations to human blood. In a study published by Clerbaux *et al.*[14] horse blood was reported to contain lower Hct, but higher mean cell haemoglobin levels when compared to human blood. In addition, Clerbaux reported that the oxygen dissociation curve of the horse was slightly shifted to the left, facilitating better oxygen delivery compared to man. In this study, the Hct range used was lower than normal levels, but still spanned levels seen in clinical situations.

The pump used in this study was a positive displacement (roller) pump which can cause low levels of haemolysis due to the occlusive nature of the pump. During the experiments, potassium was monitored as an indicator of haemolysis and the rise over the course of the whole blood experiments did not suggest haemolysis to be present (potassium range 5.5 to 5.8 mmol/l).

The calculation of MO_2 and MCO_2 assumes that the gas inlet and exhaust flow are equal for the oxygenator and deoxygenator, respectively, and that the effect of the respiratory quotient would be a negligible error.

Acknowledgements

This study was done in collaboration with Anglia Ruskin University, Cambridge, UK. The authors would like to thank Cobe (Cobe Cardiovascular, Arvada, USA) for their assistance with access to oxygenators and their technical specifications, and Terumo (Terumo Cardiovascular Systems Corporation, Egham, Surrey UK) for the use of the CDI 500 analyser.

References

1 Segers PA, Heida JF, de Vries I, Maas C, Boogaart AJ, Eilander S. Clinical evaluation of nine hollow-fibre membrane oxygenators. *Perfusion* 2001; **16**(2): 95–106.
2 Griffiths KE, Vasquez MR, Beckley PD, Lalone BJ. Predicting oxygenator clinical performance from laboratory in vitro testing, *J Extracorp Tech* 1994; **26**(3): 114–20.
3 Boschetti F, Cook KE, Perlman CE, Mockros LF. Blood flow pulsatility effects upon oxygen transfer in artificial lungs. *ASAIO* 2003; **49**(6): 678–86.
4 Muhle ML, Stammers AH, Tremain KD *et al.* An in vitro study of the effects of isoflurane on oxygen transfer. *Perfusion* 2001; **16**(4): 293–99.
5 Cotes JE. Lung function assessment and application in medicine 5th Edition, Blackwell Scientific Publications, London 1993.
6 Borland C, Chandler J, Dunningham H, Misso S, Vuylsteke A, Promnitz A. *Using a membrane oxygenator for simultaneous measurement of nitric oxide and carbon monoxide diffusing capacity.* 2003 European Respiratory Society Annual Congress.
7 Borland C, Dunningham H, Bottrill F, Vuylsteke A. *Modelling lung NO and CO transfer using a membrane oxygenator.* 2005 ATS San Diego International Conference.
8 Borland C, Dunningham H, Bottrill F, Gordon D, Vuylsteke A. *Isoflurane increases oxygen uptake by a membrane oxygenator.* 2007 ATS San Francisco International Conference.
9 Borland C, Dunningham H, Bottrill F, Vuylsteke A. Can a membrane oxygenator be a model for lung NO and CO transfer? *J Appl Phys* 2006; **100**: 1527–38.
10 AAMI *ISO 7199:1996(E), Cardiovascular implants and artificial organs – Blood-gas exchangers (oxygenators),* International Organisation for Standardisation, Switzerland (1997).
11 Fried DW. Rethinking the AAMI/ISO International Standard for oxygen transfer performance of artificial lungs. *Perfusion* 1994; **9**(5): 335–42.
12 Bethune DW. Standards for blood gas exchange devices. *Perfusion* 1994; **9**(3): 207–209.
13 Ueyama K, Niimi Y, Nose Y. How to test oxygenators for extracorporeal membrane oxygenation:is the association for the Advancement of Medical Instrumentations Protocol enough? *Artif Org* 1996 Jul; **20**(7): 741–42.
14 Clerbaux T, Gustin P, Detry B, Cao ML, Frans A. Comparative study of the oxyhaemoglobin dissociation curve of four mammals: man, dog, horse and cattle. *Comp Biochem Physiol* 1993; **106**A(4): 687–94.

APPENDIX 8

Borland CDR, Bottrill F, Dunningham H, Vuylsteke A, Yilmaz C, Dane DM, Hsia CCW. Significant erythrocyte membrane resistance to nitric oxide diffusion in the lung. ATS 2009, Vienna.

Lung diffusing capacity for nitric oxide (DL_{NO}) is used to measure alveolar membrane conductance (DM_{NO}) but disagreement remains as to whether DM_{NO} equals DL_{NO}, i.e., whether theta-NO is infinity or less. We previously showed in a membrane oxygenator circuit that theta-NO is less than infinity since hemolysis increased D_{NO} (*J Appl Physiol* 2006;100:1527-1538). Here we progressively added free haemoglobin (Hb) blood substitute (bovine Hb glutamer-200, Dechra, Overland Park, KS), to our oxygenator circuit observing an increase in D_{NO} from 13.4 to 18.6 ml min^{-1} $torr^{-1}$ (n=3 P<0.001) . In 3 anesthetized dogs, DL_{NO} and DL_{CO} measured by rebreathing before and after each of 3 successive equal volume exchange transfusions with bovine Hb glutamer-200 (10 ml/kg each, total exchange of 30 ml/kg). At baseline, DL_{NO} averaged 4.5 x DL_{CO}. After exchange transfusion DL_{NO} rose 57 ±16% (mean ±SD) from baseline (p<0.01).

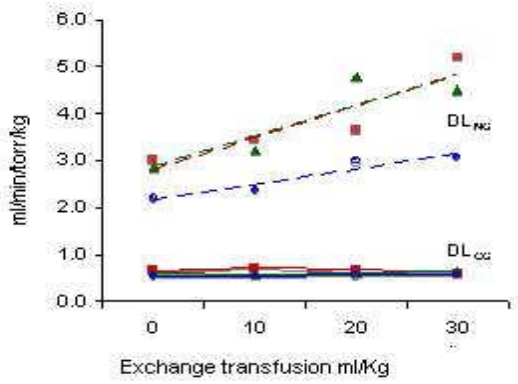

Thus, both *in vitro* and *in vivo* data demonstrate a finite theta-NO. We conclude that erythrocyte membrane imposes considerable resistance to alveolar-capillary NO uptake. DL_{NO} is sensitive to dynamic hematological factors, and is not a pure index of the conductance of the alveolar tissue membrane.

APPENDIX 9

Borland CDR, Dunningham H, Bottrill F, Vuylsteke A, Yilmaz C, Dane DM, Hsia CCW. Significant blood resistance to nitric oxide transfer in the lung. JAP 2010; 108:1052-1060.

J Appl Physiol 108: 1052–1060, 2010.
First published February 11, 2010; doi:10.1152/japplphysiol.00904.2009.

Significant blood resistance to nitric oxide transfer in the lung

Colin D. R. Borland,[1] Helen Dunningham,[2] Fiona Bottrill,[2] Alain Vuylsteke,[2] Cuneyt Yilmaz,[3] D. Merrill Dane,[3] and Connie C. W. Hsia[3]

[1]*Department of Medicine, Hinchingbrooke Hospital, Huntingdon;* [2]*Papworth Hospital, Cambridge, United Kingdom; and* [3]*Department of Internal Medicine, University of Texas Southwestern Medical Center, Dallas, Texas*

Submitted 2 August 2009; accepted in final form 10 February 2010

Borland CD, Dunningham H, Bottrill F, Vuylsteke A, Yilmaz C, Dane DM, Hsia CC. Significant blood resistance to nitric oxide transfer in the lung. *J Appl Physiol* 108: 1052–1060, 2010. First published February 11, 2010; doi:10.1152/japplphysiol.00904.2009.—Lung diffusing capacity for nitric oxide ($D_{L_{NO}}$) is used to measure alveolar membrane conductance ($D_{M_{NO}}$), but disagreement remains as to whether $D_{M_{NO}} = D_{L_{NO}}$, and whether blood conductance (θ_{NO}) = ∞. Our previous in vitro and in vivo studies suggested that $\theta_{NO} < \infty$. We now show in a membrane oxygenator model perfused with whole blood that addition of a cell-free bovine hemoglobin (Hb) glutamer-200 solution increased diffusing capacity of the circuit (D) for NO (D_{NO}) by 39%, D for carbon monoxide (D_{CO}) by 24%, and the ratio of D_{NO} to D_{CO} by 12% (all $P < 0.001$). In three anesthetized dogs, $D_{L_{NO}}$ and $D_{L_{CO}}$ were measured by a rebreathing technique before and after three successive equal volume-exchange transfusions with bovine Hb glutamer-200 (10 ml/kg each, total exchange 30 ml/kg). At baseline, $D_{L_{NO}}/D_{L_{CO}}$ = 4.5. After exchange transfusion, $D_{L_{NO}}$ rose 57 ± 16% (mean ± SD, $P = 0.02$) and $D_{L_{NO}}/D_{L_{CO}}$ = 7.1, whereas $D_{L_{CO}}$ remained unchanged. Thus, in vitro and in vivo data directly demonstrate a finite θ_{NO}. We conclude that the erythrocyte and/or its immediate environment imposes considerable resistance to alveolar-capillary NO uptake. $D_{L_{NO}}$ is sensitive to dynamic hematological factors and is not a pure index of conductance of the alveolar tissue membrane. With successive exchange transfusion, the estimated in vivo θ_{NO} [5.1 ml NO·(ml blood·min·Torr)$^{-1}$] approached 4.5 ml NO·(ml blood·min·Torr)$^{-1}$, which was derived from in vitro measurements by Carlsen and Comroe (*J Gen Physiol* 42: 83–107, 1958). Therefore, we suggest use of θ_{NO} = 4.5 ml NO·(min·Torr·ml blood)$^{-1}$ for calculation of $D_{M_{NO}}$ and pulmonary capillary blood volume from $D_{L_{NO}}$ and $D_{L_{CO}}$.

lung diffusing capacity; membrane diffusing capacity; carbon monoxide; lung diffusing capacity for carbon monoxide; lung diffusing capacity for nitric oxide; gas exchange; membrane oxygenator; exchange transfusion; bovine hemoglobin glutamer; blood substitute

NITRIC OXIDE (NO), in combination with carbon monoxide (CO), has been used to measure gas transfer in the lung since the 1980s (5, 11, 30, 31). Similar to CO, NO combines with high affinity to hemoglobin (Hb), but, in contrast to CO, the rate of combination is ~250 times faster (5, 12), so that the lung diffusing capacity for NO ($D_{L_{NO}}$) is a measure of diffusive gas conductance independent of chemical reaction. Lung transfer of a gas that combines with Hb can be described by the equation of Roughton and Forster (25), which was originally applied to CO

$$\frac{1}{D_L} = \frac{1}{D_M} + \frac{1}{\Theta Vc} \qquad (1)$$

where D_L is conductance across the lung and D_M is alveolar membrane conductance [ml gas·(min·Torr)$^{-1}$], θ is the rate of combination of gas (ligand) with erythrocyte [ml gas·(ml blood·min·Torr)$^{-1}$], and Vc is the pulmonary capillary blood volume (in ml). The left-hand term ($1/D_L$) represents the overall resistance to lung gas transfer, and the right-hand terms represent the resistance of the membrane ($1/D_M$) and the resistance of pulmonary capillary blood ($1/\theta Vc$). The equation for $1/\theta$ contains a term for diffusion resistance (*a*) and a term for chemical reaction resistance (*b*); both terms are hematocrit-dependent. Roughton and Forster exploited this and calculated D_M and Vc by measuring D_L at several P_{O_2} levels and applying known values for θ_{CO} derived from in vitro measurements using a rapid-reaction apparatus (25, 26). On the basis of their experiments in healthy adult men, resistance of the membrane was approximately equal to resistance of blood. Guenard et al. (11) assumed that since the reaction of NO with Hb is effectively infinite, θ_{NO} must be infinite; therefore, $D_{L_{NO}} = D_{M_{NO}} \approx 2\ D_{M_{CO}}$, since the ratio of diffusion of NO to diffusion of CO is directly proportional to the ratio of their respective solubility coefficients (α) and inversely proportional to the ratio of the square root of their molecular weights (MW)

$$\frac{D_{L_{NO}}}{D_{M_{CO}}} = \frac{D_{M_{NO}}}{D_{M_{CO}}} = \frac{\alpha_{NO}\sqrt{MW_{CO}}}{\alpha_{CO}\sqrt{MW_{NO}}} \approx 2 \qquad (2)$$

Implicit in their assumption is that resistance of the erythrocyte membrane, its interior, and the immediately surrounding plasma is negligible. With this assumption, *Eq. 1* can be solved from simultaneous measurements of $D_{L_{CO}}$ and $D_{L_{NO}}$ in a single maneuver and with a known value of θ_{CO}. The values for D_M and Vc obtained in this way were close to those obtained via $D_{L_{CO}}$ measured at two levels of P_{O_2} (24, 30). Combined $D_{L_{NO}}$-$D_{L_{CO}}$ measurement offered a rapid way of obtaining D_M and Vc in a variety of clinical situations, obviating the need for multiple $D_{L_{CO}}$ measurements.

However, disagreement soon arose as to whether $D_{L_{NO}} = D_{M_{NO}}$ (1, 4). The in vitro maximum rate constant of NO binding is 500–1,000 times faster with free Hb solution (2×10^5 $M^{-1}\cdot s^{-1}$) than with red blood cells (12, 33), suggesting the presence of intrinsic transmembrane or intracellular properties of the erythrocyte that limit NO uptake. In 1958, using a rapid-reaction apparatus, Carlsen and Comroe (6) measured in vitro NO reaction with human erythrocytes and found a second-order rate constant for erythrocytes (*j'*c) of 167 $mM^{-1}\cdot s^{-1}$, from which θ_{NO} = 4.5 ml NO·(min·Torr·ml blood)$^{-1}$ at Hb = 14.6 g/dl can be derived (3, 4), i.e., substantially less than infinity. To address this issue, we used a membrane oxygenator model primed with horse blood to measure in vitro NO transfer (D_{NO}) and eliminated red cell resistance by water-induced hemolysis (2). In this model, hemolysis was accompanied by a rise in D_{NO}, suggesting that red cell resistance to NO transfer was finite, i.e., $D_{NO} < D_{M_{NO}}$. Water-induced hemolysis is impracticable

Address for reprint requests and other correspondence: C. Borland, Hinchingbrooke Hospital, Huntingdon PE29 6NT, UK (e-mail: colin.borland@hinchingbrooke.nhs.uk).

in laboratory animals or isolated lung preparations, inasmuch as it disrupts the endothelium and epithelium, immediately altering in vivo D_M. However, a cell-free heme-based blood substitute (bovine Hb glutamer-200) is approved for canine clinical use (13, 14). In this study, we first progressively added bovine Hb glutamer-200 in the membrane oxygenator and examined its effect on D_{NO}, comparing it with in situ hemolysis and with hemolyzed red blood cells. Then we progressively replaced whole blood in anesthetized dogs with bovine Hb glutamer-200 and examined the effect on D_{LNO}. We reasoned that if resistance of the blood to NO were significant, in vitro D_{NO} and in vivo D_{LNO} would increase progressively as erythrocytes are "bypassed" by replacement with cell-free Hb.

METHODS

In Vitro Experiments

Membrane oxygenator circuit. Our circuit is described in detail elsewhere (2, 9). Briefly, two membrane oxygenators (Cobe Duo CML, Cobe Cardiovascular, Arvada, CO) were connected in series to form a continuous circuit perfused with 1–1.5 liters of horse blood (TCS Biosciences, Buckingham, UK) with hematocrit of 40–50% depending on batch and flowing at 2.5 l/min and 37°C. One oxygenator received a gas flow of 2.5 liters of a mixture of 22% O_2, 0.02% CO, 5 parts per million (ppm) NO, and the remainder N_2; the second oxygenator scrubbed the oxygenated blood with 8.3% CO_2 in N_2. In this way, near-physiological levels of O_2, CO_2, and pH were maintained over several hours in a steady state without apparent hemolysis (9).

Diffusing capacity measurements. D_{NO} and D_{CO} were measured from the difference in gas concentrations leaving and entering the first oxygenator as follows (2)

$$D_{NO} = \text{gas flow rate} \cdot \frac{273}{(273 + \text{Temp})[P_B - (P_{H_2O} \cdot \text{RH})]} \cdot \ln\left(\frac{NO_{in}}{NO_{out}}\right) \quad (3)$$

where Temp is ambient temperature (°C), P_B is barometric pressure (Torr), P_{H_2O} is saturated water vapor pressure (Torr), RH is relative humidity, and NO_{in} and NO_{out} are NO concentrations at the inlet and outlet ports. For CO, the calculations were identical, except CO_{in} and CO_{out} were substituted for N_{in} and N_{out}.

Addition of blood substitute. Bovine Hb glutamer-200, a cell-free heme-based blood substitute licensed for canine clinical use (Oxyglobin, Dechra, Overland Park, KS), was added in 25-ml aliquots at 5-min intervals to a total of 250 ml via the oxygenator blood-sampling port, and D_{NO} and D_{CO} were measured after each addition.

Addition of free Hb. For preparation of Hb, the cells were allowed to separate in a 1-liter bag of horse blood overnight; then the plasma was expressed by a separating clamp. Tap water was added to a total volume of 1 liter to achieve complete hemolysis.

Comparison with hemolysis. Oxyglobin was added to a total of 250 ml in 25-ml aliquots, and hemolysis was induced by addition of 100-ml aliquots to a total of 700 ml and a potassium concentration >9.5 mmol/l.

Statistical analysis. D_{NO} was entered as a dependent variable in ANOVA (SPSS version 17.0, SPSS, Chicago, IL). Solution added (Hb or Oxyglobin) was entered as an independent variable, and volume added was entered as a covariate.

Animal Experiments

The Institutional Animal Care and Use Committee at the University of Texas Southwestern Medical Center approved all protocols and procedures. Three purpose-bred adult male foxhounds [28.3 ± 1.0 kg body wt (mean ± SD)] were studied. Circulating blood, plasma, and red cell volumes were determined by the Evans blue dye-dilution method (22) on a separate day before the main study while the animal was awake and at rest.

Anesthesia and catheterization. The animal was fasted overnight and premedicated with acepromazine (0.2 mg/kg) and glycopyrrolate (0.01 ml/kg) by subcutaneous injection. A peripheral intravenous catheter was inserted. Anesthesia was induced with intravenous propofol and maintained by an infusion of ketamine and diazepam titrated to effect. Additional boluses of propofol (0.3–0.5 mg/kg iv) were administered as needed to maintain deep anesthesia and minimize fluid load. A urinary catheter was placed to monitor fluid balance. The animal was intubated with a cuffed endotracheal tube, placed supine, and mechanically ventilated (model 607, Harvard Apparatus, Millis, MA) at a tidal volume (10–12 ml/kg) and rate (18–24 breaths/min) sufficient to suppress spontaneous ventilation. Transcutaneous O_2 saturation and heart rate were monitored continuously. One external jugular vein was catheterized with an 8.5-French introducer and one femoral artery with a 5-French catheter. Through the jugular introducer, a pulmonary artery catheter was placed, and its position was verified by pressure tracing. The catheters were flushed with heparinized saline and sutured to skin. A balloon-tipped polyethylene catheter was positioned in the distal one-third of the esophagus, and the balloon was inflated with 0.5–1.0 ml of air for measurement of esophageal pressure.

Blood analyses. Arterial and mixed venous blood samples (3 ml) were drawn, at baseline and on completion of rebreathing maneuvers following each exchange transfusion, for measurement of Hb concentration, conventional blood gases, and O_2 saturation by blood analyzers (models ABL720 and OSM3, Radiometer America, Westlake, OH). The instruments were calibrated for dog blood. Hematocrit was determined using a microcapillary centrifuge.

Pressure-volume curves. Static pressure-volume curves were measured at the beginning and end of the experiment by stepwise increments and then decrements (15, 30, 45, and 60 ml/kg) of inflation volume delivered using a calibrated syringe from end-expiratory lung volume. Transpulmonary pressure was calculated as the difference between mouth and esophageal pressures. Paired measurements at each volume were averaged.

Rebreathing measurements. Rebreathing was measured as described elsewhere (19). Briefly, a known volume (45 ml/kg) of test gas mixture containing 0.3% CO, 0.3% methane, 0.8% acetylene, and 40–55 ppm NO in balance of 21% or 99% O_2 was delivered from end-expiratory lung volume via a calibrated syringe and mixed with resident gas in the lung by rebreathing maneuvers for 20 s. Gas concentrations were measured at the end of the endotracheal tube. Concentrations of methane, acetylene, and CO were measured using rapid-response infrared analyzers (Act II S, Sensors, Saline, MI). NO concentration was measured by chemiluminescence (model NOA 280, GE Analytical Instruments, Boulder, CO). Duplicate measurements at each inspired O_2 fraction were averaged. On completion of these procedures, a separate rebreathing maneuver (20 s) was performed while the animal breathed 100% O_2 followed by slow (over 7 s) exhalation, during which alveolar NO concentration was measured. In addition, CO backpressure was measured.

Exchange transfusion. After baseline measurements, 10 ml/kg of blood was removed via the femoral artery catheter into a collection bag containing citrate-phosphate-dextrose-adenine (CPDA-1, Fenwal, Lake Zurich, IL) and replaced with an equal volume of Oxyglobin solution warmed in a water bath to 37°C and infused via the central venous port. The exchange transfusion took ~1 h. Then arterial and venous blood analyses and rebreathing measurements were repeated. The exchange transfusion-and-measurement procedure was performed twice more for a total exchange volume of 30 ml/kg. The removed blood was refrigerated.

Recovery. The catheters were removed, and pressure was applied until bleeding stopped. On the next day, a venous blood sample was collected for measurement of hematocrit and Hb concentration, and a portion (10 ml/kg) of the removed blood was warmed to body temperature and

Table 1. *A summary of methods and assumed values for estimating Dm_{CO} and Vc*

Method	$1/\theta_{CO}$	Dm_{CO}	$1/\theta_{NO}$
1) Roughton-Forster (RF)	(0.93 + 0.0052 alveolar Po_2)·(14.6/Hb)	Calculated using θ_{CO} at 2 alveolar Po_2 levels	Not used
2) NO-CO	(0.93 + 0.0052 alveolar Po_2)·(14.6/Hb)	= Dl_{NO}/2.34	0
3) NO-CO	(0.93 + 0.0052 alveolar Po_2)·(14.6/Hb)	= Dl_{NO}/2	0.222

Vc, pulmonary capillary blood volume; θ, rate at which gas [carbon monoxide (CO) or nitric oxide (NO)] combines with erythrocytes; Dm_{CO}, alveolar membrane conductance of CO.

reinfused into the dog via a peripheral vein with use of a blood filter (Baxter, Deerfield, IL). This procedure was performed twice more on consecutive days until all the removed blood had been reinfused.

Data analysis. Lung volumes were calculated from methane dilution. Pulmonary blood flow was calculated from the logarithmic disappearance of acetylene relative to methane, corrected for the intercept of CO disappearance. DL_{CO} and DL_{NO} were calculated from end-tidal logarithmic disappearance of CO and NO, respectively, relative to methane (27, 30). Gas exchange septal (tissue + blood) volume was calculated from the extrapolated intercept of the acetylene disappearance curve (28). DM_{CO} and Vc were estimated by three methods, each with the assumption of different values of θ_{CO} or θ_{NO} (Table 1): *1*) by the Roughton-Forster (RF) method *(Eq. 1)* from DL_{CO} measured at two alveolar Po_2 (PA_{O_2}) levels and the θ_{CO} value given by Holland (18) for canine whole blood incorporating a temperature correction for 39°C and made at pH 7.4 using a stopped-flow apparatus (17), calculated from the mean PA_{O_2} during rebreathing and Hb concentration ([Hb])

$$\frac{1}{\theta_\infty} = (0.929 + 0.00517 \cdot P_{AO_2}) \cdot \frac{14.6}{[Hb]} \quad (4)$$

2) from simultaneously measured DL_{NO} and DL_{CO} (NO-CO method) (5, 11) with the assumption that $\theta_{NO} = \infty$ ($DL_{NO} = DM_{NO}$) and an empirical DL_{NO}-to-DM_{CO} ratio = 2.34 measured in 69 dogs cumulatively studied in our laboratory (unpublished observation), and *3*) by the NO-CO method as described above, but with the assumption of a finite θ_{NO} = 4.5 ml NO·(ml blood·min·Torr)$^{-1}$ derived from the *j'*c of Carlsen and Comroe (6) and $DM_{CO} = DM_{NO}/2$. *Equation 1* was solved for CO and NO in turn using Mathematica software (Wolfram Research, Champaign, IL). This approach gives a solution identical to that previously published (3). These data were expressed as means ± SD and compared before and after exchange transfusion by repeated-measures ANOVA. $P < 0.05$ was considered significant.

RESULTS

In Vitro Experiments

Addition of Oxyglobin to our oxygenator circuit increased D_{NO} from 13.4 ± 0.115 to 18.6 ± 1.659 (SD) ml·(min·Torr)$^{-1}$ ($n = 3$, $P < 0.001$), while D_{CO} increased from 1.075 ± 0.05 to 1.33 ± 0.139 ml·(min·Torr)$^{-1}$ ($n = 3$, $P = 0.006$; Fig. 1). The increase in D_{NO} after addition of Oxyglobin was not significantly different ($P = 0.44$) from that after addition of hemolyzed free Hb, whereas the mean D_{CO} was significantly greater with Oxyglobin than with free Hb ($P = 0.001$). No significant further increase in D_{NO} or D_{CO} was observed after hemolysis was induced in the oxygenator circuit (Fig. 2). A highly significant between-run effect was observed for D_{NO} ($P < 0.001$) and D_{CO} ($P = 0.002$).

In Vivo Experiments

Baseline hematological parameters measured during wakefulness at rest were normal in all three animals [hematocrit = 0.45 ± 0.02, plasma volume = 74.5 ± 6.3 ml/kg, red cell volume = 60.0 ± 6.6 ml/kg, and total blood volume = 134.6 ± 11.5 ml/kg (mean ± SD)]. All animals recovered from exchange transfusion without adverse effects, except for temporary darkening of the mucous membrane and the urine. From baseline to postexchange, pressure-volume curves and systemic and pulmonary arterial blood pressures were unaltered (data not shown). Hematological data and arterial blood gases are shown in Fig. 3. DL_{CO} was not corrected for reduction in Hb, since the anticipated alteration was <10%.

As expected, exchange transfusion reduced arterial hematocrit from 40.3 ± 3.3% to 23.2 ± 1.4%. There were also absolute declines in postexchange Hb concentration from 13.5 ± 1.5 to 11.4 ± 0.3 g/dl and in arterial O_2 saturation from 100 ± 0% to 95 ± 4% ($P < 0.05$) without significant changes in arterial P_{CO_2} or pH.

Rebreathing data obtained during 21% O_2 breathing are summarized in Table 2 and Fig. 4. Compared with baseline, DL_{NO} increased 59% after exchange transfusion ($P = 0.021$), while mean PA_{O_2}, lung volumes, and DL_{CO} did not change. With use of *Eq. 4* and the assumption that $\theta_{NO} = \infty$, estimates of DM_{CO} by the RF or NO-CO method (*methods 1* and *2*, respectively, in Table 1) were similar at baseline. As a result of a rising DL_{NO} with each

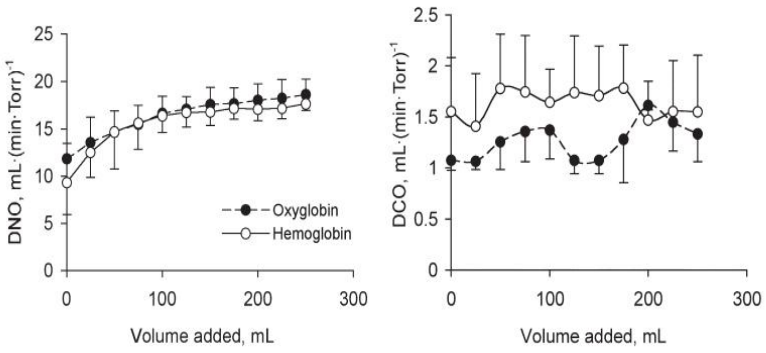

Fig. 1. In vitro diffusing capacity for nitric oxide (D_{NO}) and carbon monoxide (D_{CO}) measured in the membrane oxygenator model after successive addition of free Hb or bovine Hb glutamer-200 (Oxyglobin) solution. Values are means ± SD of 3 replicate runs.

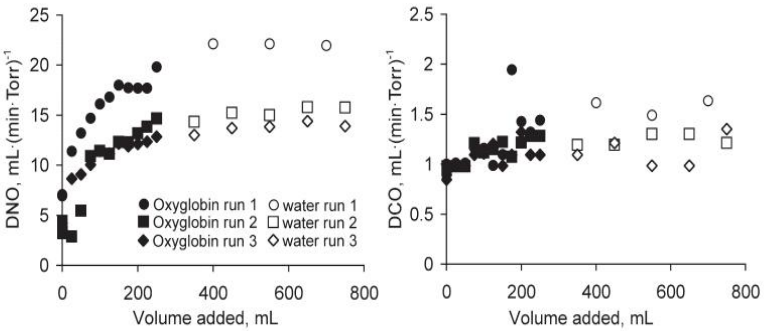

Fig. 2. In vitro D_{NO} and D_{CO} measured in the membrane oxygenator model with successive addition of bovine Hb glutamer-200 (Oxyglobin) solution followed by water hemolysis. Individual runs are shown.

exchange transfusion, D_{MCO} estimated by *method 2* progressively increased, whereas the corresponding D_{MCO} estimated by *method 1* did not change (Fig. 5, *left*). In a reciprocal relationship, Vc estimated by *method 2* progressively declined with exchange transfusion compared with the corresponding Vc estimated by *method 1* (Fig. 5, *right*).

D_{MCO} and Vc calculated using different values of θ_{NO} and θ_{CO} are given in Table 2, and their comparisons are shown in Table 3. At baseline, *methods 1* and *2* (NO-CO assuming $\theta_{NO} = \infty$) yielded similar estimates of D_{MCO} and Vc. *Method 3* [NO-CO assuming θ_{NO} = 4.5 ml NO·(ml blood·min·Torr)$^{-1}$] approximately doubled the estimated D_{MCO} and halved the estimated Vc compared with *method 2*. With successive exchange transfusions, estimates of D_{MCO} and Vc by *method 1* remained relatively stable until 30 ml/kg of blood had been exchanged. In contrast, *method 2* yielded progressively increasing values of D_{MCO} and declining values of Vc with each exchange transfusion. *Method 3* also yielded increasing values of D_{MCO} with exchange transfusion, while the estimates of Vc were more stable.

Using the in vivo data (Table 2) and applying *Eq. 1* to NO and CO individually (rearranged in *Eq. 5*), we may estimate the likely range of θ_{NO} values

$$\theta_{NO} = \theta_{CO} \times (1/D_{L_{CO}} - 1/D_{M_{CO}})/(1/D_{L_{NO}} - 1/D_{M_{NO}}) \quad (5)$$

At baseline, D_{LCO} = 0.61 and D_{LNO} = 2.69 ml·(min·Torr)$^{-1}$. Since D_{MCO} = 0.5 D_{MNO}, 1/D_{MCO} = 2/D_{MNO}. θ_{CO} was calculated at 141 Torr arterial P_{O_2} (Table 2) = 0.6 ml CO·(ml blood·min·Torr)$^{-1}$. With the assumption that with each successive exchange transfusion the measured D_{LNO} (line 10, Table 2) more closely approximates true conductance of the tissue membrane ($D_{LNO} \rightarrow D_{MNO}$),

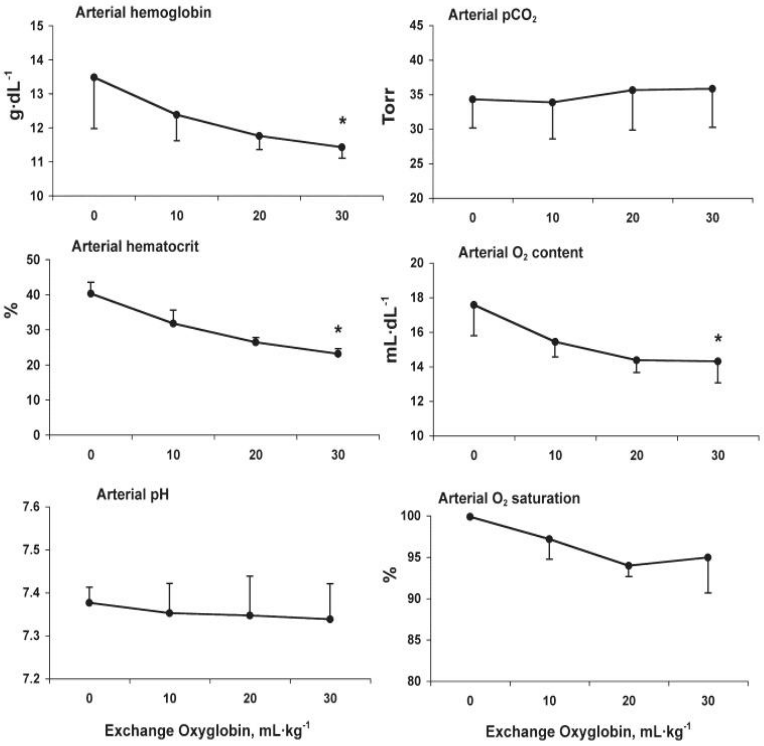

Fig. 3. Blood parameters before and after successive in vivo exchange transfusion with Oxyglobin solution. Values are means ± SD. *$P < 0.05$ vs. baseline.

Table 2. *In vivo data*

	Exchange Transfusion, ml/kg				
	0	10	20	30	*P*
Hb, g/dl	13.5 ± 1.5	12.4 ± 0.8	11.8 ± 0.4	11.4 ± 0.3	*
Hematocrit, %	40.3 ± 3.3	31.8 ± 3.8	26.5 ± 1.3	23.2 ± 1.4	*
Mean alveolar P_{O_2}, Torr	141 ± 3	141 ± 6	137 ± 7	135 ± 2	
Heart rate, beats/min	119 ± 5	107 ± 11	100 ± 22	106 ± 10	
Pulmonary blood flow, ml·(min·kg)$^{-1}$	121 ± 5	114 ± 20	119 ± 18	109 ± 10	
End-expiratory lung volume, ml/kg	32 ± 5	32 ± 5	31 ± 5	31 ± 8	
End-inspiratory lung volume, ml/kg	84 ± 5	84 ± 4	83 ± 5	83 ± 8	
Septal tissue volume, ml/kg	5.10 ± 2.15	4.88 ± 1.84	3.80 ± 1.45	4.30 ± 1.92	
Dl_{CO}, ml·(min·Torr·kg)$^{-1}$	0.61 ± 0.05	0.61 ± 0.10	0.61 ± 0.06	0.60 ± 0.03	
Dl_{NO}, ml·(min·Torr·kg)$^{-1}$	2.69 ± 0.44	3.01 ± 0.57	3.81 ± 0.92	4.27 ± 1.08	*
		Method 1 (RF)			
Dm_{CO}, ml·(min·Torr·kg)$^{-1}$	1.08 ± 0.11	1.07 ± 0.23	1.21 ± 0.10	1.01 ± 0.21	
Vc, ml/kg	2.75 ± 0.33	2.96 ± 0.19	2.73 ± 0.26	3.47 ± 0.64	*
		Method 2 (NO-CO, $\theta_{NO} = \infty$)			
Dm_{CO}, ml·(min·Torr·kg)$^{-1}$	1.15 ± 0.19	1.29 ± 0.29	1.63 ± 0.39	1.82 ± 0.46	*†
Vc, ml/kg	2.57 ± 0.33	2.42 ± 0.22	2.18 ± 0.05	2.06 ± 0.35	*†
		Method 3 (NO-CO, $\theta_{NO} = 4.5$)			
Dm_{CO}, ml·(min·Torr·kg)$^{-1}$	2.23 ± 0.70	2.68 ± 0.86	4.55 ± 2.28	4.28 ± 2.31	†
Vc, ml/kg	1.70 ± 0.25	1.66 ± 0.12	1.52 ± 0.06	1.66 ± 0.03	†

Values are means ± SD. RF, Roughton-Forster method using θ_{CO} from *Eq. 4*. NO-CO method assumes $Dl_{NO}/Dm_{CO} = 2.34$ and $\theta_{NO} = \infty$ or $\theta_{NO} = 4.5$. Repeated-measures ANOVA and post hoc Fisher's protected least significant difference: *$P < 0.05$ vs. exchange transfusion; †$P < 0.05$ vs. *method 1*.

in vivo θ_{NO} values were as follows: $0.6 \times (1/0.61 - 2/3.01)/(1/2.69 - 2/3.01) = 14.8$, $0.6 \times (1/0.61 - 2/3.81)/(1/2.69 - 2/3.81) = 6.1$, and $0.6 \times (1/0.61 - 2/4.27)/(1/2.69 - 2/4.27) = 5.1$ ml NO·(ml blood·min·Torr)$^{-1}$ after 10, 20, and 30 ml/kg exchange, respectively; i.e., with each exchange, the in vivo θ_{NO} declined in a nonlinear fashion toward the in vitro value of 4.5 ml NO·(ml blood·min·Torr)$^{-1}$ (4).

DISCUSSION

Summary of Findings

In vitro and in vivo replacement of whole blood with hemolyzed blood and a cell-free Hb solution (Oxyglobin) caused D_{LNO} to increase progressively, suggesting that D_{MNO} exceeds D_{LNO}.

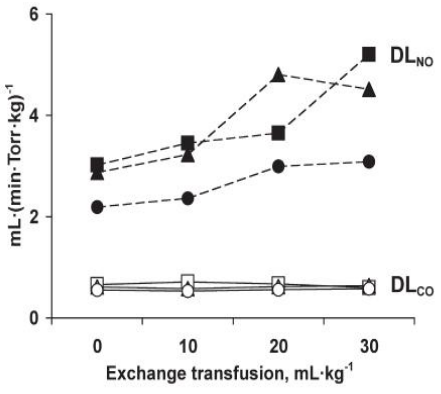

Fig. 4. In vivo lung diffusing capacity for NO (D_{LNO}) in individual animals (closed symbols, dashed lines) rose significantly after successive exchange transfusion with Oxyglobin solution compared with baseline ($P < 0.05$ by repeated-measures ANOVA), while DL_{CO} in each animal (open symbols, solid lines) remained unchanged.

The final value achieved using Oxyglobin in vitro is identical to that after hemolysis. The cell-free Hb solution penetrates the plasma surrounding the erythrocytes and between the erythrocytes and the endothelial layer; it reduces blood resistance by "bypassing" the erythrocyte membrane and interior and increases the effective surface area of tissue membrane available for gas exchange by allowing all perfused tissue surfaces to directly contact Hb. On the basis of our data, it is almost certain that θ_{NO} in vitro and in vivo is substantially less than infinity; the true in vivo θ_{NO} is probably close to the in vitro estimate of 4.5 ml NO·(ml blood·min·Torr)$^{-1}$ given the results from *Eq. 5*. The only (and unlikely) alternative explanation would be the presence of a periendothelial plasma layer that offered the sole blood resistance to NO transfer. Estimates of D_{MCO} and Vc obtained by the combined NO-CO methods (*methods 2* and *3*) are highly sensitive to the addition of cell-free Hb, while estimates obtained by the RF method (*method 1*) are relatively insensitive, because the former use D_{LNO} in their calculation. D_{LNO} increases with exchange transfusion.

Critique of Methods

Although the in vitro post-Oxyglobin, post-hemolyzed blood, and post-Oxyglobin posthemolysis values of D_{NO} are similar, they are appreciably lower than those reported in our previous work (2). The marked between-run variation observed on the same day with blood from a single horse shows that the variation is between oxygenators.

Oxyglobin does not cause hemolysis (14), and repeated administration over 1 yr caused no adverse physiological effects in dogs (13). The Hb content of Oxyglobin (13 g/dl) is similar to that of baseline canine blood under anesthesia (13.5 g/dl). After equal volume exchanges of blood with the Hb solution, arterial Hb concentration progressively declined to 11.4 g/dl, likely because of the known plasma-

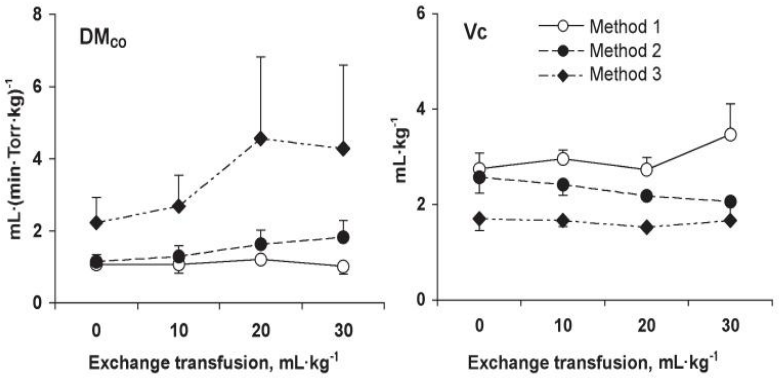

Fig. 5. Membrane diffusing capacity for CO (D_{MCO}) and pulmonary capillary blood volume (Vc) estimated by the Roughton-Forster method (*method 1*), the NO-CO method with the assumption that specific transfer conductance of blood per milliliter for NO (θ_{NO}) = ∞ (*method 2*), and the NO-CO method with the assumption that θ_{NO} = 4.5 ml NO·(ml blood·min·Torr)$^{-1}$. Values are means ± SD. Estimates by all 3 methods were significantly different from one another by repeated-measures ANOVA (all $P < 0.05$).

expanding effect of Oxyglobin. We followed the clinical slow-infusion protocol (10 mg/kg over 1 h) up to the recommended maximum (30 mg/kg total) to minimize, but not eliminate, the effect. Hemodilution would have reduced D_{LCO} more than D_{LNO}, because the blood resistance to CO transfer is greater than that to NO transfer.

A small decrease in D_{LCO} due to hemodilution could have offset a small expected increase in D_{LCO} because of reduced erythrocyte diffusion resistance with Oxyglobin, thereby explaining why in vitro D_{CO} increased with exchange transfusion but in vivo D_{LCO} did not. In the oxygenator, D_{CO} increased more with blood replacement by Oxyglobin than with blood replacement by lysed blood; given the predominant reaction dependence of D_{CO}, this likely reflects a slower reaction rate of CO with free Hb in lysed blood than with Oxyglobin. We have no in vitro data for the reaction kinetics of CO or NO with Oxyglobin. Using the oxygenator, we observed a considerably higher D_{NO}-to-D_{CO} ratio than was observed in vivo (D_{LNO}-to-D_{LCO} ratio); the difference has been discussed previously (2) and attributed to the design of the multipore membrane, where gas directly contacts a thin boundary layer of blood, resulting in a higher D_M-to-Vc ratio in the oxygenator than in the lung.

There was a modest reduction in arterial and mixed venous O_2 saturation with exchange transfusion, consistent with a rightward shift of the O_2 dissociation curve caused by Oxyglobin [P_{O_2} necessary to obtain 50% O_2 saturation of Hb (P_{50}) = 34 Torr] (8). We observed a similar rightward shift when using the oxygenator (Dunningham and Borland, unpublished observations).

Estimation of D_M and Vc by the NO-CO method requires knowledge of the D_{MNO}-to-D_{MCO} ratio, which theoretically is ~2 (*Eq. 2*). Experimentally, we observed D_{LNO}/D_{MCO} = 2.42 in healthy human subjects and 2.24 in patients with pulmonary sarcoidosis (24, 30). The empirical value in dogs (2.34) is within this range. This variability in the D_{LNO}-to-D_{MCO} ratio per se makes little difference to *method 2*, which assumes $D_{LNO} = D_{MNO}$. If we assumed a ratio of 2.42, instead of 2.34, the estimated D_{MCO} would be only 3.4% lower and the estimated Vc would be 3.1% higher. With the assumption that θ_{NO} is infinite, the empirical D_{MNO}-to-D_{MCO} ratio (2.24–2.42) is modestly (12–20%) higher than the theoretical value. This difference may be explained by the range of θ_{CO} values given in the literature, which easily causes a 20% variation in the estimated D_{MCO}. Other possible explanations have been discussed previously (24). *1*) The NO solubility coefficient may be higher in plasma than in water. *2*) Facilitated NO diffusion may occur in plasma; NO interacts with sulfhydryl groups in plasma lipids and proteins and can be transported as *S*-nitrosothiols.

Relative Resistance of Tissue and Erythrocyte Membranes

From Table 2, the baseline and postexchange transfusion D_{LCO} values [0.61 and 0.60 ml·(min·Torr·kg)$^{-1}$, respectively] may be used in conjunction with D_{MCO} [1.08 and 1.01 ml·(min·Torr·kg)$^{-1}$, respectively] obtained by *method 1* to estimate the percentage of in vivo resistance to CO uptake ($1/D_{LCO}$) due to resistance of the tissue-plasma-erythrocyte diffusion barrier ($1/D_{MCO}$), i.e., 100 × D_{LCO}/D_{MCO}. At baseline, the combined barrier resistance was (100 × 0.61/1.08) = 56% of total CO resistance. After exchange transfusion, the barrier resistance was (100 × 0.60/1.01) = 59% of total CO resistance. These values agree with previous estimates showing about equal diffusion and reaction limitation for CO uptake (20). Exchange of erythrocytes for cell-free Hb contributed little (3%) to overall CO resistance. For NO uptake, $1/D_{LNO\ pre}$ = membrane + red cell resistance, while $1/DL_{NO\ post}$ = membrane

Table 3. *Comparison of methods*

	Exchange Transfusion, ml/kg			
	0	10	20	30
Dl_{NO}/Dl_{CO}	4.44 ± 0.40	4.94 ± 0.54	6.22 ± 1.38	7.07 ± 1.68*‡
	NO-CO method using different θ_{NO} (method 3/method 2)			
Dm_{CO} $\theta_{NO4.5}/\theta_{NO\infty}$	1.90 ± 0.33	2.04 ± 0.31	2.68 ± 0.71	2.53 ± 0.75
Vc $\theta_{NO4.5}/\theta_{NO\infty}$	0.66 ± 0.03	0.69 ± 0.03	0.72 ± 0.04	0.74 ± 0.02*†

Values are means ± SD. Repeated-measures ANOVA and post hoc Fisher's protected least significant difference: *$P < 0.05$ vs. 0 ml/kg; †$P < 0.05$ vs. 20 ml/kg; ‡$P < 0.05$ vs. 10 ml/kg.

resistance only; mean values of $D_{L_{NO}}$ before and after exchange transfusion were 2.69 and 4.27 ml·(min·Torr·kg)$^{-1}$, respectively (Table 2). Thus

$$\%\ \text{overall resistance due to erythrocytes} = 100 \times \frac{\left(\frac{1}{D_{L_{NOpre}}} - \frac{1}{D_{L_{NOpost}}}\right)}{\frac{1}{D_{L_{NOpre}}}} = \left(1 - \frac{D_{L_{NOpre}}}{D_{L_{NOpost}}}\right) = \left(1 - \frac{2.69}{4.27}\right) \times 100 = 37\% \quad (6)$$

This value (37%) represents a lower-limit underestimation of true erythrocyte-related barrier resistance in alveolar capillaries, since only a fraction of erythrocytes was removed.

Values for θ_{CO}

The initial justification for the veracity of the NO-CO method (*method 2*) used by Guenard et al. (11) was the apparent agreement between values for D_M and Vc obtained by their method and by the traditional RF method (*method 1*) using the θ_{CO} values given by Roughton and Forster (25) as $1/\theta_{CO} = a + b \cdot P_{A_{O_2}} = 0.34 + 0.0061 \cdot P_{A_{O_2}}$. Until now, the greatest challenge to their method came from Robert E. Forster himself (10). He acknowledged that the earlier θ_{CO} value had been obtained at pH 7.8–8.0 and, in 1987, repeated the measurements in red blood cells from five normal individuals at pH 7.4 and 37°C obtaining a new relationship: $1/\theta_{CO} = a + b \cdot P_{A_{O_2}} = 1.3 + 0.0041 \cdot P_{A_{O_2}}$. Using the 1987 value, instead of the 1957 value, of θ_{CO} gives a 36% lower value for Vc and a twofold greater $D_{M_{CO}}$ in normal adult subjects (20), an observation also made by others (35). These later values no longer agree with those obtained from the NO-CO method (*method 2*) with the assumption that $\theta_{NO} = \infty$.

DL_{NO} and Hb

One way to determine whether θ_{NO} is infinity or less might be to examine the effect of altering Hb concentration, which might alter θ_{NO}, were it less than infinity, while leaving D_M and Vc unchanged. However, clinical studies involving patients with anemia have yielded conflicting results (1, 23, 32) at least partly attributed to the difficulty of selectively altering θ without altering D_M and Vc in pathological states. For example, patients with renal failure, especially those undergoing dialysis, will have permanent or temporary alteration in D_M and Vc. Because D_M is intrinsically "coupled" to Vc (20), it will vary as Vc varies (3). Furthermore, clinical alterations in Hb may not be sufficient to allow the effect of θ to be dissected out from other changes. Because the membrane oxygenator is a rigid structure, we were not only able to alter Hb without changing Vc or D_M, but we were also able to alter Hb 1,000% between 1 and 10 g/dl (2).

There is also a fundamental chemical kinetic reason why θ_{NO} may be less than infinity and yet independent of hematocrit. θ derives from the rate constant for the reactions of Hb and ligands. For NO, the reaction is second order: $d[NO]/dt = j'[NO][HbO_2]$. Roughton and Forster and colleagues extended chemical kinetic theory to red blood cells in vitro and in vivo, so that the reaction for NO becomes $d[NO]/dt = j'c[NO][HbO_2]$, where $j'c$ is the second-order rate constant for red blood cells (167 l·mmol^{-1}·s^{-1}), which equates to θ_{NO} = 4.5 ml NO·(ml blood·min·Torr)$^{-1}$ (4). There are good grounds for thinking that this reaction could be zero-order with respect to Hb and, therefore, just pseudo-first-order for NO. If the Hb concentration is great compared with NO concentration, then so few binding sites would be used in the reaction that altering Hb concentration would have little effect on reaction rate. Inhaling 40 ppm NO gives a plasma concentration of 2.5×10^{-9} M compared with 9×10^{-3} M for Hb concentration; i.e., Hb is greatly in excess. This argument assumes that the Hb is well mixed in solution. If Hb is packaged in red blood cells and there is an advancing front effect (20), then the effective Hb concentration would be much smaller. Nevertheless, pseudo-first-order kinetics could explain why some clinical studies (32) found no effect of Hb on $D_{L_{NO}}$.

True Values for θ_{NO}

An apparent inconsistency in the approach of Guenard et al. (11) (*method 2*) was to accept the earlier θ_{CO} value in the RF method (25) but reject the data of Carlsen and Comroe (6), which gave a finite value for θ_{NO} obtained in the same laboratory using the same continuous-flow rapid-reaction apparatus. Their approach may not be as illogical as it first appears: the values for θ_{CO} and θ_{NO} may be underestimated unpredictably by diffusion limitation in stagnant layers in the apparatus. This effect is likely to be greater for NO, since it is exclusively diffusion limited, in contrast to CO, which is equally reaction and diffusion limited. The stagnant layer effects are likely to be less in the continuous-flow than in the stopped-flow apparatus. In support of the approach of Guenard et al. (*method 2*), indirect estimates of θ_{NO} using thin layers of blood are significantly higher than that reported by Carlsen and Comroe; Heller and Schuster (16) used a value of 14 ml NO·(ml blood·min·Torr)$^{-1}$, which appears to have been calculated from (θ_{O_2} = 9.2) obtained from Heidelberger and Reeves (15) by multiplying by the ratio of water solubilities (α_{NO}/α_{O_2}) and Krogh diffusion constants (k_{NO}/k_{O_2}), although we obtain a higher value: $9.2 \times 0.041/0.021 \times 1.76 = 27.7$ ml NO·(ml blood·min·Torr)$^{-1}$. Chakraborty et al. (7), using computer simulation to eliminate the stagnant layer effect, report $\theta_{NO} = 4.2 \times 10^6$ ml NO·(ml blood·min·Torr)$^{-1}$! This raises the counterargument that stagnant layers could well be present in alveolar capillaries in vivo, a possibility that Hughes and Bates (20) emphasize strongly. Indeed, if, as suggested by this and our previous work (2, 4), θ_{NO} approximates 4–5 ml NO·(ml blood·min·Torr)$^{-1}$, then the thin film work (15) supports the argument that the major resistance to red cell-associated NO diffusion lies immediately adjacent to, rather than within, the cell or its membrane. This fits in neatly with recent work examining Hb and red cell effect on vasoconstriction and the effect of chemically and physically altering the red cell membrane and observing red cell NO uptake (21). These experiments point to diffusion limitation of NO in vivo by a cell-free zone along the endothelium, an unstirred layer around the red blood cell, and, finally, the red cell membrane itself (21). The respective contribution of these three barriers remains in dispute.

Taken together, our in vitro experiments favor the red cell membrane and its surrounding layer as a major source of the

diffusion resistance to NO. Reducing hematocrit will proportionately increase plasma and reduce red cell surface area by approximately (hematocrit)$^{2/3}$. Although we found a statistically significant relationship between 1/Hb and 1/D_{NO} in vitro, there was little change in D_{NO} above Hb ~4 g/dl. By contrast, the effect of hemolysis and bypassing the red cell membrane using Oxyglobin is striking. One way to circumvent some of these difficulties is to consider the entire diffusion barrier from air-tissue-plasma-erythrocyte to intracellular Hb as a single dynamic resistance (1/D_B), measured as 1/D_{NO}, separate from the chemical reaction rate with Hb; then the latter becomes the empirically measured gas uptake by 1 ml of free Hb solution at a given concentration (θ_{Hb}), i.e., $1/D_L = 1/D_B + 1/(\theta_{Hb} \cdot Vc)$. This approach assumes similar chemical reaction kinetics between free extra- and intraerythrocyte Hb; this assumption may or may not be true (29) and requires further examination.

Use of Blood Substitutes

It is increasingly clear that the "encapsulation" of Hb within erythrocytes markedly slows NO scavenging by heme-binding sites, allowing NO to act as a vasodilator "downstream." Cell-free heme-based blood substitutes accelerate removal of NO, risking local vasoconstriction and potentially limiting their application (34). This work should encourage the development of encapsulated heme-based blood substitutes, and our oxygenator circuit could be used to test the NO-scavenging properties of blood substitutes.

Implication for Clinical Use of D_{LNO}

All the recent reports of D_{LNO} have assumed θ_{NO} to be infinite and used D_{LNO} as a pure and direct measure of membrane conductance, i.e., unaffected by any diffusive resistance associated with capillary erythrocytes. Our findings showed this assumption to be untrue: 1/D_{LNO} is 37% erythrocyte resistance and 63% nonerythrocyte resistance. Caution is warranted when interpreting isolated D_{LNO} measurements. Reconciling the different methods and θ values remains challenging. *Method 1* (the RF method) yields stable estimates of D_M and Vc during exchange transfusion until 30 ml/kg of blood has been exchanged. *Method 2* yields D_M and Vc that change in opposite directions with exchange transfusion. *Method 3* yields relatively stable estimates of Vc, whereas D_M increases with exchange transfusion. The important point is to ensure internal consistency within a given study. On the basis of current data, when calculating D_{MNO} and Vc from D_{LNO} and D_{LCO}, we recommend the use of θ_{NO} = 4.5 ml NO·(min·Torr·ml blood)$^{-1}$.

Red cell dependence also raises the following question: Should D_{LNO} be adjusted for Hb concentration? With use of the finite θ_{NO} = 4.5, D_{MNO} = 4.27 ml·(min·Torr·kg)$^{-1}$, and Vc = 1.7 ml/kg, substituting in *Eq. 1* the reduction in D_{LNO} is ~0.1 ml·(min·Torr·kg)$^{-1}$ per (g/dl) until Hb <8 g/dl. Therefore, a Hb correction is not needed in routine clinical practice.

ACKNOWLEDGMENTS

The authors thank the staff of the University of Texas Southwestern Animal Resources Center for veterinary assistance.

GRANTS

This research was supported by National Heart, Lung, and Blood Institute Grants R01 HL-040070, HL-054060, and HL-062873.

DISCLAIMER

The contents of this article are solely the responsibility of the authors and do not necessarily represent the official views of the National Heart, Lung, and Blood Institute or of the National Institutes of Health.

DISCLOSURES

No conflicts of interest are declared by the author(s).

REFERENCES

1. **Borland C.** NO and CO transfer. *Eur Respir J* 3: 977–978, 1990.
2. **Borland C, Dunningham H, Bottrill F, Vuylsteke A.** Can a membrane oxygenator be a model for lung NO and CO transfer? *J Appl Physiol* 100: 1527–1538, 2006.
3. **Borland C, Mist B, Zammit M, Vuylsteke A.** Steady-state measurement of NO and CO lung diffusing capacity on moderate exercise in men. *J Appl Physiol* 90: 538–544, 2001.
4. **Borland CD, Cox Y.** Effect of varying alveolar oxygen partial pressure on diffusing capacity for nitric oxide and carbon monoxide, membrane diffusing capacity and lung capillary blood volume. *Clin Sci (Lond)* 81: 759–765, 1991.
5. **Borland CD, Higenbottam TW.** A simultaneous single breath measurement of pulmonary diffusing capacity with nitric oxide and carbon monoxide. *Eur Respir J* 2: 56–63, 1989.
6. **Carlsen E, Comroe JH.** The rate of uptake of carbon monoxide and of nitric oxide by normal erythrocytes and experimentally produced spherocytes. *J Gen Physiol* 42: 83–107, 1958.
7. **Chakraborty S, Balakotaiah V, Bidani A.** Diffusing capacity reexamined: relative roles of diffusion and chemical reaction in red cell uptake of O_2, CO, CO_2, and NO. *J Appl Physiol* 97: 2284–2302, 2004.
8. **Driessen B, Jahr JS, Lurie F, Griffey SM, Gunther RA.** Effects of haemoglobin-based oxygen carrier hemoglobin glutamer-200 (bovine) on intestinal perfusion and oxygenation in a canine hypovolaemia model. *Br J Anaesth* 86: 683–692, 2001.
9. **Dunningham H, Borland C, Bottrill F, Gordon D, Vuylsteke A.** Modelling lung and tissue diffusion using a membrane oxygenator circuit. *Perfusion* 22: 231–238, 2007.
10. **Forster RE.** Diffusion of gases across the alveolar membrane. In: *Handbook of Physiology. The Respiratory System. Gas Exchange.* Bethesda, MD: Am. Physiol. Soc., 1987, sect. 3, vol. IV, chapt. 5, p. 71–88.
11. **Guenard H, Varene N, Vaida P.** Determination of lung capillary blood volume and membrane diffusing capacity in man by the measurements of NO and CO transfer. *Respir Physiol* 70: 113–120, 1987.
12. **Hakim TS, Sugimori K, Camporesi EM, Anderson G.** Half-life of nitric oxide in aqueous solutions with and without haemoglobin. *Physiol Meas* 17: 267–277, 1996.
13. **Hamilton RG, Kelly N, Gawryl MS, Rentko VT.** Absence of immunopathology associated with repeated IV administration of bovine Hb-based oxygen carrier in dogs. *Transfusion* 41: 219–225, 2001.
14. **Hamilton RG, Kickler TS.** Bovine hemoglobin (glutamer-250, Hemopure)-specific immunoglobulin G antibody cross-reacts with human hemoglobin but does not lyse red blood cells in vitro. *Transfusion* 47: 723–728, 2007.
15. **Heidelberger E, Reeves RB.** Factors affecting whole blood O_2 transfer kinetics: implications for θ_{O_2}. *J Appl Physiol* 68: 1865–1874, 1990.
16. **Heller H, Schuster K.** Role of reaction resistance in limiting carbon monoxide uptake in rabbit lungs. *J Appl Physiol* 84: 2066–2069, 1998.
17. **Holland RA, Forster RE.** The effect of size of red cells on the kinetics of their oxygen uptake. *J Gen Physiol* 49: 727–742, 1966.
18. **Holland RAB.** Rate at which CO replaces O_2 from O_2Hb in red cells of different species. *Respir Physiol* 7: 43–63, 1969.
19. **Hsia CCW, Herazo LF, Ramanathan M, Johnson RL Jr.** Cardiopulmonary adaptations to pneumonectomy in dogs. IV. Membrane diffusing capacity and capillary blood volume. *J Appl Physiol* 77: 998–1005, 1994.
20. **Hughes JM, Bates DV.** The carbon monoxide diffusing capacity (D_{LCO}) and its membrane (D_M) and red cell (θ_{Vc}) components. *Respir Physiol Neurobiol* 138: 115–142, 2003.
21. **Kim-Shapiro DB, Schechter AN, Gladwin MT.** Unraveling the reactions of nitric oxide, nitrite, and hemoglobin in physiology and therapeutics. *Arterioscler Thromb Vasc Biol* 26: 697–705, 2006.

22. **McDonough P, Dane DM, Hsia CC, Yilmaz C, Johnson RL Jr.** Long-term enhancement of pulmonary gas exchange after high-altitude residence during maturation. *J Appl Physiol* 100: 474–481, 2006.
23. **Moinard J, Guenard H.** Membrane diffusion of the lungs in patients with chronic renal failure. *Eur Respir J* 6: 225–230, 1993.
24. **Phansalkar AR, Hanson CM, Shakir AR, Johnson RL Jr, Hsia CC.** Nitric oxide diffusing capacity and alveolar microvascular recruitment in sarcoidosis. *Am J Respir Crit Care Med* 169: 1034–1040, 2004.
25. **Roughton FJW, Forster RE.** Relative importance of diffusion and chemical reaction rates in determining the rate of exchange of gases in the human lung, with special reference to true diffusing capacity of the pulmonary membrane and volume of blood in lung capillaries. *J Appl Physiol* 11: 290–302, 1957.
26. **Roughton FJW, Forster RE, Cander L.** Rate at which carbon monoxide replaces oxygen from combination with human hemoglobin in solution and in the red cell. *J Appl Physiol* 11: 269–276, 1957.
27. **Sackner MA, Greenletch D, Heiman M, Epstein S, Atkins N.** Diffusing capacity, membrane diffusing capacity, capillary blood volume, pulmonary tissue volume and cardiac output by a rebreathing technique. *Am Rev Respir Dis* 111: 157–165, 1975.
28. **Sackner MA, Markwell G, Atkins N, Birch SJ, Fernandez RJ.** Rebreathing techniques for pulmonary capillary blood flow and tissue volume. *J Appl Physiol* 49: 910–915, 1980.
29. **Sirs JA.** The kinetics of the reaction of carbon monoxide with fully oxygenated haemoglobin in solution and erythrocytes. *J Physiol* 236: 387–401, 1974.
30. **Tamhane RM, Johnson RL Jr, Hsia CC.** Pulmonary membrane diffusing capacity and capillary blood volume measured during exercise from nitric oxide uptake. *Chest* 120: 1850–1856, 2001.
31. **van der Lee I, Zanen P.** Diffusion capacity for nitric oxide and carbon monoxide. *Chest* 126: 1708–1710, 2004.
32. **van der Lee I, Zanen P, Biesma DH, van den Bosch JM.** The effect of red cell transfusion on nitric oxide diffusing capacity. *Respiration* 72: 512–516, 2005.
33. **Vaughn MW, Huang KT, Kuo L, Liao JC.** Erythrocytes possess an intrinsic barrier to nitric oxide consumption. *J Biol Chem* 275: 2342–2348, 2000.
34. **Winslow RM.** Red cell substitutes. *Semin Hematol* 44: 51–59, 2007.
35. **Zavorsky GS, Cao J, Murias JM.** Reference values of pulmonary diffusing capacity for nitric oxide in an adult population. *Nitric Oxide* 18: 70–79, 2008.